Investigating the contribution of astrocytes and neuroinflammation to pathological tau changes in Alzheimer's disease

Phillips, Emma Claire

Awarding institution:
King's College London

Investigating the contribution of astrocytes and neuroinflammation to pathological tau changes in Alzheimer's disease

Emma Phillips

Thesis submitted in fulfilment of the degree of Doctor of Philosophy

Department of Basic and Clinical Neuroscience

Institute of Psychiatry, Psychology and Neuroscience

King's College London

September 2016

Declaration

I hereby declare that all of the work presented in this thesis is my own, with the exception of the following:

- Electron microscopy of synthetic $Aß_{1-42}$ was carried out by Covance (Princeton, NJ, US).
- Immunohistochemical staining of post-mortem brains was carried out by the London Neurodegenerative Diseases Brain Bank.

Emma Phillips

September 2016

Acknowledgements

Firstly, many thanks to Dr Wendy Noble for her continual guidance and support. Wendy was always able to provide encouragement and advice when most needed. Thank you also to Prof Diane Hanger for her invaluable additional input and guidance. I also appreciate the perspective gained by being mentored by two strong women so early in my career.

Thanks also to Dr Michael O'Neill and everyone at Eli Lilly for being so helpful and making me feel so welcome. In particular, thank you to Dr Joanna Wolak and Dr Daniel Ursu. Also, Emma, Sarah, Yugesh, Elena, Jasmeet and Silvia, without your help I would have been completely lost.

Thanks to Fiona for helping me with the CHO cells. A huge thank you to Team Tau, particularly the Noble group. Also, especially to Dawn and Teresa for being lovely right from the start. Lizzie, for early morning neuron prep gossips and Charlotte for wanting to throw yourself over obstacles just as much as me. Also to Martina, for the chocolate and Mount Everest chat!

Thank you to my friends who supported me along the way: my ice skating family, GoodGym friends and the Wadhamites. Particularly thanks to Sam, Dan, Ella and Ella for the pub and tube walks, Abi and Emily for the girl's nights, and to Becca, without whom I wouldn't have got through the last four years - thank you for the wine, feminism and Meryl Streep films!

A special thanks goes to my family who have always been there, even when I'm a crying mess ruining our Canadian holiday! Thank you to my parents who support and believe in me no matter what. To my sisters, Sal, Soph and Grace (adopted sister!), who always know how to lighten the mood and remind me what life is actually about – fun! Most importantly, thanks to Ed, literally my other half, without you this thesis would not have happened. Thank you for caring about Alzheimer's and tau even though it's really not your thing!

Finally, this thesis is dedicated to my Gransha, Mac Norgrove, whose love, laughter and dignity in the face of neurodegeneration sparked this whole journey off.

Abstract

Alzheimer's disease (AD) is a progressive neurodegenerative disease characterised by accumulation of ß-amyloid in extracellular plaques, intracellular neurofibrillary tangles composed of abnormally phosphorylated and aggregated tau, and widespread synaptic dysfunction and neuron loss that underlie the clinical symptoms of AD. Glial activation and a neuroinflammatory immune response is also a key aspect of the pathological progression of AD. The activation of astrocytes appears to be particularly associated with pathological changes in tau. This thesis aims to investigate the association between astrocyte activation and abnormal tau processing using primary cell culture and human post-mortem brain. Furthermore, it aims to explore possible regional differences in this role of astrocytes, and the molecular signalling pathways by which astrocytes exert their effects on tau.

Experiments in primary astrocyte and neuron co-cultures demonstrated that astrocytes were involved in accelerating Aß-induced neurotoxicity in hippocampal cultures, but not cortical cultures although the differences were quite subtle. Interestingly, astrocytes were important for the neuronal release of tau from cortical neurons under basal conditions, suggesting that astrocytes may be important for pathological tau spread in AD. Analysis of human post-mortem brain showed differences in astrocytic changes in hippocampus and cortex as AD progresses. In addition, these experiments also suggested regional differences in mechanisms related to synaptic dysfunction and loss as disease progresses. These data suggest that different mechanisms may underlie the neurodegenerative effects of ß-amyloid and/or activated astrocytes in distinct brain regions; an important consideration when considering therapeutic strategies for AD.

In addition, the potential benefits for tauopathy of repurposing an already licenced drug with anti-inflammatory action were investigated. Despite showing significant modulation of tau phosphorylation in primary cultures, dimethyl fumarate had little influence on disease-associated tau species when tested *in vivo* in a mouse model of tauopathy.

Overall, the findings of this thesis suggest that there are regional differences in astrocyte activation during the development of AD, that are somewhat associated with AD-relevant changes in tau. This work also supports a role for astrocytes in physiological tau release. Further elucidating these differences will increase understanding of neurodegenerative mechanisms. Moreover, these data suggest that regional involvement at different disease stages could be an important consideration when targeting specific mechanisms for therapeutic development.

Contents

List of Figures

List of Tables

Publications arising from this studentship

Croft CL, Wade MA, Kurbatskaya K, Mastrandreas P, Hughes MM, **Phillips EC**, Pooler AM, Perkington MS, Hanger DP, Noble W. (Submitted). Differential membrane association and release of wild-type and pathological tau. Biological Psychiatry.

Lau DHW, Hogseth M, **Phillips EC**, O'Neill MJ, Pooler AM, Noble W, Hanger DP. (2016). Critical residues involved in tau binding to fyn: implications for tau phosphorylation in Alzheimer's disease. Acta Neuropath. Comms. 4(1):49.

Kurbatskaya K*, **Phillips EC***, Dentoni G, Hughes MM, Croft CL, Wade MA, Al-Sarraj S, Troakes C, Hanger DP, Noble W. (2016). Upregulation of calpain activity precedes tau phosphorylation and loss of synaptic proteins in Alzheimer's disease brain. Acta Neuropath. Comms. 4:34.

Phillips EC, Croft CL, Kurbatskaya K, O'Neill MJ, Hutton ML, Hanger DP, Garwood CJ, Noble W. (2014). Astrocytes and neuroinflammation in Alzheimer's disease. Biochem. Soc. Trans. 42, (5), 1321-5.

Hanger DP, Lau DHW, **Phillips EC**, Bondulich MK, Guo T, Woodward BW, Pooler AM, Noble W. (2014). Intracellular and extracellular roles for tau in neurodegenerative disease. J. Alz. Dis. 40, (Suppl 1), S37-45.

Abbreviations

Aß	ß-amyloid
AD	Alzheimer's disease
ADAM	A disintegrin and metalloprotease domain containing protein
AICD	APP intracellular domain
Alphascreen	Amplified luminescent proximity homogenous assay screen
ALS	Amyotrophic lateral sclerosis
AMPA	α-amino-3-hydroxy-5-methyl-4-isoxazolepropionic acid
ANOVA	Analysis of variance
APH	Anterior pharynx-defective 1
ApoE	Apolipoprotein E
APP	Amyloid precursor protein
APP/PS1 mice	Amyloid precursor protein / presenilin 1 mice
APS	Ammonium persulphate
AraC	Cytosine arabinoside
ATP	Adenosine triphosphate
BACE1	ß-site APP-cleaving enzyme 1
BCA	Bicinchoninic acid
BDNF	Brain derived neurotrophic factor
BSA	Bovine serum albumin
CaMKII	Calcium and calmodulin dependent kinase II
Caspase	Cysteine dependent aspartate-specific proteases
cdk5	Cyclin-dependent kinase 5
CHO	Chinese hamster ovary
ck1	Casein kinase-1

CNS	Central nervous system
CSF	Cerebrospinal fluid
CTFα	C-terminal fragment α
CTRL	Control
D421	Aspartate 421
DAMP	Damage-associated molecular pattern
DIV	Days *in vitro*
DMEM	Dulbecco's modified Eagle's medium
DMF	Dimethyl fumarate
DMSO	Dimethyl sulfoxide
DNA	Deoxyribonucleic acid
DNase	Deoxyribonuclease
dNTPs	Deoxynucleoside triphosphates
DTT	Dithiothreitol
DYRK1A	Dual specificity tyrosine-population-regulated kinase 1A
E18	Embryonic day 18
EAE	Experimental autoimmune encephalomyelitis
EDTA	Ethylenediaminetetraacetic acid
EGTA	Ethylene glycol tetraacetic acid
EFS	Electrical field stimulation
ER	Endoplasmic reticulum
ERK1/2	Extracellular signal-related kinase 1/2
FBS	Foetal bovine serum
FTD	Frontotemporal dementia
g(av)	G-force
GFAP	Glial fibrillary acidic protein

GFP	Green fluorescent protein
GLAST	Glutamate aspartate transporter
GLUT	Glucose transporter
GSK-3	Glycogen synthase kinase 3
GWAS	Genome-wide association studies
H	Hours
H&E	Hematoxylin
HBSS	Hank's balanced salt solution
HBT	HEPES buffered Tyrode
HCl	Hydrochloride
HEPES	4-(2-hydroxyethyl)-1-piperazineethanesulfonic acid
HRP	Horseradish-peroxidase
HSS	High speed supernatant
Hz	Hertz
Iba1	Ionised calcium-binding adaptor molecule 1
ICC	Immunocytochemistry
IFN-γ	Interferon γ
IHC	Immunohistochemistry
Iκ-Bα	Nuclear factor of κ light polypeptide gene enhancer in B-cells inhibitor, α
IL	Interleukin
IL-1RA	Interleukin 1 receptor antagonist
iNOS	Inducible nitric oxide synthase
INT	2-p-iodophenyl-3-p-nitrophenyl-5-phenyl tetrazolium chloride
IP-10	IFN-γ-inducible protein 10
IP_3	Phospholipase C/inositol 1, 4, 5-triphosphate
iPS cells	Induced pluripotent stem cells

JNK	c-Jun N-terminal kinases
Keap1	Kelch-like ECH-associated protein 1
Kb	Kilobases
kDa	Kilodaltons
KPI	Kunitz protease inhibitor
LDH	Lactate dehydrogenase
LSS	Low speed supernatant
LTP	Long term potentiation
MAP2	Microtubule-associated protein 2
MAPK	Mitogen activated protein kinase
MAPT	Microtubule-associated protein tau
MCI	Mild cognitive impairment
MCP1	Monocyte chemoattractant protein 1
MIP-1α	Macrophage inflammatory protein 1 α
Min(s)	Minute(s)
Minocycline	Minocycline hydrochloride
MS	Multiple sclerosis
MSD	Meso Scale Discovery
MWM	Morris water maze
N	Number
NAD^+	Nicotinamide adenine dinucleotide
NADH	Nicotinamide adenine dinucleotide (reduced form)
NDP52	Nuclear dot protein 52
NF-κB	Nuclear factor κ-light-chain-enhancer of activated B cells
NFT	Neurofibrillary tangles
NMDA	N-methyl-D-aspartate

Nrf2	Nuclear factor erythroid 2-related factor 2
ns	Not significant
NSAIDs	Non-steroidal anti-inflammatory drugs
NSE	Neuron specific enolase
NT	Neuropil thread
p-tau	Phosphorylated tau
PAGE	Polyacrylamide gel electrophoresis
PAMP	Pathogen-associated molecular pattern
PBS	Phosphate buffered saline
PBS-T	PBS-Tween 20
PCR	Polymerase chain reaction
PDL	Poly-D-lysine
PET	Positron emission tomography
PFA	Paraformaldehyde
Phe	Phenylalanine
PHF	Paired helical filament
PMD	Post-mortem delay
PNS	Peripheral nervous system
PP1	Protein phosphatase 1
PSD-95	Postsynaptic density protein 95
RANTES	Regulated on activation, normal T-cell expressed and secreted protein
ROS	Reactive oxygen species
Sarkosyl	Sodium lauroyl sarcosinate
SDF-1α	Stromal cell-derived factor 1 α
SDS	Sodium dodecyl sulfate
Sec	Seconds

SEM	Standard error of the mean
Ser	Serine
Src	Sarcoma
t-tau	Total tau
TAE	Tris-acetate-EDTA
TBE	Tris-borate EDTA
TBS	Tris buffered saline
TBS-T	TBS-Tween 20
TEMED	N,N,N',N'-Tetramethylethylenediamine
Thr	Threonine
TLR	Toll-like receptor
TNFα	Tumour necrosis factor α
TREM2	Triggering receptor expressed on myeloid cells 2
TW buffer	Tris-western buffer
Tween 20	Polyethylene glycol sorbitan monolaurate
USD	US dollars
V	Volts
Val	Valine
VEH	Vehicle
WT	Wild-type
XSLB	Extra strong lysis buffer

Chapter 1: Introduction

1.1 Historical perspective

Alzheimer's disease (AD) is a progressive, neurodegenerative disease first described by Alois Alzheimer in 1906. He presented the case of a fifty year old, Auguste D, who showed "a peculiar severe disease of the cerebral cortex" (Hippius and Neundorfer, 2003). Alzheimer went on to describe how Auguste D showed progressive deteriorating psychological symptoms beginning with paranoia and, over the five years he studied her, continued with memory problems, sleep disorders, aggressiveness, hallucinations and increasing confusion. After her death, Alzheimer was able to histologically investigate her brain, first describing the senile plaques and neurofibrillary tangles that are still used today to diagnose the disease post-mortem (Alzheimer et al., 1995).

It is now known that AD clinically presents as progressive memory loss, confusion and often changes in behaviour and personality. However, diagnosis cannot be definitively confirmed until after death with the histopathological observation of ß-amyloid extracellular plaques and intracellular tau neurofibrillary tangles in the brain (McKhann et al., 1984). AD is currently the most common cause of dementia worldwide. The World Alzheimer Report 2015 estimates there are 46.8 million people living with dementia and that 58 % of these people live in developing countries. In 2015 the total worldwide cost of dementia was estimated to be USD 818 billion, 1.09 % of global GDP (Prince, 2015). In the 2014 Alzheimer's Society Dementia UK Update it was estimated that, in the UK alone, there are over 850,000 people living with dementia with an overall economic impact of £26.3 billion – approximately £32,250 per person annually. The number of people living with dementia is estimated to rise to over 2 million by 2051 and there are still no clinically approved disease-modifying treatments available (Dementia UK Update).

1.2 Neuropathology

AD brain shows clear pathology and atrophy compared to a healthy brain. Final diagnoses of AD can be made after demonstrating the presence of microscopic senile plaques and neurofibrillary tangles (NFTs) (**Figure 1.1 A**). In addition to the classical hallmarks of AD there is a characteristic pattern of neuron loss throughout the brain, with hippocampal and medial temporal lobe atrophy being so prominent that changes in hippocampal mass are used as a clinical diagnostic tool (**Figure 1.1 B**) (Schroder and Pantel, 2016). These changes start long before memory and behavioural symptoms present, with ß-amyloid and tau aggregates, synaptic dysfunction and axonal and dendrite loss occurring decades before the onset of symptoms (Braak and Braak, 1991, 1995). By the time the first clinical symptoms are present and recognised as distinct from the normal aging process there is already widespread pathology and neuron loss. This results in an additional challenge in successful drug development: by the time symptoms present neuronal damage may already be irreversible (Cutler and Sramek, 2001). For this reason biomarkers, for example levels of ß-amyloid and tau in blood or cerebrospinal fluid (CSF), to diagnose or highlight high-risk individuals easily and reliably, are needed in order to increase the window of time available to treat and slow the disease (Waite, 2015).

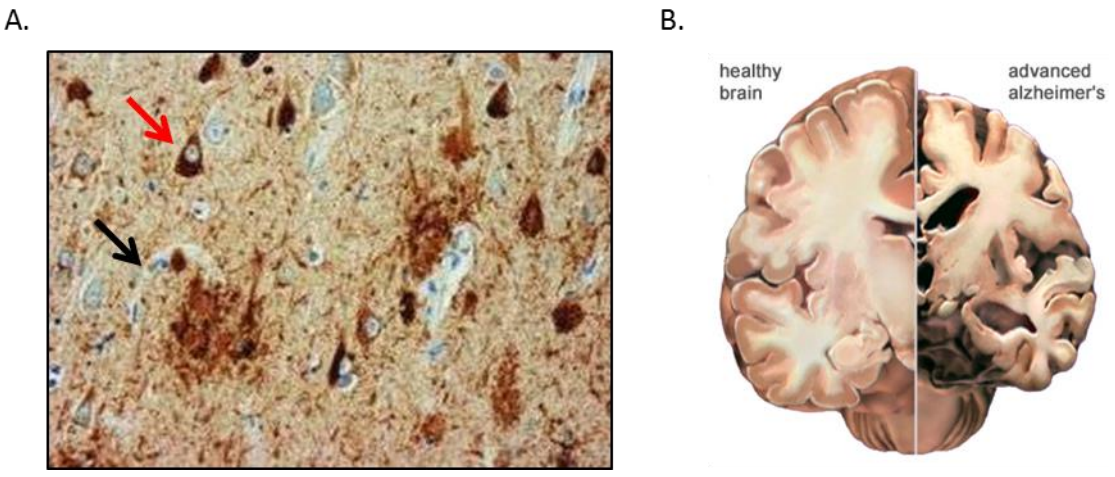

Figure 1.1: Pathological changes in AD
A. Microscopically, ß-amyloid and tau aggregate to form extracellular senile plaques (indicated by black arrow) and intracellular neurofibrillary tangles (red arrow) respectively (Washington University School of Medicine). **B.** Advanced AD shows significantly reduced brain volume, severe hippocampal atrophy and increased ventricle volume compared to healthy brain (www.alz.org).

1.2.1 ß-amyloid plaques

ß-amyloid (Aß) or senile plaques are pathological lesions found in the grey matter of the cortex and hippocampus (Glenner and Wong, 1984). Amyloid plaques can be described as being diffuse or dense-core. Dense core plaques have deposits of fibrillar Aß at their centre. These hydrophobic plaques are found in the extracellular space surrounded by a halo of soluble oligomeric Aß species, neuron debris, activated astrocytes and microglia and degenerating synapses (Koffie et al., 2009; Bouvier et al., 2016). Diffuse plaques do not contain fibrillar Aß, have no defined structure and are usually not associated with glial responses or synaptic loss (Serrano-Pozo et al., 2011). The abundance and spread of Aß pathology through diseased brain has been described as five progressive phases (Thal et al., 2002):

I) Aß plaques are found only in the neocortex,

II) Aß plaque pathology has spread into allocortical brain regions,

III) Plaques present in some subcortical areas such as the striatum, diencephalic nuclei and the cholinergic nuclei of the basal forebrain,

IV) Aß plaques have spread to the brainstem,

V) Spread of plaque pathology to the cerebellum.

It was originally thought that these stages could be used to define the severity of AD, however it has since been found that plaque staging does not correlate with the clinical severity of the disease except for at the most severe phases (Boluda et al., 2014) (**Figure 1.2**).

1.2.2 Neurofibrillary tau tangles

NFTs are intracellular aggregates composed primarily of the microtubule-associated protein tau (Grundke-Iqbal et al., 1986) that is abnormally phosphorylated, cleaved and aggregated, and is arranged into paired helical filament structures (PHFs) (Bancher et al., 1989). In most individuals, the spread of NFTs across diseased brain occurs in a stereotypical spatial and temporal pattern as AD progresses. This staging of this spread by Braak and Braak, known as Braak staging, is commonly used as an indicator of disease severity (Braak and Braak, 1991).

Braak stages I and II are pre-symptomatic, occurring many years before the clinical symptoms of AD are apparent (Caselli and Reiman, 2013). During stage I moderate NFT pathology is found only in the pre-α layer (layer II) of the transentorhinal cortex. Neuropil threads (NTs), abnormal neurites made from PHFs and straight filaments, are found in AD throughout disease progression and first appear in the pre-α layer of the transentorhinal in stage I. In stage II NFTs and NTs in the transentorhinal cortex are more numerous and small numbers have spread to the subiculum and CA1 of the hippocampus (Braak and Braak, 1991). Stages III and IV are known as the 'limbic stages' and generally correlate with a diagnosis of mild cognitive impairment (MCI). Clinically, individuals show some cognitive and possible memory deficits but these symptoms are not severe enough to interfere with everyday life (Golomb et al., 2004). Stage III is histologically characterised by severe NFT pathology in the pre-α layer in both the transentorhinal and entorhinal cortices and modest involvement of CA1. 'Ghost tangles', NFTs left behind in the extracellular space once a neuron has died, are also first seen at this stage. NFT pathology is also present, but mild, in the magnocellular forebrain nuclei, the anterodorsal nucleus of the thalamus and the amygdala. Stage IV is identified by many ghost tangles in the transentorhinal and entorhinal cortices and numerous NFTs in the hippocampus. NFTs also appear in some nuclei of the basal ganglia and severe NFT deposition is apparent in the anterodorsal nucleus of the thalamus. It is important to note, however, that at stages III/IV cortical areas are predominantly unaffected by tangle pathology (Braak and Braak, 1991). Clinical symptoms of AD occur mainly during stages V and VI when NFTs begin to significantly spread into cortical areas (Braak and Braak, 1995). Stage V is defined by significant NFT and NT formations in the temporal and frontal cortices and severe pathology in almost all areas of the hippocampus. Synapse degeneration and neuron loss is also present in affected brain areas; however, it is unclear whether synaptic degeneration is a cause or effect of abnormal tau function and pathology (Thies and Mandelkow, 2007). At this stage both primary sensory and motor cortices are still relatively spared. By stage VI, NFTs have spread throughout the cortex, with the exception of the motor cortex. Severe neuron loss and ghost tangles can be seen in the hippocampus and

other limbic regions with significant neuron loss also present in the cortex (Braak and Braak, 1991). The presence of NFTs correlates well with synaptic degeneration and the clinical symptoms of disease, leading many to believe that their presence is necessary for neurodegeneration in AD (**Figure 1.2**) (Braak and Braak, 1995; Perez-Nievas et al., 2013). However, there is also a school of thought which suggests that the production of NFTs may be a protective mechanism, as cells attempt to prevent the damage of potentially more toxic tau oligomers and fibrils (Rodriguez-Martin et al., 2013).

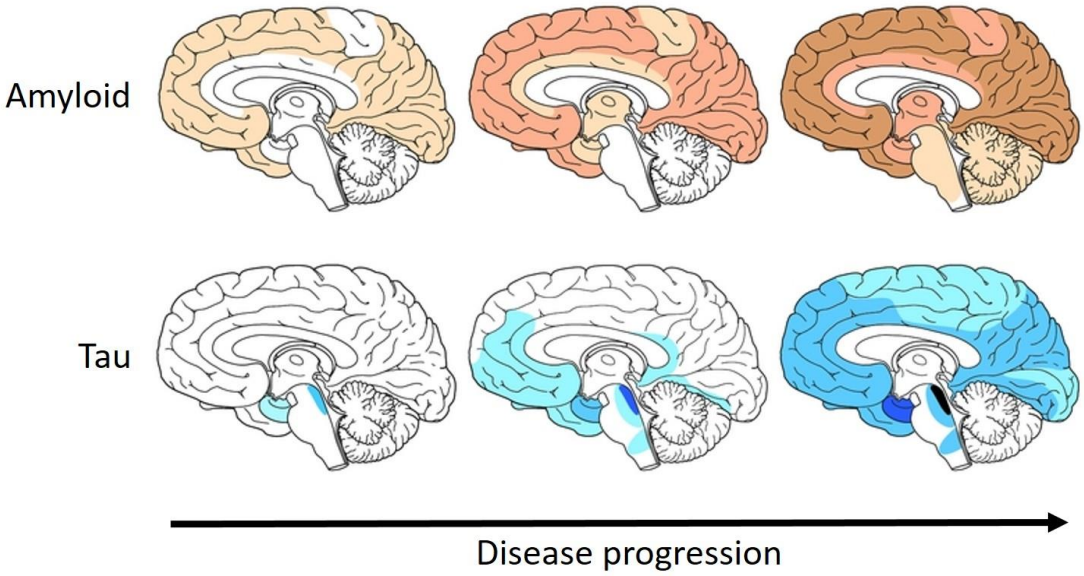

Figure 1.2: Aß and tau pathology spread across the brain in AD
Representative spread of pathology across the brain as disease progresses (from left to right of the figure). Darker colouring indicates increased pathology density. Top row of diagrams indicate the pattern of Aß spread. Bottom row of diagrams indicates tau spread. Adapted from Jucker and Walker (2011).

1.3 The genetics of AD

AD occurs most commonly in a sporadic and late-onset form, and rarely as a familial, autosomal dominant, early-onset disease (Khanahmadi et al., 2015). Autosomal dominant mutations that cause early-onset, familial AD are found in one of three genes: *APP* (St George-Hyslop et al., 1987; Goate et al., 1991; Sorbi et al., 2001), *PS1* (encoding presenilin 1; PS1) or *PS2* (encoding presenilin 2; PS2) (Levy-Lahad et al., 1995; Sherrington et al., 1995). Indications that AD has a

genetic component were first found in a study of adult development in Trisomy 21 (Down's syndrome) individuals. Approximately 70 % of individuals over 40 with Down's syndrome (DS) begin to show AD-like symptoms (Wilcock and Griffin, 2013) with post-mortem studies finding the widespread presence of amyloid plaques by the age of 30 and NFTs by the age of 50 (Hyman et al., 1995; Lemere et al., 1996). The *APP* gene is located on chromosome 21, so these patients carry three copies of *APP*, suggesting that an excess of APP protein can cause disease (St George-Hyslop et al., 1987; Wisniewski et al., 1985). Indeed, duplication of the *APP* gene has since been found to cause familial AD (Rovelet-Lecrux et al., 2006; Sleegers et al., 2006). A number of autosomal dominant mutations of *APP* have also been shown to cause familial AD. These pathogenic mutations occur close to the Aß domain of APP and act to enhance or alter Aß production (Schellenberg and Montine, 2012; Tanzi, 2012). In particular, some mutations increase total Aß production, some mutations increase the relative levels of the more pathogenic $Aß_{42}$ peptide and some mutations make Aß more prone to aggregation or more "amyloidogenic". Interestingly, one *APP* mutation has been identified that protects against AD and this inhibits the production of Aß (Jonsson et al., 2012).

Mutations in *PS1* and *PS2* are the most common cause of familial AD. The presenilins form part of the γ-secretase complex that is involved in the proteolytic cleavage of APP to produce Aß (De Strooper and Annaert, 2010). Familial AD-linked *PS1/2* mutations are loss-of-function mutations that alter the production of Aß from APP by influencing the specificity of γ-secretase cleavage. *PS1/2* cause an increase in the Aß42/Aß40 ratio, either by decreasing the production of Aß40 or increasing the production of Aß42 (Duff et al., 1996; Scheuner et al., 1996; Bentahir et al., 2006; Shen and Kelleher, 2007; De Strooper and Annaert, 2010; Kretner et al., 2011; Fernandez et al., 2014). Other PS1 mutations in FAD, such as mutations at D257A and D385A, are dominant negative, and cause decreased Aß peptide secretion and the accumulation of the C-terminal fragments of the precursor protein (Kim et al., 2001).

Genetic variations in a number of genes increase risk of developing AD (Rosenberg et al., 2016). Apolipoprotein E (ApoE) is involved in cholesterol transport and, in the CNS, is mainly expressed

in astrocytes. Located on chromosome 19, the gene has three isoforms: ε2, ε3 and ε4. The ε3 isoform is most common, however the presence of the ApoE ε4 isoform is the largest risk factor for AD development identified to date. Individuals harbouring one copy of ApoE ε4 have a three-fold higher risk of AD, whereas those with both copies have a ten-fold higher risk. In contrast, the ε2 allele is neuroprotective and carriers of this allele have lower risk of AD (Strittmatter et al., 1993; Riedel et al., 2016). Since its discovery as an AD risk gene, ApoE has been well characterised as an APP chaperone and has been shown to play a role in Aß processing (Bu, 2009). The ε4 isoform was demonstrated to increase levels of Aß production, reduce Aß clearance and encourage Aß oligomerisation, compared to the ε3 allele (Ye et al., 2005; Castellano et al., 2011; Hashimoto et al., 2012). Evidence from mouse models suggests blocking the ApoE/Aß interaction can ameliorate ε4-related Aß pathology further supporting the role of ApoE in the late-onset disease process (Pankiewicz et al., 2014).

Recent genome-wide association studies have identified over twenty other genes that are associated with AD (Harold et al., 2009; Bertram et al., 2010; Seshadri et al., 2010; Hollingworth et al., 2011; Karch et al., 2014; Naj et al., 2014). These can be broadly grouped into genes involved in lipid metabolism, protein trafficking and inflammation (Schellenberg and Montine, 2012; Karch and Goate, 2015). To date, variations in triggering receptor expressed on myeloid cells 2 (TREM2) are most strongly associated with developing AD, increasing risk by 2-4 fold (Guerreiro et al., 2013; Heneka et al., 2016; Ulrich and Holtzman, 2016). TREM2 is expressed in immune cells throughout the body, including microglial cells in the brain. In microglia, TREM2 is known to be involved in controlling reactive state, including upregulating phagocytic pathways possibly involved in clearing Aß deposits (Guerreiro et al., 2013; Heneka et al., 2016). Further support for this comes from studies demonstrating TREM2 upregulation in microglia located close to Aß deposits in animal models (Frank et al., 2008; Varvel et al., 2015; Heneka et al., 2016). It has been proposed that high risk variants of TREM2 result in a loss of function at the protein level, possibly increasing apoptosis and reducing microglial proliferation (Heneka et al., 2016; Ulrich and Holtzman, 2016; Villegas-Llerena et al., 2016). This would reduce the number of

microglia surrounding Aß plaques, possibly resulting in reduced phagocytosis of plaques or Aß oligomers in the surrounding area (Forabosco et al., 2013; Heneka et al., 2016; Ulrich and Holtzman, 2016).

The *MAPT* gene encodes tau and resides on chromosome 17. To date, no mutations in *MAPT* have been found that cause familial AD. Instead they lead to the development of some forms of frontotemporal dementia (Lee et al., 2001; Spillantini and Goedert, 2013; Simic et al., 2016). *MAPT* mutations either alter the ability of tau to bind to microtubules or alter the ratio of tau isoforms via alternative splicing changes (Spillantini and Goedert, 2013). Both types of mutations are believed to enhance tau aggregation into intracellular NFTs (Spillantini and Goedert, 2013).

1.4 Amyloid precursor protein and ß-amyloid

1.4.1 Amyloid precursor protein processing

APP is a highly-conserved large transmembrane protein found in many tissues. Within the brain, APP is particularly localised to the cerebral cortex and hippocampus, areas that are affected in AD (Bahmanyar et al., 1987; Arai et al., 1991). APP is found at particularly high concentrations in synapses, where it has been implicated in synapse formation and neuronal plasticity underlying learning and memory (Turner et al., 2003; Priller et al., 2006). APP completely spans the membrane, with a large N-terminal extracellular region, a transmembrane domain and a smaller C-terminal intracellular region (Kang et al., 1987). The Aß encoding sequence is located in the extracellular and transmembrane domains (Dyrks et al., 1988). APP undergoes alternative splicing of exons to generate a number of different isoforms. Three major isoforms of APP are produced, which contain 695, 751 or 770 amino acids. The two longer isoforms contain a Kunitz protease inhibitor (KPI) domain and APP_{770} also contains an Ox2 domain. APP_{695} is the main APP isoform expressed in brain tissue, while APP_{751} and APP_{770} are expressed ubiquitously throughout many cell types (Kitaguchi et al., 1988; Ponte et al., 1988; Tanzi et al., 1988; Oltersdorf et al., 1989; Zhang et al., 2011).

APP processing occurs through two main and well-described mutually exclusive pathways: the first, the non-amyloidogenic pathway, is the predominant pathway in healthy individuals, but early in the development of AD the balance changes resulting in increased amyloidogenic processing of APP leading to enhanced Aß production (Zhang et al., 2011).

The non-amyloidogenic pathway (**Figure 1.3**) is initiated by cleavage of APP by α-secretase in the extracellular region of APP close to the plasma membrane and the middle of the Aß peptide region. α-secretase is thought to be a metalloprotease of the a disintegrin and metalloprotease (ADAM) family. ADAM9, ADAM10 and ADAM17 are all capable of α-secretase cleavage of APP and there appears to be some functional redundancy among these proteins (Kuhn et al., 2010; Vingtdeux and Marambaud, 2012). Overexpression of ADAM10 leads to increased cleavage of APP via the non-amyloidogenic pathway (Lammich et al., 1999). The cleavage of APP by α-secretase produces a large soluble extracellular cleavage fragment known as sAPPα (Zhang et al., 2011). The smaller C-terminal fragment α (CTFα) is left in the membrane and later cleaved by γ-secretase in the transmembrane region producing a small fragment, p3, and the APP intracellular domain (AICD) that translocates to the nucleus to modulate gene expression (Muller et al., 2008; Minogue et al., 2009).

In the amyloidogenic pathway (**Figure 1.3**), cleavage of APP occurs first by ß-secretase in the extracellular domain close to the plasma membrane. ß-secretase has been identified as ß-amyloid cleaving enzyme (BACE), a type-1 membrane-spanning aspartyl protease that is active in the low pH environment of the endosomal/lysosomal system and Golgi, where it cleaves APP (Shoji et al., 1992; Sinha et al., 1999; Vassar et al., 1999; Yan et al., 1999). APP cleavage by ß-secretase releases the soluble N-terminal cleavage fragment sAPPß and is followed by the cleavage of APP by γ-secretase in the transmembrane region. This releases the AICD and Aß (Zhang et al., 2011) which are then secreted from the cell (Chow et al., 2010; Haass et al., 2012). γ-secretase is a multiprotein complex consisting of aspartic proteases PS1/2, PS enhancer 2 (PEN-2), nicastrin and anterior pharynx-defective phenotype-1 (Aph-1). PEN-2, nicastrin and Aph1 are believed to be chaperone proteins or involved in targeting the γ-secretase complex to

its substrates (Minogue et al., 2009; De Strooper et al., 2012). The low sequence specificity of γ-secretase accounts for the creation of varying lengths of Aß peptide of which $Aß_{1-40}$ and $Aß_{1-42}$ are the best studied (Zhang et al., 2011). Recently, N-terminal extended Aß peptides were also described (Welzel et al., 2014; Szczepankiewicz et al., 2015). In a physiological state, the Aß produced is predominantly $Aß_{1-40}$ with only low levels of $Aß_{1-42}$. However, in AD the Aß 40:42 ratio is altered to promote $Aß_{1-42}$ production. $Aß_{1-42}$ has a higher propensity to aggregate and an increase in its production leads to higher levels of neurotoxic Aß oligomers being produced (Hellstrand et al., 2010; O'Brien and Wong, 2011; Qiu et al., 2015).

Recently a new APP processing pathway was discovered whereby APP is cleaved by membrane-bound metalloproteinases, now named η-secretase in the plasma membrane (Willem et al., 2015). Evidence suggests this cleavage by η-secretase releases a larger C-terminal fragment (CTFη) while the remainder of APP can be cleaved again by α-secretase and ß-secretase to produce two new amyloid fragments: Aη-α and Aη-ß. These fragments were found to be enriched in dystrophic neurons, in humans and transgenic mice, and they inhibited activity in hippocampal slices (Willem et al., 2015). This provides evidence that APP cleavage products other than Aß are involved in the biological basis of learning and memory and this new APP cleavage pathway is likely to play some role in the development of AD, possibly providing new therapeutic targets for drug development. Furthermore, it may explain why drugs targeting traditional amyloidogenic pathway proteins, such as BACE1 inhibitors, have not been as successful as hoped. For example, Willem *et al.* found inhibiting BACE1 pharmacologically and genetically results in increased Aη-α and impaired long-term potentiation supporting the idea that there are other toxic APP fragments that could drive AD pathology alongside Aß (Willem et al., 2015).

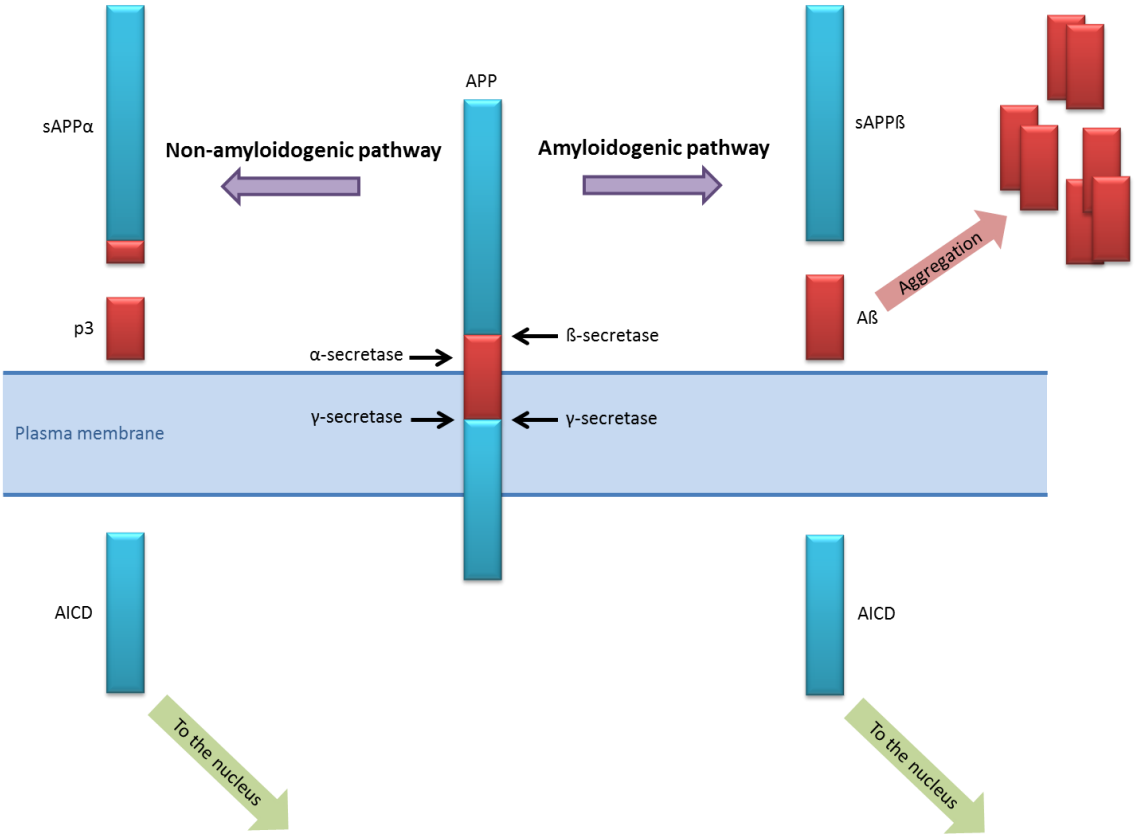

Figure 1.3: APP processing
APP can be proteolytically cleaved via two pathways. The non-amyloidogenic pathway (left) involves APP cleavage by α and γ-secretases to produce non-toxic peptide products. The second, amyloidogenic pathway (right) results in Aß production due to APP cleavage by ß and γ-secretases.

1.5 Tau

1.5.1 Protein structure

Abnormally phosphorylated, cleaved and aggregated tau are the major component of the NFTs found in AD brain (Grundke-Iqbal et al., 1986). Human tau is encoded by the microtubule-associated protein tau (*MAPT*) gene on chromosome 17q21.3 and comprises sixteen exons that can be alternatively spliced resulting in the presence of six tau isoforms in the adult human CNS. Exons two and three at the N-terminus can be alternatively spliced to result in tau protein that has 0, 1 or 2 N-terminal inserts (0, 1 or 2N). Alternative splicing of exon 10 results in tau isoforms that contain either three (no exon 10; 3R) or four (exon 10 included; 4R) microtubule binding domains (Andreadis et al., 1992) (**Figure 1.4**). Tau expression is developmentally regulated, and

during foetal development only 0N3R is expressed (Goedert and Jakes, 1990). In healthy adult humans the ratio of 3R to 4R tau is approximately equal, and in AD brain both 3R and 4R tau are deposited in NFTs (Hasegawa et al., 2014; Qian and Liu, 2014). However, other tauopathies are characterised by aggregation of predominantly 3R (e.g. Pick's disease (Buee and Delacourte, 1999)) or 4R tau (e.g. corticobasal degeneration (Kouri et al., 2011)) and there is some evidence that disruption of the equal ratio of the isoforms may be involved in tau aggregation in AD (Yasojima et al., 1999; Glatz et al., 2006).

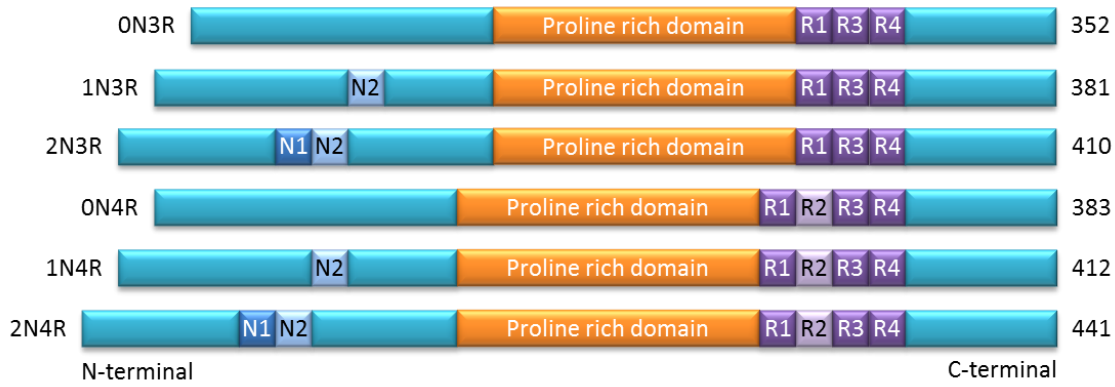

Figure 1.4: Tau protein structure showing the six isoforms of tau found in adult human CNS
The six different isoforms of tau are generated upon alternate splicing of exons 2, 3 and 10. Inclusion of exons 2 and 3 result in additional amino acid inserts near the N-terminus of tau, N1 and N2, respectively. Inclusion of exon 10 results in tau isoforms containing four (4R) rather than three (3R) microtubule binding repeats (R1-R4). R2 is encoded by exon 10. Tau contains a large proline rich domain to the middle of the tau protein. Tau isoforms range in size from 352 to 441 amino acids, the size of each isoform is shown to the right.

1.5.2 Post-translational modifications of tau

Tau can be post-translationally modified in a number of ways and at many epitopes, however phosphorylation of tau is the best studied modification. Tau has approximately 80 phosphorylatable serine (Ser), threonine (Thr) and tyrosine (Tyr) residues, over half of which are known to be abnormally or hyperphosphorylated in AD brain (**Figure 1.5**), in stark contrast to the few sites phosphorylated in healthy adult brain (Ksiezak-Reding et al., 1992; Hanger et al., 2007; Hanger et al., 2009).

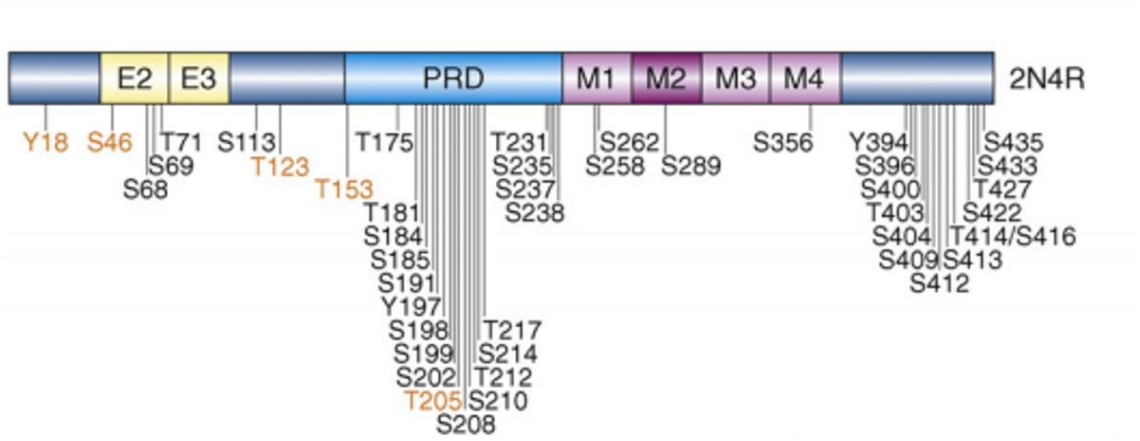

Figure 1.5: Abnormal tau phosphorylation in AD
Forty-five of over sixty phosphorylation sites on the tau protein found to be abnormally phosphorylated in AD brain. Sites cluster in the proline-rich domain (PRD) and C-terminal region. Five phosphorylation sites in orange were only identified by phospho-specific labelling at the time of the original making of this figure, rather than direct means (mass spectrometry or Edman degradation). E2/3: exons 2/3, M1-4: microtubule-binding regions, Y: tyrosine, S: serine, T: threonine. Adapted from Hanger et al. (2009).

Tau phosphorylation is a dynamic process and is regulated by the activity of protein kinases and phosphatases. Phosphate is added to tau by the action of kinases and removed by protein phosphatases. Multiple kinases have been shown to phosphorylate tau *in vitro* and *in vivo*, including the proline-directed kinases GSK-3, cyclin-dependent protein kinase 5 (cdk5), extracellular signal-regulated kinase 1/2 (ERK1/2), mitogen activated protein kinase (MAPK), p38, c-Jun N-terminal kinases (JNK) and 5' adenosine monophosphate-activated protein kinase (AMPK) (Hanger et al., 1992; Baumann et al., 1993; Hanger et al., 2009; Thornton et al., 2011; Martin et al., 2013), the non-proline directed protein kinases calcium and calmodulin dependent kinase II (CaMKII), protein kinase A, casein kinase-1 (ck1), microtubule affinity-regulating kinases (MARKs), and dual specificity tyrosine-phosphorylation-regulated kinase 1A (DYRK1A) (Hanger et al., 2009; Martin et al., 2013), and tyrosine kinases including Fyn, Abl and Syk (Lee et al., 2004; Derkinderen et al., 2005; Lebouvier et al., 2008). In addition, several phosphatases dephosphorylate tau, including protein phosphatase-1, -2A, and -5 (PP1, PP2A, and PP5) (Liu et al., 2005).

Other post-translational modifications of tau have also been implicated in AD. Tau in post-mortem AD brains, mouse models of AD and in *in vitro* studies has been found to be abnormally

acetylated, nitrated, glycated and glycosylated (Takahashi et al., 1999; Cohen et al., 2011; Beharry et al., 2014; Song et al., 2015; Liu et al., 2016). Mimicking acetylation in mice slows tau turnover, increases its accumulation and results in cognitive deficits. Additionally, inhibiting acetylation after phenotype onset in transgenic mice expressing frontotemporal dementia (FTD)-causing P301S tau not only reduced the levels of total tau but also rescued memory deficits and hippocampal atrophy (Min et al., 2015).Nitration has been found to reduce the ability of tau to self-associate and nitrated tau has been found in fibrillar lesions in AD and other tauopathies (Reynolds et al., 2006). Glycosylation of tau may be neuroprotective with a reduction in glycosylated tau occurring early in the disease process, possibly mediating early pathological phosphorylation (Liu et al., 2002). Additionally, there is evidence that tau glycosylation may be responsible for the formation and maintenance of the helical structure of PHFs (Wang et al., 1996; Takahashi et al., 1999). *O*-GlcNAcylation, a distinct form of glycosylation where tau is modified by ß-linked N-acetylglucosamine (Arnold et al., 1996), has also been linked to intracellular glucose metabolism. Hypotheses suggest that impaired glucose metabolism years before disease onset may lead to decreased *O*-GlcNAcylation and, later, increased tau phosphorylation and AD (Gong et al., 2006; Iqbal et al., 2016).

1.5.3 Tau cleavage

Tau can also be cleaved at multiple sites (Hanger and Wray, 2010; Zhao et al., 2016). In particular, cleavage at aspartate 421 (Asp421) by caspase-3 has been implicated in the progression of AD. Caspase-3-cleaved tau has a higher propensity to aggregate than full-length tau, and may form a seeding nidus that promotes the aggregation and fibrillisation of full-length tau species supporting a role for tau cleavage in NFT formation (Gamblin et al., 2003). The abundance of tau cleaved at Asp421, along with tau cleaved at Glu391, is associated with ApoE genotype and positively correlates with a clinical dementia index (Basurto-Islas et al., 2008).

Several other proteases have been implicated in abnormal tau cleavage in AD (Gamblin et al., 2003; Zhang et al., 2014a). For example, calpain-1 and -2 cleave tau at the N-terminus to produce a 17 kDa fragment found to cause neurotoxicity in hippocampal cultures (Park and Ferreira,

2005). Investigations in human tissues have found evidence of multiple cleaved tau fragments including 37 kDa, 35 kDa and 26-28 kDa species (Johnson et al., 1997; Wang et al., 2007; Wray et al., 2008). While the functional relevance of all cleaved tau species is not fully understood, recent evidence has shown that sub-endogenous expression in mice of a 35 kDa tau fragment identified in PSP brain causes a behavioural and molecular phenotype similar to that of human tauopathies (Bondulich et al., 2016).

1.5.4 Tau aggregation

The relationship between tau phosphorylation, cleavage and aggregation is poorly understood, however, the amyloid cascade hypothesis posits that post-translational modifications of tau directly encourage tau aggregation as disease progresses (Selkoe and Hardy, 2016). Indeed, induction of tau phosphorylation in transgenic models of tauopathy induces tau aggregation (Cruz et al., 2003; Noble et al., 2003; Engel et al., 2007), suggesting that phosphorylation precedes aggregation *in vivo*. Aggregation cannot occur while tau is bound to microtubules, therefore phosphorylation of specific tau epitopes is believed to occur prior to aggregation since phosphorylation of tau removes it from microtubules leading to increased concentration of free tau in the cytoplasm where it is open to other post-translational modifications including acetylation and cleavage (Meraz-Rios et al., 2010). These post-translational modifications, and further phosphorylation, not only prevent tau from re-binding to microtubules as it might under normal conditions but also increase its local concentration supporting aggregation (Marcus and Schachter, 2011; Martin et al., 2011; Wang and Mandelkow, 2016). Changes in the conformation of tau, also known to occur early in AD progression (Mondragon-Rodriguez et al., 2008a) increasing the percentage of ß-pleated sheets in the secondary structure of tau (Hanger and Wray, 2010), encouraging side chain/side chain interactions that promote the formation of tau dimers (Meraz-Rios et al., 2010). Stable tau dimers are thought to undergo a process of nucleation leading to fibrillisation dose- and time-dependent manner (Yin and Kuret, 2006; Congdon et al., 2008).

It is important to note here that significant evidence now suggests that tau oligomers are the most toxic species of tau. Tau oligomers are closely correlated with cognitive decline *in vivo* (Berger et al., 2007), have been shown to cause synaptic dysfunction and neuron death, and most recently to play a critical role in tau propagation across diseased brain (Lasagna-Reeves et al., 2011; Benilova et al., 2012). In keeping with this, tau aggregates have been proposed to be an inert end-stage pathology resulting from endogenous neuroprotective mechanisms in an attempt to minimise oligomer toxicity (Cowan and Mudher, 2013).

1.5.5 Tau functions in health and disease

Tau was first discovered as a protein required for tubulin to form microtubules *in vitro* (Weingarten et al., 1975). A readily post-translationally modified protein, in healthy neurons tau stabilises and polymerises microtubules. Found predominantly in the axon, normal tau function is important for maintaining efficient and successful axon transport (Spittaels et al., 1999). The microtubule binding strength of tau is determined largely by phosphorylation of multiple sites in the microtubule binding domains: increased phosphorylation results in decreased microtubule binding (Selden and Pollard, 1983). Phosphorylation of all sites in the microtubule binding domains of tau, but particularly threonine (Thr) 231, serine (Ser) 262 and Ser356 (**Figure 1.5**), are thought to inhibit the ability of tau to promote microtubule polymerisation while phosphorylation at epitopes in the proline-rich region of tau inhibit *de novo* microtubule construction (Hanger et al., 2007). Easy assembly and disassembly of microtubules is important in embryonic development when neurons are growing rapidly and the cytoskeletal structure, including their microtubule architecture, is very dynamic (Watanabe et al., 1993). However, hyperphosphorylation of tau in adult neurons can result in breakdown of microtubules and disruption of axonal transport. In AD, tau is abnormally phosphorylated and microtubule binding is reduced, leading to the breakdown of microtubule structure and axonal transport (Ksiezak-Reding et al., 1992). With microtubule integrity impaired, mitochondria, proteins and nutrients cannot be transported to the synapse for effective synaptic function. Organelles and protein build up where microtubules have broken down, further blocking transport along the axon

(Stamer et al., 2002). As less and less reaches the synaptic terminal, synapses become dysfunctional and are eventually lost (Stamer et al., 2002). The polymerisation and stabilisation of microtubules in the axon is the best known physiological function of tau (Weingarten et al., 1975), however more recent evidence shows that tau has a diverse range of functions in neurons (Wang and Mandelkow, 2016).

In the axon, tau actively promotes and regulates microtubule assembly including dynamic reorganisation of microtubules to allow for cytoskeletal flexibility (Feinstein and Wilson, 2005). Tau microtubule binding domains bind to heterodimers of tubulin to polymerise microtubules (Scott et al., 1991). Knocking down tau in cultured rat neurons results in inhibition of neurite growth and axon formation suggesting that tau, and microtubules, are involved in the development and elongation of axons (Caceres and Kosik, 1990). Tau also plays a critical role in microtubule-dependent axonal transport (Dixit et al., 2008), regulating kinesin- and dynein-dependent transport of many protein cargoes (Trinczek et al., 1999; Stamer et al., 2002; Dixit et al., 2008) via activation of GSK-3 and PP1 (Kanaan et al., 2011). Phosphorylation of N-terminal tau residues reduces GSK-3/PP1 activation and the subsequent kinesin-cargo binding inhibition (Kanaan et al., 2012), and reduction of tau levels can rescue Aß-induced axon transport deficits by blocking GSK-3 activation (Vossel et al., 2015).

The N-terminal projection domain of tau binds to plasma membranes where it may be involved in signal transduction (Pooler et al., 2012). For example, in the post-synaptic terminal plasma membrane-bound tau binds to Fyn and directs it to dendrites where Fyn, phosphorylates NMDA receptor subunit 2B (NR2B) to mediate Aß toxicity at the synapse (Ittner et al., 2010). At the pre-synaptic terminal tau can be released into the extracellular space, and extracellular tau can activate muscarinic receptors mediating intracellular calcium in post-synaptic neurons (Gomez-Ramos et al., 2009). This evidence suggests that tau may play a physiological role in intercellular signalling.

Finally, tau has also been found in the nucleus of cells and has been suggested to play multiple roles there. Particularly, it has been suggested that tau may be involved in protecting DNA and

RNA from cellular distress. Under heat stress and oxidative stress largely dephosphorylated tau binds to DNA and RNA in the nucleus protecting the nucleic acids from damage (Violet et al., 2014). Additionally, FTD-causing P301L tau mutation are linked with chromosome instability (Rossi et al., 2008), and tau has also been implicated in RNA and DNA transcription (Thurston et al., 1996; Sjoberg et al., 2006).

1.5.6 Tau spread and seeding

Recent studies have shown that tau propagates through diseased brain in a 'prion-like' manner (de Calignon et al., 2012; Jucker and Walker, 2013). It is thought that monomeric and small order oligomers are released from neurons into the extracellular space via a currently unknown mechanism (Chai et al., 2012; de Calignon et al., 2012; Hanger et al., 2014) that might involve unconventional secretory pathways (Chai et al., 2012; Fontaine et al., 2016), tau association with exosomes (Saman et al., 2012; Polanco et al., 2016) or ectosomes (Dujardin et al., 2014), or alternatively "free" tau (Pooler et al., 2013). However, most tau is thought to be released at or near the synapse, resulting in the spread of pathology between synaptically connected neurons rather than those that are anatomically adjacent (Liu et al., 2012). Evidence suggests that most extracellular tau is dephosphorylated, indicating that tau is either dephosphorylated before its release or soon after it is extruded (Diaz-Hernandez et al., 2010; Pooler et al., 2013). Whether tau is intact, C-terminally or N-terminally cleaved remains a matter of debate (Pooler et al., 2013).

The mechanisms underlying the spread of pathological tau forms is also under investigation. Injections of brain homogenate, either from post mortem AD brain or transgenic mouse models of tauopathy, into the brain of transgenic mice expressing wild-type human tau demonstrates that tau from the seeded brain material is taken up by neurons. The mechanisms for tau uptake remain unclear but, once in the cell, the seeded tau is able to recruit endogenous tau (Ahmed et al., 2014; Iba et al., 2015). Furthermore, the conformation of the seeded tau is thought to be critical since injecting tau from an argyrophilic grain disease brain into wild-type human tau expressing mice results in grain-like tau aggregates, tau from PSP brain leads to tufted astrocyte-

like tau pathology and CBD tau injection leads to the development of astrocytic plaques in the injected mice (Clavaguera et al., 2013).

Furthermore, pathological tau spreads further and more rapidly and causes greater neurotoxicity in the presence of Aß (Pooler et al., 2015). Similar effects are seen *in vitro* where Aß influences the species and amount of tau released from neurons (Kanmert et al., 2015). These results suggest that there is an important relationship between extracellular tau and Aß, however the specifics of this relationship are yet to be fully defined.

Tau release and its subsequent functions is still a field in its infancy. There is still a lot to be discovered about the mechanisms of tau release and uptake, and how these mechanisms are involved in both physiological and pathological tau processing, spread and synaptic function.

1.6 The amyloid cascade hypothesis

The amyloid cascade hypothesis was first proposed by Hardy and Allsop in 1991 and since this time has been influential in directing research in the field. In its simplest form, the amyloid cascade hypothesis proposes that, whether due to a genetic mutation in *APP* or *PSEN1/2* or through another cause, toxic forms of Aß are produced that initiate a signalling cascade leading to abnormal phosphorylation and cleavage of tau, impairing tau function and initiating its aggregation into paired helical filaments (PHFs) and NFTs that cause neurodegeneration (Hardy and Selkoe, 2002; Selkoe and Hardy, 2016).

Amyloid plaques were originally thought to be the directly toxic Aß species. However, it is now believed that, although aggregate stress contributes to neuron disease and death, pre-fibrillar soluble Aß oligomers are more toxic, leading to neuron excitotoxicity and detrimental calcium dysregulation, particularly at synapses (Ittner et al., 2010; Cavallucci et al., 2012; Zhang et al., 2016a). Damage caused by Aß at the synapse is thought to lead to abnormal processing of tau, including its hyperphosphorylation and abnormal cleavage by calpains and caspases (Decker et al., 2010; Kurbatskaya et al., 2016). These modifications alter tau function, resulting in instability

of microtubules and failure of fundamental cell processes such as axonal transport. As axons die back, synaptic connectivity is lost and neurons degenerate, further disrupting synapses and perpetuating neuronal dysfunction (Hanger et al., 2014; Iqbal et al., 2016). This pathological cascade, which occurs alongside continued overproduction of $Aß_{1-42}$, is suggested by the amyloid cascade hypothesis, to eventually result in dementia and the accompanying clinical symptoms typical of individuals with AD (Selkoe and Hardy, 2016).

While the amyloid cascade hypothesis' simplicity is appealing, the theory has been criticised for being too linear. A large amount of research suggests that there are multiple pathways involved at many stages of the cascade. For example, Aß is known to activate multiple membrane receptors either directly or indirectly, resulting in a complex cascade of intracellular signalling pathways being activated, many of which can positively and negatively regulate each other (Benilova et al., 2012; De Strooper and Karran, 2016). Additionally, evidence suggests that tau is not only affected by synaptic changes but also has important functions at synapses that may become detrimental in pathological conditions (Pooler et al., 2013; Pooler et al., 2014). Revisions to the original cascade have been made to take into account recent advances in the field. For example, it has become clear that the neuron-glial interactions and neuroinflammation are closely associated with the development of AD (Cai et al., 2013; Phillips et al., 2014; Wes et al., 2016), and now the inflammatory response is indicated as part of the amyloid cascade (**Figure 1.6**), which, together with oxidative stress, link Aβ to pathological tau processing (McGeer and McGeer, 2013; Selkoe and Hardy, 2016).

Finally, there is some research that the hypothesis struggles to explain. For example, the level of Aß plaques do not correlate well with the progression of disease symptoms and a small percentage of individuals show Aß pathology with no clinical symptoms of disease (Elobeid et al., 2014). In fact, tau mislocalised to the synapse and glial activation have been suggested as the most reliable predictors of dementia in AD suggesting that Aß oligomers and plaques may not be as directly critical to disease pathology as the amyloid cascade hypothesis suggests,

however it is possible that they are required upstream of these changes in tau and glia (Perez-Nievas et al., 2013).

Therefore, the causative link between Aβ generation, or even general altered APP processing and tau hyperphosphorylation, remains largely unknown. Indeed, most APP animal models of AD do not develop tau pathology, requiring mutations of both *APP* (or APP processing-linked) and *MAPT* genes to fully model disease (Elder et al., 2010; Richardson and Burns, 2002). Despite this, the genetic cause of AD cannot be ignored, and the amyloid cascade hypothesis is still a valuable starting point for research in this field (Selkoe and Hardy, 2016).

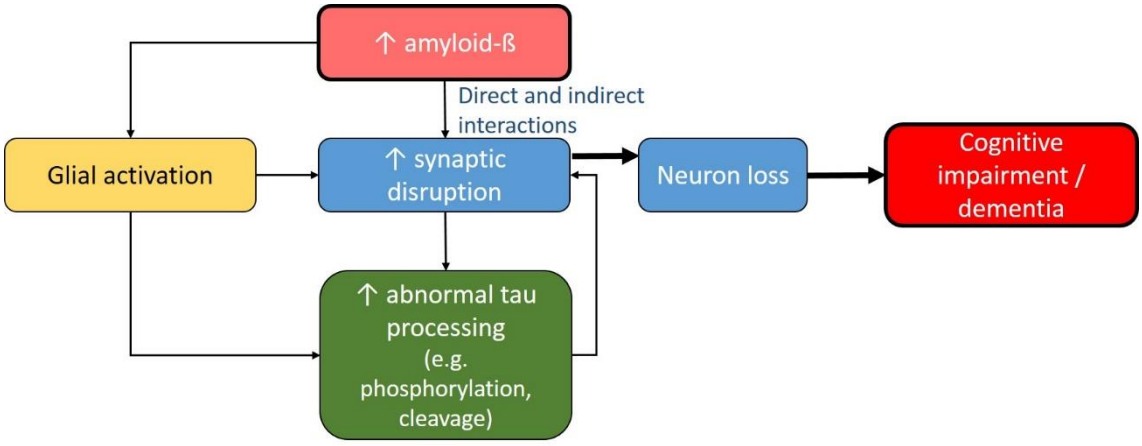

Figure 1.6: Updated amyloid hypothesis cascade
Diagram showing the updated amyloid cascade hypothesis from increased Aß (amyloid-ß) production to cognitive impairment and dementia, including glial activation.

There is a large amount of experimental evidence supporting the role of Aß in the initiation and development of AD (Butterfield, 2002; Decker et al., 2010; Benito et al., 2012; Ferreira et al., 2012; McGeer and McGeer, 2013; Sengupta et al., 2016). Studies in both cell culture and mouse models of AD show that Aß causes AD-like changes in tau (Selenica et al., 2013; Pooler et al., 2015). For example, treatment of hippocampal neurons with Aß dimers isolated from AD brain induced tau hyperphosphorylation and neuritic degeneration. This degeneration was tau-dependent however, as it was prevented by knocking down tau and was exacerbated by over-expressing human tau (Jin et al., 2011). Furthermore, injections of $Aß_{1-42}$ fibrils into the brains of a mouse model of tauopathy resulted in a localised five-fold increase in the number of NFTs with

tau phosphorylation and fibril formation occurring as early as 18 days after Aß fibril injections (Gotz et al., 2001). Crossing mouse models of tauopathy with those that over-produce Aß also accelerates tau-dependent neurodegeneration (Gotz et al., 2001; Lewis et al., 2001; Pooler et al., 2013). However, this is not a unidirectional effect since double APP/tau transgenic mouse models also show exacerbation of Aß production (Ribe et al., 2005).

Evidence demonstrates Aß can cause toxicity independent of tau pathology. For example, Aß oligomers impair NMDA receptor function, disrupt calcium homeostasis and impair axonal transport (Decker et al., 2010; Ferreira et al., 2012; Talantova et al., 2013). One study found that synapse function is directly affected by Aß oligomers associating with post-synaptic densities as well as promoting dysfunction via tau pathology (Ferreira et al., 2012). Furthermore, a 'halo' of Aß oligomers have been found to collect around senile plaques. The density of this Aß 'halo' was shown to correlate with local excitatory synapse loss (Koffie et al., 2009). In addition, inflammation is exacerbated by Aß regardless of the presence of tau, supporting an important role for inflammation in AD (Benito et al., 2012; Cai et al., 2013).

However, Aß-induced neurotoxicity is reported to be reduced in tau-deficient neurons (Rapoport et al., 2002), and *in vivo* tau knockout significantly reduces Aß-induced synaptic deficits, network dysfunction and cognitive decline (Roberson et al., 2007; Ittner et al., 2010; Roberson et al., 2011), indicating that there is likely to be a critical co-pathogenic relationship between tau and Aß in AD.

1.6.1 Modelling the amyloid cascade in vitro

To provide a tractable cell model with which to study the effects of Aß on downstream pathways, various species of Aß have been widely used to treat rodent neural cell cultures. Many of these studies have used synthetic $Aß_{1-42}$ since this allows use of precisely known concentrations and forms of human Aß in the absence of any other biological contaminants (Finder et al., 2010). However, variation in synthetic Aß produced by different suppliers, and batch-to-batch differences, has been found to affect the properties of Aß including its solubility and propensity to form fibrils and ß-sheets (Soto et al., 1995). Moreover, peptide solubility and neurotoxicity

are thought to be affected by even very low levels of impurities in the sample, something that is difficult for the end user to control (Zagorski et al., 1999). Furthermore, the high concentrations of Aß required to generate an effect from synthetic Aß is considered to be unphysiological. As a result of these and other issues, the results of experiments using Aß can be very variable and are sometimes not reproducible, making the use of Aß in *in vitro* experiments controversial. This is partly due to there being no standard protocol for the preparation of the Aß, with some groups solubilising the peptide immediately before use and others encouraging it to aggregate into small amyloid diffusible ligands, oligomers or fibrils, protocols that can give extremely variable results in our hands, and using different solvents and different peptide lengths (Zagorski et al., 1999).

There have been several attempts to develop a more physiologically-relevant source of Aß for these types of experiment. Two of the most common systems used for this purpose and that have been used in this thesis are:

1. Aß released from immortalised cell lines that over-express a FAD-causing mutant human form of *APP*. For example, 7PA2 cells express the Val717Phe APP mutation. These cells release small Aß oligomers at sub-nanomolar levels, similar to those seen in the brain and CSF of patients with AD (Walsh et al., 2002; Walsh et al., 2005). While these Aß oligomers do not cause cell death, they have been found to impair long term potentiation (LTP) and synaptic activity both *in vitro* and *in vivo* suggesting they may be modelling early pathology-induced changes in AD (Walsh et al., 2002; Klyubin et al., 2005).

   However, in addition to the release of Aß, 7PA2 cells have also been found to release larger N-terminal fragments of APP that extended across the BACE1 cleavage site (Portelius et al., 2013). These fragments are distinct from the Aß oligomers released by 7PA2 cells and have also been found to impair synaptic plasticity (Welzel et al., 2014), possibly resulting in difficulties in using these oligomers as a synthetic Aß alternative.

2. Aß released from primary neurons cultured from transgenic mice over-expressing APP mutations, such as the Tg2576 mice which expresses mutant human APP with the Swedish double APP mutations (Lys670Asn, Met671Leu) (Wu et al., 2012). When wildtype neurons are treated with Aß-containing conditioned medium from cultured Tg2576 neurons, changes in dendritic spine numbers and morphology linked to calcium signalling (Wu et al., 2012) and activation of tau kinases such as GSK-3, resulting in Aß-induced neuritic damage (DaRocha-Souto et al., 2012) have been reported. These Aß-induced changes with Tg2576 conditioned medium treatment suggest the Aß species released from these neurons may also be modelling early AD stages since induction of degenerative pathways are observed in the absence of widespread neuron death.

1.7 Neuroinflammation

Since the amyloid cascade hypothesis was first proposed in 1991 (Hardy and Allsop, 1991), numerous studies have shown that neuroinflammation is a dominant feature of AD development (Crehan et al., 2012; Phillips et al., 2014; Heneka et al., 2015; Heppner et al., 2015; Zhang and Jiang, 2015). Rather than being a side-effect of abnormal Aß and tau processing, neuroinflammation is now thought to play an active and significant role in mediating disease progression. This idea has been bolstered by initial evidence from recent GWAS studies which demonstrated that variants of several immune genes, including *TREM2*, *CR1* and *CD33* result in increased susceptibility of developing AD (Di Bona et al., 2008; Guerreiro et al., 2013; Villegas-Llerena et al., 2016).

Astrocytes and microglial cells are the main types of cells involved in neuroinflammation. Activated microglia are closely associated with Aß plaques (Olabarria et al., 2010; Bouvier et al., 2016), whereas reactive astrocytes are particularly associated with NFTs (Bouvier et al., 2016). Importantly, elevated levels of activated microglia and astrocytes are one of the key features associated with dementia in AD (Perez-Nievas et al., 2013).

However, the role of immune cells in AD development is unclear since microglia and astrocytes have both neuroprotective and neurotoxic roles, depending on their phenotype or activation state (Heneka et al., 2016), and this is supported from reports using different models of disease (Thornton et al., 2006; Bhaskar et al., 2010; Garwood et al., 2011; Kraft et al., 2013; Avila-Munoz and Arias, 2014; Zheng et al., 2016). Deciphering the role of individual immune mechanisms is likely to be complex and involve overlapping signalling pathways. However, inflammation and glial activation is an area with promising therapeutic options (Garwood et al., 2010; Skaper, 2011; Birch et al., 2014; Zhang et al., 2014b).

1.7.1 Glia

Glia were originally thought to provide only structural support in the CNS, 'binding' neurons in the brain, however we now know glia have an active and regulatory role in the CNS.

There are two main types of glia in the brain: microglia and macroglia (Garcia-Segura and McCarthy, 2004). The term macroglia encompasses four cell types:

- ependymal cells that line the walls of the brain ventricles,
- Schwann cells that form the myelin sheath of peripheral neurons,
- oligodendrocytes that form the myelin sheath of axons in the CNS,
- astrocytes.

Astrocytes and microglia will be discussed further below since they are the best studied in the context of AD and the focus of this thesis.

Astrocytes

The word 'astrocyte' was first coined in 1893 by von Lenhossek when referring to star-shaped glial cells (Garcia-Marin et al., 2007a). Differentiated from neural stem cells, astrocytes have a similar developmental path to neurons and are native to the CNS (Zuchero and Barres, 2015). Astrocytes can be broadly split into two different classes according to their location and morphology: protoplasmic astrocytes reside largely within grey matter, and fibrous astrocytes are found mainly within white matter (Molofsky et al., 2012). Morphologically, these two classes

of astrocytes differ according to their function. Protoplasmic astrocytes form connections with neurons at the synapse, displaying dense, ramified processes for multiple local connections. Fibrous astrocytes, on the other hand, require long fibre-like processes to extend through white matter forming connections with neurons at nodes of Ranvier, the unmyelinated areas of axons required for successful action potential propagation (Barres, 2008). However, this two class split over-simplifies the differences seen in astrocyte type throughout the brain. It has been suggested that there may be as many types of astrocytes as there are neurons in the brain, with different types found in different brain regions (Grolla et al., 2013; Rodriguez et al., 2014; Hu et al., 2016). This idea is supported by evidence of region-specific glial cells such as Mueller cells in the retina and Bergmann glial cells in the cerebellum (Mochizuki et al., 2014; De Zeeuw and Hoogland, 2015). Furthermore, research has shown that culturing neurons with astrocytes from a different brain region can impair neuron outgrowth suggesting neurons are healthiest when cultured with their corresponding regional astrocytes (Barbin et al., 1988). From this research it could be suggested that astrocytes from different regions have different functions, supporting different neuron types according to their own specific needs. This is, perhaps, unsurprising as patterns of neurodegenerative disease clearly demonstrate that different neuron types can withstand different insults with varying levels of tolerance (Eisen and Turner, 2013). However, functional differences in astrocyte type also suggest that different types of astrocytes may have differential responses in disease, and therefore the role of astrocytes in diseases such as AD may change as the neurodegenerative process spreads to brain areas (Rodriguez et al., 2014).

Astrocytes were originally thought to be passive, resting cells, providing only structural support to neurons (Verkhratsky et al., 2012). However, research now shows that astrocytes play an active and critical role in the CNS, forming a network of communicating cells that monitor and support neurons in multiple ways including the provision of structural, trophic and metabolic support, maintaining the blood brain barrier, regulating CNS energy metabolism and mediating neurotransmitter levels at synapses (Volterra and Meldolesi, 2005; Abbott et al., 2006; Bernardinelli et al., 2014).

Glial fibrillary acidic protein (GFAP) is the major intermediate filament (IF) protein in astrocytes, and at least 10 different isoforms have been discovered to date (Middeldorp and Hol, 2011; Hol and Pekny, 2015). In addition to GFAP, the astrocyte IF network also includes vimentin, nestin and synemin (Eng et al., 2000; Jing et al., 2007; de Pablo et al., 2013; Hol and Pekny, 2015). Together these IFs form a highly dynamic network, the most motile of cytoskeletal polymers (Wiche and Winter, 2011). Vimentin is the favoured polymerisation partner of GFAP, but GFAP can also form polymers in the absence of vimentin (Eliasson et al., 1999). Vimentin and nestin are also highly expressed in immature astrocytes, whereas GFAP is the main IF in mature astrocytes (Middeldorp and Hol, 2011). GFAP is also thought to have a role in anchoring GLAST, a glutamate transporter expressed by astrocytes, as well as having a role in cell motility and maintaining the mechanical strength of astrocytes (Hughes et al., 2004; Sullivan et al., 2007). Under pathological conditions the upregulation of IFs, in particular GFAP, is one of the earliest changes observed in astrocytes. Concomitantly, a change in astrocyte morphology is observed (Pekny and Pekna, 2004; Pekny and Nilsson, 2005; Sofroniew and Vinters, 2010; Middeldorp and Hol, 2011; Pekny et al., 2014). The extent of astrocyte activation depends on the severity of the triggering insult, however, severe activation can result in astrocyte proliferation and increased density of cells with overlapping processes. Extreme insult can lead to the production of an astrocytic or glial scar (Sofroniew and Vinters, 2010). Scar formation protects healthy tissue from areas of severe inflammation and toxicity by building a compact wall of astrocytes, glial cells and other cell types around the border of the damaged tissue. The benefits of glial scarring have been debated. Glial scarring has been demonstrated to protect from oxidative stress and promote the degradation of Aß. However, glial scar formation also inhibits axon regeneration and isolates damaged tissue (Sofroniew, 2009).

At the synapse, astrocytes mediate multiple signalling pathways to ensure successful communication between neural cells. Both neurons and astrocytes express glucose transporters (GLUT3 and GLUT1, respectively) (Maher et al., 1991; Maher, 1995), however, astrocyte end-feet are well positioned to take up glucose from blood vessels (Morgello et al., 1995; McKenna,

2012). Glucose is the main energy substrate of the CNS under physiological conditions (Mergenthaler et al., 2013), and is utilised either in the tricarboxylic acid (TCA) cycle to provide neurons with energy or is converted into lactate or glycogen (Pellerin et al., 2007). Astrocytes store glucose as glycogen, and evidence suggests that astrocytes convert this glycogen into lactate in order to supply neurons with energy when synaptic activity is high (Pellerin et al., 1998; Pellerin and Magistretti, 2012). The breakdown of glycogen and lactate release via this "lactate shuttle" are crucial for the maintenance of long-term potentiation and long-term memory formation (Suzuki et al., 2011).

In the rodent brain glutamate transporters GLAST and GLT1 (EAAT1 and EAAT2 in the human brain) control the uptake of glutamate by astrocytes via coupling transport of Na^+ and K^+ with the inward movement of glutamate (Allaman et al., 2011; Pellerin and Magistretti, 2012). Expression of both GLAST and GLT1 on astrocytes is concentrated on areas adjacent to neuronal dendritic spines, suggesting that these transporters play an important role in the clearance of synaptic glutamate (Kondo et al., 1995; Lehre et al., 1995; Matute et al., 2005; Sheldon and Robinson, 2007). GLAST expression is most prominent in Bergmann glia, and at lower levels in other astrocyte populations throughout the CNS, whereas GLT1 expression is more apparent in the mature CNS and abundant in the forebrain (Tanaka, 2000; Beart and O'Shea, 2007).

Unlike neurons, astrocytes are not electrically excitable cells, but they do play an active role in information processing through the propagation of intracellular Ca^{2+} waves (Agulhon et al., 2012; Perea & Araque, 2005; Wang & Bordey, 2008). It has since become apparent that communication between astrocytes is mediated independently of external stimuli through transient increases in intracellular Ca^{2+} that can spread into neighbouring astrocytes to form synchronised Ca^{2+} waves (Fiacco & McCarthy, 2006; Kuga et al, 2011; Scemes & Giaume, 2006). This Ca^{2+} signalling mechanism also allows bidirectional information processing between neurons and astrocytes. Intercellular Ca^{2+} waves can cause Ca^{2+} transients that trigger neuronal activation, whereas neuronal signalling in turn may activate Ca^{2+} waves within networks of astrocytes (Araque & Navarrete, 2010; Perea & Araque, 2005; Perea et al., 2009). Astrocytic

uptake and release of Ca^{2+} (Agulhon et al., 2012; Allen & Barres, 2009; Parpura & Verkhratsky, 2012; Perea & Araque, 2005), allowing the cells to regulate post-synaptic excitatory activity, has been implicated in synaptic transmission and plasticity (Navarrete et al., 2013). Dysregulated astrocytic glutamate and calcium signalling is thought to be involved in synaptic dysfunction and loss in AD, suggesting astrocytes may play multiple roles in neurodegeneration (Agulhon et al., 2012; Ferreira et al., 2012; Talantova et al., 2013).

Research has shown gliotransmitters allow astrocytes to communicate with each other and other cell types (Liu et al., 2011b; Petrelli and Bezzi, 2016). Extracellular adenosine triphosphate (ATP) is important for neuron-astrocyte communication, as it can act as a signalling molecule in an activity dependent manner (Verderio and Matteoli, 2001; Orellana et al., 2011; Cisneros-Mejorado et al., 2015). Additionally, it plays a crucial role in intercellular astrocyte interaction, due to the role of ATP signalling in the propagation of the Ca^{2+} wave (Guthrie et al., 1999). ATP binding to either metabotropic or ionotropic purinergic receptors results in Ca^{2+} being released from intracellular stores or Ca^{2+} membrane influx respectively. Both mechanisms are crucial for cellular communication and responses to disease (James and Butt, 2001; Verkhratsky et al., 2009; Alloisio et al., 2010).

Although astrocytes do express ionotropic receptors, a large proportion of these receptors are metabotropic (Perea et al., 2009). The binding of neurotransmitters to metabotropic, G-protein coupled receptors activate the phospholipase C/inositol 1, 4, 5-triphosphate (IP_3) pathway resulting in the release of Ca^{2+} from intracellular IP_3-sensitive Ca^{2+} stores, such as the endoplasmic reticulum (ER) (Fiacco and McCarthy, 2006; Scemes and Giaume, 2006; Illes et al., 2012). Ca^{2+} release from the ER is considered to be crucial for gliotransmission and is highly regulated (Zorec et al., 2012).

Astrocytic inflammatory activity is also becoming widely accepted as important for neurodegeneration in AD (Phillips et al., 2014). Astrocytes exacerbate neuroinflammation by releasing small signalling molecules such as cytokines and chemokines (Choi et al., 2014; Rothhammer and Quintana, 2015). In AD, these molecules and activated astrocytes are

associated with increased tau pathology and neurodegeneration (Mrak and Griffin, 2005; Zilka et al., 2012; Zheng et al., 2016). As a result, the role of astrocytes in AD is complicated by a mixed activated response, both protecting from and exacerbating Aß insult.

Astrocyte activation is a response to multiple causes. Some, such as oxidative stress are environmental, while on other occasions astrocytes are responding to the release of cytokines from other nearby cells (Sofroniew and Vinters, 2010). Experiments have demonstrated that Aß can also activate astrocytes, possibly directly or by increasing oxidative stress (Butterfield, 2002), causing abnormal calcium signalling (Lim et al., 2013; Navarrete et al., 2013), disrupted glutamate processing (Talantova et al., 2013) and increased release of pro-inflammatory cytokines such as IL-1ß (Thornton et al., 2006; Carrero et al., 2012). By mediating many of the affected systems in AD, astrocytes are able to influence the progression of disease at multiple stages.

At early stages of disease, astrocytes have been found to atrophy, in both transgenic mouse models and post-mortem AD brain (Olabarria et al., 2010; Rodriguez-Arellano et al., 2016). It has been suggested that this atrophy may reduce the area of the domain of each astrocyte, resulting in a reduction in the number of neurons and synapses that each astrocyte can maintain. This could lead to problems with neuronal and synaptic homeostasis as astrocytic maintenance is reduced, weakening synaptic connections and resulting in dysfunction, the first signs of pathology seen in AD (Coleman et al., 2004). In particular, this atrophy may disrupt glutamate and calcium homeostasis, both key roles of astrocytes at the synapse (Anderson and Swanson, 2000; Agulhon et al., 2012).

Astrocytic glutamate uptake by GLAST and GLT-1 is impaired by Aß treatment in astrocytic cultures via reductions in the levels of both transporters, increasing levels of extracellular glutamate (Matos et al., 2008). Additionally, pathological glutamate release by astrocytes in response to Aß treatment has been shown in hippocampal slices. Furthermore, this increase in extracellular slices results in increased excitotoxicity via activation of extrasynaptic NMDA receptors (Talantova et al., 2013). Furthermore, this increased excitotoxicity has been found to

inhibit LTP in hippocampal slices, a key mechanism underlying memory and learning (Li et al., 2011). Excitotoxicity is also known to increase Ca^{2+} influx into the neuron in AD (Ferreira et al., 2012; Navarrete et al., 2013). Alongside excess glutamate effects on neuronal Ca^{2+} levels, astrocytes appear to directly affect Ca^{2+} homeostasis in AD. Ca^{2+}-dependent endoplasmic reticulum stress has been found to correlate with astrogliosis in Aß-treated astrocytes and in the 3xTg-AD mouse model (Alberdi et al., 2013). However, Aß-induced astrocytic calcium signalling effects have not always been seen in cell culture (Toivari et al., 2011). This is likely to reflect functional differences between types of astrocytes. In fact regional differences have been found in the calcium signalling response of astrocytes to Aß treatment suggesting there could be large variations in the astrocytic response in AD and AD-like pathology (Grolla et al., 2013).

As AD progresses, both Aß and tau aggregate, resulting in increased glial activation, chronic inflammation and neurodegeneration (**Figure 1.7**). Astrocytic activation, along with levels of phosphorylated tau in the synapse, show good correlation to clinical disease progression (Perez-Nievas et al., 2013). In more severe stages of AD and AD-like pathology, astrocytes, along with microglia, have been found to localise around Aß plaques in AD brain in a similar way to astroglial scar formation, possibly attempting to minimise the spread of Aß toxicity (Olabarria et al., 2010; Bouvier et al., 2016). Additionally, there is evidence that activated astrocytes may also take up phosphorylated tau, again possibly in an attempt to minimise pathological spread (de Calignon et al., 2012). Increasingly severe astrogliosis, along with increased microglial activation, also results in increased release of cytokine and chemokines, triggering chronic inflammation and a feed-forward neurodegenerative loop producing widespread neuronal loss (**Figure 1.7**) (Heneka et al., 2015).

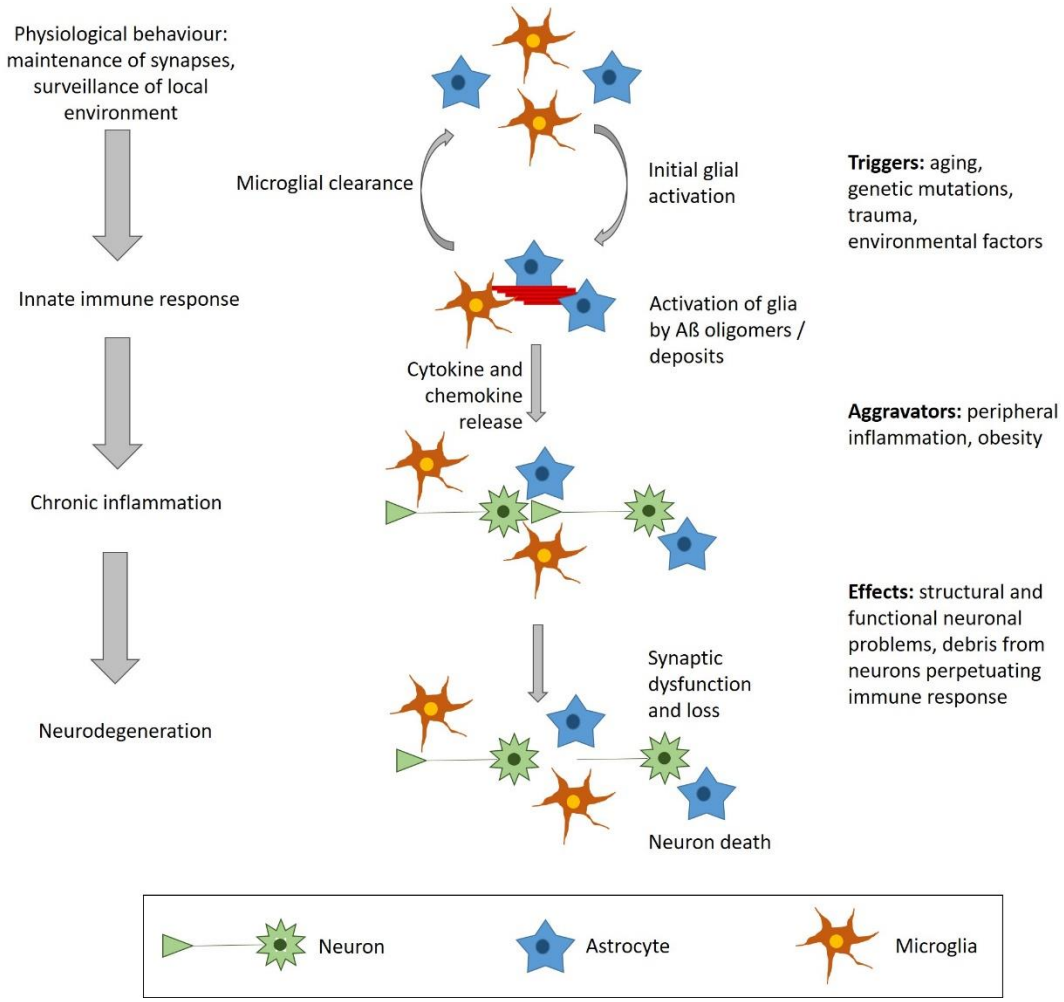

Figure 1.7: Neuroinflammation in AD
Schematic diagram demonstrating development of neuroinflammation and neurodegeneration in AD. Adapted from Heneka et al. (2015).

Microglia

Microglia were originally identified by Rio-Hortega in 1919 (Garcia-Marin et al., 2007a). Part of the mononuclear phagocytic system, they develop outside of the CNS and migrate to the brain in late pre- and early post-natal development (Ransohoff and Cardona, 2010). However, once inside the brain, normal proliferation is thought to occur locally (Lawson et al., 1992; Perry, 2016). Microglia have traditionally been viewed as the resident 'immune cells of the brain', surveying and responding to abnormal or foreign material in order to protect neurons from infection and toxicity (Wirenfeldt et al., 2011; Perry, 2016). However, evidence shows microglia also play important roles in the maintenance and plasticity of synapses and neuronal circuits in the healthy brain (Ji et al., 2013).

Criteria for describing microglial activation state has been adapted from that used for peripheral macrophages (Gordon and Martinez, 2010; Martinez and Gordon, 2014), subsequently revised to explain the range of microglial responses to disease (Biber et al., 2014; Tam and Ma, 2014). In the M0 state, microglia are considered to be "resting". These cells have a ramified morphology and show dynamic cytoskeletal rearrangement as they actively survey the local environment (Nimmerjahn et al., 2005; Sierra et al., 2014). The M1 phenotype is associated with microglia taking on an amoeboid morphology and increased release of pro-inflammatory factors such as tumour necrosis factor α (TNFα), interleukin-1ß (IL-1ß), inducible nitric oxide synthase (iNOS) and production of reactive oxygen species (ROS) (Block et al., 2007). Alternatively, microglia may adopt a M2 phenotype characterised by an increased release of anti-inflammatory mediators such as brain derived neurotrophic factor (BDNF), IL-10 and Arginase-1 and deactivation of the M1 phenotype (Biber et al., 2014). The M2 phenotype is linked with tissue regeneration and repair.

Through active surveillance of their environment, microglia can transition between these states/phenotypes rapidly (Biber et al., 2014; Gomez-Nicola and Perry, 2016), and the resulting state may depend on maturity of the brain since, like astrocytes (Zhang et al., 2016b), different expression profiles have been observed during murine development (Crain et al., 2013). Similarly, repeated activation, or "priming" (Perry and Holmes, 2014) of microglia has been suggested to predispose them towards a pro-inflammatory phenotype. This is often associated with aging, and increased sensitivity to inflammatory stimuli has been found in aged rodent and primate brain (Perry and Teeling, 2013). However, genetic mutations and specific genetic expression, such as that found in the APP/PS1 transgenic mouse have also been associated with primed microglia (Orre et al., 2013). The mechanisms through which microglia transition between activation states are unclear, however the TREM-2 receptor has been linked to an M2 phenotype (Takahashi et al., 2005). The highly varied response of microglia to pathological events remains controversial, and it is to be seen whether manipulating the transition between M1/M2 phenotypes may provide new therapeutic opportunities (Biber et al., 2014).

Complement receptors on the cell surface can detect insults such as disruption of the blood brain barrier (Jacob and Alexander, 2014) and can trigger microglial activation (Crehan et al., 2013). While other receptors including toll-like receptors (TLRs) and scavenger receptors can detect and respond to damage-associated molecular patterns (DAMPs) and pathogen-associated molecular patterns (PAMPs) (Jack et al., 2005). A wide range of proteins and molecules come under the umbrella terms DAMPs (endogenous stimuli) and PAMPs (foreign pathogen stimuli), including heat-shock receptors, ATP, bacterial lipopolysaccharides, viral nucleic acids and Aß, and stimulate microglia to respond to a range of possibly toxic situations with the aim of protecting neuron health (Akira and Hemmi, 2003; Stewart et al., 2010; Pisetsky, 2012; Venereau et al., 2015). Additionally, glutamate receptors are present on the surface of microglia allowing them to detect and respond to excess glutamate in the extracellular space, for example in cases of excitotoxicity (Pocock and Kettenmann, 2007). Furthermore, astrocytes are able to activate microglia through cytokine release in cases of infection and neurodegeneration (Tanuma et al., 2006; Ovanesov et al., 2008). A combined astrocyte and microglial immune response is important as together these two cell types may be able to respond more effectively to toxic stimuli such as Aß, however, as with astrocyte activation, the benefits of microglial activation in AD are unclear.

Support for a microglial response in AD has been established for significantly longer than that of astrocyte activation (Rodriguez et al., 2010). A wealth of evidence demonstrates that microglia display two types of behaviour in response to Aß and AD pathology: phagocytosis and an inflammatory response. Microglia have been found to phagocytose Aß and debris from synapse loss and neuron death (Eugenin et al., 2016). Largely, removal of Aß and this possibly toxic waste is considered beneficial. However, as with the astrocytic immune response, the microglial immune response results in the release of cytokines and chemokines that can trigger detrimental signalling pathways in other glial cells and neurons, and lead to further disease progression (Pocock and Liddle, 2001; Maphis et al., 2015; Wes et al., 2016). Evidence suggests that Aß alone can be sufficient to activate microglia and initiate an inflammatory response

(Heneka et al., 2015). However, microglial priming by peripheral inflammation, and other factors such as obesity, could exacerbate the innate immune system response to Aß and have been suggested to increase risk of chronic inflammation and subsequent neurodegeneration (**Figure 1.7**) (Whitmer et al., 2008; Cunningham et al., 2009; Heneka et al., 2015).

As previously mentioned, some genetic variants of TREM2 significantly increase risk of developing AD (Forabosco et al., 2013; Guerreiro et al., 2013; Villegas-Llerena et al., 2016). The effects of these variants and TREM2 function in physiological and pathological conditions still remains unclear, with conflicting results from different studies (Heneka et al., 2016; Ulrich and Holtzman, 2016). However, it is likely TREM2 is involved in multiple stages of the development of chronic inflammation and neurodegeneration. For example, knocking out TREM2 in mouse models of AD prevents microglia clustering around Aß plaques suggesting TREM2 may be involved in microglial migration (Forabosco et al., 2013; Wang et al., 2015). Moreover, the same study found reduced levels of general microglia activation in TREM2 knock out animals, suggesting TREM2 is involved in a wide range of functions aiming to limit Aß pathology (Wang et al., 2015). Further investigations have suggested that TREM2-positive cells surrounding plaques are peripheral macrophages entering the CNS, rather than resident microglia (Savage et al., 2015). Additionally, TREM2 knock out mice showed very little infiltration of peripheral macrophages and significantly reduced inflammation, unexpectedly indicating a detrimental role for TREM2 in AD (Jay et al., 2015). Regional differences have also been seen in the influence of TREM2, with a reduction in both Aß plaques and soluble Aß oligomers found in the hippocampus, but not cortex, of TREM2 knockout transgenic mouse models of AD (Heneka et al., 2016). This supports findings from experiments investigating astrocyte function that suggest the immune response to AD pathology may differ depending on the brain region and disease stage (Yeh et al., 2011; Rodriguez et al., 2014).

Analysis of TREM2 in peripheral monocytes found other AD-associated alleles of other genes could affect TREM2 biology. In particular, those involved in innate immunity have been found to affect and be effected by TREM2 variants, providing further suggestions of the complex role

TREM2 may play in AD development (Forabosco et al., 2013; Chan et al., 2015). Overall, results from investigations into the role of TREM2 have provided mixed results. However, TREM2 appears to function together with other aspects of the immune system, in particular the innate immune system, in response to Aß and AD-like pathology.

An important part of the microglial innate immune system that is likely to be involved in the response of TREM2 to Aß oligomers and plaques is the inflammasome. Inflammasomes are inducible protein complexes key to microglial function. Four different inflammasomes have been characterised, however the NLRP3 inflammasome seems to be most involved in pathological mechanisms (Gold and El Khoury, 2015). The NLRP3 inflammasome can be activated via two steps: the first requires activation of the transcription factor NF-κB, its translocation to the nucleus and the transcription of the different elements of the inflammasome, resulting in inflammasome 'priming' (Bauernfeind et al., 2009). The second step is the oligomerisation and construction of the inflammasome, where all three protein components join together to form the inflammasome complex (Baroja-Mazo et al., 2014).

A wealth of evidence supports the role of NF-κB in AD. Activation of the transcription factor can be caused, indirectly, by Aß oligomers binding to TLRs. This results in increases in transcription of cytokines and the NLRP3 inflammasome (Kaltschmidt et al., 1997; Lin et al., 2013; Shi et al., 2016). Furthermore, the NLRP3 inflammasome has been found to be activated in human AD brain and contribute to pathology in the APP/PS1 transgenic mouse model of AD, including possibly reducing microglial phagocytosis of Aß (Heneka et al., 2012). Once activated, the complex can control the release of IL-1ß, a pro-inflammatory cytokine associated with AD pathology (Thornton et al., 2006; Di Bona et al., 2008; Ghosh et al., 2013), along with other pro-inflammatory cytokines (Gold and El Khoury, 2015; Freeman and Ting, 2016). Once released, cytokines can activate a range of signalling pathways, switching the microglial innate immune response to chronic neuroinflammation, contributing to the progression of AD pathology (**Figure 1.7**) (Zheng et al., 2016).

1.7.2 Inflammatory mediators

As described above, astrocytes and microglia are part of the brain's innate immune system (Dong and Benveniste, 2001; Barres, 2008; Graeber et al., 2011). Both microglia and astrocytes respond to injury and disease by altering their morphology and changing their protein expression and secretion profile (Allen and Barres, 2009; Rodriguez et al., 2016). Numerous inflammatory mediators, including both pro- and anti-inflammatory cytokines, have been implicated in both the progression and attenuation of AD pathology (Zheng et al., 2016). Furthermore, evidence suggests cytokines and chemokines are involved throughout AD development, including Aß accumulation, tau phosphorylation and aggregation, and synaptic and neuron loss (Mrak and Griffin, 2005; Rubio-Perez and Morillas-Ruiz, 2012; Avila-Munoz and Arias, 2014).

Cytokines

Cytokines are a group of small immune cell signalling molecules that aid intercellular communication during an immune response (Dinarello and Mier, 1986; Zheng et al., 2016). The group comprises of several types of signalling molecules, including interleukins (ILs), interferons (IFN), tumour necrosis factors (TNF) and growth factors (Rothwell and Relton, 1993). Upon glial activation cytokine expression and release is upregulated, however they are also released at low levels throughout the normal peripheral nervous system (PNS) and CNS (Tchelingerian et al., 1994; Rothwell and Luheshi, 2000; Holmin and Hojeberg, 2004). Additionally there is some redundancy in these inflammatory mediators, with multiple cytokines activating similar signalling pathways (Anisman, 2009). Astrocytes have detrimental effects on neurons through cytokine production, which in turn may lead an increased production of reactive oxygen species, exacerbated neuroinflammation, BBB disruption and the release of potentially neurotoxic levels of glutamate (Sofroniew, 2009; Sofroniew and Vinters, 2010; Burda and Sofroniew, 2014; Pekny et al., 2014). Astrocytes also release a wide range of soluble factors including IFNγ, IL-4, IL-6 and TNF-α and express a variety of cytokine receptors (Cahoy et al., 2008; Wang and Bordey, 2008; Sofroniew, 2009; Sofroniew and Vinters, 2010; Agulhon et al., 2012; Hamby et al., 2012).

Consequently, cytokine signalling may occur both in an autocrine and paracrine fashion. As already discussed, establishing the effect of cytokine signalling is difficult as different expression levels can provoke distinct outcomes, and similarly interactions between secreted proteins may also alter their effects. For example, low concentrations of IFNγ had a beneficial effect on astrocytic glutamate clearance in culture, but the effect was lost when both IL-4 and IFNγ were added to the cultures (Garg et al., 2009). Many cytokines have been shown to have neuroprotective, as well as harmful, effects depending on the context. Indeed, through the release of soluble factors, astrocytes can regulate neuronal function, as well as that of other glial cells such as microglia (Sofroniew, 2009; Sofroniew and Vinters, 2010; Colangelo et al., 2014).

Many cytokines have been found to be upregulated in AD brain, compared to control brain (Zheng et al., 2016), and inflammatory cytokine levels have been found to correlate with Aß levels in transgenic mouse models of AD (Patel et al., 2005). Cytokines have been implicated in almost all stages of disease development (Heneka et al., 2015; Zheng et al., 2016), for example, IL-1ß is robustly upregulated in disease brain and polymorphisms in the IL-1ß gene may be associated with an increased risk of AD (Di Bona et al., 2008). Additionally, IL-1ß has been associated with increased tau phosphorylation via activation of tau kinases and increased astrocyte-induced caspase activity in cell culture (Li et al., 2003; Thornton et al., 2006). Similarly, IL-1ß levels correlate well with tau phosphorylation in htau mice (Garwood et al., 2010). Treating the mice with minocycline, a tetracycline with anti-inflammatory action, reduces IL-1ß levels and rescues tau pathology (Garwood et al., 2010). A study crossing another mouse model of AD with mice overexpressing IL-1ß further supported the role of IL-1ß in tau phosphorylation. However, mice also showed reduced Aß load, possibly due to the 4-6-fold increase in plaque-associated microglia suggesting an increase in Aß phagocytosis. In addition to demonstrating the complexity of the immune response and cytokine roles in AD, this paper highlights a divergence between the development of Aß and tau-associated neurodegeneration in AD models (Ghosh et al., 2013).

Increased expression of IL-18 has also been found in post-mortem AD brain suggesting it may have a role in disease progression (Ojala et al., 2009). In particular, evidence supports a role for IL-18 in early AD pathology since increases in peripheral IL-18 levels are found in individuals with MCI (Salani et al., 2013). Furthermore, increases in peripheral IL-18 correlate with cognitive impairment suggesting that IL-18 may play an active role in disease pathogenesis (Bossu et al., 2008). The mechanisms underlying this role are unclear, however, IL-18 has been demonstrated to increase BACE1 and PSEN1 levels in neuron-like cells possibly leading to increases in $Aß_{1-42}$ production during the early stages of disease (Sutinen et al., 2012). IL-18 has also been implicated in the development of tau pathology via the regulation of NMDA receptor function (Curran and O'Connor, 2001). NMDA receptor activity influences tau pathology in multiple ways, including increasing phosphorylation and cleavage of tau that is mediated by elevated extracellular-signal related kinase (ERK) and calpain activity (Amadoro et al., 2006). Furthermore, tau release is dependent on synaptic activity both *in vivo* and *in vitro*, suggesting that IL-18 may influence the spread of tau pathology via NMDA receptor function (Pooler et al., 2013; Yamada et al., 2014).

In addition to IL-1ß and IL-18, there is evidence to support the role of many other cytokines in AD progression. Studies attempting to tease apart which cytokines influence which pathological signalling pathways are on-going and complex. However, it is thought that cytokines could be promising drug targets for AD treatment, hopefully allowing specific signalling pathways to be carefully controlled (Jiwrajka et al., 2016; Zheng et al., 2016).

Chemokines

Chemokines are a group of small (8-10 kDa) cytokines first described by Oppenheim in 1991 (Oppenheim et al., 1991). The name chemokine is derived from their ability to induce chemotaxis, movement in response to a chemical stimulus, in nearby cells. Like other cytokines, chemokines are released from both astrocytes and microglia and they bind G-protein linked receptors on both neuronal and other glial cells (Griffith et al., 2014). Chemokine function can be split into two broad categories: homeostatic or inflammatory, either controlling cell

migration during normal development or recruiting cells to sites of infection, respectively. All chemokines share similar structural and genetic characteristics and can alternatively be classified in four subfamilies: CXC, CC, CX3C and XC however, these subfamilies are not definitively associated with chemokine function (Liu et al., 2014). Chemokine receptors have also been classified, approximately according to the chemokine to which they bind. For example, chemokine CXCL1, also known as GRO-α, binds to receptor CXCR1 (Lu et al., 2005). However, this system has become confused as new research has demonstrated that many chemokines can bind to multiple receptors (CXCL1 can also bind to CXCR2), and many receptors interact with multiple chemokines (evidence suggests CXCR2 can bind more than nine different chemokines) (Liu et al., 2014).

Multiple chemokines have been implicated in the development or progression of AD (Azizi et al., 2014), including MCP-1 (Madrigal et al., 2009; Vukic et al., 2009), SDF-1α (Laske et al., 2008), MIP-1α (Xia et al., 2000), IP-10 (Lai et al., 2013), IL-8 (Ashutosh et al., 2011), and RANTES (Tripathy et al., 2010). Like cytokines, the signalling pathways triggered and the effects caused by these molecules is complex. For example, robust evidence supports the role of fractalkine (CX3CR1) in AD (Kim et al., 2008; Sheridan and Murphy, 2013). However, it is currently unclear whether fractalkine activity promotes or helps rescue the progression of AD. Knocking out the fractalkine receptor in htau transgenic mice exacerbates tau phosphorylation and aggregation via p38/MAPK, and overexpression of fractalkine suppresses tau pathology *in vivo*, suggesting a neuroprotective role for this chemokine that is dependent upon keeping microglia in a resting state (Bhaskar et al., 2010; Nash et al., 2013). However, when mice overexpressing mutant human APP and PSEN1 (APP/PS1) were crossed with fractalkine receptor knockout mice, reduced Aß deposition was found (Lee et al., 2014), which again might reflect an upregulation of microglial phagocytosis as their “rest” signal from neurons is removed. Indeed, fractalkine is suggested to influence autophagy leading to an accumulation of Aß and changes in tau clearance (Hebron et al., 2013).

The studies described here, and others in the literature, demonstrate the complexity of cytokine and chemokine signalling. There is abundant evidence showing that distinct inflammatory mediators play important roles in many stages of disease, and this might diverge depending on whether tau or Aß-mediated neurodegeneration is being studied. Moreover, both cytokines and chemokines mediate multiple signalling pathways, often displaying overlapping functions. This makes elucidating the roles of specific mediators very complex. However, drugs targeting one or several inflammatory mediators may have potential benefit in AD, and there has been renewed interest in anti-inflammatory treatment strategies in recent years (Heneka et al., 2016).

1.7.3 Neuroinflammation as a therapeutic target in AD

Broad anti-inflammatory agents, such as non-steroidal anti-inflammatory drugs (NSAIDs) have shown promise as treatments for Parkinson's disease (Powers et al., 2008). However, multiple clinical trials investigating NSAID efficacy as treatment for AD have found no improvement or prevention of symptoms following NSAID treatment (Miguel-Alvarez et al., 2015). However, glial cell behaviour can both exacerbate and protect from disease progression and it is possible that more specific anti-inflammatory drugs may be needed to ensure that appropriate signalling pathways are up- or downregulated. Drugs targeting specific cytokines are beginning to be tested. For example, IL-1ß receptor antagonists, aiming to rescue or reduce IL-1ß-mediated tau phosphorylation and aggregation, are currently in use for other inflammatory diseases (Braddock and Quinn, 2004). Additionally, evidence from AD mouse models suggests that IL-1ß receptor antagonists show promising effects and may improve AD symptoms (Ben-Menachem-Zidon et al., 2014).

Repurposing drugs already in the clinical is a quick and effective way to find new disease-modifying drugs. Since clinical trials investigating the safety of the drug for humans do not have to be repeated, only the later stages of the trial, investigating the efficacy of the drug for the specific disease, have to be implemented. This shortens the length of time and reduces the cost of clinical trials, making it easier to get effective drugs to AD patients more rapidly. Furthermore,

this approach has been shown to have better clinical trial safety as toxic drugs have already been excluded (Appleby et al., 2013).

In this thesis, two drugs, both already in clinical use for other conditions, and highlighted as being potentially promising repurposing candidates, were investigated. The first, minocycline, is currently in early-stage clinical trials for AD and was used here to investigate the role of astrocytes in the development of tau pathology in primary cell cultures. The second, dimethyl fumarate (DMF) was tested to investigate whether it could reduce tau pathology in primary cell cultures and in a mouse model of AD. Both drugs will be briefly introduced here.

Minocycline

Minocycline is a tetracycline-antibiotic derivative with anti-inflammatory action that is regularly prescribed for the treatment of acne and can cross the blood-brain barrier. Treatment of htau mice, a mouse model of tauopathy, with minocycline significantly reduced the number of activated astrocytes, and levels of pro-inflammatory cytokines and chemokines released (Garwood et al., 2010). Minocycline treatment also reduced tau phosphorylation, cleavage and aggregation in the mice suggesting that the astrocyte-directed anti-inflammatory action of minocycline may be down-regulating pathological signalling pathways that contribute to the development and progression of tau pathology (Noble et al., 2009b). Further investigations of the possible mechanisms of drug action in primary cell culture found that the effects of minocycline were astrocyte-dependent, with minocycline application reducing the release of inflammatory mediators, including IL-1ß, from astrocytes (Garwood et al., 2011). However, cytochrome c and multiple caspases were also downregulated, albeit in a manner dependent on astrocyte presence, suggesting that minocycline may downregulate multiple pathways that affect tau cleavage and aggregation, and potentially also the turnover of other proteins (Noble et al., 2009a; Garwood et al., 2011).

Dimethyl fumarate (DMF)

DMF is a known nuclear factor erythroid 2-related factor 2 (Nrf2) activator, however it also has poorly understood anti-inflammatory actions. It is these anti-inflammatory effects, via reductions in oxidative stress (Lee et al., 2012), which are thought to be exploited in the treatment of multiple sclerosis, a clinical use approved by the FDA in March 2013. Clinical trials for multiple sclerosis have shown that DMF is both non-toxic to humans at therapeutic levels and it is also able to cross the blood-brain barrier, two characteristics that are critical for a possible AD drug treatment (Fox et al., 2012; Gold et al., 2012). Furthermore, studies investigating the effects of DMF in rodent models have found reductions in both spatial memory impairments and hippocampal degeneration (Majkutewicz et al., 2016), two symptoms particularly relevant to AD. This evidence highlights the potential of DMF as a candidate drug for repurposing efforts in AD. Therefore, experiments in this thesis have investigated the effects of DMF on astrocytes and tau in primary cell cultures and the htau mouse model of tauopathy.

1.8 Aims and objectives of this thesis

This broad aim of this thesis is to investigate the association between astrocytes and tau in models of AD.

Specifically, this thesis aims to:

1. Investigate the influence of astrocytes on disease-associated changes in tau proteins in the cortex and the hippocampus using primary neural cell cultures.
2. Examine the relationship between changes in tau, glial activation and synaptic markers in cortex and hippocampus during the progression of AD in Braak-staged brain.
3. Investigate the potential of DMF as a repurposing drug candidate for AD in primary culture models and in an *in vivo* model of tauopathy.

Chapter 2: Materials and Methods

All materials were obtained from Sigma Aldrich (St Louis, MO, US) unless otherwise stated. Stock solutions and buffers were prepared using ultrapure water from a Triple Red purification system. Solution sterilisation, when required, was carried out by autoclaving for 15 min at 121 °C using a Systec VX-150 autoclave (Systec GmbH, Linden, Germany).

2.1 General buffer solutions

Phosphate buffered saline (PBS, pH 7.4)	137 mM sodium chloride, 2.7 mM potassium chloride, 10 mM disodium phosphate, 1.8 mM monopotassium phosphate
PBS-Tween (PBS-T)	1 x PBS with 0.05 % (v/v) Tween-20
Tris-buffered saline (TBS, pH 7.4)	50 mM Tris-base, 150 mM sodium chloride
TBS-Tween (TBS-T)	1 x TBS with 0.05 % (v/v) Tween-20

2.2 Cell culture

2.2.1 Rat primary neurons

Materials

Poly-D-lysine	10 µg/ml poly-D-lysine hydrobromide (molecular weight 4000 – 15000; Sigma-Aldrich P6403)
Supplemented Neurobasal medium	Phenol red free Neurobasal® medium (Invitrogen, Paisley, UK), 2 % (v/v) B-27 (Invitrogen), 2 mM GlutaMax (Invitrogen), 100 µg/ml penicillin (PAA Laboratories, Piscataway, NJ, US), 100 µg/ml streptomycin (PAA Laboratories)
Hank's Balanced Salt Solution	Hank's Balanced Salt Solution (HBSS) without Ca^{2+} or Mg^{2+} (Invitrogen)
Trypsinising solution	TrypLE ™ Express Enzyme (1x), phenol red (Invitrogen)
Trypan blue	0.4 % sterile filtered trypan blue
Foetal bovine serum (FBS)	Foetal bovine serum, qualified, heat inactivated, E.U.-approved, South America Origin (Thermo Fisher Scientific)

Cytosine arabinoside (AraC)	2 mM AraC in phenol red free Neurobasal medium

Methods

Neurons were obtained from embryonic day 18 (E18) Sprague-Dawley rat embryos (Charles River, Margate UK). Pregnant female rats were delivered to the animal house when embryoes were E13. Rats were housed singly for 5 days on a 12 h light-dark cycle and at constant temperature (21 °C). Rats had unlimited access to rodent chow (RM1, Special Diet Services) and water.

Coating plates

All plates used for cell culture were sterile. Nunc cell culture plates were coated with 10 µg/ml poly-D-lysine (PDL) and left overnight at 37 °C. On the day of the dissection, excess PDL was removed and plates were washed with sterile ultrapure H_2O three times. Phenol red free Neurobasal medium was added to each well at incubated at 37 °C until neurons were ready to be plated.

If coverslips were being used, 18 mm glass coverslips (Paul Marienfeld GmbH & Co., Lauda-Königshofen, Germany) were autoclaved and placed in the bottom of 12-well plates using sterile forceps. Plates were then coated with PDL as above.

Neuron dissection

<u>Isolation of the embryonic brain</u>

Pregnant female Sprague-Dawley rats were sacrificed using Schedule 1 methods in accordance with the Animals (Scientific Procedures) Act, 1986. The abdominal wall was cut through and the

uterus removed and placed in Hank's Balanced Salt Solution (HBSS) in a sterile petri dish. Foetuses were removed from the uterus and decapitated. Foetal heads were placed in a fresh petri dish containing HBSS. Brains were removed by making an incision in the skull from the top of the spinal cord toward the olfactory bulb. The skin and the skull were peeled back to expose the cortices. Cortices were removed using curved forceps and placed in a new sterile petri dish containing HBSS on ice.

Dissection and dissociation of the cortices

Midbrain, hindbrain and meninges were removed before the cortex and hippocampus were separated and placed into petri dishes containing HBSS on ice. Dissection took place for a maximum of 1 h from the death of the mother rat. After 1 h, cortices were cut into 3-5 parts and separated into 15 ml falcons (1 falcon/brain). All hippocampi were added to the same 15 ml falcon. For both cortices and hippocampi dissociation, 1 ml trypsinising solution was added to each falcon for 10 min at 37 °C. The trypsinisation solution was removed and brain sections were washed three times with HBSS. 1 ml of phenol red free Neurobasal medium was added to each falcon and cortices were triturated using a P1000 Gilson pipette until cells were fully dissociated. 4 ml phenol red free Neurobasal medium was added to the hippocampal cell falcon to make the total volume 5 ml. Primary neural cells were filtered through a sterile 70 µm cell strainer (Sigma Aldrich). The number of neurons was determined using Trypan blue and a haemocytometer.

Primary cortical neurons were plated in phenol red free Neurobasal medium supplemented with 5 % (v/v) foetal bovine serum (FBS) at a density of $4x10^6$ in 10 ml medium for 10 cm dishes, $1x10^6$ in 4 ml medium per well for 6-well plates or 330,000 in 2 ml medium per well for 12-well plates. Hippocampal neurons were plated in phenol red free medium at a density of 250,000 in 2 ml medium per well in 12 well plates. Cells were cultured at 37 °C with 5 % CO_2. After 24 h, medium was removed from cultures and replaced with phenol red free Neurobasal medium without FBS supplement. The health of the cell cultures was checked every 3-4 days but, except for treatment, no further changes of medium were carried out.

Cytosine arabinoside (AraC) treatment for neuronal cultures

In order to investigate the roles of astrocytes in Aß-induced neuron death in primary cell culture two different primary neuron cultures were used. The first was made as described above, resulting in both neurons and astrocytes in the same cell cultures. These are referred to as mixed cultures throughout this thesis. Neuronal cultures were also made to allow a comparison of neuron cultures containing astrocytes with neuron cultures without astrocytes. Primary neuron cultures without cultures are referred to hereafter as neuronal cultures.

To produce neuronal cultures, primary cultures were treated with cytosine arabinoside (AraC) at 3 DIV to prevent astrocyte proliferation (Garwood et al., 2011). Briefly, primary cultures underwent a 50 % medium change at 3 DIV at which time 0.5 µM AraC or vehicle (Neurobasal medium without phenol red) was added. After 8 days (at 11 DIV) the AraC-containing medium was removed and this was replaced with fresh medium and the remaining conditioned medium (part-conditioned medium).

To confirm neuronal cultures did not contain astrocytes, both mixed and neuronal cultures were stained with the astrocyte marker GFAP using immunocytochemistry (ICC) and western blots (described in Chapter 3, **sections 3.3.1, 3.3.3 and 3.3.4**).

2.2.2 Cell lines

7PA2 Chinese hamster ovary (CHO) cells stably transfected with DNA coding for the APP751 gene with the Val717Phe Alzheimer's disease causing mutation were kindly donated by Dominic Walsh. These CHO cells naturally secrete Aß monomers into the culture medium (Walsh et al., 2002). Cells were cultured in supplemented high glucose phenol-red free Dulbecco's Modified Eagle's Medium (DMEM) at 37 °C with 5 % CO_2. When cells reached 100 % confluency, medium was collected as a source of physiologically secreted Aß. Wild type (WT) CHO cells were cultured in the same way and culture medium was collected as a control.

Materials

Supplemented DMEM	Dulbecco's modified Eagle's medium (DMEM) with 4.5 g/L D-glucose, without phenol red (Invitrogen) supplemented with 10 % (v/v) FBS, 2 mM L-glutamine, 100 µg/ml penicillin, 100 µg/ml streptomycin
Trypsin	2.5 % trypsin

Methods

Passaging CHO cells

CHO cells grown for passaging, rather than medium collection were split when they reached 65 - 80 % confluency (approximately every 3-4 days). CHO cells were trypsinised using 2.5 % trypsin for 5 min at 37 °C. Cells were split 1/20 into 2 flasks: one for medium collection and one to continue the cell line. WT CHO cells were passaged in the same way.

Freezing and thawing CHO cells

CHO cells were frozen in supplemented high glucose phenol-red free DMEM with 10 % (v/v) dimethyl sulfoxide (DMSO). Cells were trypsinised as described in passaging section and added to 1 ml DMEM medium with 10 % DMSO. Immediately cells were placed in a polystyrene Eppendorf holder at -80 °C for 24 h. After 24 h cells were stored in liquid nitrogen.

To thaw cells, tubes were removed from liquid nitrogen and incubated at 37 °C until defrosted. Thawed CHO cells and medium were immediately added to flasks containing supplemented high glucose phenol-red free DMEM and incubated at 37 °C with 5 % CO_2. After 24 h culture medium was replaced with fresh medium.

2.2.3 ß-amyloid characterisation

Dynamic light scattering (DLS)

DLS is a technique used to measure the size of small molecules using the principles of Brownian motion of small particles in suspension (Berne and Pecora, 1976). Laser light shone through a sample is scattered when light waves hit a molecule with between 0.5 nm and 1000 nm radius. Scattered waves can interfere with each other resulting in fluctuations in the intensity of light detected by the detector. Faster Brownian motion results in increased frequency of intensity fluctuations as particle diffusion is faster. Therefore, larger molecules can be distinguished from smaller molecules based on the frequency of intensity fluctuations.

100 µM stock $Aß_{1-42}$ was made up by diluting 500 µM stock with autoclaved ultrapure H_2O and centrifugation at 13000 g(av) for 10 min to remove any dust and contaminating particles. 90 µl of diluted Aß was added to one well of a 96-well Corning UV Transparent Microplate (Scientific Laboratories Ltd, Hessle, Yorkshire, UK). The plate was added to a Dyna Pro Plate reader (Wyatt Technology, Santa Barbara, CA, US) with temperature control and auto-attenuation function and was read at 25 °C for 5 sec. To ensure accurate readings, the final distribution was averaged from five individual 5 sec DLS collections. This was repeated three times to ensure a stable overall reading. 90 µl of autoclaved ultrapure H_2O was also read with the plate reader as a background control. The percentage of the total Aß mass at each possible radius of Aß molecule (e.g. the radius of a monomer, dimer, trimer etc.) for each sample was obtained by the plate reader and plotted as a line graph using GraphPad Prism 6.0. Interpretation of results was qualitative so no statistical tests were carried out.

Electron microscopy

Synthetic Aß samples were prepared for electron microscopy as previously published (Guo and Lee, 2011). Briefly, samples were resuspended by vortexing for 1-2 sec, twice, and then agitated further by drawing up and ejecting 5 µl of sample 10 times. 5 µl undiluted sample was places on

a formar/carbon coated copper grid for 3 min. 2 drops of 50 nM Tris-HCl buffer, pH 7.5, were added for 5 min each to rinse samples. The samples were negatively stained by dripping 15-20 drops of 2 % (v/v) aqueous uranyl acetate with 0.5 % (v/v) glacial acetic acid over the grid before being air dried in closed containers for at least 1 h prior to viewing in a FEI Tecnai-10 TEM at 80 kV. Samples were then diluted 1:5 in PBS and the procedure was carried out again. Representative images were collected using AMT-XR-50 software.

Field and image selection were chosen as follows:

The entire grid was viewed at 2600x to determine the number and distribution of oligomers. A representative area was chosen and images were taken at 24000, 65000 and 160000x from the same grid hole opening. A second and third grid hole was chosen and images were again taken at 65000 and 160000x.

Meso Scale Discovery (MSD) assays

Assays were run according to manufacturer's instructions. Two types of MSD assay were used.

Aß-peptide panel 1 (6E10) V-Plex plates

Materials

V-PLEX Aß Peptide Panel 1 (6E10) Kit (K15200E-1, Meso Scale Discovery, Rockville, MD, US).

All reagents supplied complete by manufacturer.

Methods

These plates were used to investigate levels of $Aß_{1-38}$, $Aß_{1-40}$ and $Aß_{1-42}$ in samples of synthetic $Aß_{1-42}$, 7PA2 CHO medium and Tg2576 primary mouse neuron medium. Each well of the 96-well plates provided were pre-coated with antibodies that specifically bind to $Aß_{1-38}$, $Aß_{1-40}$ and $Aß_{1-42}$. Reagents and solutions provided in the MSD assay kit were used in the assay. In brief, non-specific binding was blocked for 1 h using the blocking solution provided at ambient temperature with vigorous shaking. After washing three times with phosphate buffered saline – Tween 20

(PBS-T), the Sulfo-tag detection antibody, MSD kit controls and samples (diluted in manufacturer's diluting solution) were added to the plate and incubated for 2 h at ambient temperature with vigorous shaking. Plates were washed a further three times with PBS-T. 2x Read Buffer, diluted in ultrapure H_2O as instructed, was added to the plates and the signals produced were read immediately using an MSD Plate Reader. The settings for reading the plate were determined automatically by the plate reader by scanning the plate bar code. Standard curves were produced from the kit controls according to the manufacturer's instructions. Aß concentrations were interpolated from each standard curve. Both blanks with no protein and WT controls (of CHO and neuron medium) were used as negative controls.

Multi-array® plates

Materials

Blocking buffer	3 % (w/v) bovine serum albumin (BSA) in 1 x PBS
Wash buffer	1x PBS
2x Read buffer	4x Read buffer (Meso Scale Discovery) diluted 1:1 with 1x PBS

Antibodies

MSD assays were blocked with the blocking buffer provided in the assay kit. Coating antibodies were incubated overnight. Detection and capture antibodies were incubated for 1 h.

Antibody	Species	Epitope	Concentration	Source
3D6	Mouse monoclonal	Amino acids 1-5 of Aß	100 ng/well	Eli Lilly and Co. (Windlesham, Surrey, UK)
A11	Rabbit polyclonal	Oligomeric Aß	100 ng/well	StressMarq Biosciences (Victoria, Canada)

Table 2.1: Coating antibodies used in MSD assays
Antibody name, species, reactivity, concentration and source shown.

Antibody	Species	Epitope	Concentration	Source
3D6	Mouse monoclonal	Amino acids 1-5 of Aß	0.5 µg/ml	Eli Lilly and Co.
Biotinylated 3D6	Mouse monoclonal	Amino acids 1-5 of Aß	0.5 µg/ml	Eli Lilly and Co.

Table 2.2: Detection antibodies used in MSD assays
Antibody name, species, reactivity, concentration and source shown.

Antibody	Dilution	Source
Goat anti-mouse Sulfo-tag	1 µg/ml	Meso Scale Discovery
Streptavidin Sulfo-tag	1 µg/ml	Meso Scale Discovery

Table 2.3: Secondary antibodies used in MSD assays
Antibody reactivity, dilution and source shown.

Methods

Multi-array® plates were used to determine the levels of Aß oligomers in samples of synthetic $Aß_{1-42}$, 7PA2 CHO medium and Tg2576 primary mouse neuron medium.

To obtain Tg2576 primary mouse neuron medium enriched with Aß, neurons overexpressing human APP containing the Swedish mutation (K670N/M671L) were cultured for 14 days without changing the medium (Hsiao et al., 1996). At 14 DIV medium was collected from primary cultures and used in Multi-array® plates to investigate Aß concentrations. WT primary mouse neurons were cultured in the same way to produce control neuronal medium.

Briefly, plates (Multi-array® 96-well plates, #L15XA-3, Meso Scale Discovery) were coated with primary capture antibody at 100 ng/well in PBS and were incubated overnight at 4 °C (**Table 2.1**).

Plates were washed three times with wash buffer and non-specific binding was blocked with blocking buffer for 1 h at ambient temperature with vigorous shaking. Plates were washed three times in PBS. Samples were diluted in PBS, and 25 µl per well were added to the plates in duplicate. For CHO cell and Tg2576 culture medium, samples were added neat for the highest concentration, while medium from synthetic Aß-treated cells was diluted 1:3 for A11 capture antibody assays and 1:9 for 3D6 capture antibody assays. All samples were then diluted in a 3-fold dilution series at least three times. This was to ensure sample concentrations were within the detection range for each antibody. Optimisation of this range was carried out by others in the group prior to these experiments taking place. Plates were incubated at ambient temperature for 1 h with vigorous shaking, the samples removed and the plates washed three times with wash buffer. 25 µl per well of detection antibody (**Table 2.2**), diluted in 1 % bovine serum albimun (BSA) in PBS, was added to the plates and incubated at ambient temperature for 1 h with vigorous shaking. Plates were washed three times with wash buffer. Sulfo-tag labelled secondary antibody (**Table 2.3**) diluted in 1 % BSA in PBS was added to the plate at 25 µl per well and incubated at ambient temperature for 1 h with vigorous shaking. The secondary antibody was removed and plates were washed three times with wash buffer. Next, 150 µl/well of 2x Read Buffer was added to the plates. Plates were read immediately at using an MSD Plate Reader. The settings for reading the plate were determined automatically by the plate reader by scanning the plate bar code. Standard curves were produced from the kit controls according to the manufacturer's instructions. Aß concentrations were interpolated from each standard curve. Both blanks with no protein and WT controls (of CHO and neuron medium) were used as negative controls.

$Aß_{1-42}$ ELISA

Materials

Human $Aß_{1-42}$ ELISA kit (Invitrogen).

All reagents supplied complete by manufacturer.

Methods

Collected CHO cell medium was run neat on $Aß_{1-42}$ ELISAs according to the manufacturer's instructions (Kurbatskaya et al., 2016). The $Aß_{1-42}$ standard was reconstituted in 55 mM sodium bicarbonate, pH 9.0, before dilution to provide a standard curve containing 0, 15.63, 31.25, 62,5, 125, 250, 500 and 1000 pg/ml of human $Aß_{1-42}$ for the assay. 50 µl of sample and standard was loaded in duplicate onto the provided ELISA plate, pre-coated with primary antibody to the N-terminus of $Aß_{1-42}$. 50 µl rabbit primary antibody against the C-terminus of $Aß_{1-42}$ was added and incubated at ambient temperature for 4 h. Plates were washed with provided wash buffer four times before 100 µl anti-rabbit horseradish peroxidase (HRP)-linked secondary antibody was added to each well and incubated for 30 min at ambient temperature. Plates were washed four times before adding the stabilised chromogen substrate for 30 min. The reaction was stopped by adding the provided stop solution, resulting in a yellow colour that was detected at 450 nm using a Wallac 1420 Victor3™ plate reader (Perkin Elmer, Waltham, MA, US). The absorbance values of the $Aß_{1-42}$ protein standards were used to create a standard curve. Sample protein concentrations were calculated from the standard curve in pg/ml.

2.2.4 Cell treatment

Materials

Minocycline hydrochloride (minocycline)	4 mM minocycline hydrochloride in sterile H_2O

ß-amyloid$_{1-42}$ (Aß$_{1-42}$)	500 µM synthetic human Aß$_{1-42}$ (California Peptide Research, Salt Lake City, UT, US) in sterile H_2O
Conditioned CHO cell medium	Neat collected CHO medium diluted 1:1 with phenol red free Neurobasal medium
Dimethyl fumarate	100 mM dimethyl fumarate (DMF) in dimethyl sulfoxide (DMSO)
S-α-amino-3-hydroxy-5-methyl-4-isoxazolepropionic acid (AMPA)	100 µM S-AMPA (Tocris Bioscience, Bristol, UK) in autoclaved H_2O
Ionomycin	10 µM ionomycin in DMSO

Methods

Minocycline

Minocycline treatment was carried out according to a protocol previously published by this group (Garwood et al., 2011). A 4 mM minocycline stock solution was made by dissolving minocycline hydrochloride in sterile H_2O at 60 °C. At 11 DIV, the medium was removed from neuronal or mixed cultures and this was replaced with part-conditioned medium. Cultures were pre-treated with 20 µM minocycline or sterile ultrapure H_20 (vehicle) for 24 h prior to ß-amyloid (Aß$_{1-42}$) addition. To ensure minocycline was not neurotoxic, cell death was measured using a LIVE/DEAD assay (assay results in Chapter 3, **sections 3.3.3 and 3.3.4**).

ß-amyloid

Synthetic $Aß_{1-42}$ (California Peptide, CA, US) was dissolved in sterile ultrapure H_20 to make a 500 µM stock solution. $Aß_{1-42}$ was added directly to primary cultured cells of 12 DIV for 48 h to give final Aß concentrations of 10 µM (Noble et al., 2009b; Garwood et al., 2011). Control wells were treated with vehicle only.

Conditioned CHO cell medium

Medium was collected from 7PA2 and WT CHO cells when cells were 100 % confluent and this was stored in 1 ml aliquots in 15 ml falcons at -20 °C since these showed low absorbance of Aß. For primary cell culture treatment, CHO medium was thawed and mixed 1:1 with conditioned Neurobasal medium. 2 ml or 4 ml of CHO cell-conditioned medium was applied to 12-well and 6-well plates, respectively. Primary neural cell cultures were treated with CHO cell conditioned medium for 48 h.

Dimethyl fumarate (DMF)

A 100 mM stock solution was made by dissolving DMF in DMSO before further diluting the resulting solution in Neurobasal medium to produce a 1 mM DMF / 0.01 % DMSO solution. This working stock of DMF was added directly to the primary culture wells at 14 DIV for 24 h to give final concentrations of 30 µM – 60 µM DMF. Controls were treated with 0.01 % DMSO only giving final DMSO concentrations of 0.0006 % (for 60 µM DMF) or 0.0003 % (for 30 µM DMF). DMF concentrations were chosen based on previous research using DMF in cell culture (Wierinckx et al., 2005; Ellrichmann et al., 2011; Scannevin et al., 2012) and preliminary experiments investigating the toxicity of DMF at these concentrations (described in Chapter 4, **section 4.3.1**).

S-α-amino-3-hydroxy-5-methylisoxazole-4-propionic acid (S-AMPA) and ionomycin treatment

S-AMPA is a specific agonist for the AMPA receptor at the post-synaptic membrane of neurons. S-AMPA was used to mimc glutamate, stimulating glutamatergic neurons in mixed primary cultures in order to investigate the effects of neuronal stimulation on levels of extracellular tau. As a positive control, the ionophore ionomycin was used to induce neurotoxicity resulting in the

breakdown of the neuronal plasma membrane and the release of all intracellular proteins, including tau, into the extracellular space. Primary rat neurons cultured in 10 cm dishes were used for S-AMPA and ionomycin cell treatment. Immediately prior to treatment, rat primary culture medium was replaced with 4 ml B27-free phenol red-free Neurobasal medium so not to block columns when concentrating the medium. Treatment of primary cell cultures with S-AMPA and or ionomycin were for 30 min. S-AMPA and ionomycin were added directly to the B27-free medium at 100 µM or 10 µM, respectively (Pooler et al., 2013). For ionomycin treatments, an equal concentration of DMSO was added to control cell cultures as a vehicle control.

2.2.5 Cell viability LIVE/DEAD assay

Methods

4 % Paraformaldehyde (PFA)	4 % (v/v) PFA in PBS from 16 % liquid stock (Alfa Aesar, Ward Hill, MA, US)

LIVE/DEAD® Fixable Far Red Dead Cell Stain kit (Thermo Fisher Scientific, Waltham, MA, US). Except PFA all reagents supplied complete by manufacturer.

Materials

LIVE/DEAD® Fixable Far Red Dead Cell Stain Assays (L10120, Invitrogen) were carried out according to the manufacturer's instructions. The LIVE/DEAD assay stains dying cells as the Far Red dye is taken up only by cells with compromised plasma membranes. Once inside the cell, the dye reacts with intracellular free animes resulting in fluroescent staining with a 665 nm wavelength. This results in cells with comprised membranes fluorescing with an intense red colour, while healthy cells are not stained (Niger et al., 2012; Sestero et al., 2012).

Briefly, LIVE/DEAD dye was dissolved in DMSO before diluting 1:500 in PBS. Cultures were washed in PBS before incubation with LIVE/DEAD solution (30 min, ambient temperature). Cells

were washed twice with PBS before being fixed with 4 % paraformaldehyde (PFA: 10 min, ambient temperature). All incubation periods were carried out in the dark. The intensity of labelling can be used as a measure of cell death. The intensity of dye incorporation was visualised and quantified using the Odyssey Imaging System and Odyssey Sa Software Version 1.1 software (Li-Cor Biosciences, Cambridge, UK). Red dye uptake of dead cells in experimental groups were anaylsed as a percentage of control group red dye uptake.

For culture characterisation, cells were also imaged using immunocytochemistry. Far Red dye stained cells were counted alongside the number of Hoescht stained nuclei and dead cells were calculated as a percentage of total nuclei counted.

2.3 Htau mice

Htau mice (Andorfer et al., 2003) were obtained from Jackson Laboratories (Bar Habor, Maine, US). These tau transgenic mice were generated by crossing 8c mice, which express the entire wild-type human tau gene under the control of the human *MAPT* promoter (Duff et al., 2000), with tau knockout mice that have a targeted disruption of exon 1 of tau caused by the introduction of eGFP (Tucker et al., 2001). Mice were then crossed onto a C57BL/6 background. Mice progressively develop tangle pathology and cognitive deficits with age (Andorfer et al., 2003; Andorfer et al., 2005; Kelleher et al., 2007; Noble et al., 2009b; Polydoro et al., 2009).

2.3.1 Genotyping and polymerase chain reaction (PCR)

Materials

All reagents were diluted in PCR-grade H_2O unless otherwise stated.

DNA extraction

1x Ten9 buffer	15 mM Tris-HCl, 35 mM Tris-base, 20 mM EDTA, 40 mM NaCl
Proteinase K storage buffer	50 mM Tris-HCl, pH 8.0, 5 mM calcium chloride, 50 % (v/v) glycerol
Digestion mix	1x Ten9 buffer, 1 % (w/v) SDS, 1 mg/ml proteinase K stored in storage buffer

PCR

<u>Primer sequences (Eurogentec, Seraing, Belgium)</u>

Human *MAPT* gene	forward (oIMR3115)	5'-ACTTTGAACCAGGATGGCTGAGCC-3'
	reverse (oIMR3116)	5'-CTGTGCATGGCTGTCCACTAACCTT-3'
Mouse *Mapt* gene	forward (oIMR3092)	5'-CTCAGCATCCCACCTGTAAC-3'
	reverse (oIMR3093)	5'-CCAGTTGTGTATGTCCACCC-3'
Disrupted *Mapt* gene / Egfp	forward (oIMR0872)	5'-AAGTTCATCTGCACCACCG-3'
	reverse (oIMR1416)	5'-TCCTTGAAGAAGATGGTG CG-3'

PCR reaction mixture	5 % (v/v) extracted template DNA, 10 µM forward primer, 10 µM reverse primer, 50 % (v/v) REDExtract-N-Amp™ PCR Reaction Mix (containing buffer, salts, deoxynucleoside triphosphates (dNTPs), Taq 95 polymerase, REDTaq dye, and JumpStart Taq antibody), 35

	% (v/v) nuclease-free H_2O (Thermo Fisher Scientific)
DNA gels	
1.5 % agarose gel	1.5 % (w/v) agarose, 40 mM Tris-base (pH 7.6), 20 mM acetic acid, 1 mM EDTA, 0.67 µg/ml ethydium bromide
TAE buffer	40 mM Tris-base (pH 7.6), 20 mM acetic acid, 1 mM EDTA
100 bp DNA ladder	Quick-Load® 100 bp DNA Ladder consisting of 12 pre-stained bands with sizes 100 bp, 200 bp, 300 bp, 400 bp, 500/517 bp, 600 bp, 700 bp, 800 bp, 900 bp, 1000 bp, 1200 bp, 1500/1517 bp when visualised with ethidium bromide on 1.5 % agarose gels (New England Biolabs, Ipswich, MA, US).

Methods

DNA Extraction

Once weaned, mice were ear punched for genotyping. 20 µl digestion mix was added to each sample and incubated for 20 min at 55 °C. Samples were removed from the water bath, vortexed and return for a further 20 min, after which 80 µl of nuclease-free H_2O was added to each sample. Samples were incubated at 100 °C for 10 min to inactivate Proteinase-K and melt DNA

strands. 20 µl of each sample was collected and added to 60 µl nuclease-free H_2O. Samples were used in PCR immediately or stored at -20 °C.

Polymerase chain reaction (PCR)

PCR was carried out to amplify DNA. Briefly forward and reverse primers (human tau, mouse tau, eGFP, Eurogentec, Seraing, Belgium) and 1 µL of extracted DNA was mixed with REDExtract-N-Amp™ PCR ReadyMix™ in nuclease-free H_2O to a final volume of 20 µl resulting in 3 primer solutions per sample. Samples were loaded into G-Storm PCR plates and set to run on in G-Storm PCR machines.

The following PCR programme was used for all primer solutions:

Initial denaturing at 94 °C for 5 min then 25 cycles of 94 °C for 30 sec (denaturation), 52 °C for 30 min (annealing) and 72 °C for 1 min (extension), with 3 min at 72 °C for a final extension step.

1.5 % agarose gels

Agarose was added to Tris-acetate-EDTA (TAE) buffer to give a final concentration of 1.5 %. The solution was heated until the agarose dissolved. Once cool, 0.67 µg/ml ethidium bromide was added before gels were poured and set. Gels were loaded with PCR samples and 100 bp DNA ladder and placed in electrophoresis tanks filled with TAE buffer. Gels were run at 150 V for 30 min. DNA was visualised immediately after running using a GelDoc-It® Imaging System and Visionworks (Ultra-Violet Products Ltd, Cambridge, UK).

2.3.2 Treatment and testing of htau mice

In this study two groups of homozygous htau mice were examined: (i) 8-9 months old, that display abnormal tau phosphorylation and the early tau aggregation, and (ii) 13-14 months old, in which a significant burden of insoluble tau is apparent. Once crossed onto a C57BL/6 background mice were bred and reared in-house. Pups were weaned at 3 weeks of age. Mice had unlimited access to rodent chow (RM3, Special Diet Services, Essex, UK) and water. Mice were housed singly or in groups (miximum of 4 animals) at a constant temperature (21 °C) on a 12 h light-dark cycle.

Materials

Dimethyl fumarate (DMF) solution	1.875 mg/ml DMF in vehicle solution of: 20 % (w/v) Splenda (Tate and Lyle, London, UK), 0.08 % (w/v) methocel, 0.1 % (v/v) chocolate flavouring for taste (Cupcake World, Holmfirth, UK) made fresh daily.
Opacifier	Acusol OP301 (DOW Chemical Company, Staines, UK)

Methods

Morris water maze

The Morris water maze is commonly used to evaluate spatial memory in rodents (Morris, 1984). Rodents learn the location of a visible platform in the maze using fixed visual cues in the experimental room. When the animal has found the platform it is rewarded by being removed from the water maze. Once the rodents have learnt the escape platform location the platform is submerged in cloudy water, making it invisible. The rodent's spatial memory is then tested by measuring how long the animal takes to navigate to the submerged platform using the previously learnt visual cues.

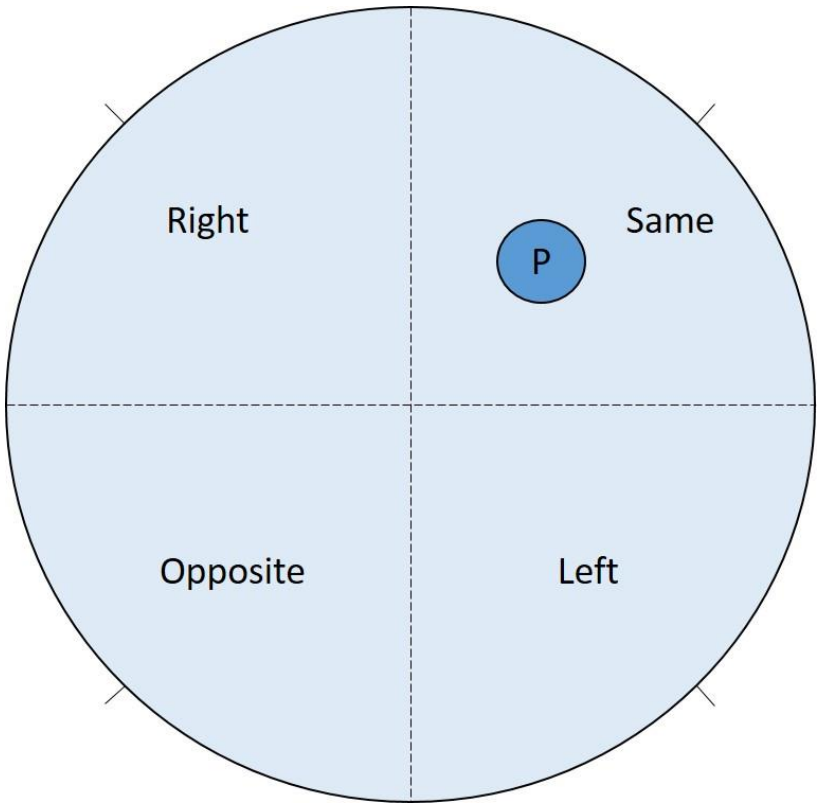

Figure 2.1: Morris water maze
The Morris water maze is divided into four quadrant according to their relation to the platform, P. Shorter lines from the edge of the maze indicate the entry point for mice for each quadrant.

Htau mice were run in a Morris water maze with a 1.2 m diameter. Opacifer was added to make the water cloudy, obscuring the escape platform when necessary. Visual cues were placed around the maze to ensure an easily navigable environment. On day 1, the mice were allowed to associate the platform with escaping the maze and learn where the platform was relative to visual cues. For this learning period the escape platform was visible above the water. The maze was split into four quadrants: same quadrant as the platform, opposite the platform and to the left and right of the platform (**Figure 2.1**). Mice were gently placed into the water in one of the four quadrants and the timer was started. Mice were allowed to swim until they reached the escape platform or for 60 secs, whichever was quickest. Once on the platform the timer was stopped and the mouse was retrieved from the water, dried and returned to its cage. Each mouse swam with the platform visible for a total of four times: from each of the four quadrant

start points. The order of quadrants was randomised for each mouse. On days 2-5 mice were tested, swimming from each quadrant, with the platform submerged. 1 h after the final swim on day 5 a probe test was also carried out. For this test the escape platform is completely removed from the maze and the percentage of time spent swimming in each quadrant is recorded. Timing, swim speed and path length of each swim were recorded using EthoVision XT 7 (Noldus, Wageningen, Netherlands). Spatial learning was analysed using a one-way ANOVA.

Treatment of htau mice

Mice were administered 15 mg/kg DMF in chocolate-flavoured vehicle solution via oral syringe twice daily (Schilling et al., 2006) for 18-20 days (**Figure 2.2**), vehicle mice were given the vehicle solution only. DMF was freshly prepared prior to each dosing. In the first group of mice an "untreated" group of mice were also included to control for possible stresses caused by the treatment. 4 h after the final treatment mice were sacrificed by cervical dislocation, at which time brains were removed and snap-frozen in liquid nitrogen for biochemical analysis.

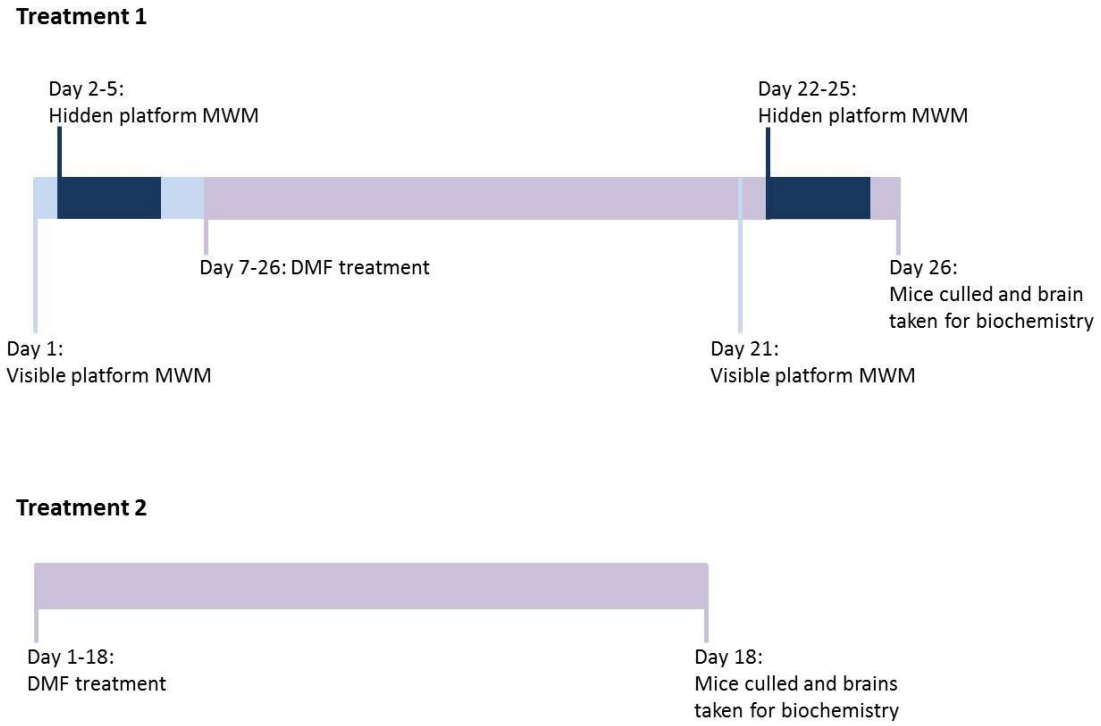

Figure 2.2: Time course for DMF mouse treatments
Two cohorts of htau mice were treated with DMF. The first cohort underwent **treatment 1**: 1 day of training and 4 days of testing on the Morris water maze (MWM) pre-treatment. Mice were then treated twice daily with 15 mg/kg DMF. Training and testing of mice on the MWM was then repeated from day 21-25 while still being treated with DMF. Mice were culled at day 26 and their brains were snap-frozen for biochemical analysis. **Treatment 2**: mice underwent twice daily treatment of 15 mg/kg DMF for 18 days. On day 18 mice were sacrificed four hours after final treatment and brains were snap-frozen in liquid nitrogen for biochemical analysis.

2.4 Sample preparation and standardisatoin

2.4.1 Sample preparation

Materials

Extra strong lysis buffer (XSLB)	10 mM tris-hydrochloride (HCl), pH 7.5, 75 mM sodium chloride, 0.5 % (w/v) sodium dodecyl sulfate (SDS), 20 mM sodium deoxycholate, 1 % (v/v) Triton X-100, 1 mM sodium pyrophosphate, 2 mM sodium

	orthovanadate, 1.25 mM sodium fluoride, 10 mM Ethylenediaminetetraacetic acid (EDTA), Mini cOmplete protease inhibitor cocktail tablet (Roche Diagnostics, West Sussex, UK)
Laemmli sample buffer (2x) (Laemmli, 1970)	125 mM Tris-HCl, pH 6.8, 4 % (w/v) SDS , 1 mM dithiothreitol (DTT), 20 % (v/v) glycerol, 0.01 % (w/v) bromophenol blue, Mini cOmplete protease inhibitor cocktail tablet
Tau fractionation buffer	50 mM sodium phosphate, pH 7.0, 10 nM sodium pyrophosphate, 2 mM Ethylene glycol tetraacetic acid (EGTA), 2 mM EDTA, 20 mM sodium fluoride, 1 mM DTT, Phosphatase inhibitor cocktail 2, Mini cOmplete Protease inhibitor cocktail tablet, 2 mM sodium orthovanadate
Homogenisation buffer	50 mM TBS, pH 7.4, 2 mM EGTA, 10 mM sodium fluoride, 1 mM sodium orthovanadate, cOmplete protease inhibitor cocktail
Sodium lauroyl sarcosinate (Sarkosyl)	N-laurosylsarcosine sodium salt solution, 20 %

Methods

Cell lysis

Cells were washed once with PBS and lysed in extra strong lysis buffer (XSLB) before brief sonication (15 sec, 40 %) using a Vibra-Cell sonicator (Sonics & Materials, Newtown, CA, US) and centrifugation in a benchtop Spectrafuge 24D (Jencons-PLS, East Grinstead, West Sussex, UK; 16,300 g(av) for 20 min at 4 °C). XLSB is a lysis buffer with high concentrations of detergent in order to ensure full breakdown of cell membranes. If necessary, the resulting supernatant was standardised for total protein and normalised samples were diluted 1:1 with 2x Laemmli buffer. Samples used for Alphascreen assays were lysed in tau fractionation buffer as the high levels of detergents in XSLB interfere with the Alphascreen assay.

Concentrating tau from primary cell culture medium

For use on the tau sandwich ELISA, cell culture medium as concentrated using a protocol previously published by this group (Pooler et al., 2013). 2 ml cell culture medium was collected from primary cultured neurons and spun at 4 °C at 16100 g(av) for 5 min. Supernatants were pipetted into filters of constructed centrifugal filter units (with a molecular weight cut off of 30 kDa) and spun in a Sorvell Legend RT centrifuge with swinging bucket at 4 °C at 3000 g(av) for 20 min. Once finished, the filtrate collection tube was removed and discarded, the rest of the unit was inverted and centrifuged again at 4 °C at 1000 g(av) for 5 min. The filter was removed and discarded. Concentrate was pipetted from collection tube to Eppendorfs, and the volume of concentrate was recorded. 2x Laemmli buffer was added to concentrate so concentrate to buffer ratio was 4:1. Samples were heated at 100 °C for 20 min and then stored at -20 °C until required.

Human brain homogenisation

London Neurodegenerative Disease Brain Bank, Brains for Dementia Research and the Medical Research Council provided all frozen human brain samples as frozen blocks (500 mg for cortical samples, 200 mg for hippocampal samples). For each individual one frozen block of temporal cortex was tested. Hippocampal samples (one 200 mg frozen block) were obtained from as many individuals providing cortical samples as possible however, due to the small volume of the hippocampus, it was not possible to obtain hippocampal samples for each individual. For full details of individuals samples refer to Chapter 5, **section 5.2**.

Samples in pilot experiments (using only temporal control and Braak stages V/VI samples) were homogenised directly in 2x Laemmli buffer with 5 % (v/v) ß-mercaptoethanol with a Tissue Master-125 Omni International mechanical homogeniser (Kennesaw, GA, US), at 200 mg/ml. All other samples (temporal and hippocampal control and Braak stages I-VI) were homogenised in XSLB (Kurbatskaya et al., 2016). Whilst being kept on ice, all samples were sonicated for 15 sec using a Vibra-Cell sonicator and then centrifuged in an Eppendorf 5415 R benchtop centrifuge (Eppendorf UK Limited, Stevenage, UK) at 16300 g(av) for 20 min at 4 °C. Supernatants were collected and, if not already, mixed 1:1 with 2x Laemmli buffer with 5 % (v/v) ß-mercaptoethanol. Samples were run on western blots to standardise for neuron-specific enolase (NSE) levels. Based on the amounts of NSE detected, samples were standardised to give equal NSE content using 2x Laemmli buffer. Aliquots were stored at -80 °C until used for western blotting.

Mouse brain homogenisation

<u>Cortical sections</u>

Frozen cortical sections of htau mouse brain were homogenised in XSLB using a Tissue Master-125 Omni International mechanical homogenised with a final concentration of 100 mg/ml. Whilst being kept on ice, all samples were sonicated for 15 sec using a Vibra-Cell sonicator and

then centrifuged in an Eppendorf 5415 R benchtop centrifuge at 16300 g(av) for 20 min at 4 °C. Supernatants were collected and mixed 1:1 with 2x Laemmli buffer. Samples were run on western blots to standardise for ß-actin levels. Based on the amounts of ß-actin detected, samples were standardised to give equal ß-actin content using 2x Laemmli buffer. Aliquots were stored at -20 °C until used for western blotting.

Hippocampal sections (Sarkosyl extraction preparation)

Sarkosyl extraction preparation is a method of extracting insoluble and soluble tau from brain homogenates or cell lysates using sarkosyl as a detergent to separate insoluble tau from soluble tau. Since the initial publication of the method, sarkosyl-insoluble tau has been considered a good approximation to aggregated tau, while sarkosyl-soluble tau is thought to consist of soluble tau monomers and oligomers (Greenberg and Davies, 1990; Julien et al., 2012).

For sarkosyl extraction, frozen mouse hippocampal sections were homogenised in fresh homogenisation buffer using a Tissue Master-125 Omni International mechanical homogeniser with a final concentration of 100 mg/ml. Samples were centrifuged in a desktop centrifuge (Spectrafuge 24D, Jencons-PLS) at 16,300 g(av) for 20 min at 4 °C. Supernatant (low speed supernatant, LSS) was collected and an aliquot was frozen at -20 °C for total brain western blots. This fraction is the total brain homogenate fraction. Pellets are stored at -20 °C. Sodium lauroyl sarcosinate (sarkosyl) was added to the rest of the supernatant resulting in a final sarkosyl concentration of 1 %. Samples are incubated at ambient temperature for 30 min with shaking before centrifuging at 100,000 g(av) for 1 h at ambient temperature using a Beckman Ultracentrifuge with a TLA 55 rotor. High speed supernatant (HSS) was collected at stored at -20 °C, this is the sarkosyl-soluble tau fraction. The remaining pellet was washed with 1 % sarkosyl by centrifuging at 100,000 g(av) for 10 min, then resuspended in 2x Laemmli buffer with 5 % (v/v) ß-merceptoethanol. This is the sarkosyl insoluble tau fraction and was stored at -20 °C. For western blots the LSS and HSS fractions were mixed 1:1 with 2x Laemmli buffer with 5 % (v/v) ß-mercaptoethanol.

2.4.2 Protein standardisation

Two protein standardisation assays were used in this thesis. The first, the bicinchoninic acid (BCA) assay was used for all experiments (all experiments except Alphascreen assays) carried out at King's College London. However, the Bradford assay was used to standardise protein for Alphascreen experiments carried out at Eli-Lilly UK, as this was the standard total protein assay used in this laboratory.

Bicinchoninic acid (BCA) assay (Smith et al., 1985)

Materials

BSA	2 mg/ml BSA (Thermo Fisher Scientific)
BCA protein assay	BCA Reagent A (Thermo Fisher Scientific) BCA Reagent B (Thermo Fisher Scientific)

Methods

2 mg/ml BSA was diluted with XSLB to create a set of protein standards ranging in concentration from 0 mg/ml to 2 mg/ml. Protein standards were made fresh for each assay. Equal volumes of samples and protein standards were added to a 96-well plate in duplicate and BCA assay reagents were added according to the manufacturer's instructions. Samples were incubated in the dark at 37 °C for 30 min before the plate was read at 550 nm using a Wallac 1420 Victor3™ plate reader. A standard curve was determined and the sample readings were compared to this to determine sample concentrations in µg/ml. Samples were diluted as appropriate using XSLB to normalise protein concentrations.

Bradford assay

Materials

BSA	2 mg/ml BSA
Coomassie Plus	Coomassie Plue protein assay reagent (Thermo Fisher Scientific)

Methods

Medium samples used in Alphascreen assays were standardised to the total protein concentration of their equivalent cell lysates. Total protein concentration was determined using a Bradford assay (Bradford, 1976). 2 mg/ml BSA was diluted in tau fractionation buffer according to the manufacturer's instructions to create a set of standards of known protein concentration ranging from 0 mg/ml to 2 mg/ml. Cell lysates were diluted 1:1 with tau fractionation buffer. Samples and protein standards were added to a 96-well plate in duplicate. 300 µl coomassie plus reagent was added to each well. The colour reaction was read at 595 nm immediately using a Molecular Devices Precision Microplate Reader. A standard curve was determined and the sample readings were compared to this to determine sample concentrations in µg/ml. Samples were diluted as appropriate using tau fractionation buffer to normalise protein concentrations.

2.5 Immunostaining

2.5.1 Immunocytochemistry (ICC) of primary rat cultures

Materials

4 % Paraformaldehyde (PFA)	4 % (v/v) PFA in PBS from 16 % liquid stock

Permeabilisation solution	0.1 % (v/v) Triton X-100 in PBS
Blocking solution	3 % (w/v) BSA in PBS with 0.05 % (v/v) Tween 20
Hoechst 33342	5 µg/ml Bisbenzimide H33342 trihydrochloride in PBS

Antibodies

Immunocytochemistry (ICC) antibodies were blocked with 3 % BSA with 0.05 % Tween-20. Primary antibodies were incubated for 2 h. Secondary antibodies were incubated for 1 h.

Antibody	Species	Epitope	Dilution	Source
GFAP	Rabbit polyclonal	Glial fibrillary acidic protein	1:1000	Dako (Ely, UK)
MAP2	Rabbit polyclonal	Microtubule-associated protein 2	1:500	Merck Millipore (Watford, UK)
MAP2 (5F9)	Mouse monoclonal	Microtubule-associated protein 2	1:500	Merck Millipore
NF-κB	Mouse monoclonal	Residues 120-239 on the N-terminus of NF-κB p50	1:50	Santa Cruz Biotechnology

Table 2.4: Primary antibodies used in ICC
Antibody name, species, reactivity, dilution and source shown.

Antibody	Species	Dilution	Source
Anti-mouse Alexa-Fluor 568	Goat	1:1000	Invitrogen
Anti-rabbit Alexa-Fluor 488	Goat	1:1000	Invitrogen

Table 2.5: Secondary antibodies used in ICC
Antibody reactivity, species, dilution and source shown.

Methods

ICC was carried out according to the protocol published in Garwood et al. (2011). Cells grown on coverslips were washed in PBS, fixed with 4 % PFA (10 min, ambient temperature) and permeabilised with permeabilisation solution (3 min, ambient temperature). Blocking solution was used to block non-specific binding for 30 min at ambient temperature. Cultures were incubated, in the dark, with primary antibodies in blocking solution for 2 h at ambient temperature (for antibody list, see **Table 2.4**). The primary antibodies were removed and the cells were washed and fluorophore conjugated secondary antibodies diluted blocking solution added (see **Table 2.5**; 1 h, ambient temperature, in the dark). After washing, DNA in cell nuclei was stained with Hoescht-33342 dye (5 µg/ml, 2 mins, ambient temperature, dark) before being washed and mounted onto microscope slides using fluorescent mounting medium (Dako). Cells were visualised, and images taken, using a Leica DM5000 B fluorescence microscope (Leica Miscrosystems CMS, Mannheim, Germany).

2.5.2 Immunohistochemical (IHC) staining of human post-mortem brain sections

Materials

BOND Polymer Detection 3,3'-diaminobenzidine (DAB) kit	All reagents supplied complete by manufacturer, except the following:
Formic acid	80 % (v/v) formic acid
Hydrogen peroxidase	3 % (v/v) hydrogen peroxidase

Methods

As previously published (Kurbatskaya et al., 2016) staining of human post-mortem brain samples was carried out as follows: 7 µm tissue sections were cut from formalin-fixed, paraffin-

embedded post-mortem human brain samples. Sections were stained using a BOND-MAX autostainer (Leica) and BOND Polymer Detection (DAB) kits.

For tau staining, sections were incubated with BOND Epitope Retrieval Solution 1 for 20 mins for heat induced epitope retrieval to improve antigen binding. Sections were deparaffinised and endogenous peroxidase activity inhibited by a 30 min sample incubation in hydrogen peroxidase. Sections were incubated overnight with a total tau antibody (AT8, Thermo Scientific; dilution factor 1:500) at 4 °C. Sections were incubated with the linking post-primary antibody and then the polymeric HRP-secondary antibody conjugates, according to the manufacturer's instructions. The antibody complex was visualised with DAB.

For Aß staining, sections were pre-treated with 80 % formic acid for 1 h. Sections were deparaffinised and endogenous peroxidase activity inhibited by a 30 min sample incubation in hydrogen peroxidase. Sections were incubated overnight with a Aß antibody (ß-A4; Covance; dilution factor 1:6000) at 4 °C. Sections were incubated with the linking post-primary antibody and then the polymeric HRP-secondary antibody conjugates, according to the manufacturer's instructions. The antibody complex was visualised with DAB.

All samples were counterstained with hematoxylin and eosin (H&E).

2.6 Western blotting

2.6.1 Materials

Sodium dodecyl sulphate-polyacrylamide gel electrophoresis (SDS-PAGE)

Gels for SDS-PAGE were prepared using stock solutions purchased from National Diagnostics (Atlanta, GA, US). Final gel compositions in ultrapure H_20 were:

Tris-glycine gels

10 % Resolving gel, pH 8.8	10 % (v/v) acrylamide, 25 % (v/v) resolving buffer, 0.01 % (w/v) ammonium persulphate (APS), 0.1 % (v/v) N,N,N',N' tetramethylethylenediamine (TEMED)
12 % Resolving gel, pH 8.8	12 % (v/v) acrylamide, 25 % (v/v) resolving buffer, 0.01 % (w/v) APS, 0.1 % (v/v) TEMED
4 % Stacking gel, pH 6.8	4 % (v/v) acrylamide, 25 % (v/v) stacking buffer 0.075 % (w/v) APS, 0.1 % (v/v) TEMED
Running buffer	25 mM Tris (Fisher Scientific, Fairlawn, NJ), 192 mM glycine (Fisher Scientific), 1 % (w/v) SDS
Protein molecular weight marker	Precision Plus Protein™ All Blue Prestained Protein Standards (BioRad Laboratories, Hercules, CA)

Tris-tricine gels

Tris-HCl/SDS, pH 8.45	3 M Tris-HCl, pH 8.45 with 0.3 % (w/v) SDS
16 % Resolving gel	990 mM Tris-HCl/SDS, pH 8.45, 16 % (v/v) acrylamide, 10 % (v/v) glycerol, 0.025 % (w/v) APS, 0.05 % (v/v) TEMED

10 % Spacing gel	990 mM Tris-HCl/SDS, pH 8.45, 10 % (v/v) acrylamide, 10 % (v/v) glycerol, 0.025 % (w/v) APS, 0.05 % (v/v) TEMED
4 % Stacking gel	750 mM Tris-HCl/SDS, pH 8.45, 4 % (w/v) acrylamide, 0.1 % (w/v) APS, 0.025 % (v/v) TEMED
Cathode buffer, pH 8.25	100 mM Tris-base, pH 8.2, 100 mM tricine, 1 % (w/v) SDS
Anode buffer, pH 8.9	200 mM Tris-HCl, pH 8.9

Western blotting

Transfer buffer	25 mM Tris-base, 192 mM glycine, 20 % (v/v) methanol in ultrapure H_20
Washing buffer	TBS containing 0.05 % (v/v) Tween-20 (TBS-T)
Blocking solutions	5 % (w/v) non-fat skimmed milk powder in TBS-T Odyssey block buffer (Li-Cor Biosciences, Lincoln, NE, US)

Native PAGE gels and western blots

All reagents were diluted in ultrapure H_2O unless otherwise stated.

Tris-borate EDTA (TBE), pH 8.3	90 mM Tris, 90 mM boric acid, 2 mM EDTA, pH 8.0
4 % Non-denaturing resolving gel	1 % (v/v) TBE, 4 % (w/v) acrylamide, 0.05 % (w/v) APS, 0.06 % (v/v) TEMED
22 % Non-denaturing resolving gel	1 % (v/v) TBE, 22 % (w/v) acrylamide, 0.05 % (w/v) APS, 0.06 % (v/v) TEMED
4 % Non-denaturing stacking gel	1 % (v/v) TBE, 4 % (w/v) acrylamide, 0.05 % (w/v) APS, 0.1 % (v/v) TEMED
4x Loading buffer	60 % (w/v) sucrose, 0.1 % (w/v) bromophenol blue
Protein molecular weight marker	NativeMark molecular weight marker (Invitrogen)
Ponceau S solution	0.1 % (w/v) ponceau S, 5 % (v/v) acetic acid
Tris-western (TW) buffer	150 mM NaCl, 10 mM Tris-HCl, 0.1 % (v/v) Tween-20

Blocking buffer	7 % (w/v) non-fat powdered milk in TW buffer

Enhanced chemiluminesence (ECL)

ECL detection solution	Pierce ECL Detection Reagent A (Thermo Fisher Scientific) and Pierce ECL Detection Reagent B (Thermo Fisher Scientific) mixed according to the manufacturer's instructions.

2.6.2 Antibodies

Antibodies were blocked with 5 % non-fat skimmed milk in TBS-T, unless otherwise stated. Primary antibodies were incubated overnight. Secondary antibodies were incubated for 1 h.

Antibody	Species	Epitope	Dilution	Source
Actin	Mouse monoclonal	ß-Actin	1:10000	Abcam (Cambridge, UK)
Actin	Rabbit polyclonal	ß-Actin	1:5000	Abcam
ß-amyloid (3D6)	Mouse monoclonal	Residues 1-5 on ß-amyloid	1:1000	Eli Lilly and Co.
ß-amyloid (4G8)	Mouse monoclonal	Residues 17-24 on ß-amyloid	1:1000	Covance (Princeton, NJ, US)
ß-amyloid (6E10)	Mouse monoclonal	Residues 1-16 on ß-amyloid	1:1000	Covance
Cdk5 (J-3)	Mouse monoclonal	Cyclin-dependent kinase 5	1:25	Santa Cruz Biotechnology
CP13	Mouse monoclonal	Tau: phosphorylated serine residue 202	1:400	P. Davies (The Feinstein Institute for Medical Research, Manhasset, NY, US)
CP27	Mouse monoclonal	Total human tau	1:200	P.Davies

GFAP	Rabbit polyclonal	Glial fibrillary acidic protein	1:2000	Dako
GSK-3α/ß	Mouse monoclonal	Gycogen synthase kinase 3 α/ß	1:1000	Enzo Life Sciences (Exeter, UK)
Iba1	Mouse monoclonal	Human Iba1	1:500	Merck Millipore
IκBα	Rabbit monoclonal	Serine 32 region on IκBα	1:1000	Abcam
Nrf2	Rabbit polyclonal	Nuclear factor erythroid 2-related factor 2	1:500	Abcam
Nrf2 (Ser40)	Rabbit polyclonal	Nrf2: phosphorylated serine residue 40	1:200	Bioss (London, UK)
NSE	Mouse monoclonal	Neuron specific enolase	1:10000	Dako
p35 (C-19)	Rabbit polyclonal	C-terminus of p35	1:25	Santa Cruz Biotechnology
pGSK-3α/ß (Ser21/9)	Rabbit polyclonal	GSK-3α/ß: phosphorylated Ser residues 21(α) & 9 (ß)	1:1000	Cell Signaling Technology (Danvers, MA, US)
PHF1	Mouse monoclonal	Tau: phosphorylated residues Ser396/404	1:2000	P. Davies
PSD-95	Rabbit polyclonal	Post-synaptic density 95	1:1000	Cell Signaling Technology
PSD-95 (6G6-1C9)	Mouse monoclonal	Post-synaptic density 95	1:1000	Merck Millipore
Synapsin	Mouse monoclonal	Synapsin-1	1:1000	Merck Millipore
Synaptophysin	Rabbit polyclonal	Synaptophysin	1:1000	Enzo Life Sciences
Tau-1	Mouse monoclonal	Tau: dephosphorylated Ser199/202/Thr205	1:5000	Merck Millipore
Total tau	Rabbit polyclonal	Tau: residues 243-441 on C-terminus	1:10000	Dako
TP007	Rabbit polyclonal	Amino acids 1-16 of tau (N-terminus)	1:2000	Made in house
TP70	Rabbit polyclonal	Amino acids 428-441 of tau (C-terminus)	1:1000	Made in house
Vimentin	Rabbit polyclonal	Epitopes surrounding Arg28 of human vimentin	1:500	Cell Signalling Technology

Table 2.6: Primary antibodies used in western blotting
Antibody name, species, reactivity, dilution and source shown.

Antibody	Species	Dilution	Source
Anti-mouse Alexa Fluor 680	Goat	1:10000	Invitrogen
Anti-mouse HRP-linked secondary antibody	Goat	1:2000	GE Healthcare (London, UK)
Anti-rabbit HRP-linked secondary antibody	Goat	1:2000	GE Healthcare
Anti-rabbit IRDye800	Goat	1:5000	Invitrogen

Table 2.7: Secondary antibodies used in western blotting
Antibody reactivity, species, dilution and source shown. Antibodies were compatible with Li-Cor Odyssey Imaging System or ECL.

2.6.3 Methods

All gels run were 10 % tris-tricine gels unless otherwise stated. Likewise, all western blots were developed using the Odyssey Imaging System unless stated otherwise.

Tris-glycine gels

Samples were loaded into 12 % or 10 % (w/v) tris-glycine resolving gels with 4 % (w/v) tris-glycine stacking gel and a protein ladder. Proteins were electrophoresed at 150 V for 80 min in tris-glycine running buffer using BioRad Mini-PROTEAN® Tetra Cell Systems (83 mm x 73 mm gels; BioRad Laboratories). Proteins were transferred onto 0.45 µm nitrocellulose membrane (Whatman, Maidstone, UK) using a Mini Trans-Blot® Cell (BioRad Laboratories) wet transfer system at 100 V for 60 min in transfer buffer.

Tris-tricine gels

Samples were loaded onto 16 % (w/v) tris-tricine resolving gels (83 mm x 73 mm gels) with a 1 cm 10 % (w/v) tris-tricine spacer gel and 4 % (w/v) tris-tricine stacking gel and a protein ladder. Proteins were electrophoresed at 80 V for 15 min, or until samples had passed through the stacking gel. Electrophoresis then continued at 100 V for 6 h. Electrophoresis was carried out using BioRad Mini-PROTEAN® Tetra Cell Systems. Proteins were transferred onto 0.2 µm nitrocellulose membrane using a Mini Trans-Blot® Cell (BioRad Laboratories) wet transfer

system at 13 V overnight (17 h) in transfer buffer. Membranes were incubated in 10 % acetic acid for 30 min then washed three times.

For all membranes (except native PAGE):

Non-specific binding was blocked by incubating membranes in blocking solution (5 % non-fat milk unless otherwise stated) for 1 h at ambient temperature. Membranes were then incubated in primary antibodies in blocking solution overnight at 4 °C with rocking (for antibody list see **Table 2.6**). After washing three times for 10 mins with TBS-T, membranes were incubated in secondary antibodies in blocking solution (1 h, ambient temperature, with rocking. For antibodies see **Table 2.7**). Membranes were washed three times for 10 min before visualisation and quantification with the Odyssey Clx Imaging System and Licor Image Studio Lite software, or enhanced chemiluminescence (ECL).

ECL

Nitrocellulose membranes incubated with HRP-conjugated antibodies were washed three times for 10 min and incubated in ECL detection solution (Pierce™, Thermo Scientific) according to the manufacturer's instructions. Membranes were secured in a plastic wallet inside a film cassette. In the dark room, Amersham Hyperfilm (GE Healthcare) is exposed to the membrane in the cassette and then developed using a Konica Minolta SRX-101A film processor (Konica Minolta UK Ltd., Basildon, Essex, UK).

Native PAGE gels

Non-denaturing 4 % - 22 % (w/v) gradient resolving gels were cast using a two-chamber gradient maker and peristaltic pump system and topped with 4 % (w/v) non-denaturing stacking gel. Gels were pre-run at 125 V for 30 min. Samples were prepared by mixing 1:3 with 4x loading buffer and loaded into the gels with a NativeMark protein ladder (Thermo Scientific). Gels were electrophoresed according to the following steps in tris/borate EDTA (TBE) buffer, at 4 °C:

1. 25 V for 15 min
2. 50 V for 15 min

3. 60 V for 24 h

Proteins were transferred onto 0.45 µm nitrocellulose membrane using a wet transfer system at 25 V for 45 min at 4 °C in transfer buffer. Prior to blocking, membranes were incubated in Ponceau S solution for 15 min at ambient temperature. Membranes were destained to check for efficient transfer and to highlight protein markers. Membranes were blocked in blocking buffer overnight at 4 °C with shaking. The following day, membranes were incubated in primary antibody in blocking buffer for 2 h at ambient temperature with shaking (for primary antibody list see **Table 2.6**). Membranes were washed three times with TW buffer before 1 h incubation with HRP-linked secondary antibody in blocking buffer (for secondary antibody list see **Table 2.7**). Again, membranes were washed three times with TW buffer. Membranes were incubated in SuperSignal® West Dura Extended Duration Substrate (Thermo Scientific) for 5 min and visualised using an ImageQuant machine (GE Healthcare Life Sciences, Little Chalfont, Buckinghamshire, UK).

2.7 Immunoassays

2.7.1 Standard tau ELISA

Materials

Blocking buffer	5 % (w/v) non-fat milk in PBS
TMB substrate solution	Tetramethylbenzidine (TMB)-ultra reagent (Thermo Scientific)
Stopping solution	1 M HCl

Antibodies

Standard tau ELISA antibodies were blocked in 5 % non-fat skimmed milk in PBS. Primary antibodies were incubated overnight. Secondary antibodies were incubated for 2 h.

Tau sandiwch ELISA capture antibody was incubated for 8 days and blocked with 50 % StartingBlock in TBS. The primary antibody was incubated overnight and blocked with 50 % SuperBlock in TBS. The secondary antibody was incubated for 1 h in 5 % non-fat skimmed milk in TBS.

Antibody	Species	Epitope	Dilution	Source
CP13	Mouse monoclonal	Tau: phosphorylated at Ser202	1:100	P. Davies
MC1	Mouse monoclonal	Tau: conformation dependent antibody (epitopes 312-322)	1:100	P. Davies
PHF1	Mouse monoclonal	Tau: phosphorylated at Ser396/404	1:400	P. Davies
Tau-1	Mouse monoclonal	Tau: dephosphorylated Ser199/202/Thr205	1:1000	Millipore
Total tau	Rabbit polyclonal	Tau: residues 243-441 on C-terminus	1:40000	Dako

Table 2.8: Primary antibodies used in standard tau ELISA
Antibody name, species, reactivity, dilution and source shown.

Antibody	Species	Dilution	Source
Anti-mouse HRP-linked secondary antibody	Goat	1:500	GE Healthcare
Anti-rabbit HRP-linked secondary antibody	Goat	1:500	GE Healthcare

Table 2.9: Secondary antibodies used in standard tau ELISA
Antibody reactivity, species, dilution and source shown.

Methods

A standard tau ELISA measuring levels of intracellular total and phosphorylatd tau has been developed in house (unpublished).

Samples were diluted to 30 µg/ml in PBS and added to Nunc Maxisorp 96-well plates in duplicate. XSLB diluted in PBS was used as a blank. Samples were allowed to dry onto plates overnight at 37 °C in a non-humidified incubator. Non-specific binding was blocked using blocking buffer for 1 h at ambient temperature. Primary antibodies were diluted in blocking buffer, added to the plates and incubated overnight at 4 °C with shaking (**Table 2.8**). Plates were washed five times with PBS-T. Secondary antibodies were diluted in blocking buffer, added to the plates and incubated for 2 h at ambient temperature with shaking (**Table 2.9**). Plates were washing five times with PBS-T. 3,3',5,5',-tetramethylbenzidine (TMB) substrate solution was added and incubated at ambient temperature for 1-5 minutes or until a medium strength blue colour was observed. The reaction was stopped with stopping solution and the plate was read immediately at 450 nm using a Wallac 1420 Victor3™ plate reader.

2.7.2 Tau sandwich ELISA

Materials

ELISA coating buffer, pH 7.2	15.6 mM K_2HPO_4, 25.6 mM KH_2PO_4, 136.9 mM NaCl, 1.3 mM EDTA, 7.7 mM NaN_3 in ultrapure H_2O
ELISA wash buffer	50 mM TBS containing 0.05 % (v/v) Tween-20
Block buffer	50 % (v/v) StartingBlock™ blocking buffer (Thermo Fisher Scientific) in 50 mM TBS

Primary antibody block buffer	20 % (v/v) SuperBlock™ blocking buffer (Thermo Fisher Scientific) in 50 mM TBS
Secondary antibody block buffer	5 % (w/v) skimmed milk powder in 50 mM TBS
TMB substrate solution	TMB-ultra reagent
Stopping solution	1 M HCl

Antibodies

Antibody use	Antibody	Species	Epitope	Dilution	Source
Capture	BT2	Mouse monoclonal	Total tau, epitopes 194-198	1:100	Thermo Fisher Scientific
Primary	Total tau	Rabbit polyclonal	Tau: residues 243-441 on C-terminus	1:1000	Dako
Secondary	Anti-rabbit HRP-linked secondary antibody	Goat	Rabbit IgG (heavy and light chains)	1:500	GE Healthcare

Table 2.10: Antibodies used in tau sandwich ELISA
Use of antibody in ELISA, antibody name, species, reactivity, dilution and source shown.

Methods

A sandwich ELISA for the detection of low concentrations of extracellular total tau has been developed in house (unpublished).

The capture antibody was diluted in ELISA coating buffer and added to the required number of wells of a 96-well Nunc Maxi-Sorp plate (**Table 2.10**). The plate was sealed and incubated at 4 °C with shaking for 8 days to allow the antibody to adsorb to the plastic. Plates were washed three times with ELISA wash buffer to remove any unadsorbed capture antibody before incubation with block buffer for 4 h at ambient temperature with shaking to block any non-

specific binding. After 4 h, block buffer was removed and the plate was washed a further three times with wash buffer.

To collect samples of medium containing extracellular tau, Neurobasal medium was removed from 14 DIV primary cell cultures and replaced with HBSS. Cultures were incubated for 4 h in normal conditions. After 4 h, HBSS was collected and centrifuged for 5 min at 7200 g(av) at 4 °C to remove cell debris before being added, undiluted, to the ELISA plate in triplicate. Samples were incubated at 37 °C, sealed without rocking, overnight. Blank HBSS was used as a negative control.

Samples were removed and the plate was washed three times with wash buffer. Primary antibody was diluted in primary antibody blocking solution and added to the plate (**Table 2.10**). The plate incubated overnight at ambient temperature on a rocker. The primary antibody was removed and the plate was washed three times with wash buffer. Secondary antibody was diluted in secondary antibody blocking buffer and added to the plate for incubation at ambient temperature on a rocker for 1 h (**Table 2.10**). The plate was washed five times with wash buffer. TMB substrate solution was added to the plate and incubated to allow the solution to react with the secondary antibody. The solution was stopped using stopping solution when a mid-blue colour had developed. The plate was read immediately at 450 nm using a Wallac 1420 Victor3™ plate reader.

2.7.3 Alphascreen

Amplified luminescent proximity homogenous assay (Alpha) screen is a bead-based assay used to investigate molecular interactions, particularly post-translational modifications of proteins, in microplates (Peppard et al., 2003). The technique is based on acceptor and donor beads binding to the protein of interest via two antibodies, the first conjugated to the acceptor bead, the second biotinylated. Once the acceptor bead and the biotinylated antibody have been incubated with the sample, streptavidin-coated donor beads are added. Streptavidin and biotin bind, strongly associating the donor bead with the biotinylated antibody. Donor beads contain

phthalocyanine, a photosensitiser, which converts oxygen to reactive 'singlet oxygen' when exposed to 680 nm light. Singlet oxygen is not a radical but contains one excited electron and has a half-life of 4 µsec allowing it to diffuse up to 200 nm in solution. If an acceptor bead is within range, and therefore bound to the same protein, energy from the singlet oxygen transfers the acceptor bead resulting in the emission of light at 520-620 nm, this can then be detected by a plate reader (**Figure 2.3**). If there are no acceptor beads within range, oxygen singlets fall back to their original state without producing a signal. By using a total protein antibody alongside a phospho-specific antibody, Alphascreens can be used to investigate levels and changes in levels of protein phosphorylation under different treatment conditions.

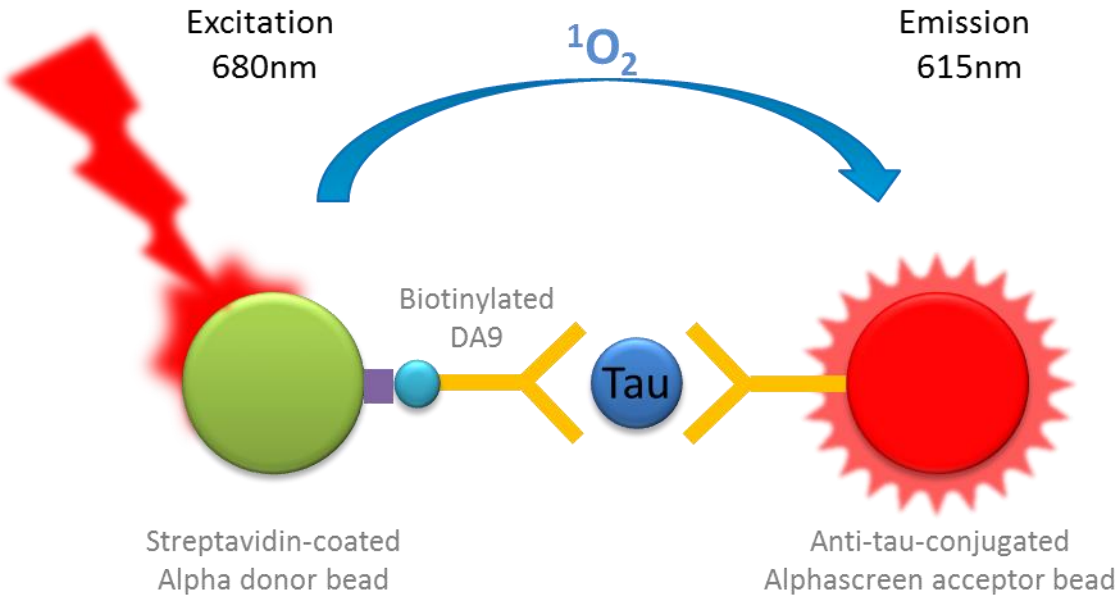

Figure 2.3: Alphascreen assay principle
Tau is bound by an anti-tau-conjugated Alphascreen acceptor bead and biotinylated DA9 (total tau antibody). When streptavidin-coated Alpha donor beads are added they bind strongly to biotinylated DA9. Excitation of a photosensitiser in the donor beads by 680 nm light converts oxygen into singlet oxygen that can transfer to donor beads also bound to the same tau protein and result in light emission at 615 nm. This light emission can be detected on a plate reader and quantified using a standard curve of known tau concentrations.

Materials

Casein buffer	0.1 % casein (from bovine milk) in Dulbecco's-PBS without Ca^{2+} or Mg^{2+}, pH 7.4 (Invitrogen)
Acceptor beads	Unconjugated Alphascreen acceptor beads (Perkin Elmer, Waltham, MA, US)
Donor beads	Alphascreen streptavidin coated donor beads, 5mg/ml (Perkin Elmer)
Edge buffer	1.25 µg/ml D-streptavidin, 1.1 mg/ml biotinylated-antibody, 20 µg/ml acceptor beads, 10 µg/ml P301S brain homogenate

Standard	Starting dilution	End dilution
P301S mouse brain homogenate	1:3	1:4374528
Tg4510 mouse brain homogenate	1:3	1:4374528

Table 2.11: Protein standards used in Alphascreen assays
Standard species, starting dilution and end dilution shown. Mouse brain homogenates were homogenised and sonicated in tau fractionation buffer, then centrifuged at 13,000 rpm to remove debris. Homogenates were then standardised to 1 mg/ml before use in Alphascreens.

Antibodies

Antibody	Species	Epitope	Concentration of biotinylated DA9 required (nM)	Source
TG5	Mouse monoclonal	Tau: residues 220-242	0.098	P. Davies
PHF1	Mouse monoclonal	Tau: phosphorylated residues Ser396/404	0.098	P. Davies
CP13	Mouse monoclonal	Tau: phosphorylated Ser202	0.0245	P. Davies

Table 2.12: Primary antibodies used in Alphascreen assay
Antibody name, species, reactivity, source and the concentration of biotinylated DA9 for required for optimal reactivity.

Methods

Alphascreen medium concentration

Medium from rat primary cultured neurons was concentrated using Centriprep 10K Centrifugal Filter Devices (Millipore). 1 ml medium from 3 wells of a 6 well plate (total 3 ml medium) was pooled into the sample containers of the centrifugal devices. Filters were reassembled and spun at 3000 g(av) for 15 min at ambient temperature in a Sigma 4-16K centrifuge with swinging bucket. Filtrate was decanted and discarded and filters were spun again at 3000 g(av) for 10 min at ambient temperature. Filtrate was discarded and the concentrated sample was collected and used for Alphascreen assays. This method resulted in samples approximately six times as concentrated as the original medium samples (approximately 500 µl volume).

Alphascreen protocol

Conjugated anti-phospho-tau antibody acceptor beads were diluted to 40 µg/ml (for antibody information see **Table 2.12**) and added to the 384-well assay plates. Biotinylated DA9 was also added to the plates at a concentration optimised for efficient interaction with each conjugated acceptor bead (**Table 2.12**). Assay plates were stored at 4 °C. Samples were added to 96-well mother plates without dilution. Two serial 2-fold dilutions in 0.1 % casein buffer were then

Mother plate 1

	1	2	3	4	5	6	7	8	9	10	11	12
A	CTRL	1:2 dilution	1:4 dilution	Minocycline	1:2 dilution	1:4 dilution	P301S	1:128				
B	CTRL	1:2 dilution	1:4 dilution	Minocycline	1:2 dilution	1:4 dilution	1:2	…				
C	CTRL	1:2 dilution	1:4 dilution	Aß+minocycline	1:2 dilution	1:4 dilution	1:4	…				
D	Aß	1:2 dilution	1:4 dilution	Aß+minocycline	1:2 dilution	1:4 dilution	1:8					
E	Aß	1:2 dilution	1:4 dilution	Aß+minocycline	1:2 dilution	1:4 dilution	1:16		…			
F	Aß	1:2 dilution	1:4 dilution	BLANK			1:32		…			
G	Minocycline	1:2 dilution	1:4 dilution	BLANK			1:64		…			
H												

Mother plate 2

	1	2	3	4	5	6	7	8	9	10	11	12
A												
B	Tg4510	1:128		PHF	1:128		14DIV	1:128				
C	1:2	…		1:2	…		1:2	…				
D	1:4	…		1:4	…		1:4	…				
E	1:8			1:8			1:8					
F	1:16		…	1:16		…	1:16		…			
G	1:32		…	1:32		…	1:32		…			
H	1:64		…	1:64		…	1:64		…			

Figure 2.4: Example plates for Alphascreen assay

Mother plate 1 and 2: Experimental samples and protein standards are pipetted into 96-well mother plates according to the plate maps. Experimental samples are diluted two-fold twice across the plate while 21-point standard curves are created down the plate. Assay plate: each coloured well of the assay plate contains biotinylated-DA9 and anti-tau conjugated acceptor beads. Experimental sample and protein standards are pipetted from mother plates into the assay plate according to the colour-coded plate plan. Uncoloured wells are empty.

made. Samples and protein standards (**Table 2.11**) were transferred to each 384-well plate in duplicate (for example plate plan see **Figure 2.4**). Plates were sealed and stored overnight at 4 °C. On day 2, streptavidin-coated donor beads were added to each well in a dim room. Edge buffer was added to the outer wells and plates were incubated in the dark at RT for 3 h with shaking. Plates were read using an EnVision 2103 Multilabel Reader (Perkin Elmer) and analysed using Microsoft Excel.

2.8 Statistical analysis

2.8.1 Protein analysis and cell death assays

All data were assessed using the D'Agostino-Pearson omnibus normality test (Graphpad Prism 6.0 Software) to test whether treatment groups showed a normal distribution. If this test was passed, all data from western blots, LIVE/DEAD assays (except experiments comparing hippocampal and cortical primary cultures) were analysed using a one-way analysis of variance (ANOVA) (Graphpad Prism 6.0 Software) with Tukey's post-hoc analysis. Experiments comparing hippocampal and cortical primary cultures were analysed using a two-way ANOVA (Graphpad Prism 6.0 Software) as there were two independent variable categories (factors), the presence of astrocytes and cell treatment, influencing the results.

One-way ANOVA compares the variability of the mean value within a group (within-group variation) to the mean differences of value between separate groups (between-group variation) (Brace, 2012). The null hypothesis for a one-way ANOVA is that there is no difference between the mean outcome between group and within groups. If there is a difference in the mean outcomes the variation between groups is larger than the variation within groups. If the difference is wide enough statistical significance may be achieved (Kirkwood, 2003).

Tukey's test is a single-step multiple comparison procedure that is used to determine which group means are significantly different from each other. The test is run after a one-way ANOVA

returns statistical significance and compares all groups to each other simultaneously. Differences were considered statistically significant when $p<0.05$.

If data did not pass the D'Agostino-Pearson omnibus normality test, or the n number was too small to carry out the test, a non-parametric Kruskal-Wallis test was used in place of one-way ANOVA, followed by Dunn's multiple comparisons test. This test assesses the differences between three or more groups by ranking all data and comparing the differences in the sum of the ranks from each group to a pre-determined critical chi-squared value. The null hypothesis for Kruskal-Wallis is that there is no difference between each group's rank sum. If the calculated value is more than the chosen critical chi-squared value, then differences can be considered statistically significant. Differences were considered statistically significant when the calculated value was greater than the critical chi-squared value equivalent to $p<0.05$.

Dunn's multiple comparisons test compares the differences in the sum of the ranks of two groups to an expected average. This test can be carried out for all groups simultaneously or for specific groups of interest. The expected average is calculated based on the number of groups and group size. Differences were considered statistically significant when $p<0.05$.

Two-way ANOVA is an extension of one-way ANOVA. The test still compares within-group variation and between-group variation for each independent variable with the null hypothesis being the between-groups variation is not larger than the within-group variation. If the between-groups variation is larger, multiple comparison post-hoc tests can be carried out to investigate which groups differ. However, the primary aim of a two-way ANOVA is to understand if there is an interaction between the effects of the two independent factors on the outcome. The null hypothesis for a two-way ANOVA is that there is no interaction between the two factors and the effects of the factors are completely independent of each other. If there is an interaction between the two factors this means the effect of one of the factors is different for different groups in your second independent variable (for example, if astrocytes improved neuron health for minocycline treated cells but not for Aß treated cells) and statistical significance may be

achieved. Multiple comparison post-hoc tests were used to determine the nature of the interaction. Differences were considered significant when $p<0.05$.

2.8.2 Analysis of Alphascreen and MSD data

Using the nonlinear regression function in GraphPad Prism 6.0, a log of the protein standard data from Alphascreen and MSD experiments was carried out to produce a sigmoidal curve in order to fit the wide data range on one standard curve. The logged concentration of each experimental data point was then read from the curve, before being unlogged to give the concentration of the sample in pg/ml for MSD assays, or an arbitrary value for Alphascreens. MSD assay results were then averaged and plotted as a bar chart to show the concentrations of Aß species. Alphascreen data was subsequently analysed using a two-way ANOVA, as described earlier.

2.8.3 Behavioural analysis of htau mice

Differences in the mouse performance on the Morris water maze were examined using one-way ANOVA with Tukey's post-hoc test or Kruskal-Wallis test, depending on data passing the D'Agostino-Pearson omnibus normality test, for the first DMF trial. The second DMF trial only used two groups of mice: vehicle-treated and DMF-treated so Student's unpaired t-test was used to assess differences between the two groups. The null hypothesis for an unpaired t-test would be that the population mean of two independent groups with an approximately normal distribution are equal. Again differences were considered significant when $p<0.05$.

Chapter 3: Investigating regional differences in Aß-induced effects of astrocytes in primary neuron cultures

3.1 Introduction

As discussed in **Chapter 1:**, there is a wealth of evidence demonstrating important roles of astrocytes in both physiological and pathological brain function (Volterra and Meldolesi, 2005; Sofroniew and Vinters, 2010; Garwood et al., 2011; Navarrete et al., 2013; Zuchero and Barres, 2015; Hu et al., 2016), including in the development of tau pathology and synaptic dysfunction in AD (McGeer and McGeer, 2003; Heneka et al., 2010; Vincent et al., 2010; Liu et al., 2014; Phillips et al., 2014; De Strooper and Karran, 2016).

Most recent updates of the amyloid cascade hypothesis have suggested glial activation and an immune response may bridge the gap between Aß plaques and the development of tau NFTs (Selkoe and Hardy, 2016). Our laboratory has previously shown that in mixed neuron and astrocytic primary cortical cultures, astrocytes accelerate Aß-induced cell death and tau phosphorylation (Garwood et al., 2011). These events were accompanied by an increased release of pro-inflammatory mediators from astrocytes and could be rescued by treatment with minocycline, a tetracycline with anti-inflammatory action (Noble et al., 2009b; Garwood et al., 2011). These findings suggested that soluble factors released by astrocytes into the culture medium are responsible for downstream effects on tau and neuron health. Several other cell culture studies have indicated the important role of astrocytes in mediating the neurotoxic effects of Aß. For example, increasing the levels of astrocyte-released growth factors, such as insulin-like growth factor 1, as opposed to pro-inflammatory signalling factors, was demonstrated to attenuate Aß toxicity (Zhou and Klein, 2012). Furthermore, astrocytes have been found to phagocytose Aß actively removing the toxic peptide (Eugenin et al., 2016).

There is a vast body of evidence linking individual cytokines with tau abnormalities and the development of other AD-related pathology (Curran and O'Connor, 2001; Thornton et al., 2006; Bhaskar et al., 2010; Ashutosh et al., 2011; Ghosh et al., 2013; Tan et al., 2014; Chakrabarty et al., 2015). Cytokine signalling pathways are complex and show many examples of compensation

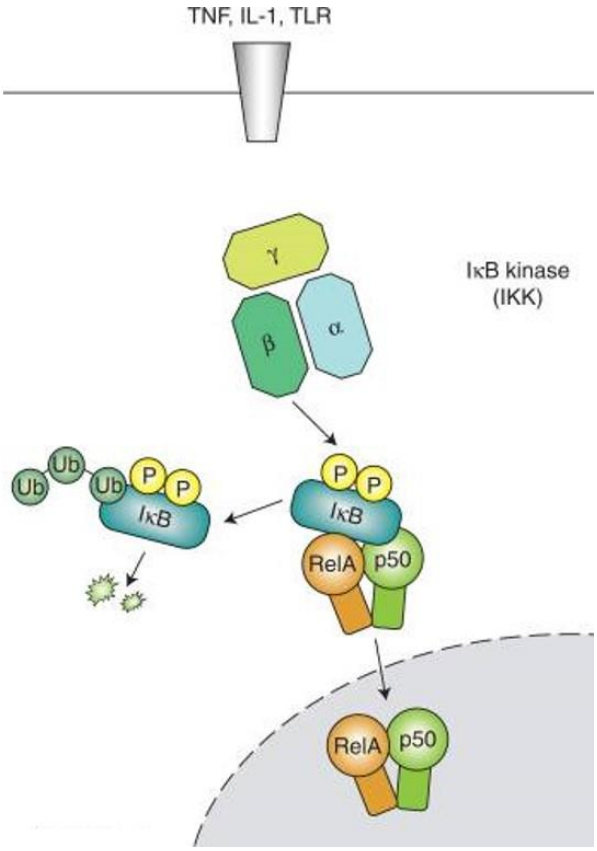

Figure 3.1: NF-κB is activated by IκBα
NF-Kb activation occurs via IκBα, a cytoplasmic protein that inhibits NF-κB activity. Phosphorylation of IκBα by TLR-mediated kinases releases NF-κB allowing it to translocate to the nucleus, while IκBα is ubiquitinated and degraded. Adapted from Lawrence (2009).

and redundancy (Anisman, 2009). There are some points of convergence, however, including the inflammatory pathways initiated by the transcription factor NF-κB (Granic et al., 2009; Shi et al., 2016). NF-κB activation as shown in **Figure 3.1** (Lawrence, 2009). Once in the nucleus NF-κB is transcriptionally active and upregulates the production of multiple pro-inflammatory cytokines, resulting in their release into the extracellular space and activation of multiple inflammatory pathways in both other glial cells and neurons (Lawrence, 2009). Aß and other pro-inflammatory signals, such as oxidative stress or pro-inflammatory cytokines, are thought to activate NF-κB via TLRs and other cell surface receptors (Murgas et al., 2012; Lin et al., 2013). Treatment of cultured glia and neurons with pathological, but not physiological, levels of Aß induces NF-κB activation (Chami et al., 2012). Oxidative stress-induced neurotoxicity, including that caused by high concentrations of Aß, is also mediated by NF-κB-controlled transcriptional upregulation of pro-inflammatory mediators (Jia and Misra, 2007). Finally, some pro-

inflammatory mediators can feedback to further upregulate pro-inflammatory NF-κB transcriptional activity. For example, IL-1ß and TNF-α both increase NF-κB nuclear localisation in neuronal progenitor cells (Taoufik et al., 2011). Thus, induction of NF-κB-driven neuroinflammatory responses can promote many potentially damaging cascades that cumulatively impact on tau processing, synapse and neuron health in AD.

Another area of interest is the trans-synaptic spread of tau pathology through AD brain (Clavaguera et al., 2015). Our laboratory showed that tau release is mediated via neuronal activity in primary culture (Pooler et al., 2013). Astrocytes are critical for synaptic function, therefore it is reasonable to assume that astrocytes may play a role in regulating neuronal tau release and/or tau propagation. Indeed, astrocytes show accumulation of tau that has spread from anatomically connected brain regions (de Calignon et al., 2012). While the mechanisms implicated in these events are not yet understood, activated astrocytes increase their production and release of pro-inflammatory cytokine, IL-18 (Ojala et al., 2009), which can regulate NMDA receptor function (Curran and O'Connor, 2001). Since stimulation of NMDA receptors increases tau release *in vivo* (Yamada et al., 2014), astrocytes may indirectly mediate tau release and spread through the action of IL-18, and possibly other inflammatory mediators. It is also important to consider the role of astrocytes in different brain regions since this is important, not only for their potential roles in tau spread, but also their other functions in a diseased environment. There is evidence suggesting that astrocyte function is specialised according to brain region, thereby allowing astrocytes in each region to best support the specific needs of local neurons (Barbin et al., 1988). Therefore, it is possible that astrocytes may contribute differently to the development of disease-associated tau changes depending on their regional origin. It is important that we develop a better understanding of these regional effects in tractable models of disease.

Previous cell culture work from this laboratory has used synthetic $Aß_{1-42}$ treatments to induce AD-like changes in primary cell cultures (Noble et al., 2009b; Garwood et al., 2011). However, synthetic Aß has been criticised for being non-physiological and often varying in efficacy and

species composition (Soto et al., 1995; Stohr et al., 2012). Aß produced by cell lines containing a mutant form of APP, such as the 7PA2 CHO cell line (Walsh et al., 2002), or Aß produced by primary neuron cultures from transgenic mice, such as Tg2576 neurons (DaRocha-Souto et al., 2012), is thought to be more physiological and is more widely accepted as a cell culture treatment. Aß produced by 7PA2 CHO cells has been found to be synaptotoxic, but does not induce neuron death, at low concentrations (Walsh et al., 2002; Walsh et al., 2005). However, it is not clear whether this Aß is a suitable alternative cell treatment to synthetic Aß. In order to investigate this further, it is important to compare differences between the two Aß sources.

To address these questions, the aims of this chapter are to:

- Characterise different preparations of Aß and compare their effects on astrocytes and neuron health.
- Confirm that astrocytes mediate Aß-induced tau changes and cell death in primary cortical cultures.
- Determine if Aß-stimulated astrocytes have similar influences in primary hippocampal cultures.
- Investigate the potential role of astrocytes in mediating tau release in primary cortical cultures.

3.2 Methods

The materials and methods used in this chapter, including detailed methodology for the production of primary cell cultures, are described in Chapter 2 (**section 2.2.1**). In brief, primary cell cultures were treated for 48 h with 0.5 µM AraC at 3 DIV, 20 µM minocycline at 11 DIV and 10 µM synthetic $Aß_{1-42}$ at 12 DIV. At 14 DIV cultures were lysed or fixed using methods described in Chapter 2, **section 2.4.1**.

Lysates were standardised to total protein concentration using a BCA assay (Chapter 2, **section 2.4.2**) and run on 10 % tris-glycine gels for western blotting (Chapter 2, **section 2.6**). LIVE/DEAD and ICC were carried out with fixed cells at 14 DIV according to methods described in Chapter 2 (**sections 2.5.1**).

Medium for the tau sandwich ELISA and Alphascreens were also collected from 14 DIV primary cultures. For the tau sandwich ELISA medium was concentrated approximately 40 times, as described before use (Chapter 2, **section 2.3**). For Alphascreens medium was concentrated approximately 6 times and was standardised to total lysate protein after use in Alphascreen assays (Chapter 2, **section 2.7.3**).

7PA2 and WT CHO medium was collected when cells were 100 % confluent and stored in 1 ml aliquots in 15 ml falcons at -20 °C. Medium was thawed before use in MSD assays (as described in Chapter 2, **section 2.2.3**) or as a cell culture treatment, when it was diluted 1:1 with Neurobasal medium as described in Chapter 2 (**section 2.2.4**).

Synthetic $Aß_{1-42}$ was frozen a maximum of once after being resuspended at 500 µM in autoclaved Ultrapure H_2O (as described in Chapter 2, **section 2.2.4**). For native and SDS PAGE gels, Aß was standardised to multiple protein concentrations and mixed with the appropriate gel loading buffer before being loaded directly into the gel (Chapter 2, **section 2.6**). For dynamic light scattering (DLS), electron microscopy (EM) and Meso Scale Discovery assay (MSD) protocols, synthetic Aß was diluted further to 50 µM in autoclaved Ultrapure H_2O. Aß was used immediately for DLS and MSD protocols as described in Chapter 2 (**section 2.2.3**). Aß was re-frozen and sent for analysis at Covance for electron microscopy (Princeton, NJ, US; according to the protocol described in Chapter 2 (**section 2.2.3**)).

3.3 Results

3.3.1 Preliminary work

Primary culture characterisation

Before experiments were carried out it was necessary to characterise the cell composition of primary cell cultures to enable proper interpretation of experimental results. Rat primary mixed cultures were prepared from E18 Sprague-Dawley rat embryos and cultured for up to 14 DIV. Cortical and hippocampal cells were cultured separately. At 7 and 14 DIV cultured cells were fixed for LIVE/DEAD assays and ICC.

In order to explore average levels of cell death as untreated cell cultures aged, LIVE/DEAD assays were carried out at 7 and 14 DIV, as described in Chapter 2 (**section 2.1**). Incorporation of dead cell dye by cells with compromised membranes gives a measure of cell death. Cell cultures were subsequently stained with an antibody against GFAP as described in Chapter 2 (**section 2.5**), as a marker for astrocytes, to investigate how much total cell death was accounted for by astrocyte death. Cells were also stained with Hoescht-33342, a nuclear dye. Dead astrocytes are indicated by the incorporation of dead cell dye in cells labelled with the GFAP antibody. Cell cultures prepared using these methods contain only neurons and astrocytes, with negliable microglia (as shown in Garwood et al., 2011). Therefore, if a cell is stained with dead cell dye but not GFAP it can be assumed that the cell is neuronal.

Images taken using a fluorescent microscope showed an increase in cell death as cultures aged for both cortical and hippocampal primary cultures. Furthermore, dead cell dye was largely incorporated into cells that are not labelled with GFAP indicating that cell death was predominantly neuronal. However, a number of large, healthy, Hoechst 33342-labelled nuclei can be observed that are not associated with astrocytes, indicating that even at 14 DIV there are many healthy neurons remaining in the cultures (**Figure 3.2**).

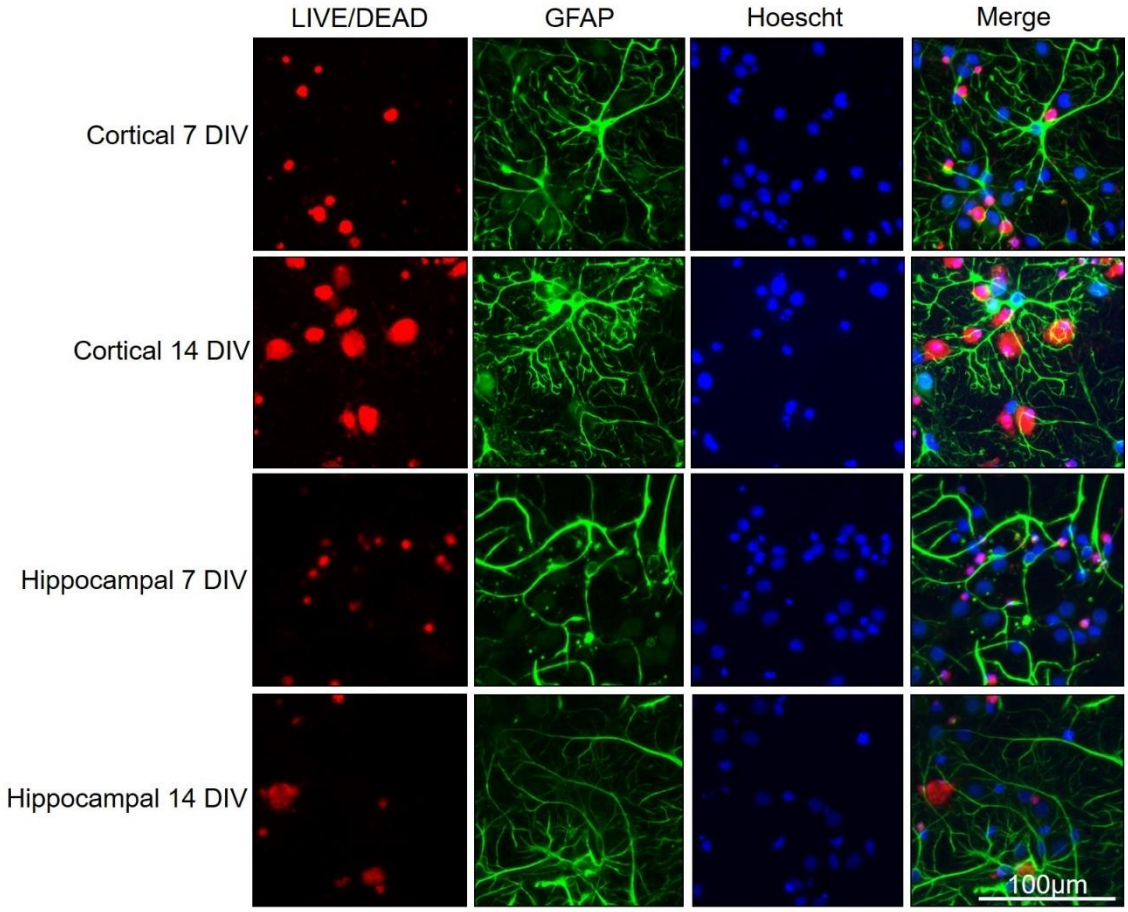

Figure 3.2: Neuronal cell death increases in rat primary mixed glial neuronal cultures with increasing DIV
Representative images, at 40x magnification, showing dead cell dye staining (red), GFAP immunolabelling (green) and Hoescht-33342 (blue) incorporation into cell nuclei in cortical and hippocampal cell cultures at 7 and 14 DIV. Culture type and age are shown on left. Right column shows merge of images. N = 14.

To further investigate the health of untreated primary cell cultures at 7 and 14 DIV, cortical and hippocampal cell cultures were cultured for 7 or 14 DIV before being fixed and immunofluorescently labelled with antibodies against microtubule-associated protein 2 (MAP2), a neuron specific marker, GFAP, an astrocyte specific marker and Hoescht-33342, a nuclear specific dye. Cell morphology was examined as an indicator of dystrophic neurons and activated astrocytes, both found in unhealthy and dying cell cultures (Chen and Herrup, 2008; Avila-Munoz and Arias, 2014). The collected images showed MAP2-labelled neurons with clear axonal and dendritic processes. In all cell culture types and ages these processes were continuous and showed little evidence of breaks or blebbing indicating that cells are healthy (Chen and Herrup,

2008). In addition, in both cortical and hippocampal cultures, neuronal processes became more complex and lengthened with increasing culture time. GFAP labelling within the same cultures showed long astrocytic processes indicative of activated astrocytes, as expected in primary culture conditions (**Figure 3.3**).

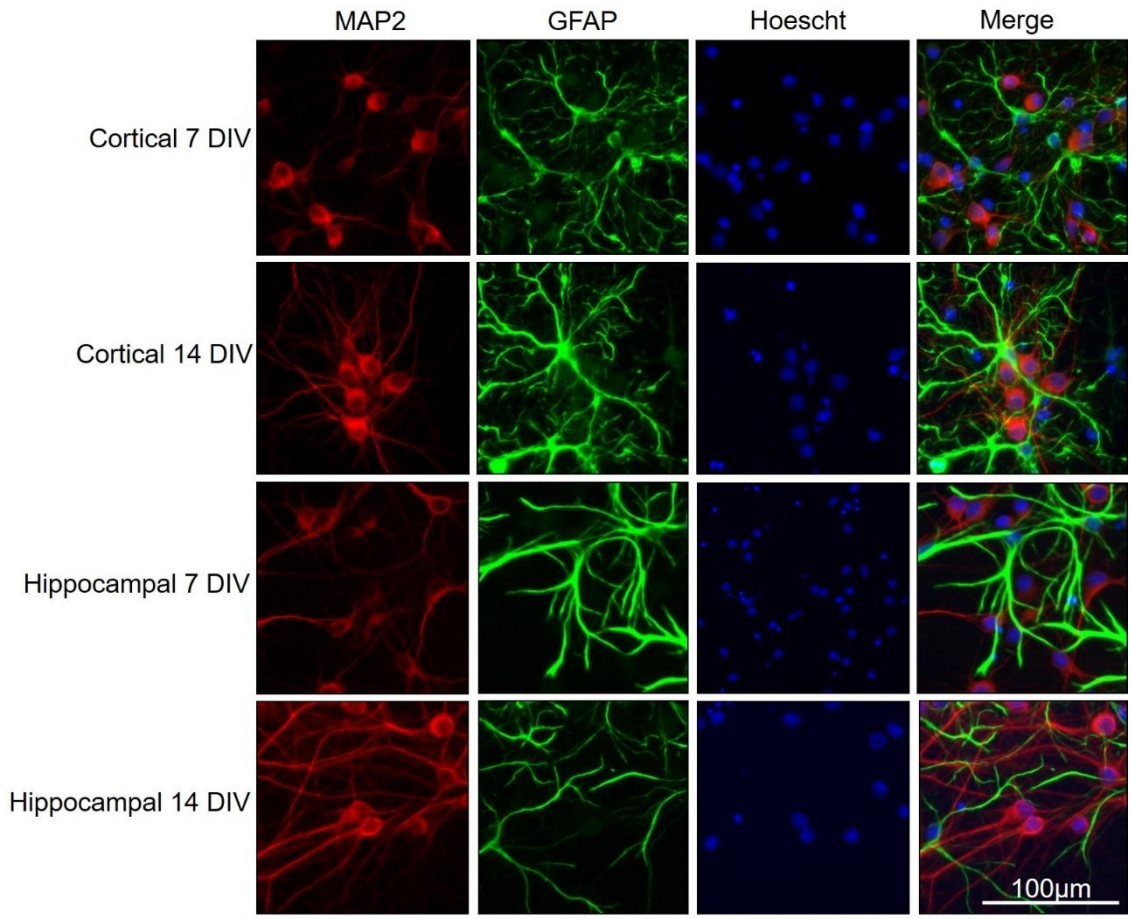

Figure 3.3: Astrocytes and neurons in rat primary mixed glial neuronal hippocampal and cortical cultures
Representative images, at 40x magnification, showing cells in 7 and 14 DIV cortical and hippocampal cell cultures immunolabelled with antibodies against the neuron marker MAP2 (red), and astrocyte marker GFAP (green). Nuclei are stained with Hoescht-33342 (blue). Culture type and age are shown on the left. The right column shows a merged image. N = 14.

As the main aim of experiments in this chapter were to investigate the contribution of astrocytes to Aß-induced tau pathology in primary cell cultures it is important to know the proportion of astrocytes in these cultures. Quantification of astrocyte numbers showed that at 7DIV, primary approximately 10 % of cells in primary cortical cultures were GFAP-positive, rising to 19 % at 14

DIV. In primary hippocampal cultures, the proportion of GFAP-positive cells was approximately 13 % at both 7 and 14 DIV (**Table 3.1**). Astrocytes are known to rapidly proliferate when activation (Sofroniew and Vinters, 2010), and these results might suggest that cortical and hippocampal cultures show different rates of astrocytic proliferation and/or activation. It should be noted that culture health varied between preparations and there were periods of time in which culture health was poor. However, care was taken to use only healthy cultures in the experiments described later in this chapter.

	% GFAP-stained cells	
	Average	± SEM
7 DIV cortical	10.7	1.7
14 DIV cortical	18.6	1.6
7 DIV hippocampal	13.6	2.9
14 DIV hippocampal	13.4	4.2

Table 3.1: The percentage of GFAP-stained cells in 7 DIV and 14 DIV rat primary mixed glial neuronal cortical and hippocampal cultures
Culture type, age, and average ± SEM % of GFAP-stained cells is shown for 7 DIV and 14 DIV cortical and hippocampal cultures. N = 14.

As a primary aim of the experiments conducted in this chapter was to examine changes in tau levels and phosphorylation, it was important to determine the optimum culture DIV for these experiments. Therefore, total and phosphorylated tau amounts were examined in primary cortical cultures at 4, 7, 10 and 14 DIV. Western blotting with antibodies against total and phosphorylation-dependent tau antibodies was performed. Total tau was examined using antibodies raised against the extreme N-terminus (TP007), extreme C-terminus (TP70) and mid-region (DAKO) of tau. Western blots showed that amounts of tau with an intact N-terminus, as detected by TP007, increased as cultures age, being significantly higher at 14 DIV compared to 4 DIV ($p<0.05$; **Figure 3.4 A, B**). Similar changes were observed for tau with an intact C-terminus (TP70) which was significantly higher at 14 DIV compared to 4 and 7 DIV ($p<0.001$ and $p<0.05$, **Figure 3.4 A, C**). These data indicate that amounts of total tau increase the longer cultures are maintained. Similar findings are reported during development *in vivo* (Larcher et al., 1992).

Phosphorylation of tau was investigated in these cultures using several different phosphorylation-specific antibodies. The antibodies selected for this characterisation are used regularly in the literature and bind to epitopes that are abnormally phosphorylated in AD (Evans et al., 2000; Hashiguchi et al., 2002; Noble et al., 2009b; Garwood et al., 2011). Tau-1 recognises tau dephosphorylated at Ser199/202/Thr 205, and no significant changes in Tau-1 levels were found with increasing time in culture (**Figure 3.4 A, D**). CP13 detects tau phosphorylated at Ser202. Tau is normally phosphorylated at this site, with the extent of phosphorylation increasing in AD (Hanger et al., 2009). There were no significant changes in CP13 amounts with increasing time in culture (**Figure 3.4 A, E**). Finally, amounts of tau detected with the PHF1 antibody, which recognises tau phosphorylated at Ser396/404, were significantly increased in 7, 10 and 14 DIV cultures when compared to those cultured for 4 DIV ($p<0.05$, **Figure 3.4 A, F**). Phosphorylation at the PHF1 sites has been found to occur early in AD and is associated with tau detachment from the microtubules (Evans et al., 2000). In human brain, PHF1 is aberrantly phosphorylated in disease conditions (Hanger et al., 2009), however, tau is commonly phosphorylated at this epitope in primary cultures (Bloom et al., 2005; Garwood et al., 2011; Pooler et al., 2012), possibly as a result of the culture conditions.

This preliminary characterisation of primary cell cultures suggests that even though they can display higher levels of cell death, 14 DIV cultures are better suited to the planned experiments since they show a higher composition of astrocytes, together with higher levels of total and phosphorylated tau. Importantly, synapse development occurs between 9-11 DIV in cortical (van Huizen et al., 1985) and slightly earlier in hippocampal (Grabrucker et al., 2009) cultures, and it was also deemed important to use cultures with functional synapses for this work.

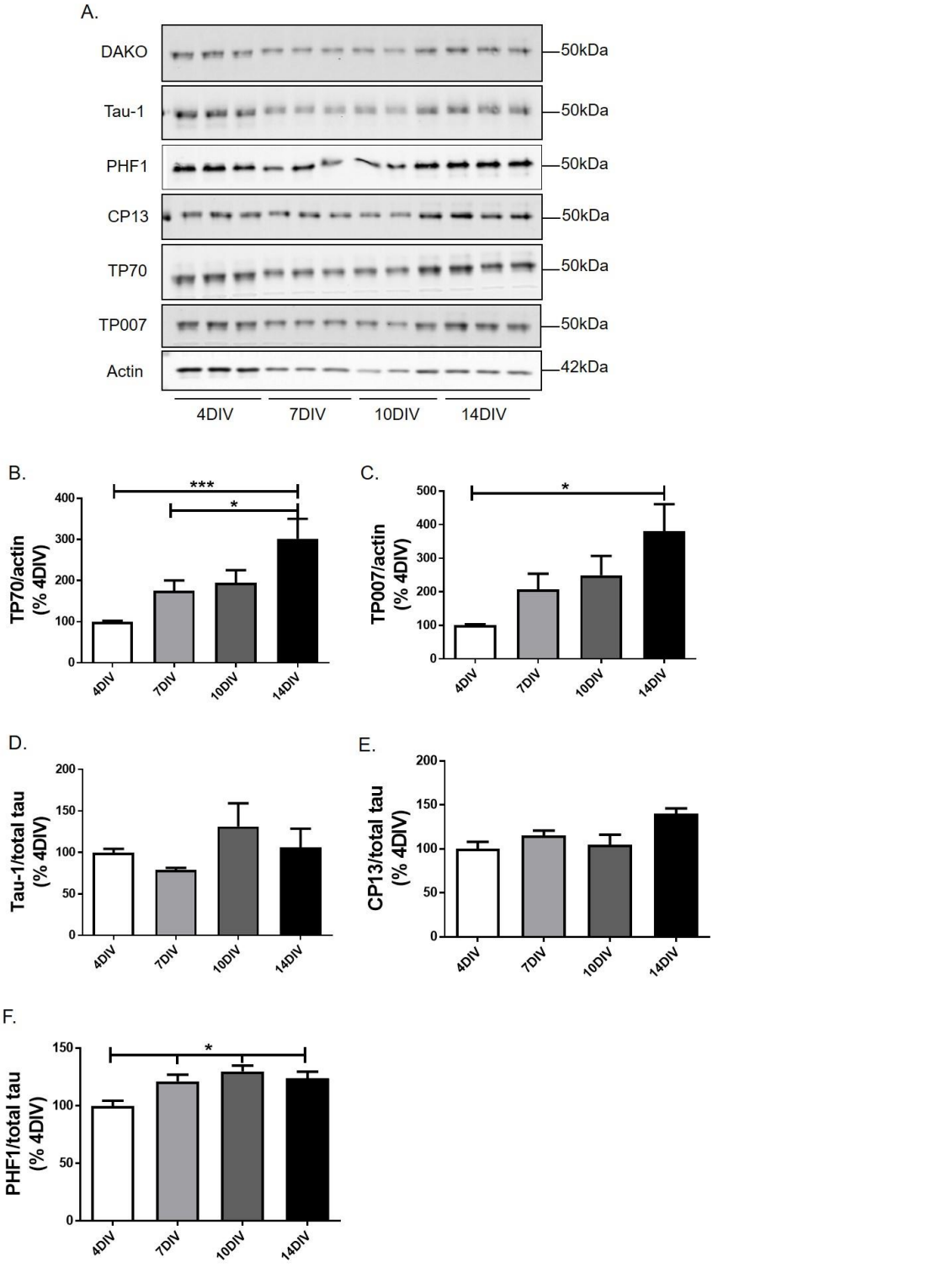

Figure 3.4: Total and phosphorylated tau amounts in rat primary mixed glial neuronal cortical cultures

A. Representative western blots of primary cortical cell culture lysates (4 DIV, 7 DIV, 10 DIV, 14 DIV) probed with antibodies against total tau (DAKO), Tau-1 (tau dephosphorylated at Ser199/202/Thr205), PHF1 (tau phosphorylated at Ser396/404), CP13 (tau phosphorylated at Ser202), TP70 (C-terminal tau), TP007 (N-terminal tau) and ß-actin as a loading control. Molecular weight markers are shown on the right. **B-F.** Bar charts show quantification of **B.** TP70 and **C.** TP007 normalised to ß-actin**, D.** Tau-1, **E.** CP13 and **F.** PHF1 as a proportion of total tau (DAKO). N=9. Values are mean ± SEM as a percentage of 4 DIV. Statistical test used: one-way ANOVA. * = $p<0.05$, *** = $p<0.001$.

3.3.2 Aß characterisation

An important aim of this chapter was to compare different preparations of Aß for use in primary cell cultures. Much of the previous work in this laboratory has used synthetic Aß (Noble et al., 2009b; Garwood et al., 2011). This type of work has been increasingly criticised since it is not considered to represent physiological events in AD brain (Finder et al., 2010). However, since there are standard and highly reproducible methods of preparation and it provides robust results, synthetic Aß is still in regular use in pharmaceutical companies. However, it was important to determine if more physiological sources of Aß provide comparable results. Therefore, different sources of Aß were also characterised.

Synthetic $Aß_{1-42}$ characterisation

To characterise the synthetic $Aß_{1-42}$ used in this chapter, 500 µM stock synthetic $Aß_{1-42}$ was further diluted to 50 µM in autoclaved Ultrapure H_2O and analysed using a dynamic light scattering Dyna Pro Plate Reader which provides information about the size of small molecules in suspension. This allows information about the size of monomers, oligomers and fibrils, and the percentage of total Aß of each size in a sample of Aß. Two types of synthetic $Aß_{1-42}$ provided by Eli Lilly and Co. were used for comparison. The results obtained showed the synthetic preparations used in our laboratory $Aß_{1-42}$ were comprised mainly of medium-high weight oligomers together with a smaller amount of large kDa $Aß_{1-42}$ fibrils (**Table 3.2**). These oligomers were slightly larger than those comprising the synthetic $Aß_{1-42}$ preparations obtained from Eli Lilly (**Figure 3.5 A**).

To further investigate the size of oligomers in synthetic $Aß_{1-42}$ preparations, different concentrations (25, 50 and 75 µM) of $Aß_{1-42}$ were run on native PAGE immunoblots and membranes were probed with 3D6 or 6E10, antibodies against total Aß. Native PAGE gels do not contain detergent and therefore do not break up detergent-soluble oligomers, allowing identification of intact oligomer sizes. Immunoblots showed a strong band indicating $Aß_{1-42}$

oligomers of approximately 100-140 kDa. Several additional bands were apparent at higher molecular weights indicating the presence of larger oligomers, supporting the results obtained from DLS experiments (**Figure 3.5 B,** 3D6 western blots not shown). 50 µM synthetic $Aß_{1-42}$ preparations were further assessed using electron microscopy also showed the relatively uniform presence of predominantly elongated $Aß_{1-42}$ oligomers (**Figure 3.5 C**). Further diluting the synthetic $Aß_{1-42}$ to 10 µM in water allowed visualisation of fibrils, associated with the oligomers, which likely represent the high molecular weight species apparent in the DLS profile (**Figure 3.5 D**). Taken together the results of these experiments provide strong evidence that the synthetic $Aß_{1-42}$ preparations used here contain approximately 86 % medium-high weight oligomers of approximately 100-140 kDa, with the remainder of the peptide aggregating into larger fibrils.

Item	Radius (nm)	Molecular weight (kDa)	% Mass
Peak 1	9.365	117	86.1
Peak 2	46.496	2147	13.9

Table 3.2: Dynamic light scattering profile showing that synthetic $Aß_{1-42}$ is composed of mainly medium-high weight oligomers
The average radius (nm), average molecular weight (kDa) and average percentage mass is shown for each DLS peak. N=3.

To investigate the stability of these $Aß_{1-42}$ oligomers, samples of $Aß_{1-42}$ were subject to SDS-PAGE immunoblotting. SDS can break weak bonds within molecules (Kramer et al., 1980), including Aß, and could, therefore, break the Aß oligomers down into their constituent monomers, dimers and low-weight oligomers which will be reflected in the molecular weights of the peptides detected on western blots. The same synthetic $Aß_{1-42}$ samples as were run on the native PAGE gels were used for this work, and membranes were probed with the same total Aß antibody (6E10). Western blots showed the presence of Aß peptides at approximately 4, 8 and 12 kDa corresponding to the expected mass of Aß monomers, dimers and trimers respectively (**Figure 3.6**), thereby demonstrating that the Aß oligomers in synthetic $Aß_{1-42}$ preparations are

SDS-sensitive, whereas the dimers and trimmers are SDS-stable. There were also smears of Aß at the top of the gel, which were particularly apparent when 50 and 75 µM synthetic $Aß_{1-42}$ was loaded. This suggests the presence of stable Aß oligomers or possibly fibrils in conditions of high Aß concentrations. This is further reflected by the absence of a dose-dependent increase in the amounts of monomers, dimers and trimers.

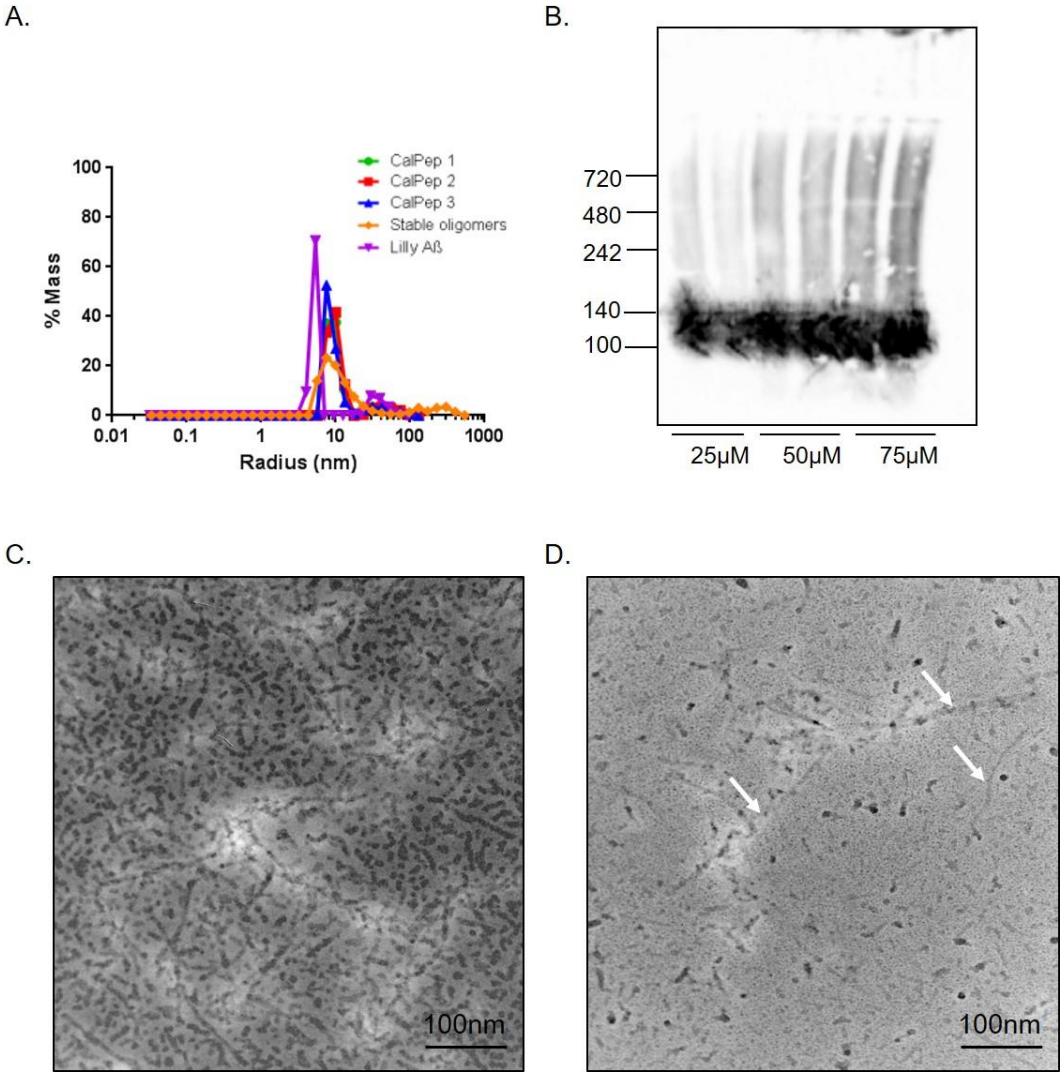

Figure 3.5: Synthetic Aß1-42 preparations are composed mainly of medium-high weight oligomers

A. Line graph showing DLS profile of synthetic $Aß_{1-42}$ with percentage of total $Aß_{1-42}$ mass against radius of molecule detected. Radius of molecule is directly correlated with oligomer size. CalPep 1, 2 and 3 indicate triplicate readings for $Aß_{1-42}$ preparations from our laboratory. Stable oligomers and Lilly Aß indicate positive controls provided by Eli Lilly. **B.** Representative native PAGE gel loaded with $Aß_{1-42}$ samples of different concentrations probed with 6E10 (antibody dilutions: 1:1000), an antibody for total Aß. Secondary antibody used at 1:2000. Molecular markers are shown on the left. **C.** Representative electron microscopy image of 50 µM synthetic $Aß_{1-42}$ sample. Scale bar at bottom right of image. **D.** Representative electron microscopy image of 10 µM synthetic $Aß_{1-42}$ sample, diluted in H_2O. White arrows indicate example fibrils. Scale bar at bottom right of image.

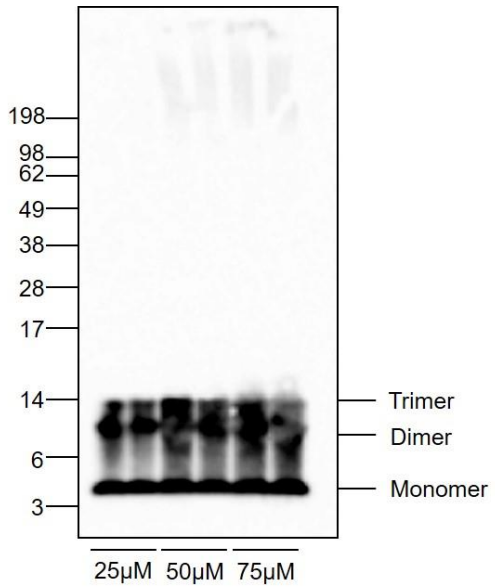

Figure 3.6: Synthetic Aß1-42 oligomers are SDS-sensitive
Representative SDS-PAGE western blot using synthetic $Aß_{1-42}$ of different concentrations (indicated at the bottom of the blot), probed with 6E10 (antibody dilution: 1:1000), a total Aß antibody. Secondary antibody used at a 1:10000 dilution. Molecular weight markers are shown on the left. Aß monomers, dimers and trimers are indicated.

Furthermore, synthetic $Aß_{1-42}$ treated primary cell culture medium was collected from cells immediately before lysis and run on two types of MSD assays to investigate the concentration of Aß and to attempt to detect Aß oligomers. First, Multi-array® plates that were coated with primary capture antibodies 3D6, for total Aß, and A11, for oligomeric Aß, in house at Eli Lilly. Results found nanomolar levels of total Aß (790 nM), very low levels of Aß oligomers (120 nM, **Table 3.3**), suggesting only a small percentage of the Aß in treated cell culture medium is oligomeric. This is inconsistent with DLS and native PAGE results suggesting that synthetic Aß samples are made up predominantly of medium-high weight oligomers. However, this may be due to the structure of the oligomers obscuring a large number of A11 antibody binding areas, resulting in a false, reduced concentration of oligomeric Aß being measured by the MSD assay.
Synthetic Aß-treated primary cell culture medium was also tested on 6E10 V-Plex plates that test for levels of $Aß_{1-38}$, $Aß_{1-40}$ and $Aß_{1-42}$. Results found no detectable $Aß_{1-38}$ or $Aß_{1-40}$ in the samples (data not shown). This is expected as these samples contain synthetic Aß, containing only $Aß_{1-42}$ peptide. The concentration of $Aß_{1-42}$, however was found to be 2.6 μM (**Table 3.3**). This is much less than the original 10 μM concentration treatment originally added to the culture

medium, likely due to the propensity of Aß to stick to surfaces (particularly plastic surfaces) and cells (Hoshino et al., 2002).

However, there is also a discrepancy between the concentration of total Aß as measured by 3D6 and 6E10 in the V-Plex plate (**Table 3.3**). This could be explained by the different primary antibodies binding to different areas of the Aß peptide, with 3D6 only binding to amino acids 1-5 and 6E10 binding to amino acids 1-16. As mentioned previously, the structure of oligomers could be obscuring more of the smaller 3D6 binding regions, resulting in a lower concentration of Aß being detected by the 3D6 antibody.

Antibody	Concentration (µM)
3D6	0.79
A11	0.12
Aß$_{1-42}$ (6E10 V-Plex plate)	2.6

Table 3.3: MSD results for synthetic Aß-treated primary cell culture medium
Antibody used and concentration of Aß (in µM) are shown.

Taken together, the results described in this section demonstrate that the synthetic Aß$_{1-42}$ used in many of the experiments in this chapter is composed of a mixture of SDS-sensitive and insensitive medium-high molecular weight oligomers. Based on the DLS profile and EM images, these oligomers are likely to be a similar size to Aß fibrils found in AD brain, suggesting they may not be as toxic as smaller Aß oligomers (Sengupta et al., 2016).

Characterisation of two more physiological alternatives to synthetic Aß

Two main sources of Aß were investigated as alternatives to synthetic Aß. The first is derived from 7PA2 CHO cells that express the familial AD-causing V717F APP mutation and secrete low levels of Aß oligomers into culture medium that are synaptotoxic (Walsh et al., 2002). The second alternative source is Aß secreted from primary neurons prepared from Tg2576 mice that over-express the familial AD-causing Swedish APP mutation. These neurons also secrete low

levels of Aß into culture medium (DaRocha-Souto et al., 2012) that induces synapse loss (Wu et al., 2012).

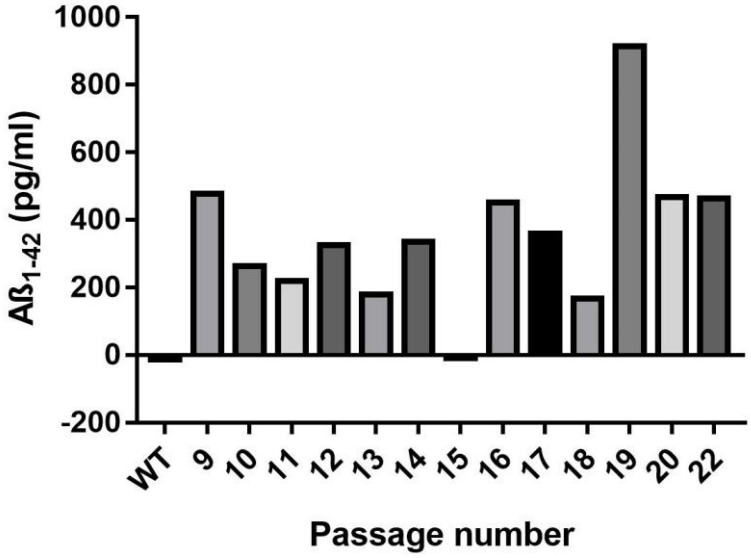

Figure 3.7: Aß$_{1-42}$ concentrations in 7PA2 CHO cell medium vary between passages
Bar chart showing results from an Aß$_{1-42}$ ELISA showing Aß$_{1-42}$ concentration (pg/ml) in 7PA2 CHO medium at different passages of this cell line (N=1).

The amounts and species of Aß secreted into culture medium from these cell sources were first investigated. Medium was collected from 7PA2 CHO cells and wild-type controls as they were passaged from passage (P)9 to P22. The amounts of Aß$_{1-42}$ in medium was determined using Aß$_{1-42}$ ELISAs. The results of this analysis showed that Aß$_{1-42}$ in the medium were at picomolar concentrations and varied with passage (**Figure 3.7**). The lack of Aß detected at P15 suggests a problem with this particular sample. The variation is likely due to changes in cell proliferation, and cell density at the time medium was collected and cells were split. However, it was apparent that, at least up to P22, there appeared to be no considerable decrease in the amount of Aß secreted into culture medium from 7PA2 cells.

In order to further characterise the levels and species of Aß in 7PA2 CHO cell medium, MSD assays were used. Samples were collected from cells at P15 (not those shown in **Figure 3.7**), and total levels of Aß$_{1-38}$, Aß$_{1-40}$ and Aß$_{1-42}$ were determined using a V-PLEX Aß Peptide Panel 1 (6E10) kit. Additionally, a sample of culture medium from Tg2576 primary mouse neurons was used in

this MSD assay to investigate the species of Aß released from these neuronal cultures. Results found levels of $Aß_{1-38}$ and $Aß_{1-40}$ were too low to be detected in 7PA2 CHO medium (**Table 3.4**). However, levels of $Aß_{1-42}$ were found to be 140 pM (648 pg/ml), consistent with the $Aß_{1-42}$ ELISA results described above (**Figure 3.7**). Tg2576 neuronal medium was found to have detectable concentrations of $Aß_{1-38}$ and $Aß_{1-40}$, with both being detected at nanomolar concentrations (**Table 3.4**). The concentration of $Aß_{1-42}$ in the Tg2576 medium was approximately 10 % of the concentration of synthetic Aß species and was at picomolar levels. These concentrations are higher than those of total Aß previously reported (DaRocha-Souto et al., 2012), however, this could be due to differences in the density of neurons plated per ml of medium.

Aß source	$Aß_{1-38}$ (nM)	$Aß_{1-40}$ (nM)	$Aß_{1-42}$ (nM)
7PA2 CHO	-	-	0.14
Tg2576	5.73	6.21	0.58

Table 3.4: Concentrations of Aß species from different Aß sources
Aß source and concentration of $Aß_{1-38}$, $Aß_{1-40}$ and $Aß_{1-42}$ shown.

Taken together these results indicate that both Aß release from 7PA2 CHO cells and Aß released from primary Tg2576 mouse neurons is present at much lower concentrations than that at which synthetic Aß is used. If found to be induce similar AD-like effects in primary neuronal cultures, 7PA2 CHO cells would be a much more sensitive and physiological Aß source. However, results also indicate that it will be important to determine the Aß concentration of each batch of conditioned medium prior to experimental use.

To be considered a synthetic Aß alternative, Aß from an alternative source needs to produce AD-like changes in treated primary cultures. To determine if Aß-containing 7PA2 culture medium affects neuron health, 12 DIV primary cortical cultures were treated with 7PA2 CHO medium in a 1:1 ratio with Neurobasal medium for 48 h. WT CHO medium was used as a control. In addition, cells were treated with 10 µM synthetic $Aß_{1-42}$ or vehicle as a comparison. For this and all future experiments using 7PA2 CHO Aß, medium from cells at passage 19 (**Figure 3.7**) were used since

this batch contained the highest levels of Aß$_{1-42}$ (approximately 950 pg/ml). A LIVE/DEAD assay was used to determine the extent of dead cell dye incorporation as a measure of cell death.

The results indicated that synthetic Aß$_{1-42}$ application resulted in an approximately 0.2-fold increase in cell death relative to its respective control, a difference that was not statistically significant in this experiment ($p = 0.07$). In contrast, 7PA2 cell medium did not result in a marked increase in cell death relative to its control (WT CHO cell medium, **Figure 3.8**). Interestingly, however, CHO medium significantly reduced cell death relative to CTRL and synthetic Aß treatments (data not shown). This is likely to be due to the FBS in the CHO cell medium.

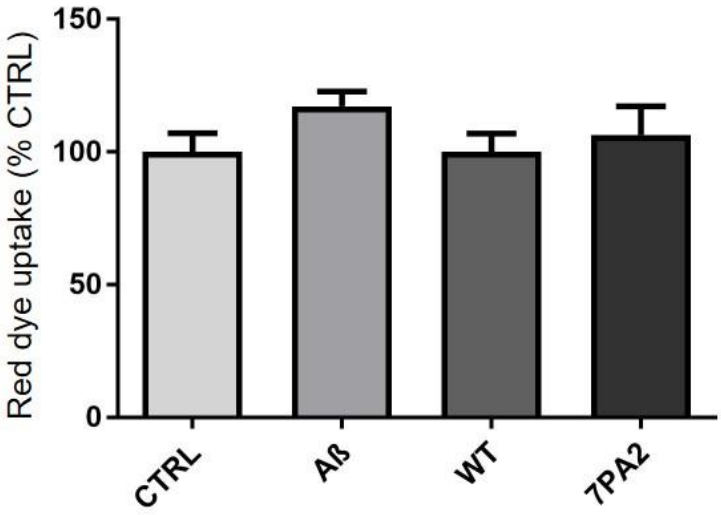

Figure 3.8: Synthetic, but not 7PA2-derived Aß decreases rat primary mixed glial neuronal culture viability

Bar chart showing the incorporation of dead cell dye in cells treated for 48 h with 10 µM synthetic Aß$_{1-42}$ or vehicle (H_2O), and 7PA2 CHO cell medium relative to its respective control of wild-type (WT) CHO cell medium. N=9. Values are mean ± SEM as a percentage of the appropriate control condition. Statistical test used: Student's t-test.

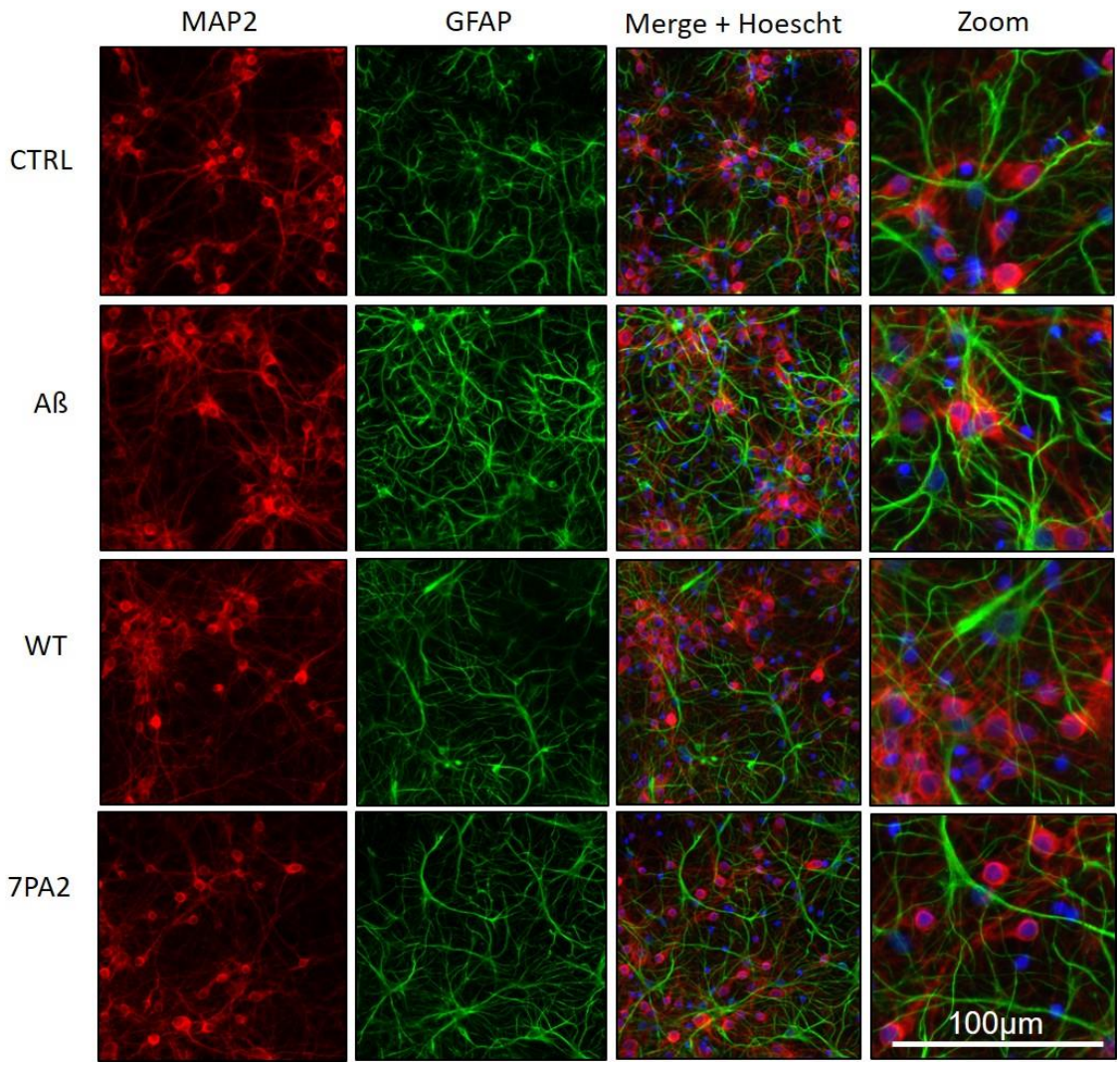

Figure 3.9: Treatment with synthetic and 7PA2-derived Aß does not affect neuronal morphology
Representative images at 20x objective magnification immunostaining of 14 DIV rat primary mixed neuronal glial cortical cell cultures treated with Aß (synthetic $Aß_{1-42}$, 10 µM) and CTRL (control: ultrapure H_2O), or (7PA2 CHO medium, 70 pM) and its control WT (WT CHO medium) for 48 h. MAP2 (red), GFAP (green) and Hoescht-33342 nuclear staining. Treatment is shown on left. Second column from right shows merged images, the far right column shows merged images at 40x objective magnification. N = 3.

ICC was used to examine the morphology of neurons and astrocytes in these cultures. Fluorescent images showed that there are no obvious changes in neuronal morphology when cells were treated with synthetic $Aß_{1-42}$ or 7PA2-derived Aß when compared to their respective controls (**Figure 3.9**), which likely reflects the mild neurotoxic effects of synthetic $Aß_{1-42}$ in this experiment. This suggests that, if 7PA2 CHO Aß is having any effects on primary cortical cultures,

the effects are likely to be subtle and may more accurately represent events in early AD, prior to substantial neuronal loss.

Although 7PA2 CHO cell medium does not cause overt cell death, it is reported to be synaptotoxic (Walsh et al., 2002). Therefore, to investigate subtler effects of 7PA2 cell -derived Aß on primary cortical cultures, changes in tau, caspase-3 and synaptic proteins were examined in these cultures. Abnormal tau processing and synaptic dysfunction are some of the earliest changes observed in AD brain (Horowitz et al., 2004; Amadoro et al., 2011; Lasagna-Reeves et al., 2011; Minano-Molina et al., 2011). Previous results from this laboratory using 7 DIV mixed cortical cultures showed that synthetic $Aß_{1-42}$ leads to increased tau phosphorylation, caspase-3 activation and increased cleavage of tau by caspase-3 (Garwood et al., 2011). Therefore, immunoblots of cell lysates were probed with antibodies against total, phosphorylated and caspase-cleaved tau, cleaved (active) caspase-3 and pre- and post-synaptic markers (**Figure 3.10 A**).

Treatment with either synthetic $Aß_{1-42}$ or 7PA2-derived Aß did not cause any changes in total tau amounts in comparison to their respective controls (**Figure 3.10 B**). This is not unexpected since total tau levels are thought to only increase at later stages of AD, when tau aggregates accumulate (Gerson and Kayed, 2016). Similarly, neither source of Aß affected tau phosphorylation at the PHF1 (Ser396/404) epitope and 7PA2-derived Aß significantly reduced phosphorylation at the CP13 (Ser202) epitope (**Figure 3.10 C, D**). This is somewhat unexpected since tau phosphorylation, particularly at the PHF1 site, is known to occur early during AD development (Evans et al., 2000) and is commonly found to increase following Aß treatment of primary neuronal cultures (Rapoport et al., 2002; Noble et al., 2009a; Jana and Pahan, 2010; Amadoro et al., 2011; Garwood et al., 2011). The reason for this discrepancy is not known, but with respect to the work conducted in this laboratory might represent differences in the

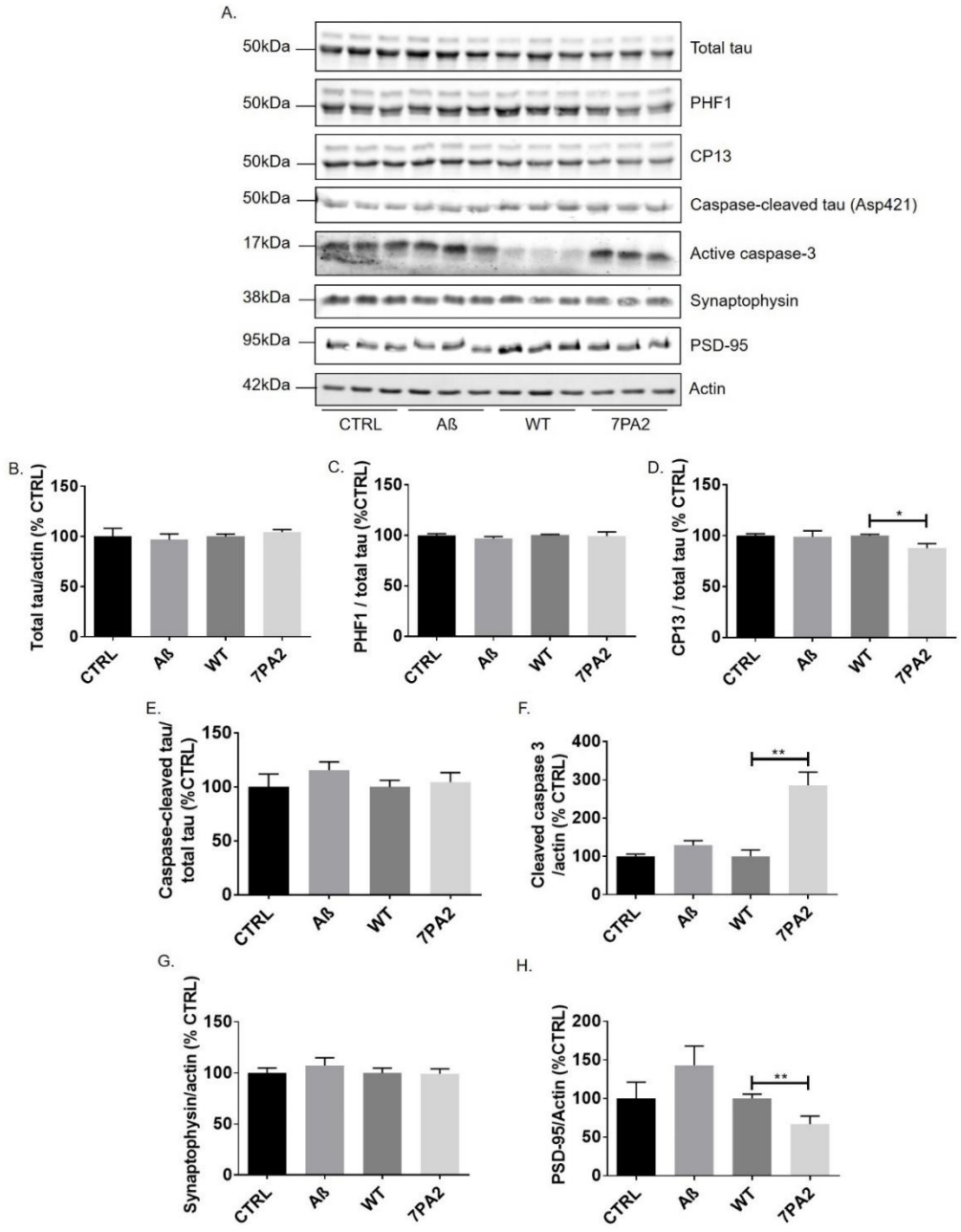

Figure 3.10: 7PA2-derived Aß increases caspase-3 activity and reduces post-synaptic protein markers

A. Representative western blots of primary cortical cell culture lysates treated with 10 µM synthetic $Aß_{1-42}$ or vehicle (H_2O), and 7PA2 CHO cell medium relative to its respective control of wild-type (WT) CHO cell medium. Blots were probed with antibodies against total tau, PHF1 (tau phosphorylated at Ser396/404), CP13 (tau phosphorylated at Ser202), caspase-cleaved tau (Asp421), cleaved caspase-3, synaptophysin, PSD-95 and ß-actin as a loading control. Molecular weight markers are shown on the left. **B-H.** Bar charts show quantification of **B.** Total tau relative to ß-actin**. C.** PHF1, **D.** CP13 and **E.** caspase-cleaved tau a proportion of total tau. **F.** cleaved caspase-3, **G.** synaptophysin and **H.** PSD-95 relative to ß-actin. N=9. Values are mean ± SEM as a percentage of the respective control. Statistical test used: Student's t-test. * = $p<0.05$, ** = $p<0.01$.

susceptibility of 14 DIV cultures (used here) and the 7 DIV cultures used in previous reports (Garwood et al., 2011).

The activity of caspase-3 and the abundance of caspase-cleaved tau were examined since increased levels of cleaved and fragmented tau encourage tau aggregation, resulting in toxic tau oligomers and eventually NFTs (Horowitz et al., 2004; Park and Ferreira, 2005; Wang et al., 2007). Caspase 3 is activated by cleavage of pro-caspase-3 at aspartate (Asp) 175 to generate active 17 kDa and 19 kDa fragments. Caspase-3 cleaves tau at Asp 421, producing large, possibly toxic, tau fragments of approximately 50 kDa (Chung et al., 2001; Liu et al., 2011a; Snigdha et al., 2012). In these experiments, neither synthetic $Aß_{1-42}$ or 7PA2-derived Aß caused significant changes in the amounts of caspase-cleaved tau antibody relative to their respective controls (**Figure 3.10 E**). In contrast, 7PA2-derived Aß caused a marked increase in the appearance of cleaved (active) 17 kDa caspase-3 species in comparison to WT CHO medium (**Figure 3.10 F**). While apparently not resulting in increased cleavage of tau, caspase-3 is an executioner caspase (Snigdha et al., 2012), linked with AD (Chung et al., 2001; Gamblin et al., 2003; Liu et al., 2011a), and this finding is indicative that 7PA2-derived Aß may have the capacity to affect neuronal viability in the long term.

Finally, synaptic proteins were examined as an indication of the effects of each Aß species on synapse health. Western blots were probed with antibodies against synaptophysin and PSD-95. Synaptophysin is a synaptic vesicle glycoprotein that regulate vesicle positioning and release by interacting with synaptobrevin (Yao et al., 2003). PSD-95 is an important scaffolding protein at the post-synapse but is also commonly used as a post-synaptic marker (Savioz et al., 2014). Synaptic dysfunction is closely linked with tau in AD, and is one of the earliest pathologies detected during AD pathogenesis (LaFerla and Oddo, 2005; Lasagna-Reeves et al., 2011; Crimins et al., 2013; Talantova et al., 2013). In the experiments shown here, neither synthetic $Aß_{1-42}$ or 7PA2-derived Aß affected the amounts of synaptophysin in comparison to their respective controls (**Figure 3.10 G**). However, 7PA2-derived Aß significantly reduced PSD-95 levels in comparison with the WT CHO medium control (**Figure 3.10 H**). This suggests that 7PA2-derived

Aß treatment is resulting in significant degeneration at the synapse, and may affect neurons in a more sensitive manner than synthetic Aß. This is consistent with results from others in the laboratory (not shown here) that have shown treatment of mouse cortical neurons with 7PA2-derived Aß reduces the density of synaptic spines, and with previous reports from Walsh et al. (2002).

In conclusion, these results indicate that 7PA2-derived Aß is having little effect in primary cortical cultures on AD-like tau changes or cell viability. However, significant alterations in caspase-3 activity and a reduction in PSD-95 levels were observed. This suggests 7PA2-derived Aß may be having more long-term effects on cell viability, possibly due to detrimental effects on dendritic levels and synaptic function. Unfortunately, by the time these findings were gained, there was not sufficient time to establish a new set of analysis criteria in this project, therefore synthetic $Aß_{1-42}$ was used for the following experiments in this chapter in which the effect of astrocytes on Aß-induced changes were investigated.

3.3.3 Astrocytes do not affect Aß-induced changes in 14 DIV primary cortical cultures

Previous research from this laboratory and others shows that astrocytes have an important effect in mediating the effects of Aß on disease-associated tau changes, synapse and neuron health (Noble et al., 2009a; Garwood et al., 2011). In work from this laboratory, astrocytes were found to accelerate Aß-induced cell death, possibly via increased pro-inflammatory cytokine release and caspase-3 activation in 7 DIV cortical cultures. Additionally, astrocytes were required for Aß-induced tau phosphorylation (Garwood et al., 2011). Garwood et al. (2011) also found that found minocycline, a tetracycline derivative with anti-inflammatory action, prevented these Aß-induced effects in astrocyte-containing cultures.

To determine if the same effects are observed in more mature neurons, that have functional synapses, these experiments were repeated here using 14 DIV primary cortical cultures. Primary cortical cells were cultured as described previously (Chapter 2, **section 2.1**). At 3 DIV some cells were treated with 0.5 µM AraC for 48 h, preventing astrocyte proliferation and resulting in

neuronal cultures, which was verified by western blotting and immunocytochemistry with cell-type specific markers. At 11 DIV, cell cultures were pre-treated with 20 µM minocycline for 24 h, prior to treatment with 10 µM synthetic Aß$_{1-42}$ for 48 h. AraC-treated cultures showed only trace amounts of GFAP when cells were lysed and western blotted. Clear ß-actin bands were apparent in these samples indicating the presence of remaining cells, predominantly neurons (**Figure 3.11**). As tau itself is a neuron-specific marker, the presence of live neurons was further confirmed by western blotting and probing resulting blots with tau to investigate changes in total and phosphorylated tau levels (**Figure 3.13**).

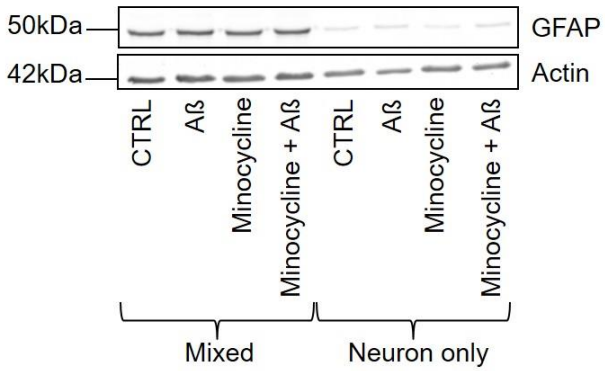

Figure 3.11: AraC treatment leaves only trace amounts of GFAP-positive cells
Representative western blot of primary cortical cultures treated with AraC (neuronal) or not (mixed) and treated with minocycline and/or Aß. Blots were probed with antibodies against GFAP and ß-actin as a loading control. Molecular weight markers are shown on the left.

The effect of synthetic Aß$_{1-42}$ on primary culture health in the presence and absence of astrocytes was next determined using LIVE/DEAD cell assays. The effect of minocycline on cell death in these cultures was also examined. The results appeared to show increases in cell death following Aß treatment of both mixed and neuronal cultures, however these differences did not reach statistical significance (**Figure 3.12**). In addition, minocycline had no effect on Aß-induced cell death in either mixed or neuronal cultures. These data suggest that astrocytes do not accelerate Aß-induced neuronal loss.

Previously, Garwood et al. (2011) found that astrocytes facilitated tau changes, including tau phosphorylation and cleavage, in 7 DIV primary cortical cultures. To determine if these are

replicated at 14 DIV, western blots were used to assess tau changes in mixed and neuronal culture lysates. In addition, an antibody against cleaved caspase 3 was used to allow comparison with caspase-cleaved tau amounts.

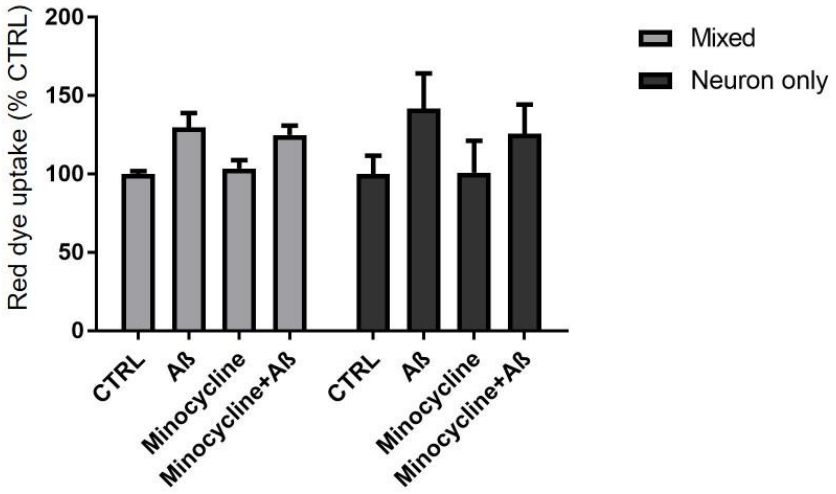

Figure 3.12: Astrocytes do not affect Aß-induced neurotoxicity in 14 DIV primary cortical cultures
Bar chart showing incorporation of dead cell dye in mixed (neuron + astrocyte) and neuronal cultures treated with 10 µM Aß for 48 h, with and without 3 h pre-treatment with 20 µM minocycline. Data is mean ± SEM as a percentage of mixed or neuronal culture CTRL conditions. N=5. Statistical test used: two-way ANOVA.

The results of this analysis showed that there were no effects of minocycline or Aß on total tau amounts or tau phosphorylation at the CP13 and PHF1 epitopes in either mixed or neuronal cultures (**Figure 3.13 A, B-D**). There were also no significant changes in caspase-cleaved tau levels in mixed or neuronal cultures treated with minocycline and/or Aß (**Figure 3.13 A, E**). Again this contradicts previous research showing that, while Aß-induced increases in caspase-cleaved tau occur in the absence of astrocytes, astrocytes can exacerbate tau cleavage (Garwood et al., 2011). In addition, the results here showed that cleaved caspase-3 levels were significantly increased following Aß treatment in neuronal, but not mixed, cultures (**Figure 3.13 A, F**).

Astrocytes may play a role in physiological tau release

Recent evidence demonstrates that tau can be released into the extracellular space under both physiological and pathological conditions (de Calignon et al., 2012; Pooler et al., 2013; Hanger

et al., 2014; Wu et al., 2016). Pathological tau release is thought to underlie the trans-synaptic spread of tau pathology along anatomical connections in diseased brains (Clavaguera et al., 2015). Tau release in physiological conditions may be involved in inter-cellular signalling (Pooler et al., 2013; Hanger et al., 2014). Little is known about the possible contributions of astrocytes to tau release. However, synaptic activity has been shown to mediate tau release, suggesting that the influence of astrocytes at synapses may be an important component of this process (Pooler et al., 2013; Avila-Munoz and Arias, 2014; Yamada et al., 2014; Wu et al., 2016).

Before investigating the role of astrocytes in tau release, it was important to first characterise the species of tau that 14 DIV mixed primary cortical cultures release. Tau release was therefore measured under basal and following stimulation with 100 μM AMPA, which this laboratory has previously shown to stimulate tau release from healthy cultured neurons (Pooler et al., 2013). As a positive control, cells were also treated with a toxic concentration (0.1 μM) of the calcium ionophore, ionomycin. Treatments were applied for 30 min at which time cells were lysed and medium was concentrated according to the protocol described in Chapter 2 (**section 2.1**). Concentrated samples of cell lysates and culture medium were determined using western blots probed with tau antibodies. Qualitative assessment of the results suggested that the amounts of tau released into culture medium are somewhat increased following AMPA treatment, as indicated by the increased density of total tau (DAKO) bands (**Figure 3.14**), supporting our previous findings (Pooler et al., 2013). There were no apparent changes in total tau amounts in the corresponding cell lysates. As expected, very low levels of tau can be seen in ionomycin-treated cell lysates since this treatment is toxic, and the high levels of tau detected in the corresponding culture medium mirror this decrease in intracellular tau (**Figure 3.14**). These experiments establish that tau release can be readily measured in culture medium under basal and stimulated conditions.

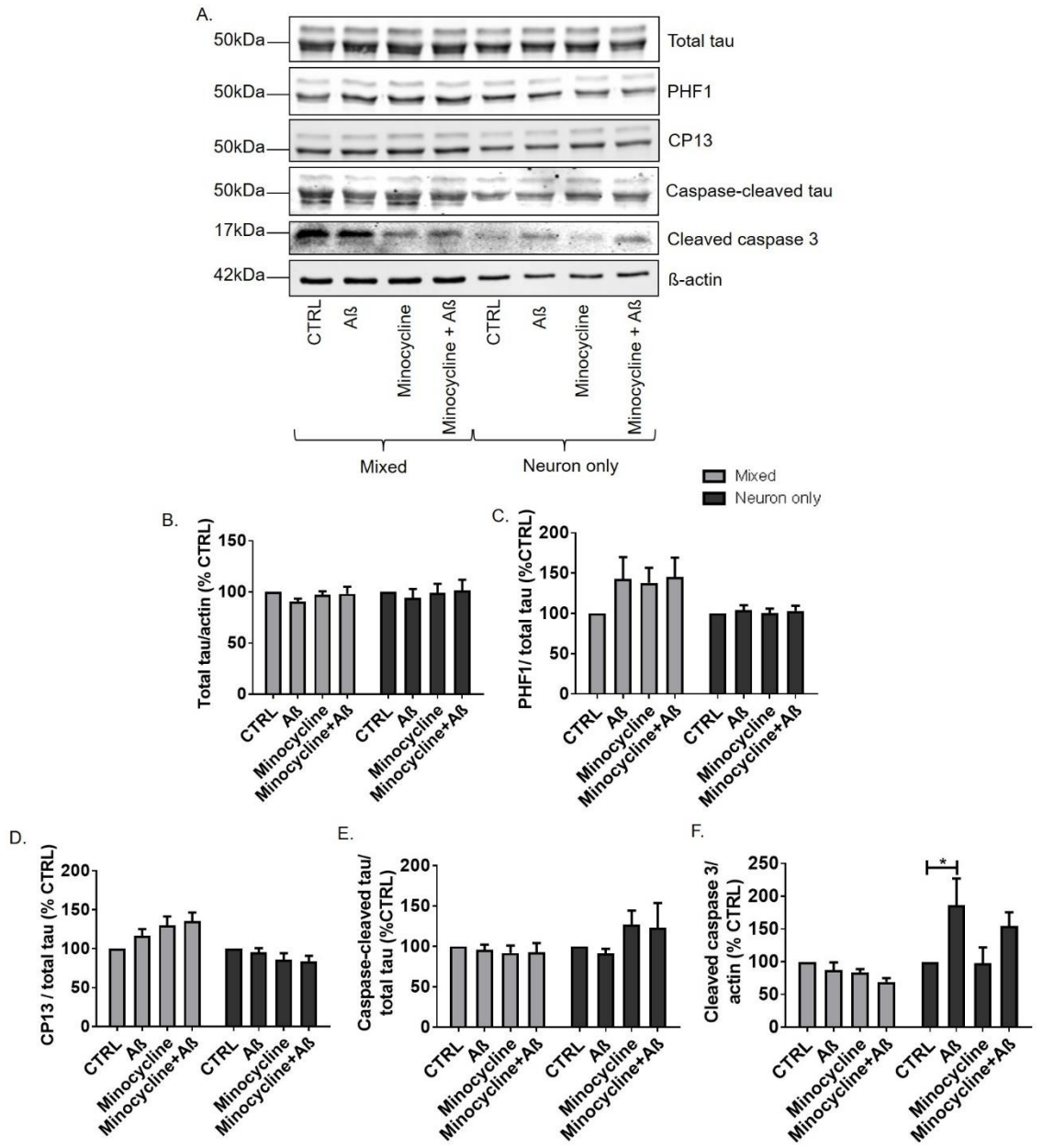

Figure 3.13: Astrocytes do not cause Aß-induced changes in tau in 14 DIV primary cortical cultures

A. Representative western blots of lysates from mixed (neuron + astrocyte) and neuronal cultures treated with 10 µM Aß for 48 h, with and without 3 h pre-treatment with 20 µM minocycline. Blots were probed with antibodies against total tau, PHF1 (tau phosphorylated at Ser396/404), CP13 (tau phosphorylated at Ser202), caspase-cleaved tau (Asp421), cleaved caspase 3, and β-actin as a loading control. Molecular weight markers are shown on the left. **B-H.** Bar charts show quantification of **B.** total tau as a proportion of ß-actin**. C.** PHF1, **D.** CP13 and **E.** caspase-cleaved tau as a proportion of total tau. **F.** cleaved caspase 3 as a proportion of ß-actin. N=9. Data is mean ± SEM as a percentage of mixed or neuronal culture CTRL conditions Statistical test used: two-way ANOVA. * = $p<0.05$.

To examine the phosphorylation status of the released tau, western blots were probed with Tau-1 antibody, which detects tau dephosphorylated at Ser199/202/Thr205. Strong immunoreactive bands are detected by this antibody in the culture medium samples (**Figure 3.14**), indicating that extracellular tau is largely dephosphorylated at these epitopes, as previously reported (Pooler et al., 2013).

To determine if the tau that is released is cleaved, as suggested by Kanmert and colleagues (Kanmert et al., 2015), or intact, as we previously reported (Pooler et al., 2013), antibodies raised against the extreme C-terminus (TP70) and N-terminus (TP007) were used. These antibodies appeared to detect the majority of tau present in culture medium at the expected size of full-length tau (**Figure 3.14**), further supporting previously published research demonstrating that extracellular tau is predominantly full-length and dephosphorylated (Pooler et al., 2013; Hanger et al., 2014).

To investigate possible contributions of astrocytes to basal and stimulated tau release, mixed and neuronal cortical cultures were established as described above. At 14 DIV, Neurobasal medium was removed and HBSS containing Ca^{2+} and Mg^{2+} applied for 30 mins. This is essential since Neurobasal medium components interfere with tau sandwich ELISAs (Pooler et al., 2013). The HBSS was collected and total tau amounts in medium were determined using a tau sandwich ELISA that we developed in-house (Chapter 2, **section 2.7**). Cell viability was measured using LIVE/DEAD assays to ensure that any changes in tau release found were not as a result of increased cell death.

The results obtained show that there are no differences in cell death between neuronal and mixed cultures (**Figure 3.15 A**). In contrast, tau content in culture medium is significantly increased in neuronal cortical cultures, when compared to mixed cortical cultures (**Figure 3.15 B**). This data suggests that astrocytes reduce the amount of tau released from neurons under basal conditions.

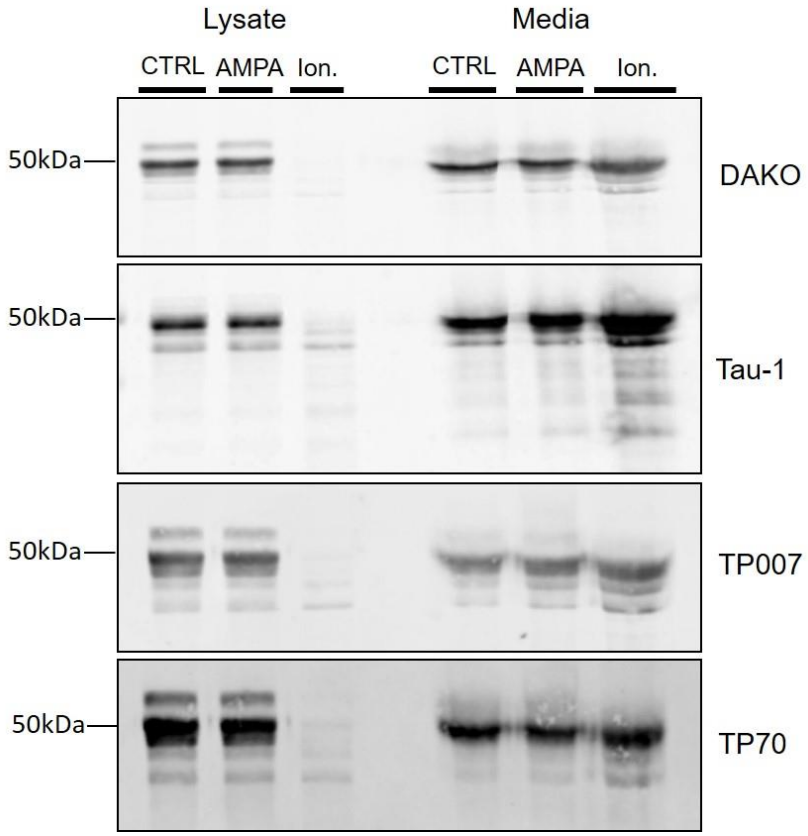

Figure 3.14: Tau released from rat primary mixed glial neuronal cortical cultures upon AMPA stimulation is intact and dephosphorylated
Representative western blots of rat primary mixed glial neuronal cortical culture lysates and concentrated medium samples from cells treated with vehicle (CTRL), 100 µM AMPA or 0.1 µM ionomycin (Ion.). Blots were probed with antibodies against total tau (DAKO), Tau-1 (tau dephosphorylated at Ser199/202/Thr205), TP007 (N-terminus of tau) and TP70 (C-terminus of tau). Molecular weight markers are shown on the left. N = 2.

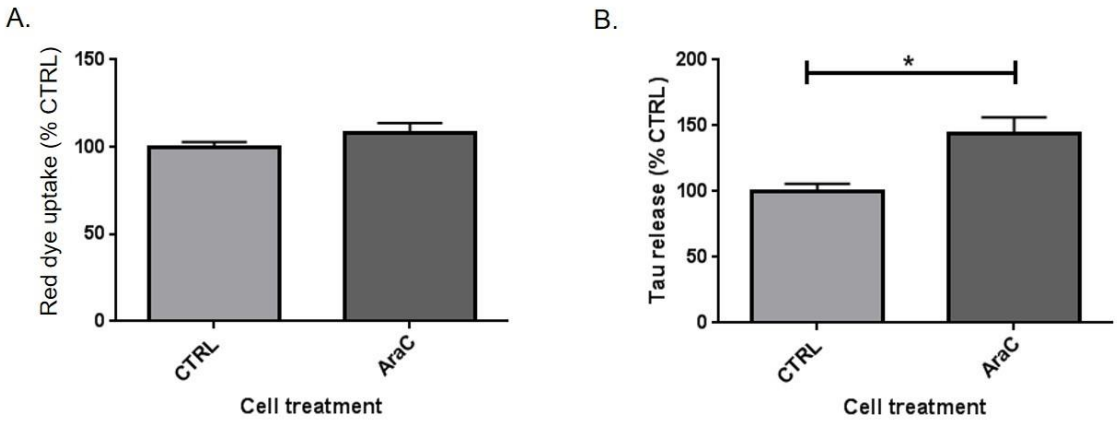

Figure 3.15: Extracellular tau amounts are increased in neuronal cultures in basal conditions
A. Bar chart showing cell death, as measured using LIVE/DEAD cell assay, in mixed (CTRL) and neuronal (AraC-treated) cortical cultures **B.** Bar chart showing total tau (DAKO) content in culture medium from these cells. N=15. Values are mean ± SEM as a percentage of CTRL. Statistical test used: Students t-test. * = $p<0.05$.

To further investigate the possible contributions of astrocytes to tau release, mixed and neuronal cortical cultures were treated with 20 µM minocycline at 11 DIV and 10 µM synthetic $Aß_{1-42}$ at 12 DIV as previously described (**section 3.3.3**). At 14 DIV, 48 h after Aß treatment, culture medium was collected and concentrated for Alphascreen assays (for method see Chapter 2, **section 2.7**) which allow detection of total and phosphorylated tau in the medium. Alphascreen is a bead-based assay based on similar principles to ELISA. Samples are incubated with two primary antibodies: a biotinylated total tau antibody, and either a total or phospho-specific tau antibody conjugated to acceptor beads. In parallel, cells were lysed and protein content determined using a Bradford protein assay (Chapter 2, **section 2.4.2**). This allowed amounts of extracellular tau to be standardised to total protein content in each sample.

Despite concentrating the medium, Alphascreens using PHF1 and CP13 antibodies conjugated to acceptor beads, were not sufficiently sensitive to detect tau in culture medium (data not shown). This problem may have been exacerbated since extracellular tau is largely dephosphorylated (Pooler et al., 2013). Using acceptor beads conjugated to Tg5, another total tau antibody, the Alphascreen results showed that there are no significant differences following Aß or minocycline treatment or between mixed or neuronal cultures (**Figure 3.16**). This is unexpected as these results could contradict the ELISA results described above. This inconsistency could possibly be explained by the reduced sensitivity of Alphascreens, the use of different total tau antibodies, potential artefacts or variation introduced when medium is concentrated for use in this assay. It is possible that repeating these experiments with different combinations of antibodies, raised to different parts of tau, may provide a more accurate determination of levels of extracellular tau in mixed and neuronal cultures under different conditions.

Overall, this set of experiments suggests that astrocytes might play a role in regulating the concentration of extracellular tau in 14 DIV primary cortical cultures under basal conditions. Further experiments are required to validate these findings and to determine the precise mechanisms involved.

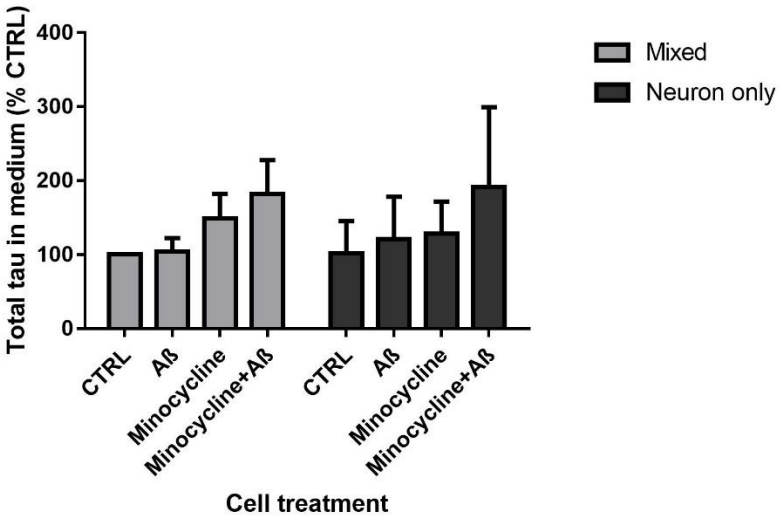

Figure 3.16: Alphascreen results suggest that tau release is not influenced by astrocytes or Aß Bar chart showing Alphascreen results with samples from mixed (neuron + astrocyte) and neuronal cultures treated with 10 µM Aß for 48 h, with and without 3 h pre-treatment with minocycline. All results are standardised to mixed control (CTRL) levels of total tau (Tg5) in the medium. N=3. Values are mean ± SEM as a percentage of CTRL. Statistical test used: two-way ANOVA.

Astrocytes show an inflammatory response to Aß treatment

The transcription factor NF-κB may mediate inflammatory roles of astrocytes, increasing production and release of pro-inflammatory cytokines in response to Aß (Shi et al., 2016). To begin to determine if Aß affects astrocytic inflammatory responses in these cultures, immunofluorescence was used to examine NF-κB in 14 DIV mixed cortical cultures, treated with Aß and minocycline treatment as described above. Cells were fixed and immunolabelled with anti-NF-κB and GFAP antibodies. Nuclear material was stained with Hoescht-33342. Images taken with a fluorescent microscope showed an increase in the intensity of NF-κB immunoreactivity following Aß treatment. Furthermore, this increase was reduced when cultures were pre-treated with minocycline (**Figure 3.17**). Average intensity of NF-Kb in each image was quantified using Image J and standardised to the average intensity of DAPI staining. Quantification confirmed a statistically significant increase in the average intensity of NF-κB staining in Aß-treated cultures compared to all other treatment groups (**Figure 3.18**), suggesting an increase in NF-κB production with Aß treatment with monocycline pre-treatment resucing

this effect. This data suggests that the cells in 14 DIV mixed primary cultures are reactive to Aß, with NF-κB induction in neural cells possibly linked to an inflammatory response. It should be noted that NF-κB immunoreactivity also appeared to be localised to neurons.

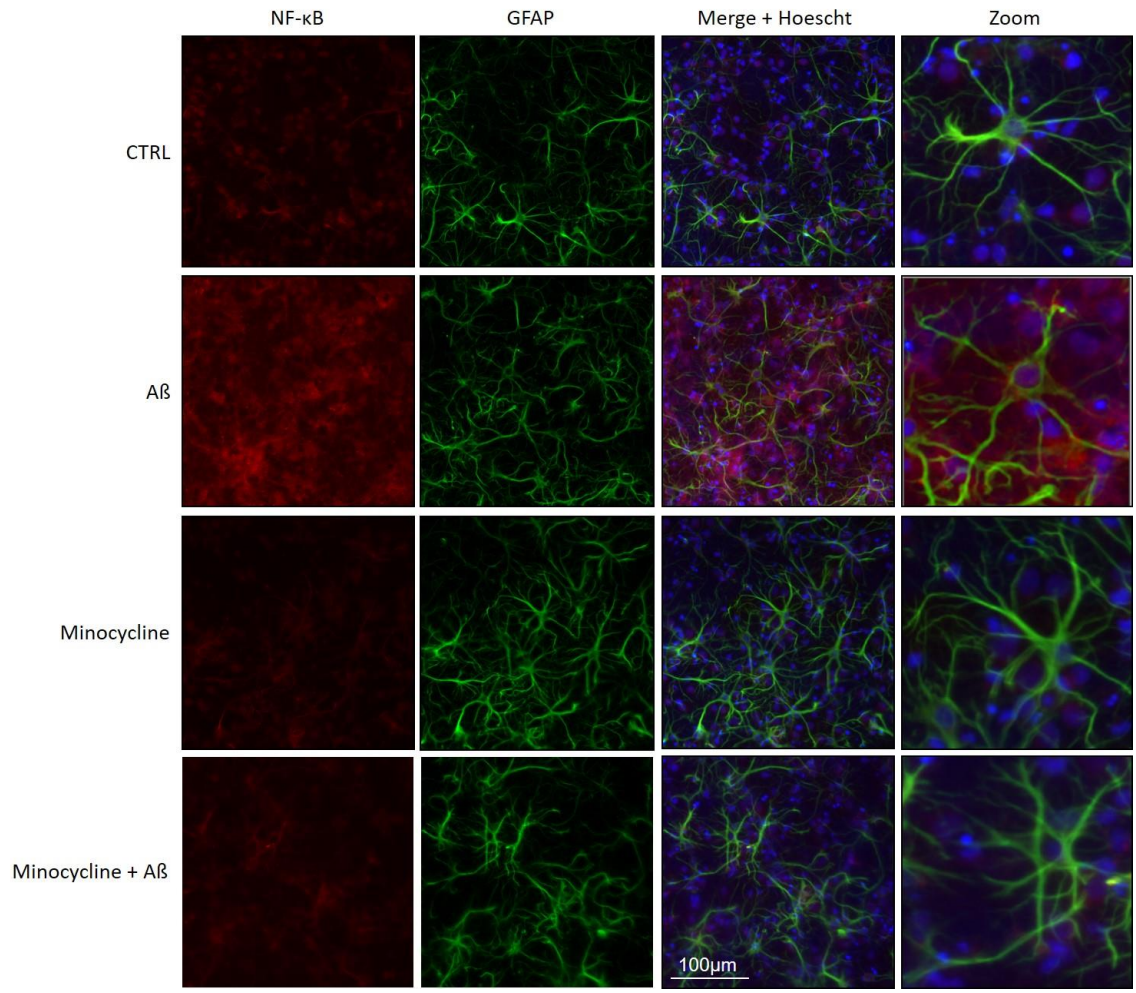

Figure 3.17: Aß-induces increases in NF-κB levels that are attenuated by minocycline pre-treatment
Representative 20x magnification images showing NF-κB (red) and GFAP (green) immunolabelling and Hoescht-33342 nuclear staining of 14 DIV mixed cortical cell cultures treated with CTRL (control: Ultrapure H_2O), Aß (synthetic $Aß_{1-42}$), minocycline or minocycline + Aß. Treatment is shown on left. Second column from right shows merged images, the far right column shows merged images at 40x magnification. N = 9.

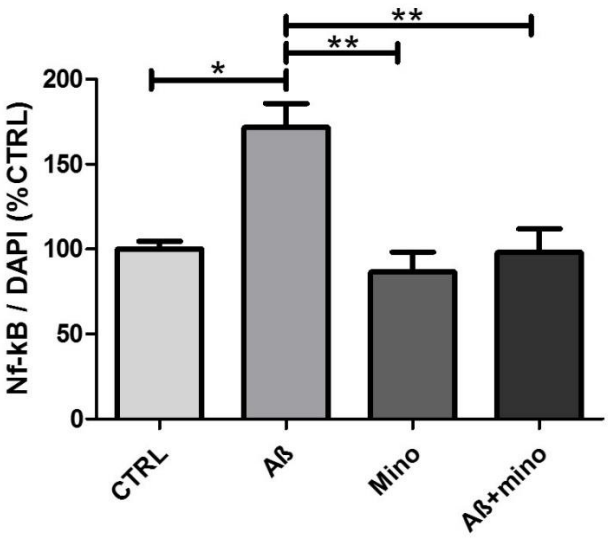

Figure 3.18: NF-κB levels are increased with Aß treatment
Bar chart show quantification of average NF-κB staining intensity as a proportion of average DAPI staining intensity. N=6. Data is mean ± SEM as a percentage of CTRL conditions. Statistical test used: Kruskal-Wallis. * = $p < 0.05$, ** = $p < 0.01$.

IκBα amounts were also examined in mixed and neuronal cultures. In astrocytes, IκBα binds to NF-κB, inactivating the transcription factor. Therefore, a decrease in IκBα results in an increase in NF-κB activity (Frakes et al., 2014). Western blots probed with an antibody specific to IκBα showed lower IκBα levels in neuronal samples when compared to those from mixed cultures (**Figure 3.19**). This is expected since IκBα is found predominantly in glia (Kopitar-Jerala, 2015). However, treatment with Aß or minocycline in either mixed or neuronal cultures did not appear to affect IκBα levels. IκBα must be phosphorylated in order to release NF-Kb. Unfortunately, reagents to examine IκBα phosphorylation were not available to allow any further investigations. In summary, the results of experiments using 14 DIV primary cortical cultures suggest that astrocytes are not important mediator of Aß-induced cell death, tau phosphorylation or cleavage. However, cortical astrocytes may play a role in mediating levels of extracellular tau.

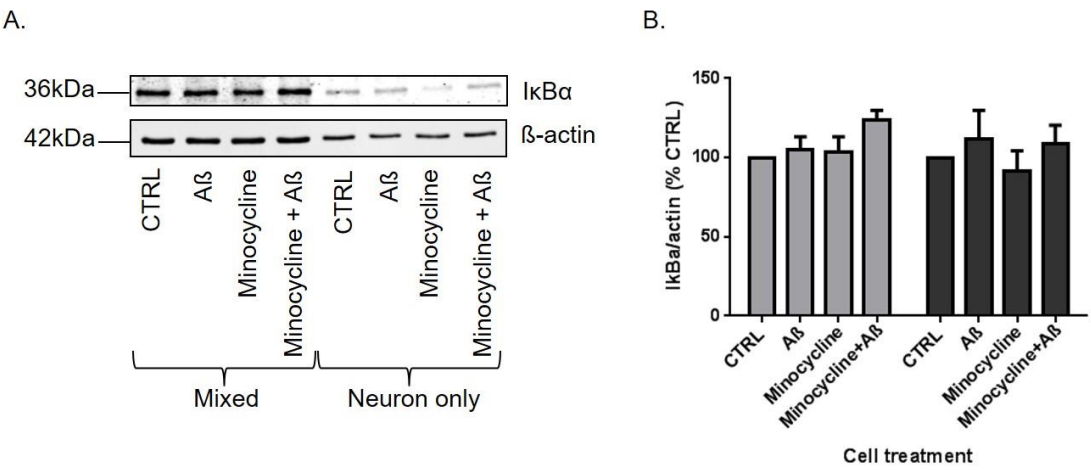

Figure 3.19: Minocycline and Aß treatment has no effect on IκBα levels in primary cortical cultures

A. Representative western blots of lysates from mixed (neuron + astrocyte) and neuronal cultures treated with 10 µM Aß for 48 h, with and without 3 h pre-treatment with 20 µM minocycline. Blots were probed with antibodies against IκBα and ß-actin as a loading control. Molecular weight markers are shown on the left. **B.** Bar chart show quantification of IκBα as a proportion of ß-actin. N=9. Data is mean ± SEM as a percentage of mixed or neuronal culture CTRL conditions. Statistical test used: two-way ANOVA.

3.3.4 Astrocytes may mediate some Aß-induced changes in primary hippocampal cultures

To determine if hippocampal astrocytes and neurons respond differently to stimulation with Aß, the experiments described above were repeated in primary hippocampal cultures. Mixed and primary hippocampal cells were cultured and treated with 20 µM minocycline and/or 10 µM synthetic $Aß_{1-42}$ treatment as described above. At 14 DIV cells were lysed and standardised to total protein levels before being run on western blots. As described for cortical neurons, lysates were first assessed using western blots probed with an antibody against GFAP to confirm the effectiveness of AraC treatment. These results showed that AraC had reduced, but not removed, astrocytes (**Figure 3.20**). For simplicity, these cultures are referred to as "neuronal", however, it should be noted that there is still an astrocyte component to these cultures.

In 14 DIV primary cortical cultures, astrocytes did not appear to influence the effects of Aß on neuron death (**Figure 3.12**). The contributions of astrocytes to Aß-induced hippocampal neuron death were investigated using the same methods. These results showed that Aß treatment significantly increased cell death compared to the control group in mixed ($p<0.01$), but not

neuronal cultures, suggesting that astrocytes contribute to Aß-induced neurotoxicity in hippocampal cultures (**Figure 3.21**). The Aß-induced increases in cell death in mixed cultures were not reduced by minocycline pre-treatment, however cell death in neuronal cultures pre-treated with minocycline were significantly reduced compared to cultures treated with Aß.

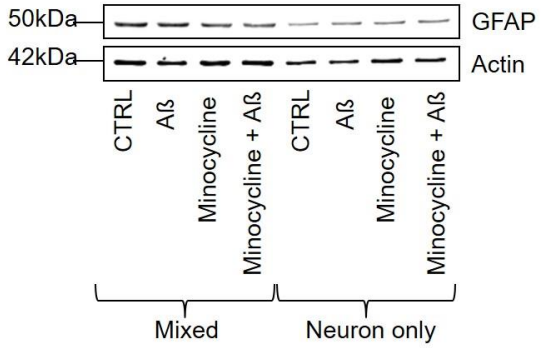

Figure 3.20: AraC treatment of primary hippocampal cultures reduces GFAP levels
Representative western blot of lysates from primary hippocampal cultures treated with AraC (neuronal) or vehicle (mixed) in addition to 20 µM minocycline and/or 10 µM Aß and probed with antibodies against GFAP. ß-actin was used as a loading control. Molecular weight markers are shown on the left.

To investigate this difference between primary cortical and hippocampal cultures further, experiments investigating the contributions of astrocytes to Aß-induced tau phosphorylation and cleavage were carried out in primary hippocampal cultures. As explained before, primary hippocampal cultures were treated with 0.5 µM AraC to create mixed and neuronal culture types. Cultures were treated with 20 µM minocycline at 11 DIV, before 10 µM synthetic $Aß_{1-42}$ treatment at 12 DIV. At 14 DIV cells were lysed and standardised to total protein levels before being run on western blots. Protein levels in each treatment group were also standardised to the levels seen in the control group of each culture type (e.g. mixed minocycline-treated cells standardised to mixed control cells).

It was next important to determine if hippocampal astrocytes affect Aß-induced changes in tau in hippocampal neurons. Therefore, lysates from these cells were immunoblotted with antibodies against total and phosphorylated tau. The results obtained showed that there was

no significant change in total tau levels in mixed or neuronal treatment groups following Aß treatment when compared to the control conditions for each group (**Figure 3.22 A, B**).

Aß did not affect tau phosphorylation at the PHF1 (tau phosphorylated at Ser396/404) or CP13 (tau phosphorylated at Ser202) epitopes in either mixed or neuronal cultures. In contrast, minocycline significantly increased phosphorylation at the PHF1 sites in mixed cultures ($p<0.01$) and at the CP13 residue in both mixed and neuronal cultures ($p<0.05$ for both, **Figure 3.22 A, C**).

No significant changes were found in amounts of caspase-cleaved tau following treatment with Aß in mixed or neuronal hippocampal cultures (**Figure 3.22 A, E**). There were apparent increases in cleaved (active) caspase-3 amounts in cells treated with Aß in both mixed and neuronal hippocampal cultures. However, statistical analysis of these results indicated that the increases were not significant, likely because of variability within groups (**Figure 3.22 F**). These results suggest that hippocampal astrocytes do not mediate tau cleavage by caspase 3, in contrast to findings in cortical cultures (Garwood et al., 2011).

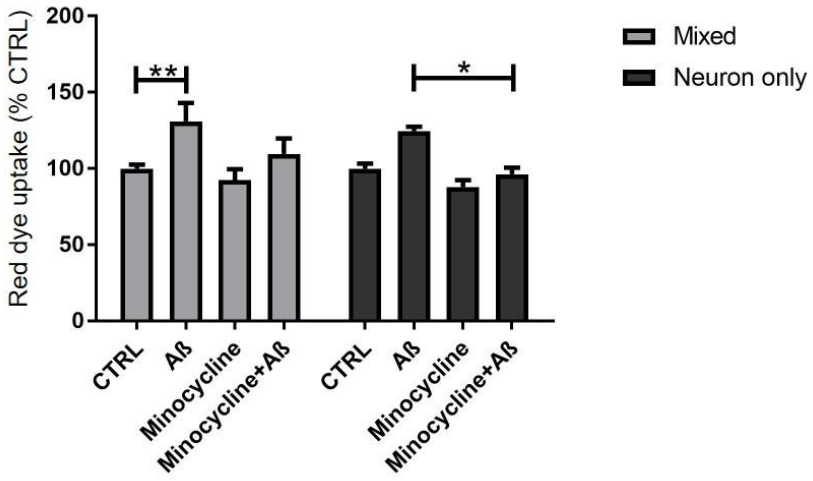

Figure 3.21: Astrocytes are involved in Aß-induced hippocampal cell death
Bar chart showing incorporation of dead cell dye in mixed (neuron + astrocyte) and neuronal hippocampal cultures treated with 10 µM Aß for 48 h, with and without 3 h pre-treatment with 20 µM minocycline. Data is mean ± SEM as a percentage of mixed or neuronal culture CTRL conditions. N=13. Statistical test used: two-way ANOVA. * = $p<0.05$, ** = $p<0.01$, *** = $p<0.001$.

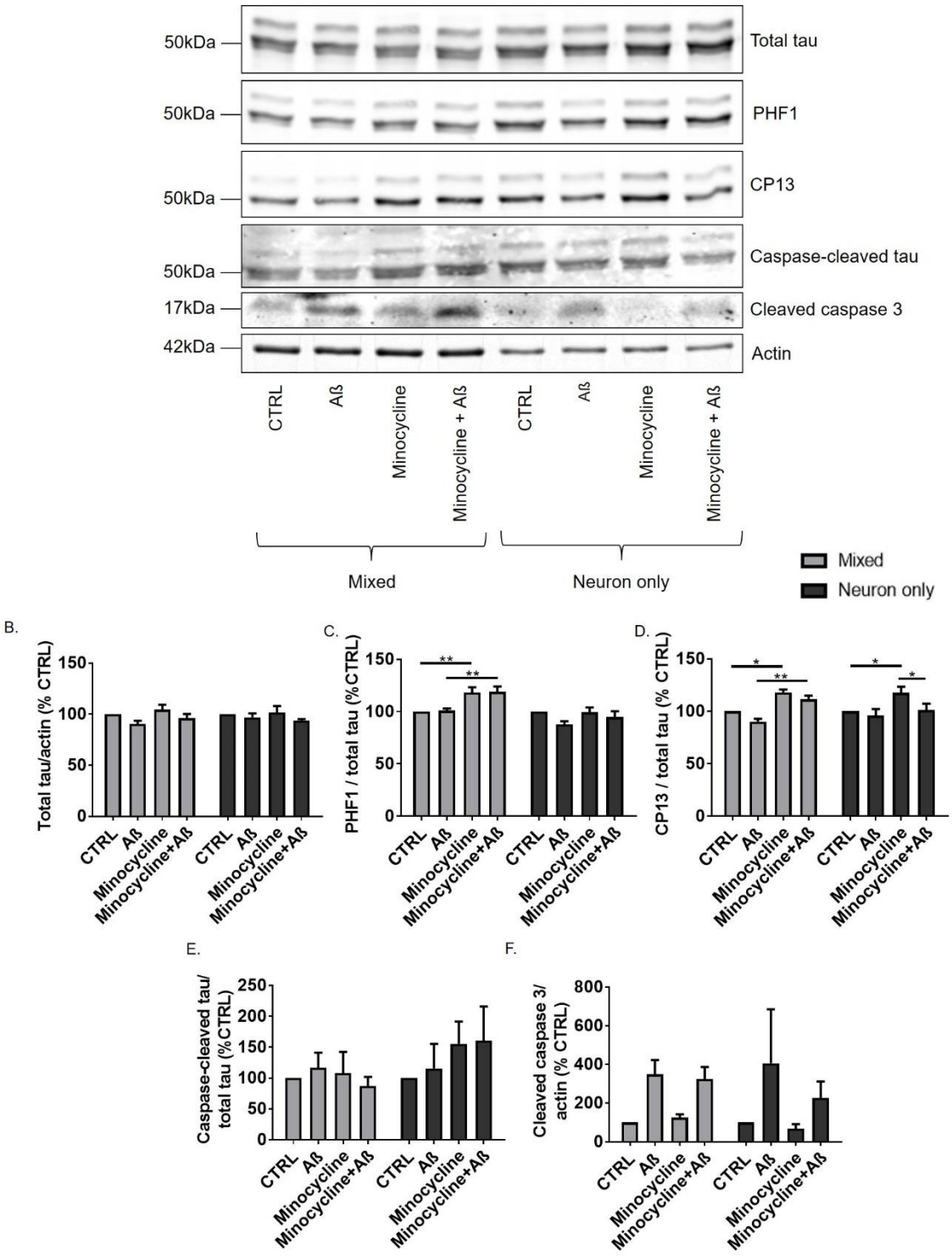

Figure 3.22: Minocycline increases tau phosphorylation in primary hippocampal cultures
A. Representative western blots of lysates from primary mixed and neuronal hippocampal cell cultures treated with 20 µM minocycline and/or 10 µM synthetic $Aß_{1-42}$ (Aß), and probed with antibodies against total tau, PHF1 (tau phosphorylated at Ser396/404), CP13 (tau phosphorylated at Ser202), caspase-cleaved tau (Asp421), cleaved caspase 3, IκBα and ß-actin as a loading control. Molecular weight markers are shown on the left. **B-H.** Bar charts show quantification of **B.** Total tau as a proportion of ß-actin**. C.** PHF1, **D.** CP13 and **E.** caspase-cleaved tau as a proportion of total tau, and **F.** cleaved caspase-3 as a proportion of ß-actin. N=5. Values represent mean ± SEM as a percentage of respective controls (CTRL). Statistical test used: two-way ANOVA. * = p<0.05, ** = p<0.01.

Overall, these results suggest that there are subtle differences in the contribution of astrocytes to Aß-induced cell death in hippocampal and cortical cultures. Astrocytes exacerbated Aß-induced cell death in hippocampal, but not cortical cultures. In addition, minocycline was found to have marked effects on tau phosphorylation in hippocampal, but not cortical cultures.

3.3.5 Summary

To summarise, the main findings of this chapter were:

- Synthetic $Aß_{1-42}$ is composed primarily of middle-high molecular weight oligomers, some of which are sensitive to SDS.
- 7PA2-derived Aß does not cause overt increases in tau phosphorylation and cleavage or cell death. However, this Aß causes robust cleavage and activation of caspase-3.
- Astrocytes appear to mediate Aß-induced cell death in 14 DIV primary hippocampal, but not cortical cultures, in contrast to previous findings in 7 DIV cortical cultures (Garwood et al., 2011).
- Astrocytes may be involved in mediating levels of extracellular tau in basal conditions.
- Primary hippocampal cultures respond to minocycline treatment differently from primary cortical cultures.

3.4 Discussion

The main aim of this chapter was to investigate possible differences in the contributions of astrocytes to Aß-induced tau changes and cell death in primary cortical and hippocampal cultures. To do this, an established model in which Aß-induced effects were mediated by the anti-inflammatory actions of minocycline on astrocytes was used (Garwood et al., 2011). The results outlined here suggest that hippocampal, but not cortical, astrocytes may mediate the toxic effects of Aß. No effects of Aß on tau phosphorylation or cleavage were indicated,

however, evidence from this chapter implicates astrocytes in the maintenance of extracellular tau levels in basal conditions. In addition, there were differences in the way that primary cultures from different brain regions respond to minocycline. Finally, investigations into signalling pathways mediating Aß-induced changes in primary cortical cultures demonstrate that NF-κB levels are increased in cortical neural cells following Aß treatment. Together, these results suggest that astrocytes may play different roles in different brain regions. However, further investigations are required to determine the reproducibility of these results and the mechanisms involved.

3.4.1 Aß characterisation

The synthetic $Aß_{1-42}$ used to treat cells in this chapter was extensively characterised. Results from multiple characterisation methods demonstrated consistently that the synthetic $Aß_{1-42}$ used here is comprised mainly of medium-high molecular weight oligomers of around 100-140 kDa. This is important since evidence suggests that the most toxic species of Aß may be lower weight oligomers (Fa et al., 2010), although this is a highly debated issue (Walsh and Selkoe, 2007). While larger oligomers and tau aggregates are thought to still be toxic, the particular batches of Aß used in these experiments may not contain the most toxic Aß species, possibly explaining why robust Aß-induced tau changes and increased neuronal death were not reliably observed.

Synthetic Aß has come under much criticism in the literature, as there is no standard preparation protocol or methods of interpreting results (Soto et al., 1995; Zagorski et al., 1999), discussed in greater detail in Chapter 6 (**section 6.4.1**). To determine if more physiological sources of Aß are a valid alternative, Aß derived from immortalised cell lines and from primary neurons expressing familial AD-causing mutant human APP (Walsh et al., 2002; Wu et al., 2012) were characterised. The first of these alternatives was Aß from primary mouse neurons cultured from Tg2576 mice (Wu et al., 2012). These mice overexpress human APP with the Swedish mutation and develop extensive amyloid pathology and age-dependent cognitive deficits (Hsiao et al., 1996). Results from this chapter found cultured neurons secrete low levels of $Aß_{1-38}$ and $Aß_{1-40}$. $Aß_{1-42}$ is also

secreted at picomolar concentrations. No oligomeric Aß was detected from this conditioned medium, however when attempting to characterise such low concentrations it may be that Aß oligomer levels are below the levels of detection of the assay. These concentrations make Tg2576-derived Aß a possible alternative source providing treatment of primary neuronal cultures produces AD-like effects. Unfortunately, time constraints meant preliminary tests to investigate any effects of Tg2576-derived Aß were not possible.

7PA2 CHO cells stably expressing familial AD causing mutant (V717F) human APP (Walsh et al., 2002) were investigated as a second alternative source of soluble Aß. In culture, these cells release pg/ml levels of Aß into culture medium, which can be collected and used to treat primary cells. Like Tg2576-derived Aß, no oligomers were detected by MSD assay, however oligomers may be present but be at such low concentration that they were undetectable. As these are an immortalised cell line, cultures are much easier to maintain compared to transgenic primary neurons, allowing larger volumes of Aß-containing medium to be readily collected. Previous research has shown that treating neurons with 7PA2-derived Aß results in synapse dysfunction and LTP inhibition (Walsh et al., 2002), may impair actin cytoskeleton changes in response to learning and memory (Davis et al., 2011), effects neuronal microRNA expression via the NMDA receptor, and possibly increases reactive oxygen species (Li et al., 2014a). Results shown in this chapter demonstrate that 7PA2-derived Aß did not cause changes in tau phosphorylation or cleavage or in primary cortical culture viability. However, 7PA2-derived Aß did cause increased cleavage, and activation of caspase-3, an executioner caspase closely linked with cell death in AD (Chung et al., 2001; Snigdha et al., 2012). These data may suggest that 7PA2-derived Aß is detrimental to neurons, but that neurotoxicity takes place over longer periods of time than examined here. In further support of this, reduced levels of PSD-95, a post-synaptic marker, was also found with 7PA2-derived Aß treatment suggesting neurotoxicity could be beginning with synaptic dysfunction. Additionally, others in our laboratory have also shown marked decreases in synaptic spine density following application of 7PA2-derived Aß to mouse primary neurons.

3.4.2 Aß-induced cell death and tau changes were not observed in 14 DIV primary cortical cultures

Results from this chapter found no Aß-induced increases in cell death, tau phosphorylation or cleavage in primary cortical cultures, or differences in the effects of Aß in mixed or neuronal cultures, although trends towards significant increases in Aß-induced cell death were present in mixed but not neuronal cultures. These results do not support previously published research supporting an important role of astrocytes in mediating disease-associated changes in tau and neuron death in AD (Garwood et al., 2010; Sofroniew and Vinters, 2010; Garwood et al., 2011; Perez-Nievas et al., 2013; Jo et al., 2014b; Phillips et al., 2014). The reasons for these discrepancies are not clear. However, one major difference between Garwood et al. (2011) and the work presented here is the age of cultures used, 14 DIV here versus 7 DIV previously. There are a number of reports showing marked differences in the species of tau, maturity of astrocytes and neurons, and the susceptibility of different ages of primary neural cell cultures to specific insults (Larcher et al., 1992; Lesuisse and Martin, 2002; Cullen et al., 2010; Schildge et al., 2013; Calvo et al., 2015), and these effects may account for some of the differences observed between this study and published data.

In addition, the synthetic $Aß_{1-42}$ used to treat the cells in these experiments can show significant variability. Each batch of synthetic $Aß_{1-42}$ bought by this laboratory is batch-tested to ensure it causes Aß-induced neurotoxicity in primary cultures. However, as previously mentioned, the literature suggests that synthetic Aß can vary not only between, but also within, batches (Stohr et al., 2012). This implies batch testing may not be thorough enough to ensure all synthetic Aß samples will cause neurotoxicity.

Furthermore, at the time that these experiments were being conducted, there were some serious problems with infrastructure, and essential repairs were not made because of our pending move to a new building. There were problems with tissue culture sterility because of failing air-flow fans, and laboratory-grade water was infected for periods of time. As a result of these, and other issues, baseline cell death in primary cultures was often higher than desired.

Although all reasonable efforts were made to use the healthiest cultures possible for these experiments, it is possible that poor culture health will have masked the effects of Aß or minocycline, particularly in the primary cortical culture experiments conducted during this period of time.

Nevertheless, the mechanisms underlying Aß-induced cell changes were investigated to explore possible influences of astrocytes. ICC experiments showed that NF-κB, a transcription factor involved in astrocyte activation and glial inflammatory responses (Lawrence, 2009), was visibly increased with Aß treatment, an increase rescued by minocycline pre-treatment. There is a wealth of evidence to suggest NF-κB and its downstream pathways have important contributions to the development of tau and other pathology in AD (Granic et al., 2009; Vincent et al., 2010; Cai et al., 2013; Shi et al., 2016). NF-κB is activated when IκBα is phosphorylated, thereby releasing NF-κB allowing it to translocate to the nucleus (Lawrence, 2009) and have transcriptional activity. Phosphorylation of IκBα is mediated by TLR function that is, in turn, mediated by stressors in the extracellular environment, for example, toxic Aß or high levels of oxidative stress (Yu and Ye, 2015). Activation of NF-κB is thought to trigger two main inflammatory reactions: upregulation of cytokine production by increasing their transcription in the nucleus (Wang et al., 2002), and secondly, induction of the inflammasome (Heneka et al., 2015). This protein complex regulates caspase-1-mediated cleavage and activation of pro-cytokines, including IL-1ß and IL-18 (Choi and Ryter, 2014). Together, these two main functions of NF-κB allow Aß and other triggers to initiate a glial inflammatory response by increasing cytokine transcription, maturation and release.

However, Aß-induced increases in NF-κB appeared not to be predominantly co-localised with GFAP, suggesting that NF-κB increases occurred in neurons. NF-κB also acts as a neuronal transcription factor (Kaltschmidt et al., 1994; Deng et al., 2014). Activation of neuronal NF-κB contributes to cell death in ischaemia and is also implicated in AD (Zhang et al., 2005). Furthermore, treatment with a neuroprotective antioxidant was shown to prevent NF-κB activation and inhibit neuronal death (Stephenson et al., 2000). However, NF-κB is also required

for neuronal survival (Lilienbaum and Israel, 2003) and may play some neuroprotective role in neurons in response to Aß (Kaltschmidt et al., 1997). However, the same paper found increases in NF-κB activation in neurons closest to Aß plaques and concluded that this increase in activity is responsible, partly, for the increase in pro-inflammatory gene transcription seen in diseased neurons (Kaltschmidt et al., 1997).

Western blots investigating the levels of IκBα did not show changes with Aß or minocycline treatment. This does not necessarily contradict the results obtained with NF-κB immunofluorescence, since IκBα must be phosphorylated to activate NF-κB (Shi et al., 2016), and there may be changes in IκBα phosphorylation following treatment with Aß or minocycline. Unfortunately, antibodies raised against phosphorylated IκBα were not available to pursue this avenue of research further.

Pro-inflammatory cytokines associated with AD, such as IL-1α and TNF-α, are thought to trigger activation of neuronal NF-κB (Pugazhenthi et al., 2013), which then upregulates transcription of a range of proteins, including BACE1, involved in APP processing and the production of Aß, inducing a pathological Aß production loop (Shi et al., 2016). While there was no robust evidence of Aß-induced cell death in these cultures, it is possible that events leading to neurotoxicity over longer periods of time may have been initiated. Observing the effects of Aß treatment (of any source) over longer periods of time may help to elucidate possible toxic outcomes related to NF-κB.

3.4.3 Astrocytes may regulate extracellular tau concentrations

Recent evidence suggests that tau pathology is released and spreads trans-synaptically along anatomical connections throughout diseased brain (de Calignon et al., 2012; Liu et al., 2012; Hanger et al., 2014). Characterisation of tau species released from primary cortical neurons showed extracellular tau is largely dephosphorylated and full-length, as has been previously published (Pooler et al., 2013). Furthermore, results presented here show that the amount of extracellular tau is significantly increased in the absence of astrocytes. There were no significant

differences in cell viability between neuronal and mixed cultures, indicating that the increased extracellular tau did not arise from unhealthy cells with compromised plasma membranes. While there was not time to fully explore the mechanisms involved in this phenomenon here, astrocytes are known to take up extracellular tau following its propagation *in vivo* (de Calignon et al., 2012), and this may also occur in primary culture. Alternatively, in the absence of astrocytes, excess glutamate at the synapse may not be cleared from the synaptic space (Anderson and Swanson, 2000) dysregulating glutamatergic synaptic activity in neuronal cultures and increasing physiological tau release.

Additional results examined tau release using Alphascreen assays and these did not substantiate the results showing the possible effects of astrocytes in regulating extracellular tau levels. The Alpha screen assay is known to be a less sensitive method for examining tau release, and this combined with the concentration of medium required for Alphascreens, may have affected these findings. Further investigations are required to better dissect possible functions of astrocytes in tau release and pathological tau propagation.

3.4.4 Differences in Aß and minocycline effects in hippocampal cultures versus cortical cultures

One of the main aims of this chapter was to determine if there are differences in roles of astrocytes in different brain regions. Therefore, hippocampal cultures were also treated with minocycline and synthetic $Aß_{1-42}$. The results of these experiments showed Aß significantly increased cell death in hippocampal cultures containing astrocytes, but not neuronal cultures, and minocycline only rescued the (non-significant) increases in Aß-induced neuron death in neuronal cultures. This is directly opposite to what has been previously published in primary cortical cultures (Garwood et al., 2011) and is also not consistent with results from primary cortical experiments described in this chapter. The potential reasons for these discrepancies are discussed above.

Furthermore, although Aß was found not to effect phosphorylation of tau at Ser396/404 or Ser202 epitopes in hippocampal cultures, phosphorylation at both epitopes was significantly increased following minocycline treatment. Some of these increases were also reduced when cultures were also treated with Aß, implying Aß treatment is rescuing the effects of minocycline. These results were unexpected and very difficult to rationalise. However, differences in the response of cytokines to minocycline in the hippocampus and cortex have been described previously (Levkovitz et al., 2015). It is possible that there are different targets of minocycline in different brain regions, indeed many different effects of this antibiotic have been described including downregulation of protein kinases and aggregation, reduced oxidative stress and increased scavenging of free radicals, and suppressed apoptosis (Chen et al., 2000; Tikka and Koistinaho, 2001; Lin et al., 2003; Familian et al., 2006; Ryu et al., 2006).

In conclusion, these results described here show that astrocytes may show differential responses in different brain regions, however, it was difficult to fully elucidate these in the cultures described here. Since this project started, there is an increasing body of research indicating astrocytes contribute differently to neuronal health in different brain regions and suggesting there are regional subspecies of astrocytes (Grolla et al., 2013; Rodriguez et al., 2014; Magnusson and Frisen, 2016). If therapeutic compounds targeting astrocytes are taken forward to clinical trials for AD, it will be of great importance to have better described these regional differences to increase the likelihood of obtaining disease modifying effects of treatments at different stages of AD.

3.4.5 Conclusions

To conclude, this chapter provides evidence that astrocytes are involved in mediating Aß-induced neurotoxicity, particularly in 14 DIV primary hippocampal cultures. There were subtle differences in responses to Aß in cortical and hippocampal cultures. In addition, experiments in primary cortical cultures provide evidence in support of the idea that astrocytes mediate extracellular tau concentrations in basal conditions. Perhaps most importantly, the experiments

described in this chapter clearly highlight the challenges with using synthetic and naturally secreted species of Aß. Experiments generally showed considerable variation, often preventing a clear result from being obtained.

Chapter 4: Exploring the potential of dimethyl fumarate repurposing for Alzheimer's disease

4.1 Introduction

As discussed in **Chapter 1:**, there is a large amount of research suggesting that neuroinflammation plays an important role in the development of AD pathology, rather than being merely a side-effect of disease progression (Olabarria et al., 2010; Perez-Nievas et al., 2013; Phillips et al., 2014; Heppner et al., 2015). Evidence suggests inflammation has an important role in the progression of early-onset AD, caused by mutations in the APP or PSEN genes, with activated astrocyte and microglia collecting around Aß plaques in cases with PSEN1 mutations (Shepherd et al., 2005). Furthermore, PSEN1 plays a key role in both age-dependent Aß accumulation and related inflammation, including glial and pro-inflammatory gene activation with early-onset AD-causing PSEN mutations accentuating inflammation (Saura, 2010). However, neuroinflammation has been particularly associated with late-onset AD as an increasing number of genes related to the immune response, including TREM2, CR1 and CD33, have been highlighted as genetic risk factors for late-onset AD (Guerreiro et al., 2013; Heneka et al., 2015; Karch and Goate, 2015; Villegas-Llerena et al., 2016). It is thought genetic variants of these inflammation-linked genes may increase the innate immune reaction and initial glial activation to a range of triggers, including aging and environmental factors. In turn, with additional activation of glia by Aß oligomers and deposits, this initial non-pathological inflammation can become chronic and pathological resulting in the synaptic dysfunction and neuron loss seen in AD (Heneka et al., 2015; Heneka et al., 2016).

In support of inflammation as an important trigger in late-onset AD, treatments aimed at reducing neuroinflammation and astrocyte activation have shown some success at improving AD-like pathology. For example, work in our laboratory has shown that minocycline, a tetracycline antibiotic derivative with anti-inflammatory action, described in **Chapter 3:**, reduces

tau pathology, astrogliosis and CNS cytokine content in htau mice (Noble et al., 2009b; Garwood et al., 2010). More recently, JQ1, a BET-bromodomain inhibitor was found to reduce pro-inflammatory modulators and tau phosphorylation at an AD-relevant site in another AD mouse model (Magistri et al., 2016). Emerging evidence suggests there are differences in the effects of anti-inflammatory treatments on amyloid- and tau-mediated neurodegeneration (Phillips et al., 2014). Attempts to attenuate astrocyte activation and inflammatory processes in AD mouse models by crossing APP/PS1 mice with GFAP and vimentin knockout mice resulted in exacerbation of Aß plaque pathology and increased dystrophic neurons (Kraft et al., 2013). However, over-expression of the pro-inflammatory mediator IL-1ß reduces Aß burden, yet exacerbates the development of tau pathology in 3xTg-AD mice (Ghosh et al., 2013).

The potential benefit of anti-inflammatory treatments for AD patients is also unclear. A review of the overall chance of individuals exposed to anti-inflammatory drugs developing AD, compared to the general population, suggested anti-inflammatory drugs have a protective effect against AD development (McGeer and McGeer, 1996). However, there is a lot of variability in the outcome of such epidemiological studies. For example, non-selective anti-inflammatory drugs such as NSAIDs (non-steroidal anti-inflammatory drugs, e.g. ibuprofen) have shown few effects in multiple clinical trials for AD and overall meta-analysis of these studies suggest NSAIDs do not improve or prevent AD symptoms (Miguel-Alvarez et al., 2015).

Astrocyte and microglial activation results in the initiation of multiple independent inflammatory signalling pathways that could be involved in either the acceleration or inhibition of disease pathology (Morales et al., 2014). By investigating the mechanisms and effects of each pathway it may be possible to highlight those that need to be upregulated, and those that need to be suppressed, in order to reverse or prevent the progression of AD. Inflammatory signalling pathways induced by astrocyte activation commonly involve an increase in the release of specific cytokines and chemokines from astrocytes into the extracellular space. These small signalling molecules are then able to activate receptors on nearby neurons, initiating signalling cascades that affect abnormal processing of Alzheimer's-relevant proteins, including tau (Zheng et al.,

2016). Effective drugs are likely to target specific inflammatory pathways, inhibiting destructive pathways or upregulating protective pathways. For example, treatment with minocycline resulted in the reduction of multiple pro-inflammatory cytokines suggesting the reduction in tau pathology could be due to reduced activity of downstream signalling pathways (Garwood et al., 2011). Furthermore, modulation of specific cytokines, such as IL-1ß and IL-10, by both pharmacological and genetic means, have shown that changes in specific cytokine levels have clear beneficial effects on the severity of tau and other AD-like pathology (Kitazawa et al., 2012; Ghosh et al., 2013; Chakrabarty et al., 2015). Thus, further investigation of compounds that have anti-inflammatory effects might reveal novel signalling targets that could be specifically targeted in future studies.

Once a drug has been shown to improve pathology and/or behavioural deficits in culture and rodent models, clinical trials investigating the efficacy and safety of these treatments must be carried out before its clinical benefit is tested in long-term, high-powered, clinical trials. These tests are time-consuming and highly costly (Institute of Medicine (US) Forum on Drug Discovery, 2010), increasing the time taken for successful treatments to reach patients. Initial phases of clinical trials (Phases 0 and I) focus on the pharmacodynamics and pharmacokinetics of therapies, for example, bloodstream absorbance, blood-brain barrier penetrance, and side effect/safety profiles. An alternative to new treatments is to focus on the repurposing of treatments already in clinical use or those that have failed efficacy trials for other medical problems. Such an approach is suggested to increase clinical trial safety since drugs with severe side effects have already been excluded (Appleby et al., 2013). Several publications have now highlighted the possibility of repurposing anti-inflammatory medications as a possible avenue for Alzheimer's drug discovery (Corbett et al., 2012; Appleby et al., 2013).

Dimethyl fumarate (DMF), also known as Tecfidera or BG-12, is a nuclear factor erythroid 2-related factor 2 (Nrf2) activator with poorly understood anti-inflammatory actions. DMF readily crosses the blood-brain barrier and was recently licenced for use in multiple sclerosis patients in both the US and the EU (FDA, March 2013; EU CHMP, Feb 2014) based on Phase III clinical

trials which demonstrated that DMF significantly reduced relapse rate and slowed rate of disability progression in relapsing-remitting multiple sclerosis (Fox et al., 2012; Gold et al., 2012). DMF was thought to have good potential for repurposing since it appears to be protective against oxidative stress (Lee et al., 2012), attenuates spatial memory impairments and hippocampal degeneration in rats (Majkutewicz et al., 2016) and reduces synucleinopathy in Parkinson's models (Lastres-Becker et al., 2016).

Therefore, it was of interest to determine the effects of DMF treatment on astrocyte-mediated changes in tau. The effects of DMF on astrocyte activation and tau phosphorylation were first investigated in rat primary mixed neuron and astrocyte cultures. Promising findings in this model prompted investigation of DMF effects in a model of tauopathy *in vivo* with the main hypothesis that DMF would reduce tau phosphorylation and related pathology (e.g. tau aggregation) in the htau mouse brain.

The *in vivo* studies were conducted using htau mice. This mouse model, generated by crossing mice over-expressing the entire wildtype human tau gene (Duff et al., 2000) with a tau knock-out mouse line (Tucker et al., 2001), was developed by Andorfer and colleagues (Andorfer et al., 2003). The resulting htau offspring overexpress the six isoforms of human tau found prominently in adult human CNS on a mouse tau knockout background. Htau mice show an age-dependent degenerative phenotype with a range of pathological brain changes. Increased tau phosphorylation, cleavage and aggregation into paired helical filaments and tangle-like structures have been well documented in these mice (Andorfer et al., 2003; Kelleher et al., 2007; Noble et al., 2009b), accompanied by astrocyte activation and neuroinflammatory changes (Garwood et al., 2010). Furthermore, htau mice show impairments in object recognition and spatial memory (Polydoro et al., 2009) followed by significant neuronal loss and cortical thinning in 8 month-old and older mice (Andorfer et al., 2005). While htau mice have no Aß pathology, the nature of the tau pathology, such as the formation of paired helical filaments indistinguishable from those extracted from AD brain when examined by electron microscopy (Andorfer et al., 2003), and marked tau-dependent behavioural deficits (Polydoro et al., 2009)

indicate that these animals are a good model for examining AD-relevant pathological changes in tau. Their relevance for examining the influence of neuron-glial interactions on tau has also been elegantly demonstrated (Bhaskar et al., 2010; Maphis et al., 2015).

The aims of this chapter were to:

- Investigate the effect of DMF treatment on astrocyte activation and tau phosphorylation in rat mixed primary cell cultures.
- Conduct pilot studies to examine the effects of DMF treatment on biochemical and behavioural phenotypes in htau mice.
- Explore possible mechanistic pathways linking DMF to changes in tau in primary cultures and htau mice.

4.2 Methods

Materials and methods used in this chapter, included detailed methodology for the production of primary cell cultures, were described in Chapter 2 (**sections 2.1**). For primer design for mouse genotyping see Chapter 2, **section 2.3.1**).

For all cell culture experiments, 13 DIV mixed primary cortical cultures were treated with DMF for 24 h and then lysed using methods described in Chapter 2, **section 2.4.1**. Lysates were standardised to total protein concentration using a BCA assay (Chapter 2, **section 2.4.2**) and run on 10 % tris-glycine gels for western blotting (see Chapter 2, **section 2.6**).

Htau mice were genotyped as outlined in Chapter 2 (**section 2.3.1**). Two separate cohorts of homozygous htau mice were used in this study to represent different disease stages:

1. 8-9 months old, show only small increases in tau phosphorylation and some tau aggregation.
2. 13-14 months old, display significant tau phosphorylation and accumulation of insoluble tau.

Both cohorts were comprised of approximately equal numbers of male and female mice. A small number of littermate wild-type (WT) mice of 13-14 months old were also assessed. Some htau mice in this cohort were left untreated to determine any effects of mouse handling for behavioural analysis and treatment (**Table 4.1**).

DMF (15 mg/kg) was administered via oral syringe twice daily (Eichenbaum et al., 2011) as described in Chapter 2 (**section 0**). 13-14 month old mice were tested for spatial memory deficits using the Morris water maze as described in Chapter 2 (**section 2.8.3**).

Following the final treatment mice were sacrificed by cervical dislocation (for full methods see Chapter 2, **section 2.3.2**) and the brains removed. The brain was crudely dissected into frontal, temporal, hippocampal, occipital/parietal and cerebellum regions then rapidly snap frozen in liquid nitrogen for biochemical analysis as described in Chapter 2, **section 2.4.1**.

Age (months)	Genotype	Treatment	Number
13-14	Htau	DMF	4
		Vehicle	5
		Untreated (CTRL)	3
	WT	DMF	1
		Vehicle	1
8-9	Htau	DMF	5
		Vehicle	5

Table 4.1: Mice used in DMF pilot study
Age, genotype, treatment and number of mice shown in each group is shown.

4.3 Results

4.3.1 Preliminary work

Generation of primary cell cultures

Rat primary mixed cortical cultures were prepared from E18 Sprague Dawley rat embryos and cultured for 13 DIV before treatment with DMF for 24 h. Cultures were assessed at 14 DIV since they have developed functional synapses by this developmental stage (Maeda et al., 1995; Grabrucker et al., 2009). These rat primary mixed cortical cell cultures are described in more detail in Chapter 3 (**section 3.3.1**).

Assessing DMF toxicity in primary cortical cultures

The literature and reagent safety data sheet suggest using low concentrations of DMSO as a vehicle for DMF, to encourage full dissolution. DMSO is a common solvent, often used for cell culture, however it is also toxic to cells at concentrations above 0.5 % (v/v) (Hanslick et al., 2009). Therefore, an assessment of primary cell culture tolerance of DMF and DMSO was first necessary. Previous studies suggest treating cell cultures with 10-30 µM DMF for 24 h (Wierinckx et al., 2005; Wilms et al., 2010; Albrecht et al., 2012). Therefore, a dose-response including these concentrations was first conducted.

A stock solution of 1 mM DMF in 1 % (w/v) DMSO was prepared. Both DMF and DMSO were diluted in culture medium to give final concentrations in culture of 0.1 µM – 1 mM DMF and 0.0001 – 1 % (v/v) DMSO. The corresponding concentration of DMSO was used as a control for each DMF treatment. Cultures were treated at 13 DIV for 24 h. Cell viability was measured at 14 DIV using a LIVE/DEAD assay, as described in Chapter 2 (**section 2.2.5**). Incorporation of the dead cell dye by cells with compromised membranes gives a measure of cell death. The results of these experiments showed that treatment with 1 mM DMF and 1 % DMSO caused increased amounts of cell death relative to control untreated cells (CTRL). Concentrations of 100 µM DMF or less, and respective DMSO treatments, did not reduce cell viability in comparison to untreated control cultures (**Figure 4.1**). As a result of these experiments treatment concentrations of 30

µM and 60 µM DMF (0.03 % and 0.06 % DMSO, respectively) were chosen for subsequent cell culture experiments since these were the highest doses tested that showed no apparent toxicity.

Breeding and genotyping of htau mice

Htau pups were ear punched and genotyped using PCR to ensure (1) the presence of the human tau gene, (2) absence of endogenous tau and (3) eGFP, the targeted insertion of which disrupts endogenous tau expression. Samples in which a GFP band (173 kb) is detected in the absence of mouse tau (187 kb) indicate a mouse with a homozygous mouse tau gene knock-out. DNA from htau mice homozygous for human tau showed a strong band at 187 kb when amplified with human tau-specific primers, while mice heterozygous for human tau show multiple faint bands at 187 kb and larger (**Figure 4.2**).

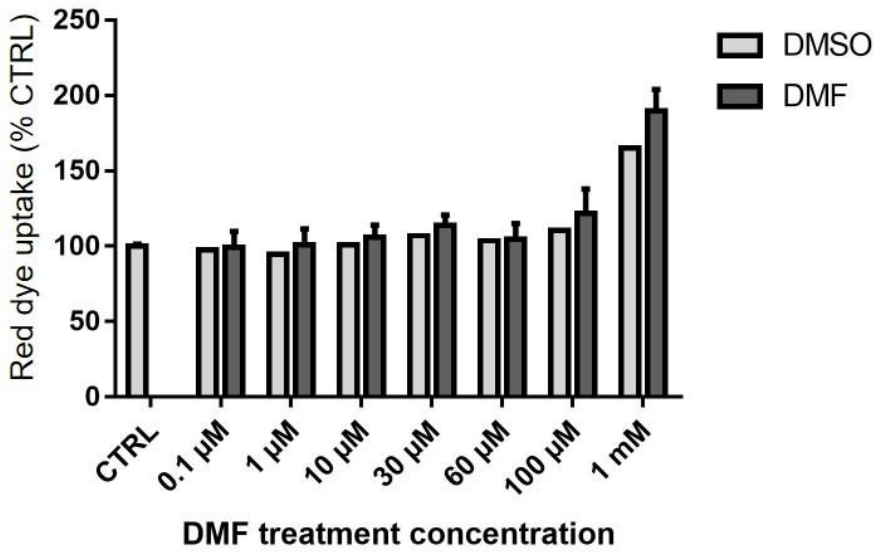

Figure 4.1: Cell death in DMF-treated rat primary mixed cortical cultures

Bar chart shows intensity of LIVE/DEAD dye incorporation, measured by the density of dye staining, as an indicator of cell death, in primary cultures treated with 0.1 µM - 1 mM dimethyl fumarate (DMF) in comparison to cultures treated with DMSO and untreated control (CTRL) cultures. Values represent mean ± SEM. CTRL: n=3, DMF: n=2, DMSO: n=1.

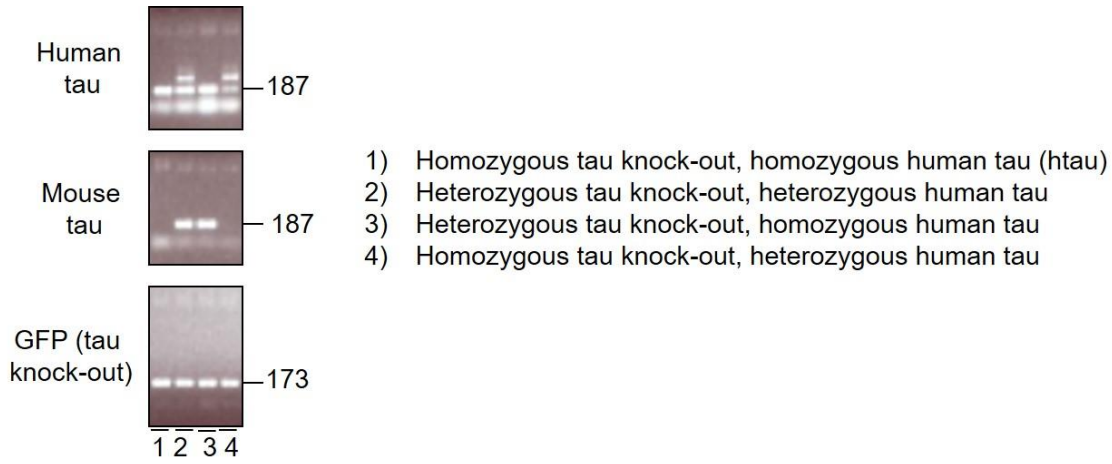

Figure 4.2: Htau genotyping
Primers against human tau amplify only the human tau transgene (187 kb), mouse tau primers detect endogenous tau only (187 kb), GFP primers detect a targeted insertion of GFP (173 kb) used to disrupt the endogenous tau gene. Examples of transcripts detected in mice homozygous or heterozygous for human tau expression and mouse tau knock-out are shown. Base pair markers on right. Lane 1 shows transcripts amplified from an htau mouse ear-punch.

4.3.2 The effects of DMF on tau and astrocytes in mixed primary cortical cultures

To begin to understand if DMF might have benefit in models of AD, 13 DIV primary mixed cortical cultures containing astrocytes and neurons were treated with 30-60 µM DMF for 24 h. Following treatment, cell lysates were collected for analysis of changes in the astrocyte marker GFAP, total tau amounts and tau phosphorylation at epitopes known to be abnormally phosphorylated in AD brain (Hanger et al., 2009).

DMF treatment reduces tau phosphorylation in primary cortical cultures

Mixed primary cortical cultures were treated with 30 µM and 60 µM DMF and lysed after 24 h. Lysates were normalised for protein content and western blotting with antibodies against total and phosphorylated tau performed. Quantification of signal intensity from total tau immunoblots showed that there was no change in total tau levels when cells were treated with 30 and 60 µM DMF relative to controls (**Figure 4.3 A**). This suggests that DMF does not affect either expression or turnover of tau.

When western blots were probed with the PHF1 antibody, no changes in tau phosphorylation at Ser396/404 were found following DMF treatment of cells in comparison to those treated with vehicle (**Figure 4.3 A**). However, when phosphorylation at Ser202 was examined using the CP13

antibody, treatment of cells with 60 µM DMF resulted in reduced signal intensity. When this signal was quantified as a proportion of total tau, 60 µM DMF was found to have significantly reduced tau phosphorylation at the CP13 epitope relative to controls ($p<0.05$). Lysates from cultures treated with 30 µM DMF also showed reduced levels of CP13 on western blots, but quantification of this change showed that this reduction did not reach statistical significance (**Figure 4.3 A, B**).

Western blots were also probed with the Tau-1 antibody that detects tau dephosphorylated at Ser199/202/Thr205 (Szendrei et al., 1993). Western blots probed with Tau-1 showed a trend towards increased Tau-1 immunoreactive tau with increasing concentration of DMF treatment, however quantification of these signals showed the differences did not reach statistical significance relative to lysates from control cultures (**Figure 4.3 A**). Since the western blotting data suggested that there might be subtle changes in phosphorylation of tau at the Tau-1 epitope, lysates from these cultures were also assessed by semi-quantitative tau ELISA using antibodies against total tau and Tau-1 (for method see Chapter 2, **section 2.7**). Using this more sensitive method, the increase in Tau-1 amount as a proportion of total tau was found to be significantly increased following treatment of cells with 60 µM DMF in comparison to vehicle-treated cultures (**Figure 4.3 C**). A clear dose-dependent effect of increasing DMF concentration could also be observed. These data indicate that DMF treatment results in significantly reduced tau phosphorylation at specific tau epitopes known to be abnormally phosphorylated in AD brain (Hanger et al., 2009) and suggest that DMF is worth pursuing to determine if it has beneficial effects in models of tauopathy.

DMF treatment does not reduce astrocyte activation in primary cortical cultures

DMF has been previously shown to have microglial and astrocytic anti-inflammatory effects (Wilms et al., 2010) so it was of interest to determine if the tau changes seen with DMF treatment may be due to DMF effects on astrocytic activation and induction of inflammatory signalling. There are no microglia in the primary cortical cultures used for these experiments, however, this laboratory has previously shown a connection between astrocytic inflammatory

signalling and changes in tau phosphorylation (Garwood et al., 2011). Therefore, changes in astrocyte activation were first explored using GFAP as a marker of activated astrocytes. Lysates from control and DMF treated cultures were assessed by western blotting using an antibody against GFAP. No apparent changes in GFAP amounts were observed on blots, and quantification of signal intensity relative to ß-actin showed that neither concentration of DMF reduced GFAP amounts relative to control cultures (**Figure 4.3 A**). This suggests the reductions in tau phosphorylation resulting from DMF treatment may not occur via alterations in astrocyte activity, although this does not necessarily exclude an effect of DMF on inflammatory signalling. Overall, these preliminary experiments show that DMF treatment readily reduces tau phosphorylation in primary cell cultures, likely independent of effects on astrocyte activation. The significantly reduced tau phosphorylation observed suggested that DMF was worth pursuing in pilot studies in an *in vivo* model of tauopathy.

4.3.3 DMF treatment of htau mice

Since DMF showed good potential for lowering tau phosphorylation in primary cell culture and has shown few side-effects when used previously to treat mice with a range of neurological conditions (Heiligenhaus et al., 2004; Schilling et al., 2006; Lee et al., 2012; Lastres-Becker et al., 2016), the effect of DMF *in vivo* was next assessed in a pilot study using the htau mouse model of tauopathy. Two ages of mice were treated, 13-14 month old mice which represent a mid-disease stage with significant tau phosphorylation and aggregation apparent, and 8-9 month old younger mice which have milder disease-associated tau abnormalities (Andorfer et al., 2003; Kelleher et al., 2007).

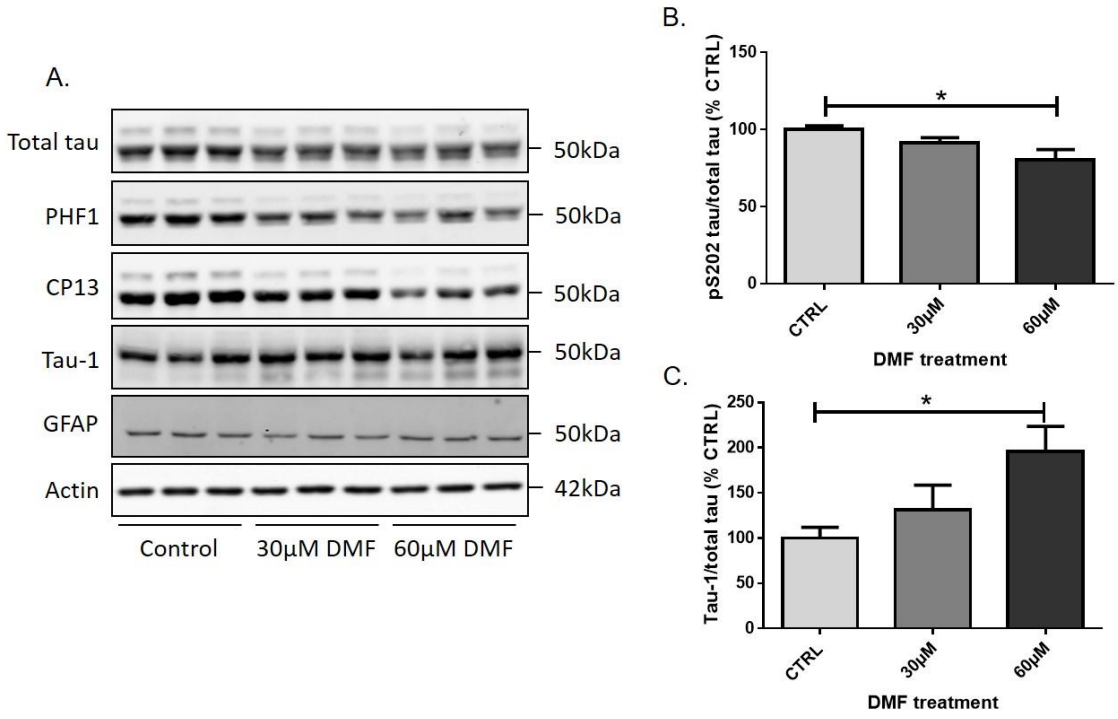

Figure 4.3: DMF treatment reduces tau phosphorylation at some residues but has no effect on total tau or GFAP levels in primary rat mixed cortical cultures
A. Representative western blots of DMF-treated lysates probed with antibodies against total tau, tau phosphorylated at Ser396/404 (PHF1), Ser202 (CP13), tau dephosphorylated at Ser199/202/Thr205 (Tau-1) and GFAP. Blots were also probed with an antibody against ß-actin as a loading control. Molecular weight markers are shown on the right. **B.** Bar chart shows quantification of western blotting. Tau phosphorylated at Ser202 was analysed as a proportion of total tau (n=15) **C.** Bar chart shows quantification of tau dephosphorylated at the Tau-1 epitope as a proportion of total tau as determined by tau ELISA (n=6). Values shown are mean ± SEM as percentage control (CTRL). Data was analysed by one-way ANOVA. * = $p<0.05$.

DMF treatment does not affect htau performance in the Morris water maze

Tau is closely associated with synaptic degeneration and dementia in AD (Perez-Nievas et al., 2013), therefore cognitive function in the 13-14 month old aged mice was examined using the Morris water maze during the period of time they were treated (see treatment schedule Chapter 2, **section 2.3.2**). The Morris water maze (Morris, 1984) has been used previously to demonstrate age-dependent spatial learning deficits in htau mice (Polydoro et al., 2009). In addition, the water maze is known to test hippocampal-dependent spatial memory (Bromley-Brits et al., 2011). This is important because hippocampal pathology and deficits in hippocampal-

dependent functions are among the earliest abnormalities observed in AD patients (Dhikav and Anand, 2011; Jahn, 2013).

Mice were trained in the Morris water maze before and after treatment with DMF to find a hidden platform for five consecutive days. To allow the mice to learn the platform location, the platform was visible on the first day. A probe trial was conducted after the final day of hidden platform testing, during which the platform was removed. The time required to find the hidden platform during training, and the percentage time spent in each quadrant during the probe trial were determined.

Mice were randomly assigned to treatment groups prior to the first administration of DMF and performance in the Morris water maze was determined for each group. Prior to administration of DMF, neither WT or htau mice showed changes in the time taken to find the hidden platform as training progressed from day 0 to day 4 (**Figure 4.4 A**). The average distance swum by the mice as the trial progressed also appeared to remain unchanged (**Figure 4.4 C**). Additionally, mice did not appear to search more in the platform quadrant when a probe test was carried out on day 4 (**Figure 4.4 B**). This might suggest that htau mouse hippocampal-dependent spatial memory is impaired which would be expected based on previous behavioural studies of this mouse model (Polydoro et al., 2009). However, results from the small number of WT mice included in the study appeared to follow the same pattern as that of htau mice, so it is not possible to state that the htau mice had a behavioural deficit with any certainty.

Following administration of DMF twice daily for 14 days, the same mice were re-tested on the Morris water maze test during the last five days of DMF treatment. No differences were apparent between DMF treated and control groups (vehicle-treated and untreated controls) or between htau mice and WTs in either the training days or the probe trial (**Figure 4.4 D-E**). Overall, the analysis of these Morris water maze results suggests DMF treatment has had no effect on the hippocampal-dependent spatial memory in treated mice. However, biochemical changes in AD-relevant proteins are apparent a long time in advance of cognitive deficits being

seen (Braak et al., 2011; Mufson et al., 2016), therefore it was important to investigate the effects of DMF on disease-relevant protein changes in htau brain.

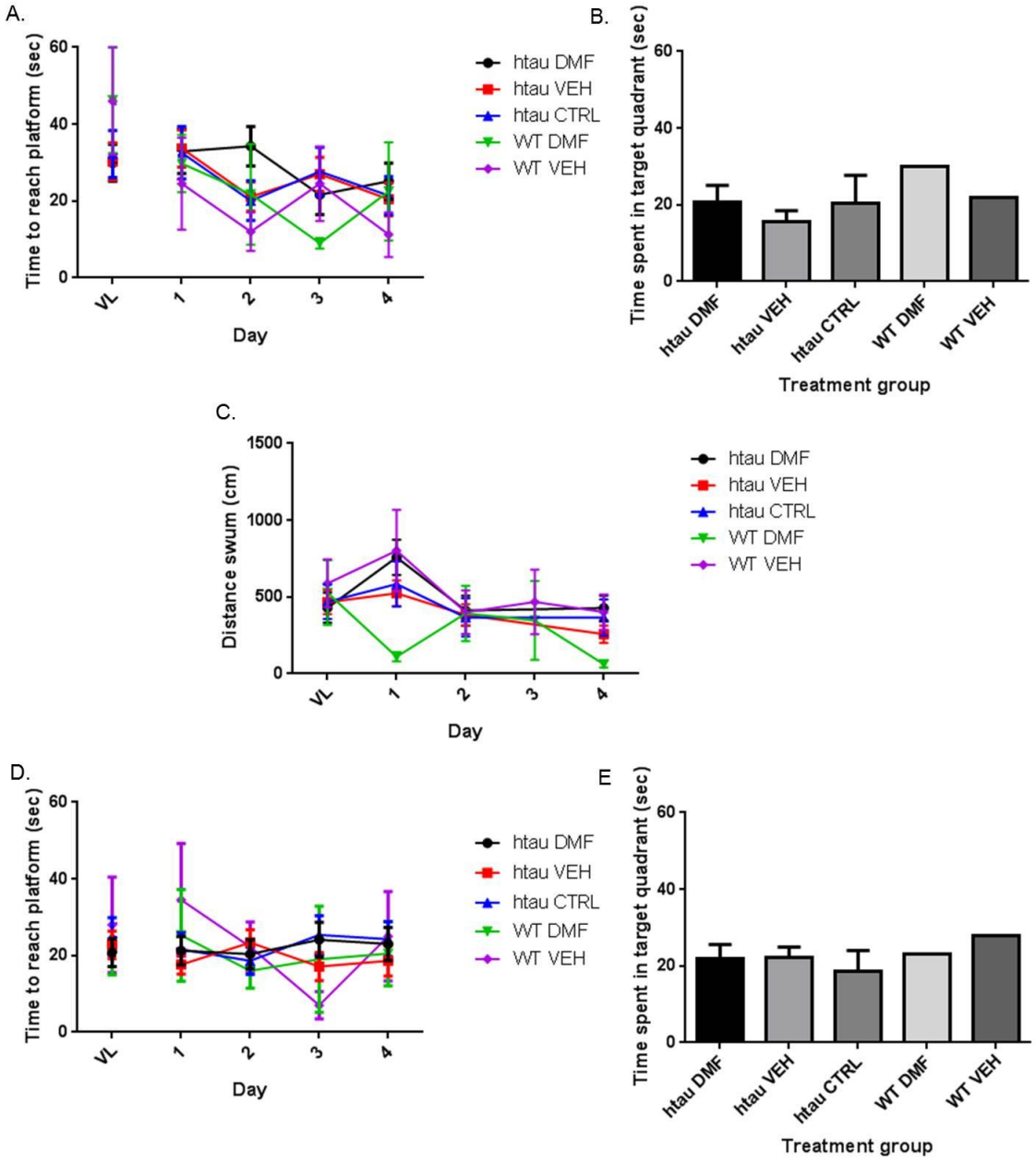

Figure 4.4: DMF treatment does not improve Morris water maze performance
A. Line graph shows time taken for 13-14 month old mice to find the hidden platform in pre-treatment water maze according to genotype and treatment group. **B.** Bar chart shows time mice spent in target quadrant during the probe test prior to DMF treatment. **C.** Line graph shows distance swum by mice to find the hidden platform in pre-treatment water maze according to genotype and treatment group. **D.** Line graphs show time taken for mice to find the hidden platform post-treatment. **E.** Bar chart shows time mice spent in target quadrant during probe test after DMF treatment. VL indicates training day when platform was visible. Days 1, 2, 3 and 4 indicate each consecutive day of hidden platform training. DMF htau: n=4, VEH htau: n=5, CTRL htau: n=3, DMF WT: n=1, VEH WT: n=1. Values represent mean ± SEM.

Analysis of the effects of DMF on tau proteins in aged htau mice

Homogenates from the frontal cortices of 13-14 month old aged mice were run on western blots and probed with antibodies against total and phosphorylated tau. Treatment with DMF led to no apparent changes in total tau as labelled by the DAKO tau antibody (**Figure 4.5 A**). However, when total tau was immunoblotted with antibody specific to human tau (CP27) there appeared to be a decrease in tau amounts in htau mice treated with vehicle or DMF relative to untreated mice, suggesting that the vehicle had an effect on human tau levels (**Figure 4.5 A**). Only daily handling and twice daily oral administration of a sugar solution differentiated the vehicle-treated and untreated control groups in the preclinical trial. It is unexpected that handling and treatment of the mice with the vehicle solution could produce significant changes in brain biochemistry. Furthermore, since htau mice only express human tau, the CP27 and total tau blots should be detecting the same tau protein, so the reason for the difference in findings when samples were immunoblotted with DAKO and CP27 is difficult to explain. These results might suggest, however, that DMF has an effect on total tau amounts through a mechanism that is not understood. Quantification of human tau and total tau immunoreactivity in htau brain samples following normalisation to ß-actin confirmed that there was a significant decrease in human, but not total, tau in DMF treated mice (**Figure 4.5 B, C**). Immunoblots of WT mouse brain showed less total tau than htau mice and no detectable human tau (**Figure 4.5 A**). This is expected as human tau is over expressed in htau mice, resulting in total tau amounts in homozygotes that are 3-4 times higher than in WT mice (Duff et al., 2000; Andorfer et al., 2003).

Since treatment of primary cortical cultures with DMF showed an effect of treatment on tau phosphorylation, it was important to determine if DMF treatment of htau mice had a similar effect. The same brain homogenates used to investigate differences in human and total tau were also probed with the same range of phospho-specific antibodies as used in DMF cell culture experiments previously described in this chapter (**section 4.3.2**). These phospho-specific antibodies were chosen because they bind to tau epitopes known to be abnormally phosphorylated in AD (Augustinack et al., 2002; Hanger et al., 2009; Mondragon-Rodriguez et

al., 2014). When western blots were probed with the CP13 and PHF1 antibodies it was obvious that there was less phosphorylation in WT brain compared to htau brain, as expected (**Figure 4.5 A**). The CP13 and PHF1 signals were quantified as a proportion of total tau in **Figure 4.5 D, E**, and suggest increased tau phosphorylation in htau mice as expected.

Probing western blots with Tau-1, an antibody that binds specifically to tau dephosphorylated at Ser199/202/Thr205, showed stronger bands in WT than in htau brain homogenates (**Figure 4.5 A**). This is reflected in the quantification of these blots in **Figure 4.5 F**. It is likely that a substantial percentage of tau in the WT mouse brain is dephosphorylated at these epitopes as increased phosphorylation at these sites has been associated with abnormal tau pathology and NFT formation (Augustinack et al., 2002).

There were no apparent differences in tau phosphorylation in DMF-treated animals relative to controls in immunoblots probed with antibodies against phosphorylated tau (**Figure 4.5 A**). Quantification and statistical analysis of tau phosphorylation as a proportion of total tau confirmed that there were no significant differences between DMF treated, vehicle-treated and untreated control aged htau mice (**Figure 4.5 D-F**). This suggests that DMF does not reduce tau phosphorylation in the frontal cortex of the htau brain, at least not at the phospho-epitopes tested here. These *in vivo* findings are in contrast to the results of cell culture experiments described earlier in this chapter (**section 4.3.2**).

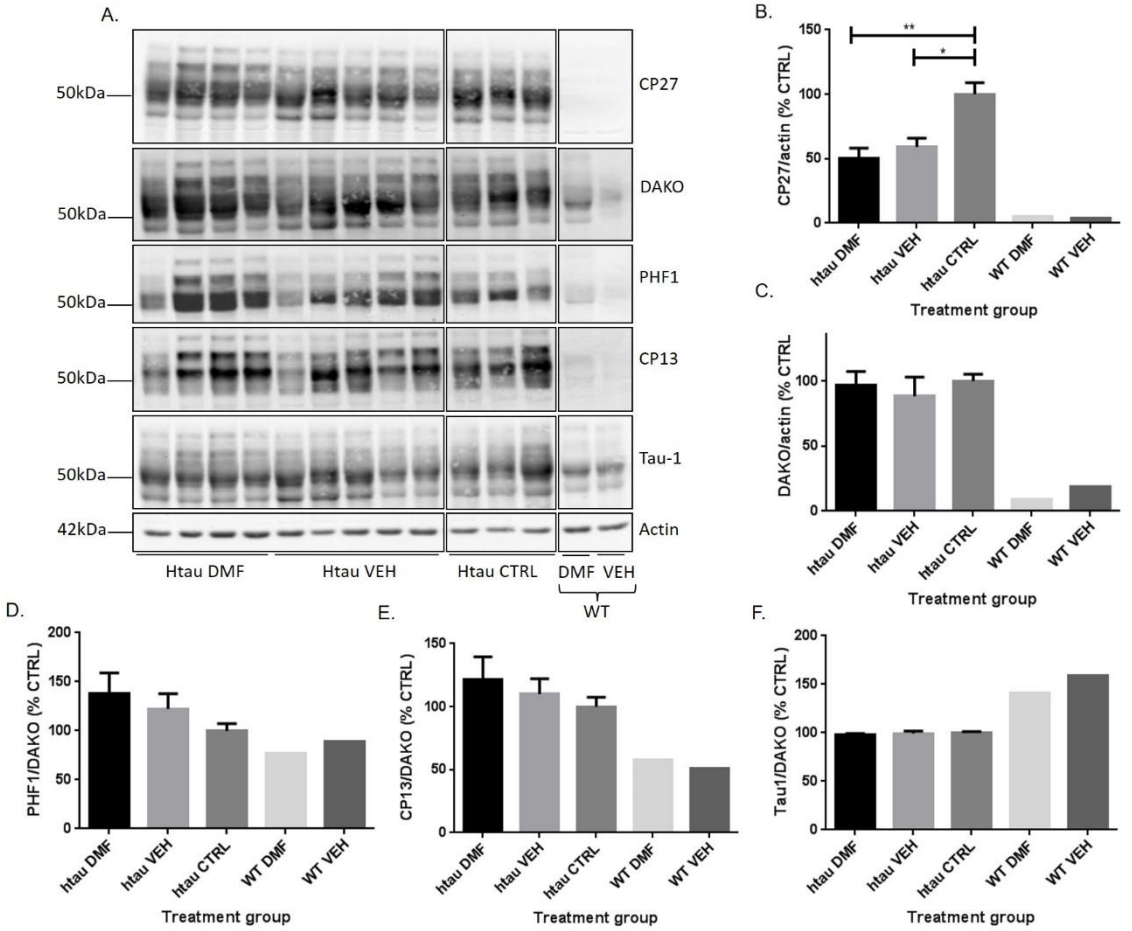

Figure 4.5: Total and phosphorylated tau levels are not changed by DMF treatment *in vivo*
A. Western blots of frontal brain homogenate from DMF or vehicle-treated and untreated control 13-14 month old htau and WT mice probed with antibodies against human tau (CP27) total tau (DAKO), tau phosphorylated at Ser396/404 (PHF1), Ser202 (CP13) and tau dephosphorylated at Ser199/202/Thr205 (Tau-1). Blots were also probed with an antibody against ß-actin as a loading control. Molecular weight markers are shown on the left. **B.-F.** Bar charts show quantification of western blotting. Human tau (**B.**) and total tau (DAKO) (**C.**) were analysed as a proportion of ß-actin. Tau phosphorylated at Ser396/404 (PHF1) (**D.**), Ser202 (CP13) (**E.**) and tau dephosphorylated at Ser199/202/Thr205 (Tau-1) (**F.**) were analysed as a proportion of total tau (DAKO). Htau DMF: n=4, htau VEH: n=5, htau CTRL: n=3, WT DMF: n=1, WT VEH: n=1. Values shown are mean ± SEM as percentage htau control (CTRL). Data was analysed by one-way ANOVA. * = p<0.05, ** = p<0.01.

Sarkosyl extraction of insoluble tau

Insoluble tau aggregates accumulate in pathological lesions in both human AD and htau mouse brain (Meraz-Rios et al., 2010; Cowan and Mudher, 2013), therefore investigating changes in tau aggregates could determine if DMF was having any effects on tau distinct from changes in phosphorylation. A sarkosyl extraction protocol was used to isolate insoluble tau from htau hippocampus. Previously published studies have used sarkosyl insolubility as a standard test for

insoluble tau aggregates and tangles (Julien et al., 2012). The tau isolated from brain by sarkosyl is representative of that deposited in NFTs (Noble et al., 2003). The sarkosyl isolation protocol gives rise to several fractions – a low speed supernatant (LSS) containing both sarkosyl soluble and insoluble tau, a high speed supernatant (HSS) containing only soluble tau, and the high speed pellet which contains sarkosyl insoluble tau. The LSS and resuspended sarkosyl-insoluble pellets from aged htau mouse brain samples were western blotted with antibodies specific to total and phosphorylated tau. WT brain samples were not used as no sarkosyl insoluble tau would be expected in these homogenates. There were no apparent changes in tau protein amounts following treatment of htau mice with DMF. Quantification of total tau amounts showed no differences in tau phosphorylation at the PHF1 epitope as a proportion of total tau in the LSS following treatment with DMF (data not shown). In addition, there were also no significant changes in sarkosyl insoluble tau amounts, once normalised to tau content in the LSS, between DMF and vehicle-treated htau mice (**Figure 4.6**). It was clear that the sarkosyl insoluble tau was somewhat phosphorylated by the signals detected on western blots, however this could not be quantified as there was too little protein detected to produce clear bands (**Figure 4.6 A**). Taken together, these results suggest that DMF treatment does not affect the pathological phosphorylation and aggregation of tau characteristic of aged htau transgenic mice. However, it is possible that the pathology in these older mice is already too severe for DMF to have a significant effect. For this reason, the same treatment protocol was repeated in younger (8-9 month old) mice which represent an early disease stage (Kelleher et al., 2007).

Analysis of the effects of DMF on tau proteins in younger htau mice

Frontal cortices of younger htau mice (8-9 month old) were homogenised and ran on western blots to investigate the effects of DMF treatment at an earlier disease stage than previously examined above. Blots were probed with antibodies against total and phosphorylated tau as before. At 8-9 months of age htau mice should show less tau pathology than those at 13-14 months of age, however tau proteins show increased phosphorylation (Andorfer et al., 2003). There were no immediately apparent differences in either tau amounts or tau phosphorylation

when blots were imaged (**Figure 4.7 A**). Quantification of western blot signals and analysis of total tau amounts revealed no significant effect of DMF treatment (**Figure 4.7 A-B**). This is consistent with results obtained from analysis of 13-14 month old htau mice and in cell culture experiments (**section 4.3.2**). Analysis of changes in tau phosphorylation at the PHF1, CP13 and Tau-1 epitopes as a proportion of total tau in each sample also showed that there were no differences between treatment groups (**Figure 4.7 C-E**). This is consistent with the results found with the previous mouse cohort and suggest that DMF treatment does not reduce tau phosphorylation *in vivo*.

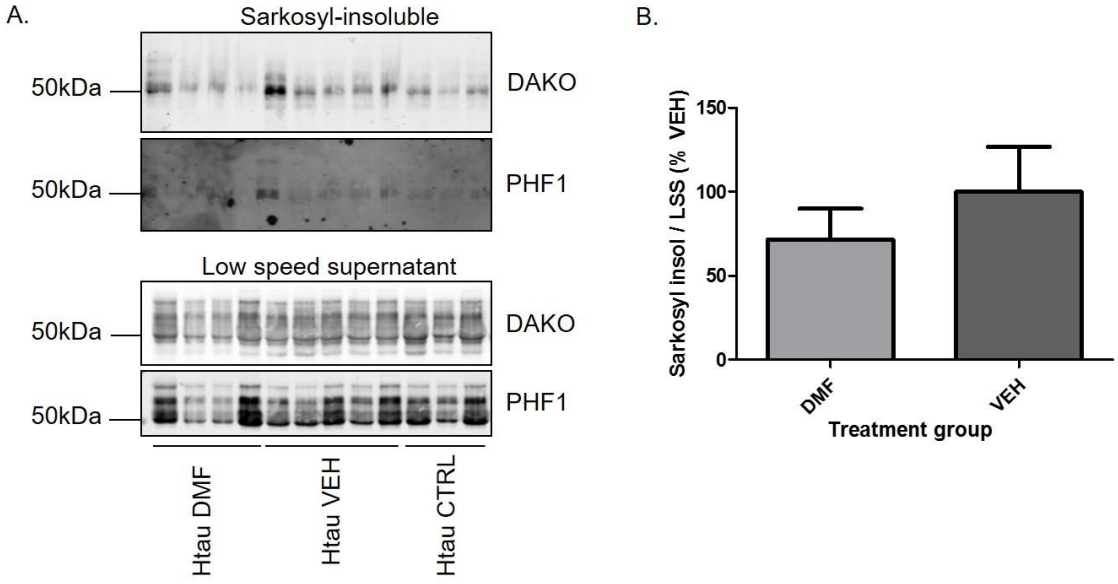

Figure 4.6: DMF treatment does not affect the accumulation of sarkosyl-insoluble tau
A. Western blots of sarkosyl-insoluble and LSS (sarkosyl-soluble and insoluble) fractions isolated from hippocampus of 13-14 month old htau mice and probed with total tau (DAKO) and PHF1 (pSer396/404) antibodies. Molecular weight markers are shown on the right. **B.** Bar chart showing total tau amounts in the sarkosyl-insoluble fraction following normalisation to tau amounts in the LSS. Only DMF and vehicle-treated brain samples were included in the statistical analysis to reduce statistical noise. Values represent mean ± SEM as percentage vehicle (VEH). DMF n=4, VEH n=5.

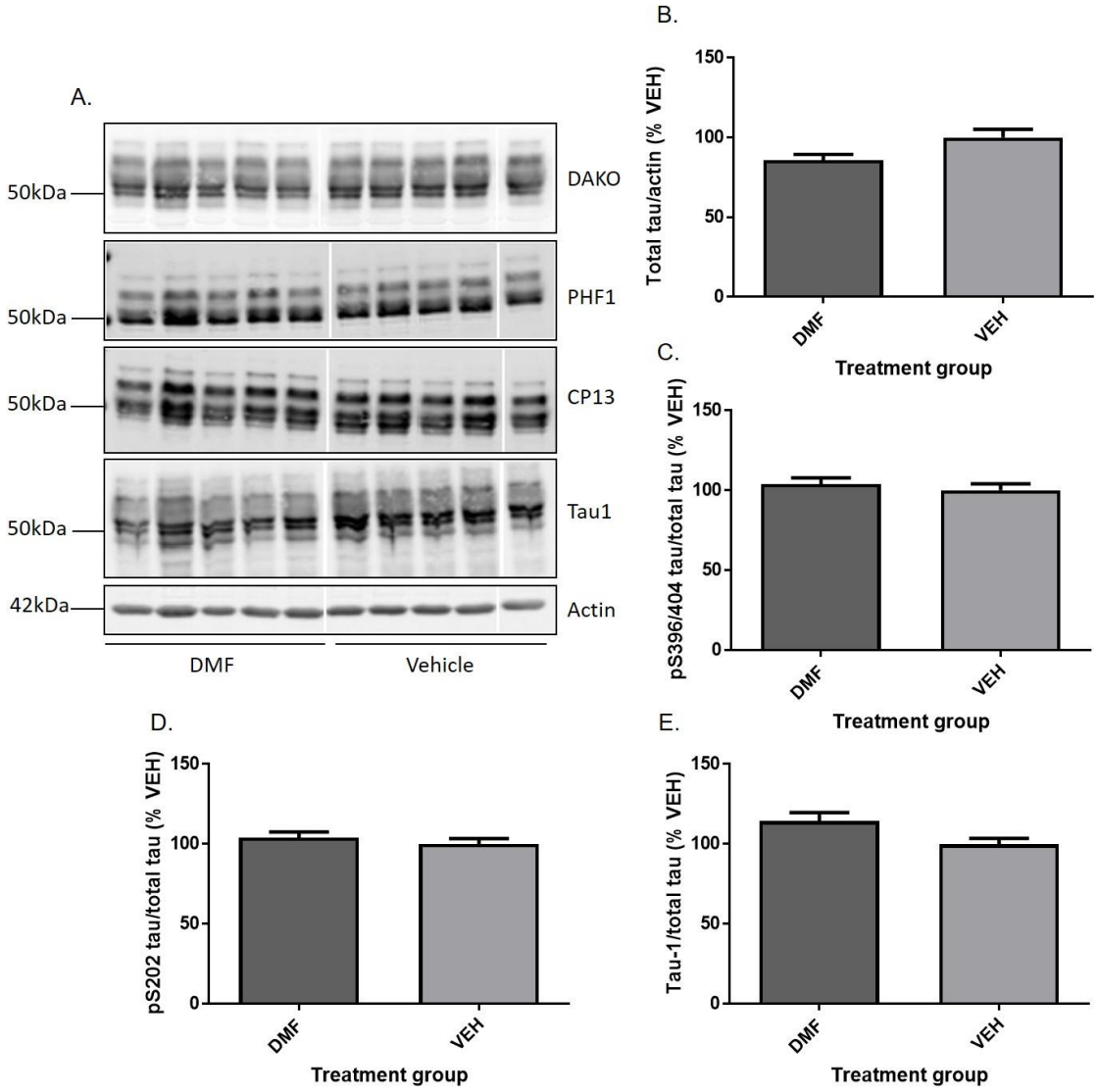

Figure 4.7: There is no effect of DMF treatment on tau phosphorylation in cortex from 8-9 month old htau mice

A. Western blots of frontal brain homogenate from DMF-and vehicle-treated 8-9 month old htau mice probed with antibodies against total tau (DAKO), tau phosphorylated at Ser396/404 (PHF1), Ser202 (CP13) and tau dephosphorylated at Ser199/202/Thr205 (Tau-1). Blots were also probed with an antibody against ß-actin as a loading control. Molecular weight markers are shown on the left. **B.-E.** Bar charts show quantification of western blotting. (**B.**) Total tau (DAKO) was analysed as a proportion of ß-actin. (**C.**) Tau phosphorylated at Ser396/404 (PHF1), (**D.**) Ser202 (CP13) and (**E.**) tau dephosphorylated at Ser199/202/Thr205 (Tau-1) were calculated as a proportion of total tau (DAKO) in each sample. DMF: n=5, VEH: n=5. Values shown are mean ± SEM as percentage vehicle-treated (VEH). Data was analysed by Student's t-test.

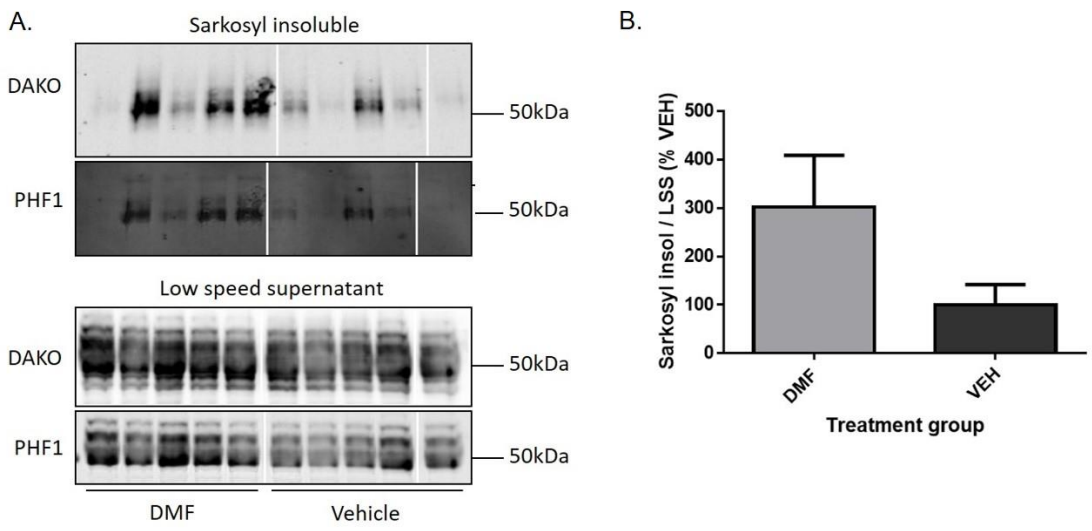

Figure 4.8: There is a trend towards an increase in sarkosyl insoluble tau levels with DMF treatment

A. Western blots of sarkosyl-insoluble and low speed supernatant (sarkosyl-soluble and insoluble) fractions isolated from hippocampus of 8-9 month old htau mice and probed with total tau (DAKO) and PHF1 (pSer396/404) antibodies. Molecular weight markers are shown on the right. **B.** Bar chart showing total tau amounts in the sarkosyl-insoluble fraction following normalisation to tau amounts in the LSS. Values represent mean ± SEM as percentage vehicle (VEH). DMF n=5, VEH n=5.

Sarkosyl extraction of insoluble tau

Brain pathology and behavioural deficits are age-dependent in the htau mouse; therefore, it would be expected that these younger mice have less insoluble tau aggregates than the aged mice. However, previous characterisation of the htau mouse model shows tau aggregates are present, albeit in lesser amounts, in 9 month old htau mice (Andorfer et al., 2003). Therefore, sarkosyl-insoluble tau was isolated from the hippocampus of 8-9 month old htau mice as described earlier in this chapter. Western blots showed approximately equivalent amounts of total tau and tau phosphorylated at the PHF1 epitope in the LSS from DMF- and vehicle-treated mice (**Figure 4.8 A**). Quantification of tau phosphorylation at PHF1 relative to total tau confirmed that there were no significant differences between groups (data not shown). Similarly, levels of tau phosphorylated at the PHF1 epitope in the sarkosyl insoluble fraction appeared to be higher in the DMF-treated brain homogenates (**Figure 4.8 A**). Quantification of tau phosphorylation at PHF1 relative to total tau found that this difference was not statistically significant (data not

shown). However, western blots showed higher levels of sarkosyl-insoluble tau in samples from DMF-treated htau brains in comparison to vehicle-treated htau brains (**Figure 4.8 A**). When the amounts of sarkosyl-insoluble tau were calculated as a proportion of tau in the LSS, this difference did not reach statistical significance (p=0.057; **Figure 4.8 B**), but showed a clear trend towards higher levels of tau aggregates in DMF-treated brains. This was an unexpected finding since DMF was hypothesised to reduce pathological changes in tau. In particular, results showing reduced tau phosphorylation in cell culture experiments would predict a reduction in tau aggregation since abnormally high levels of tau phosphorylation are widely believed to be an important driver of tau aggregation and NFT formation (Simic et al., 2016).

4.3.4 Possible signalling pathways for DMF action

The results presented above suggest that DMF may affect the aggregation of tau *in vivo* and tau phosphorylation *in vitro*. Elucidating some of the signalling pathways and mechanisms affected by DMF may provide clues as to which pathways are important for the abnormal processing of tau in AD and other tauopathies. DMF is a known Nrf2 activator with anti-inflammatory action (Wilms et al., 2010; Lastres-Becker et al., 2016) therefore the following investigations focussed on the effects of DMF on glial activation and Nrf2 in treated htau mice. In addition, the activities of key tau kinases were investigated in cortical cell lysates to determine if changes in kinase activity underlie the alterations observed in tau phosphorylation following DMF treatment.

Glial activation is not changed by DMF treatment

Astrocyte activation

DMF has previous been shown to have anti-inflammatory actions so it was of interest to investigate whether it was having an effect on glial activation seen in htau mice. Previous research from our laboratory has demonstrated robust astrocyte activation and increased

cytokine content in the htau mouse brain (Garwood et al., 2010), so changes in astrocyte activation was first investigated.

Homogenates from the hippocampus of 8-9 and 13-14 month old htau mice were immunoblotted and probed with an antibody against GFAP, a cytoskeletal protein that is increased when astrocytes become activated (Eng et al., 2000). There were no apparent differences in GFAP amounts in homogenates from DMF-treated relative to vehicle-treated 13-14 month old htau mice (**Figure 4.9 A**). Quantification of GFAP immunoreactivity relative to ß-actin amounts in the same sample confirmed that there was no effect of DMF treatment on GFAP levels (**Figure 4.9 B**). Similar findings were obtained when cortical homogenates from 8-9 month old htau mice were examined (**Figure 4.9 C**, **D**). This is consistent with results previously described in primary cell cultures which also showed no effect of DMF on astrocyte activation.

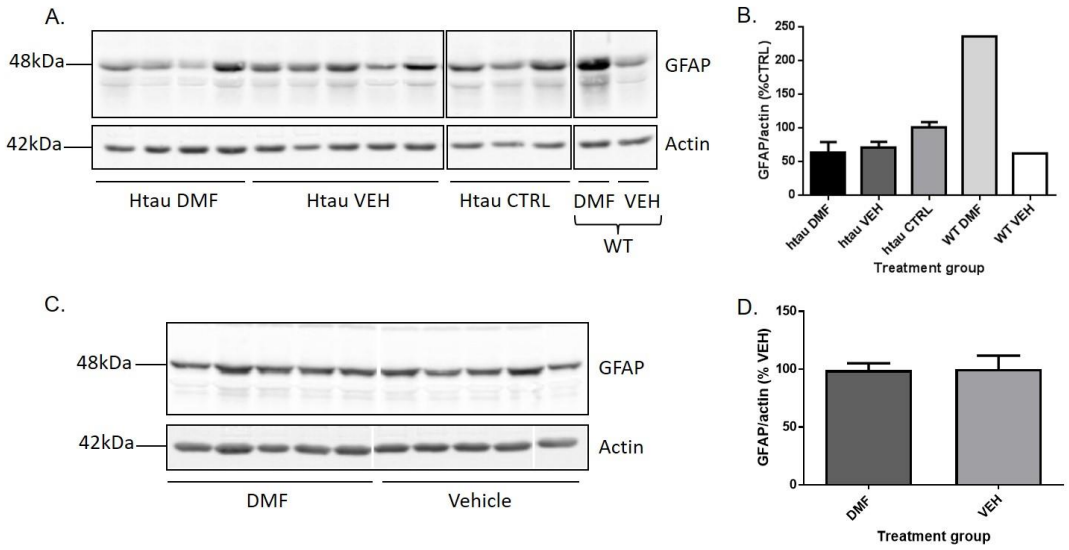

Figure 4.9: DMF does not change GFAP levels in 8-9 or 13-14 month old htau mice
A. Western blot of hippocampal homogenate from 13-14 month old DMF- and vehicle-treated htau and WT mice probed with an anti-GFAP antibody. The blot was also probed with an antibody against ß-actin as a loading control. Molecular weight markers are shown on the left. **B.** Bar chart shows quantification of GFAP amounts following normalisation to ß-actin in homogenates from 13-14 month old mice. Data from htau samples was analysed by one-way ANOVA. Values shown are mean ± SEM as percentage htau control (CTRL). **C.** Western blots of frontal cortex homogenates from 8-9 month old DMF- and vehicle-treated htau mice probed with an anti-GFAP antibody. The blot was also probed with an antibody against ß-actin as a loading control. Molecular weight markers are shown on the left. **D.** Bar chart shows GFAP amounts relative to ß-actin. Data was analysed by Student's t-test. Values shown are mean ± SEM as percentage vehicle-treated htau (VEH). Aged mice: DMF: n=5, VEH: n=5. Younger mice: DMF: n=5, VEH: n=5.

Microglial activation

Microglia are known to have key roles in the development and progression of AD, and microglial signalling pathways are being explored as possible drug targets for AD treatment (Crehan et al., 2012; Wes et al., 2016). Specifically, research suggests microglia are involved in tau aggregation: a study crossing htau mice with fractalkine receptor knockout mice which show sustained microglial activation, found that reactive microglia drive the development of tau pathology, including tau phosphorylation and aggregation, and the spread of tau pathology across the brain (Maphis et al., 2015).

To determine if DMF affects microglia in htau mice, frontal cortex homogenates from 8-9 month old htau mice were run on 12 % tris-glycine gels and immunoblotted for the microglial marker, Iba1. Iba1, though not necessarily a marker of activated microglia (Boche et al., 2013) is increased during inflammatory states (Streit and Xue, 2009) so any changes in the abundance of this protein after DMF treatment would indicate an effect of DMF on microglial inflammatory signalling. Despite several attempts and optimisation steps, a clear signal for Iba1 could not be detected by western blotting (**Figure 4.10**), and bands were not clear enough to allow signal quantification. Qualitative observation of Iba1 bands suggests that there is no obvious change in Iba1 levels following DMF treatment of htau mice, however, definitive conclusions about the potential effects of DMF on microglial inflammatory responses cannot be drawn from the data shown here.

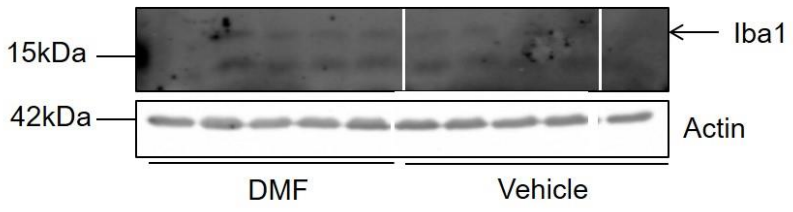

Figure 4.10: DMF treatment does not appear to affect Iba1 levels in htau mouse cortex
Western blots of frontal cortex homogenate from 8-9 month old htau mouse brains probed with an antibody against the microglial marker, Iba1. Immunoblot shows a band at the correct size for Iba1 at 17 kDa (indicated by arrow) and several non-specific bands. Molecular weight markers are indicated on the left. The blot was also probed with an antibody against ß-actin as a loading control. DMF: n=5, VEH: n=5.

DMF may affect Nrf2 activation in htau mice

DMF is a known activator of the transcription factor, Nrf2 (Brennan et al., 2016). Nrf2 is known to induce the transcription of a range of genes that could be involved in AD and neurodegeneration (Tebay et al., 2015). Under normal conditions, Nrf2 is found in the cytoplasm, where it is inactive and bound by Kelch-like ECH-associated protein 1 (Keap1). Activation of Nrf2 occurs under stressful conditions, such as oxidative stress, and is caused by phosphorylation of Nrf2 at Ser40. This allows Nrf2 to stabilise and translocate to the nucleus (Niture et al., 2014). Of particular relevance, Nrf2 controls transcription of autophagy adaptor protein, nuclear dot protein 52 (NDP52) (Jo et al., 2014a). NDP52 associates with phosphorylated tau, facilitating tau clearance by autophagy (Kim et al., 2014). In support of this, Nrf2 knock-out animals show reduced levels of NDP52 and neuronal accumulations of phosphorylated and sarkosyl-insoluble tau (Jo et al., 2014a). Therefore, it was important to assess the effects of DMF on Nrf2 activation in htau mouse brain and primary culture lysates.

Western blots of frontal cortex homogenates from 8-9 month old htau mice treated with DMF or vehicle were probed with an antibody that detects total Nrf2. Lysates from DMF- or vehicle-treated primary cortical cultures were immunoblotted in the same way. A single prominent band of approximately 64 kDa was detected in both sets of samples, corresponding to the predicted size of Nrf2. Western blots showed no apparent change in Nrf2 amounts between treated and control mouse brain homogenates. However, there was an apparent reduction in total Nrf2 amounts in cell cultures treated with 30 µM DMF in comparison to control treated or 60 µM DMF treated cells. When the amounts of DMF were normalised to ß-actin content in each sample, and the results were quantified, analysis showed that this difference was not significant. No other significant changes in Nrf2 amounts were found following DMF treatment of cell cultures or mouse brain when compared to control samples (**Figure 4.11 A-D**). This data indicates that DMF treatment does not increase total Nrf2 amounts.

Nrf2 is activated when the protein is phosphorylated at Ser40, and measurements of the amounts of phosphorylated Nrf2 are commonly used as indicators of Nrf2 activity (Huang et al., 2002; Tebay et al., 2015). To test the efficacy and specificity of an antibody against phosphorylated Ser40 on Nrf2, homogenates were prepared from rat primary cortical culture lysate, mouse and human brain and these were immunoblotted with a phospho-Nrf2 antibody. Unfortunately, the phospho-Nrf2 antibody did not display clear protein bands at the correct

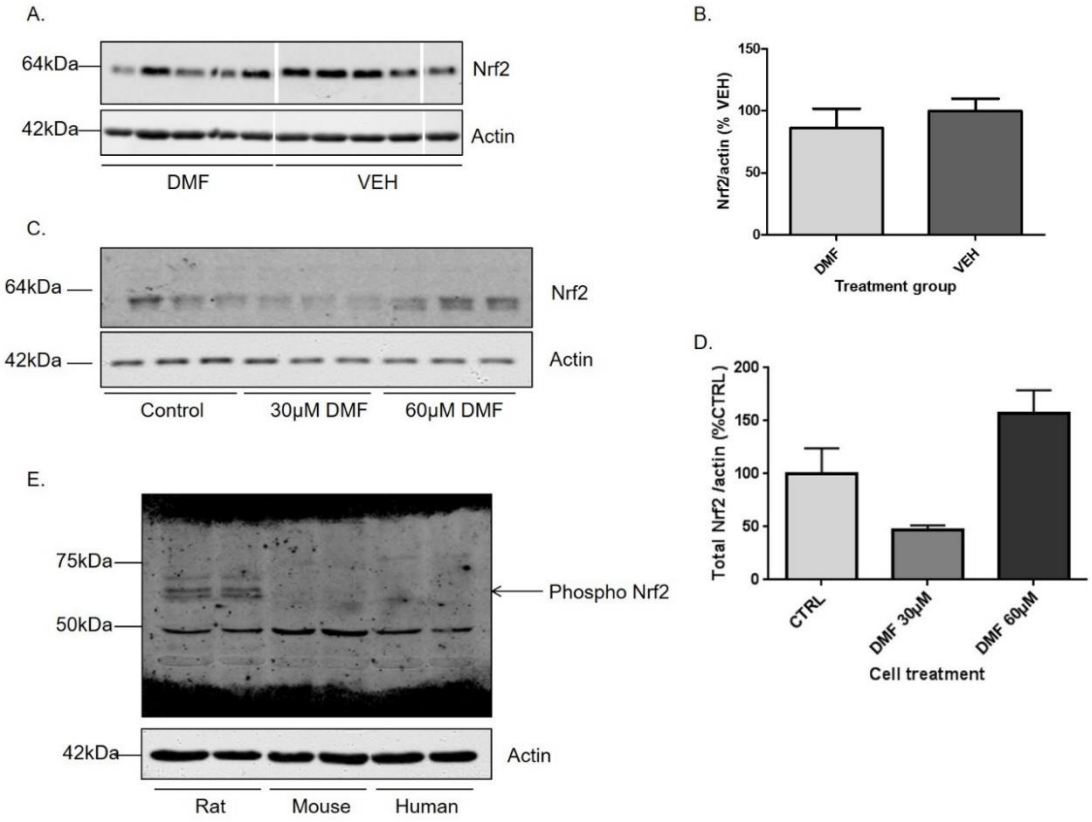

Figure 4.11: DMF treatment does not significantly affect Nrf2 amounts in htau mice or rat primary cortical cultures

A. Western blot of frontal cortex homogenate from 8-9 month old htau mice treated with vehicle or DMF and probed with an antibody against total Nrf2. Blots were also probed with an antibody against ß-actin as a loading control. Molecular weight markers are shown on the left. **B.** Bar chart shows quantification of western blotting. Nrf2 amounts were determined following normalisation to ß-actin in each sample. Values represent mean ± SEM as percentage vehicle-treated htau (VEH). Data was analysed using Student's t-test. **C.** Representative western blots of rat primary cortical culture lysates probed with an antibody against total Nrf2. Blots were also probed with an antibody against ß-actin as a loading control. Molecular weight markers are shown on the left. **D.** Bar chart shows quantification of total Nrf2 amounts relative to ß-actin. Values represent mean ± SEM as percentage control (CTRL). Data was analysed using a Kruskal-Wallis test. **E.** Representative western blot of rat cell lysate, homogenised mouse brain and homogenised post-mortem human brain probed with an antibody against Nrf2 phosphorylated at Ser40. The expected size of phospho-Nrf2 (64 kDa) is indicated with arrow. Molecular weight markers are shown on the left. Htau mouse brain: n=5. Cell lysates: n=3. Phospho-Nrf2 test: n=2 per sample type.

size (64 kDa) for mouse and human samples and only very faint bands in rat sample lanes (**Figure 4.11 E**). Therefore, it was not possible to determine if DMF has caused any changes in Nrf2 activity, as indicated by its phosphorylation at Ser40. In an attempt to further investigate Nrf2 activation by determining if any proteins downstream of Nrf2 activation were affected, blots were also probed with an antibody against NDP52. Unfortunately, this antibody also gave insufficient signal and it was not possible to draw any conclusions (data not shown).

DMF treatment reduces the activity of cdk5

Finally, to investigate the mechanism by which DMF application caused reductions in tau phosphorylation in primary cell cultures, the activities of key tau kinases were examined. Many kinases and phosphatases are involved in post-translational modifications of tau and have been implicated in the development of tau pathology in AD (Hanger et al., 2009). Multiple kinases and phosphatases regulate phosphorylation of the same tau residues (Hanger et al., 2009), and there is complex interplay between kinases (Engmann and Giese, 2009) making any attempts to elucidate the signalling pathways regulating tau phosphorylation difficult. However, glycogen synthase kinase 3 (GSK-3) and cyclin-dependent kinase 5 (cdk5) are well recognised to regulate phosphorylation at both the Tau-1 and CP13 epitopes (Hanger et al., 2007; Hanger et al., 2009), the sites affected by DMF treatment in primary cultures. Therefore, lysates from primary cortical cultures treated with vehicle, 30 µM or 60 µM DMF were immunoblotted with antibodies against these kinases.

GSK3

Antibodies against total GSK-3α/ß and GSK-3α/ß phosphorylated at Ser21/9 were used and western blots were developed by ECL. GSK-3 activity is regulated by inhibitory phosphorylation at Ser21/9 (Fang et al., 2000) and therefore increases in phosphorylation at these sites indicates a decrease in GSK-3α/ß activity. Proteins of the sizes corresponding to GSK-3α/ß were detected by both antibodies (51 and 47 kDa, respectively). There were no apparent differences in the amounts of either total or phosphorylated GSK-3 on western blots, and when phosphorylated

GSK-3 was quantified as a proportion of total GSK-3, there was no statistical difference in phosphorylated GSK-3α/ß between treatment groups (**Figure 4.12 C**). This suggests that reduced GSK-3α/ß activity is likely not to be responsible for the decrease in tau phosphorylation resulting from DMF treatment of these cultures.

Cdk5

Cdk5 activity is controlled by its association with neuronal regulatory subunits including p35 (Kesavapany et al., 2004). Evidence suggests that in neurodegenerative diseases p35 is cleaved to form p25. p25 has a longer turn-over rate than cdk5 and therefore not only activates cdk5, but sustains this activity resulting in increased tau phosphorylation and degeneration (Patrick et al., 1999). It should be noted that the role of p25 in neurodegeneration is somewhat controversial (Engmann and Giese, 2009; Giese, 2014).

Therefore, western blots run with DMF-treated cell lysates from vehicle- and DMF- treated primary cell cultures. Antibodies against cdk5 and p35 were used. The p35 antibody was raised against the C-terminus of this protein and therefore should also detect the cleaved p25 fragment. There appeared to be a dose-dependent reduction in cdk5 immunoreactive signals in lysates from cells treated with DMF (**Figure 4.12 B**) and quantification of signal intensity relative to ß-actin showed that 60 µM DMF significantly reduced cdk5 protein amounts relative to controls (**Figure 4.12 F**). The p35/p25 antibody detected p35 protein at 35 kDa, but unfortunately did not p25 at 25 kDa (**Figure 4.12 B**). However, there also appeared to be a dose-dependent reduction in p35 amounts with DMF treatment. Quantification of the p35 signal as a proportion of ß–actin amount in each sample showed that 60 µM DMF significantly reduced p35 amounts in comparison to control cultures (**Figure 4.12 E**). When p35 amounts were normalised to cdk5, this significance was lost, most likely since cdk5 amounts were also reduced (**Figure 4.12 D**). This data shows that DMF reduced both total protein amounts of cdk5 as well as that of its main neuronal activator, p35. Therefore, it is reasonable to assume that the reduced tau phosphorylation observed in DMF treated cultures may have resulted from inhibition of cdk5 activity by DMF.

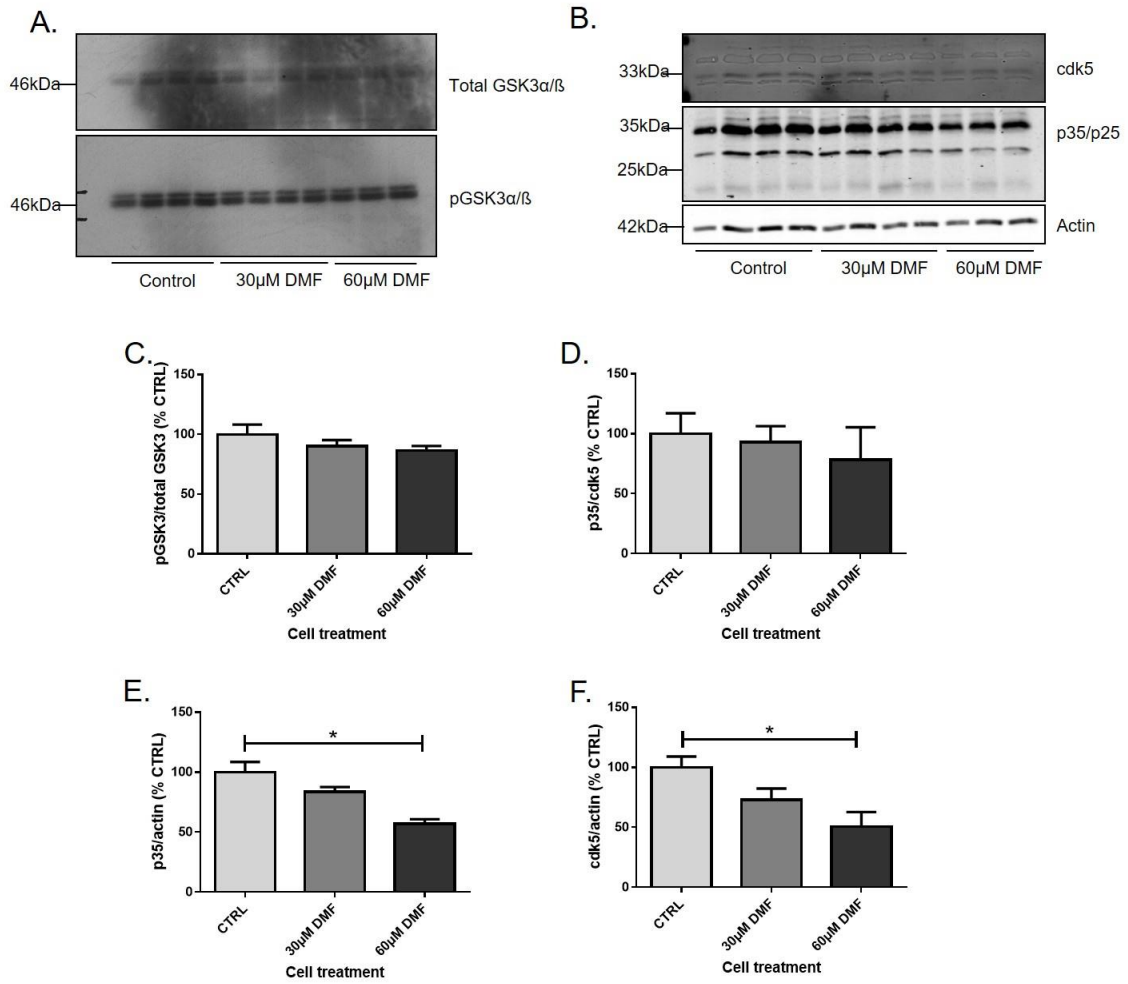

Figure 4.12: DMF reduces cdk5 and p35 levels in primary mixed cultures
Representative western blot of lysates from 13 DIV primary cortical cultures treated with vehicle or DMF for 24 h. Immunoblots were probed with antibodies against **A.** total GSK-3α/ß and GSK-3α/ß phosphorylated at Ser21/9 (pGSK-3α/ß), and **B.** cdk5 and p25/p35. Blots were also probed with ß-actin as a loading control. Molecular weight markers are shown on the left. Bar charts show quantification of **C.** pGSK-3α/ß as a proportion of total GSK-3α/ß, **D.** p35 was as a proportion of cdk5, **E.** p35 as a proportion of ß-actin, **F.** cdk5 as a proportion of ß-actin. Values represent mean ± SEM as percentage control (CTRL). CTRL and 30 μM DMF: n=4, 60 μM DMF: n=3. Data analysed using a Kruskal-Wallis test. * = $p<0.05$.

4.3.5 Summary

To summarise, the main results of this chapter were:

- DMF treatment reduces amounts of cdk5, p35 and tau phosphorylation in primary cortical cultures at concentrations that do not affect cell viability.
- The DMF-induced reduction in tau phosphorylation is not accompanied by decreases in markers of astrocytic activity.

- DMF treatment of 13-14 month old htau mice had no effect on htau mouse spatial memory impairment as measured by training on the Morris water maze, tau phosphorylation, tau aggregation or markers of active astrocytes.
- DMF treatment of 8-9 month old htau mice did not affect amounts of total or phosphorylated tau, but appeared to increase insoluble tau amounts compared to age-matched vehicle-treated htau mice. These changes were not accompanied by alterations in Nrf2 amounts.

4.4 Discussion

The main aim of this chapter was to investigate the possibility of repurposing DMF, a drug already approved for multiple sclerosis (MS), as an AD therapeutic. The results outlined in this chapter show that DMF robustly reduces tau phosphorylation and the activity of the tau kinase cdk5 in primary cell cultures. Unfortunately, similar findings were not found following treatment of htau mice, a more complex and pathologically accurate model of disease. In fact, data suggested that tau aggregation may be exacerbated when DMF is administered at early disease stages to 8-9 month old htau mice. Analysis of treated mouse brain failed to identify changes in glial activation or in Nrf2 amounts, and there were no changes in behavioural measures of cognitive function following DMF treatment. Further investigation into alternative mechanisms and signalling pathways were carried out but due to methodological difficulties these still remain unclear. Overall, these results do not support efforts to repurpose DMF for Alzheimer's treatment.

4.4.1 DMF effects in primary cortical cultures

DMF reduces tau phosphorylation in primary cortical cultures

Tau phosphorylation is one of the earliest pathological changes in tau in AD and is thought to be a trigger for further abnormal tau processing (Ballatore et al., 2007; Hanger et al., 2009; Noble et al., 2013). For this reason, phosphorylation of tau at AD-relevant epitopes was investigated following DMF treatment of primary cortical cultures. A reduction in tau phosphorylation at the Ser199/202/Thr205 epitopes, as indicated by both CP13 and Tau-1 antibodies, was found. However, phosphorylation of tau at Ser396/404 were not similarly reduced. All five of these tau residues are hyperphosphorylated in NFTs isolated from AD brain (Hanger et al., 2009). Additionally, all sites are substrates of multiple tau kinases, including GSK-3 and cdk5 (Hanger et al., 2007). However, evidence suggests that phosphorylation at these sites occurs at different disease stages. A study of fixed sections from multiple stages of AD and Down's syndrome brain found that phosphorylation at the PHF1 epitope (Ser396/404) is one of the earliest events in disease progression (Mondragon-Rodriguez et al., 2014). Conversely, NFTs were found to be enriched in tau phosphorylated at Ser199/202/Thr205 sites, suggesting that this post-translation modification of tau is closely associated with tau aggregation and tangle formation, an event that occurs later in disease progression (Augustinack et al., 2002). A different situation appears to exist in tau transgenic mice where increased phosphorylation at Ser202 is commonly found prior to that at the PHF1 epitope (Lewis et al., 2001; Sahara et al., 2002; Kelleher et al., 2007). The difference in timing of phosphorylation at the Tau-1 and PHF1 epitopes may explain why phosphorylation at Tau-1 sites, but not PHF1, was significantly reduced in these cell culture experiments. However, tau phosphorylation is artificially increased in embryonic stages, and in primary cell cultures likely as a result of cell stress, and therefore the contribution of developmental stage or the action of stress-activated kinases cannot be discounted.

4.4.2 DMF effects on the htau mouse model of tauopathy

Two small pilot studies into the effects of DMF in htau mice were carried out. The first study investigated DMF treatment of 13-14 month old htau mice, which are reported to display phenotypic characteristics of mid-stage AD including tau phosphorylation, aggregation, behavioural and cognitive deficits, while the second group of 8-9 month old mice show milder and possibly more reversible, tau abnormalities (Andorfer et al., 2003; Andorfer et al., 2005; Polydoro et al., 2009). Htau mice are considered to be a highly relevant model of the tau pathology that develops in AD since the express only human tau on a mouse tau knockout background and show abnormal tau processing very similar to that observed in AD brain (Noble et al., 2009b). In particular, electron microscopy of filamentous tau extracted from aged htau brain shows that it has a paired helical filament conformation (Andorfer et al., 2003), rather than the straight filaments seen in other tauopathies and that are characteristic of the vast majority of other tau transgenic lines (Noble et al., 2010). Additionally, astrogliosis is prominent in htau brain (Garwood et al., 2010), further recapitulating characteristics of human AD brain and making the mice appropriate for experiments investigating potential astrocytic inflammatory changes. However, it is important to remember that abnormal APP processing and Aß over-production are not mimicked in these mice, therefore they do not represent a full model of AD. However, since the experiments in this chapter are looking specifically at the effects of DMF on astrocyte activation and tau pathology, the htau mouse model was considered an appropriate model to use.

Unfortunately, the effects of DMF treatment were limited in the htau mice. In particular, the reductions in tau phosphorylation observed in primary cultures were not found following treatment of either 8-9 or 13-14 month old htau mice. Analysis of the amounts of sarkosyl insoluble tau extracted from hippocampal tissue of younger, but not aged, htau mice showed a trend towards an increase in insoluble tau levels with DMF treatment. Sarkosyl insoluble tau is widely used as a marker for the presence of tangle-like tau (Hasegawa, 2006; Julien et al., 2012). Traditionally, insoluble tau aggregates and NFTs found in brain from tauopathy patients and the

brains of multiple mouse models of tauopathy have been viewed as both pathological and toxic (Augustinack et al., 2002; Hasegawa, 2006; Hanger et al., 2007). Tau aggregates have been widely reported to disrupt axonal transport, both because they block narrow axons and by sequestering tau, resulting in the destabilisation of axon microtubules (Terwel et al., 2002; Mandelkow et al., 2003; Spires-Jones et al., 2009). Additionally, insoluble tau aggregates have been suggested to reduce autophagy levels while reduced autophagy has been found to promote the formation of insoluble tau aggregates, possibly creating a pathological feed-forward loop inhibiting autophagy and increasing aggregate formation (Lim et al., 2001; Rodriguez-Martin et al., 2013). The mechanistic pathways involved in this complex circular pathophysiology are unclear (Liu et al., 2015b). However, increasing autophagic activity increases aggregated tau clearance and improves neuronal function and cognitive impairments resulting in research into autophagy as a drug target in AD (Yang et al., 2011; Jo et al., 2014a; Friedman et al., 2015).

Therefore, possible increases in insoluble tau aggregation with DMF treatment in mouse brain could be due to activation of cellular pathways reserved for final attempts at reducing tau toxicity. Mechanisms increasing tau aggregation are likely to reduce immediate toxicity of soluble oligomers of tau but result in serious long term problems, such as exacerbation of impairments in axonal transport and autophagic clearance. Moreover, another study investigating DMF treatment for MS also found that the drug activated mechanisms (via Nrf2) that lie on the border between cell protection and toxicity, supporting the results seen here (di Nuzzo et al., 2014). This further indicates that DMF is not an ideal candidate for the long term treatment of AD in human patients.

4.4.3 Possible pathways underlying the effects of DMF

Some of the pathways through which DMF may be acting were investigated since this information may provide insights into the mechanisms and signalling pathways involved in the development of tau pathology. The experiments in this chapter focussed on three potential mechanisms: glial activation, Nrf2 activation and reductions in kinase activity.

Glial activation does not appear to be reduced with DMF treatment

DMF has astrocyte-mediated anti-inflammatory effects (Wilms et al., 2010) and previous research from this laboratory has found that anti-inflammatory agents can reduce abnormal tau pathology by reducing levels of activated astrocytes (Garwood et al., 2010). However, no effects of DMF on GFAP, a widely-used marker of astrocyte activation, were observed in primary cortical cultures or in treated htau mice, suggesting that perhaps astrocytic inflammation did not contribute to the effects of DMF on tau. However, GFAP knockout mice still display astrogliosis demonstrating that GFAP is not essential for astrocytic activation (Pekny et al., 1995; Yang and Wang, 2015). Therefore, it is not possible to exclude the possibility that DMF could have affected specific inflammatory pathways in the absence of a reduction in GFAP levels. Unfortunately, there was not sufficient time to explore this possibility in more detail.

The primary cortical cultures used here contain only neurons and astrocytes and, as a result, any inflammatory effects must be mediated by astrocytes. However, the htau mouse brain also contains microglial cells. Microglia have long been implicated in the progression of AD and they modulate inflammatory pathways via the release of cytokines and other small signalling molecules alongside astrocytes (Meyer-Luehmann and Prinz, 2015). In addition, mutations in microglial genes, such as TREM2, have been found to significantly increase risk of developing sporadic AD suggesting that microglial activity and function are key in the development of the disease (Villegas-Llerena et al., 2016). Therefore, anti-inflammatory effects of DMF could occur via changes in microglial activation and behaviour. An attempt at measuring microglial activation, using an anti-Iba1 antibody, was carried out, however western blotting with this antibody was not successful despite attempts to optimise conditions. Time permitting, further investigation of microglial changes could have provided useful information about DMF mechanisms. Experiments using alternative antibodies for active microglial markers, such as CD68, or other methods, such as immunohistochemical analysis of brain sections, could provide useful information about possible signalling pathway affected by DMF. In addition, unbiased cytokine arrays could highlight specific pathways targeted by the drug treatment although

whether these pathways were controlled by astrocytic or microglial activity, or both, would remain unclear.

The effects of DMF on Nrf2 and cdk5 activities

As DMF is a known Nrf2 activator, differences in Nrf2 in DMF-treated cells and mouse brain compared to control samples were investigated. No significant changes were found in Nrf2 amounts following treatment of primary cortical neurons with DMF. A previous study found that DMF treatment of Huntington's disease mouse models increased neuronal Nrf2 activation in the absence of increased astrocytic Nrf2 activation (Ellrichmann et al., 2011). This suggests that DMF activation of Nrf2 and downstream pathways could affect tau pathology without astrocytic involvement, as suggested from these experiments.

Unfortunately, it was not possible to successfully optimise the antibody against phosphorylated (active) Nrf2 so any changes in activation by DMF are still unknown. However, knocking out Nrf2 in mice inhibits DMF-mediated rescue of experimental autoimmune encephalomyelitis (EAE), an animal model of multiple sclerosis, suggesting that Nrf2 is necessary for DMF action, at least when it is used as a treatment for multiple sclerosis (Brennan et al., 2016). Furthermore, the same study found that Nrf2 activation resulted in changes in the expression of multiple genes involved in oxidative stress, cell death and cell signalling, including GFAP, apolipoprotein E (ApoE) and NF-κB inhibitor, all of which have been implicated in AD (Chartier-Harilni et al., 1994; Granic et al., 2009; Garwood et al., 2011). Additionally, as mentioned earlier in this chapter, NDP52, an autophagy adaptor protein whose transcription is Nrf2-dependent, is known to co-localise with phosphorylated tau and increase tau clearance (Jo et al., 2014a; Kim et al., 2014). Taken together, these studies suggest Nrf2 activation and downstream transcription changes are likely to be involved in any tau changes caused by DMF treatment.

DMF activity through Nrf2 activation, increased NDP52 production and increased clearance of phosphorylated tau is another, alternative explanation for the effects of DMF treatment described in the cell culture experiments in this chapter. However, activation of this pathway in the htau mice would be expected to result in reduction, rather than the increase, in sarkosyl-

insoluble tau observed here. However, DMF effects are wide-ranging, both via Nrf2 and independent of the transcription factor (Brennan et al., 2016), making it difficult to tease out possible alternative pathways that could explain a trend toward increased tau aggregation following treatment of 8-9 month old htau mice. However, Nrf2 has been found to also be activated by cdk5, which primary culture data indicates is inhibited by DMF. Activation of Nrf2 by cdk5 has been proposed as a neuronal survival mechanism in the face of reactive oxygen species and oxidative stress (Jimenez-Blasco et al., 2015). It is possible, therefore, that the increase in p35/cdk5 that is observed in aged htau mice (Kelleher et al., 2007) could potentially have been inhibited by DMF treatment of htau mice, leading to inhibition of Nrf2, reduced downstream levels of NDP52 and inhibition of autophagy, leading to an accumulation of insoluble tau. If time had permitted, this potential pathway could have been explored experimentally.

DMF did not affect cognitive function in htau mice

No effect of DMF treatment on cognitive function was observed. The Morris water maze was used to investigate any changes in hippocampal-dependent spatial memory in aged (13-14 month old) htau mice treated with DMF. This is considered a relevant test of cognitive function in AD since impairment in hippocampal-dependent tasks, including spatial memory tasks, is one of the first symptoms seen in individuals with AD (Dhikav and Anand, 2011; Jahn, 2013). Htau mice have previously been reported to show impairment in this task compared to age-matched WT animals (Polydoro et al., 2009). In a previous study, as training progressed, htau performance in the water maze improved but at a slower rate than observed for control mice (Polydoro et al., 2009). However, in the study reported in this chapter throughout both pre-treatment and post-treatment testing, no improvement was found in any mice (transgenic or WT) tested despite using the same testing methods as Polydoro and colleagues (Polydoro et al., 2009). This is generally regarded as a very robust behavioural task and therefore the abnormal WT results could simply be a result of the very low numbers used in these pilot studies (only two WT mice, each in a different treatment group). However, it could also potentially be due to problems

stemming from the relatively short testing protocol used here, possibly suggesting the mice may not have associated finding the platform with the reward of being removed from the water, or did not perceive leaving the water as a reward. This association between the platform and a reward is crucial as without the promise of a reward there is no reason for the mice to remember the location of the platform. Circling behaviour and the fact that all mice demonstrated impaired learning could both be associated with mice not learning a platform-reward association. If this study was to be repeated an increase in the number of visible platform trials could increase the chances of platform-reward associations. To ensure mice fully understood this pairing, visible platform trials could be carried out until mice consistently swum directly to the platform. In addition, larger group sizes would, of course, be beneficial.

Differences between cell culture and htau brain findings

The potential increases in tau aggregation found in the hippocampus of the younger mice are particularly surprising, not just because DMF was expected to reduce htau tau pathology, but also because these results appear to contrast with the findings from cell culture, where DMF led to a dose-dependent reduction in tau phosphorylation. While the reasons for this apparent discrepancy are not clear, htau mice are a model of tauopathy (Komuro et al., 2015), whereas the primary cell cultures used in these experiments originate from WT rats and have not been treated with additional reagents (e.g. synthetic Aß) to imitate abnormal AD-like processes including abnormal tau processing. Neurons cultured *in vitro* are clearly different from those grown normally *in vivo* and face more challenges and stressors than non-dissociated neurons (Chen and Herrup, 2008). As a result, neurons cultured in primary cultures may have increased levels of tau phosphorylation due to increased cellular stress (Alavi Naini and Soussi-Yanicostas, 2015), however, generally, these neurons are representative of normal, control brain cells. Therefore, the *in vitro* experiments described in this chapter are examining the effects of DMF treatment on normal, physiological tau phosphorylation, rather than pathological tau phosphorylation seen in the htau mouse brain. Physiological tau phosphorylation is an important process in all neurons, particularly developing neurons. However, in normal neurons

tau phosphorylation occurs at much lower levels and reversibility is key to its microtubule stabilising functions (Wang and Mandelkow, 2016). Therefore, tau phosphorylation in physiological primary cell cultures may be more prone to reversal or prevention than the pathological phosphorylation seen in the htau mouse brain. This difference could explain the inconsistencies seen in the results from this chapter. Furthermore, htau tau levels are approximately 3-4 times those expressed in wildtype animals (Duff et al., 2000; Andorfer et al., 2003). Small reductions in tau phosphorylation that may be seen in primary cells with normal total tau levels, may be obscured by increased levels of both phosphorylated and dephosphorylated tau in the htau mouse neurons.

Furthermore, in light of results described in Chapter 3 (**section 3.3**), it is important to note that primary cells were cultured from the cortices of E18 rats while sarkosyl extraction preparations were carried out with hippocampal htau brain tissue. As previous results have shown, hippocampal and cortical cultures can respond very differently to both insult (e.g. Aß treatment) and possibly protective drugs (e.g. minocycline or DMF). Additionally, the roles of astrocytes in these different brain regions appear to differ significantly (Yeh et al., 2011; Grolla et al., 2013; Rodriguez et al., 2014). This could also partly explain the differences seen between cell culture and htau brain results.

Finally, practical differences in the way primary cultures and mice are treated could also explain discrepancies seen. In primary culture experiments, dissolved DMF was added directly to the culture medium ensuring cells were in direct contact with the drug molecules. Oral treatment of the htau mice, however, results in much higher chances of DMF not reaching the brain. Research has shown DMF is both able to cross into the bloodstream from the digestive system and cross the blood brain barrier (Schilling et al., 2006; Moharregh-Khiabani et al., 2010). However, levels of absorption could vary and it is unlikely that all of the drug that is administered will reach the brain. Oral gavage ensures that all of the prescribed drug dose is consumed, but has increased health risks for the mice being treated (Schilling et al., 2006; Eichenbaum et al., 2011). Here, DMF was administered via oral syringe, reducing the health risks to the mice as

feeding is not forced and there is no risk of physical damage to the oesophageal tract. This makes using an oral syringe more appealing as a method of drug delivery but also reduces the chances of all of the drug solution entering the mouse's digestive system. As mice are not force fed it is possible for them to avoid drinking some drug solution. While it is very unlikely that a mouse could avoid a whole dose, variability of DMF concentrations reaching the brain could be increased. Every effort was made to encourage the mice to drink the drug solution; including attempting to make the taste appealing, but it is unavoidable that some mice will find the solution more appealing than others. If this experiment was repeated the only way of ensuring equal DMF concentrations reach each mouse's brain would be via an alternative drug administration method, for example via gavage or intraperitoneal injection. However, both of these methods have drawbacks, either compromising either the mouse health risks posed or reducing the similarities to human drug consumption.

In summary, differences in the results obtained following DMF treatment of primary cortical cultures and htau mouse brain could have multiple explanations, including the presence of physiological and pathological tau, the different brain regions assessed and differences in drug administration. It would be highly challenging to tease out these causes and determine which has had the greatest effect on the results presented here, however, it seems clear that the results from these two different experimental set-ups are not directly comparable.

4.4.4 Conclusions

To conclude, this chapter provides evidence that DMF treatment of both primary neuron cell cultures and the htau mouse model of tauopathy can influence pathological tau changes. In primary cell culture, DMF treatment reduces tau phosphorylation at some AD-related sites. These effects were associated with reduced cdk5 activity through an as yet, unidentified, pathway.

DMF treatment of htau mice did not rescue spatial memory deficits or affect tau phosphorylation in aged mice (13-14 months old) but possibly increased tau aggregation in

younger (8-9 months old) mice. No changes in astrocyte activation were observed in association with increased tau aggregation. It is possible that this finding could reflect an attempt by cellular repair mechanisms to reduce the damage caused by highly toxic soluble tau oligomers.

Overall, the experiments presented in this chapter do not support the repurposing of DMF as a potential AD therapeutic, at least not when using the models and methods of administration used here.

Chapter 5: Temporal and regional changes in glial markers in post-mortem Alzheimer's disease brain

5.1 Introduction

Experiments described in the previous two chapters used primary cell cultures and transgenic mice to model AD-like pathology. Using these models, the contributions of astrocytes and possible pathology-improving drugs were investigated. However, these experiments cannot provide insights into the development and treatment of AD if the models used do not reflect the development of the human disease.

As options for investigating neurological diseases in human brain are limited, exploration of disease in post-mortem brain can provide valuable insights into a disease and validate animal and cell culture models. Initial studies into AD and other neurodegenerative diseases were carried out in post-mortem brain, including Alois Alzheimer's first report of the pathological changes seen in cells in AD (Alzheimer et al., 1995; Garcia-Marin et al., 2007b, a). More recently, IHC studies of sections of post-mortem brain have demonstrated distinctions between different tauopathies, showing characteristic differences in tau aggregates from different diseases (Kovacs, 2015). Studies showing that tau, rather than Aß, spread throughout the human brain correlated best with AD symptoms prior to death were also key to demonstrating tau plays an important role in AD pathology (Braak and Braak, 1995; Braak et al., 2011; Perez-Nievas et al., 2013). These studies, providing robust evidence for the importance of tau spread throughout the human brain, have ensured tau pathology features in the amyloid cascade hypothesis, the major AD development theory dominating AD research (Hardy and Allsop, 1991) in the absence of AD-causing tau mutations (Hardy et al., 1998). Furthermore, findings from post-mortem brain studies, such as the discovery of a 35 kDa cleaved fragment of tau in multiple tauopathies (Wray et al., 2008), have directly influenced the development of new models of AD and tauopathy. In this example, the tau35 mouse, a mouse expressing the 35 kDa tau fragment described above, was developed to further investigate the role of the cleaved tau fragment (Bondulich et al., 2016).

However, many studies focus only on differences between control and late-stage AD brain, and as a result changes seen in early and mid-stage disease that may provide evidence about specific disease mechanisms, may be over-looked. Levels of synaptic markers indicating the health or number of synapses, for example, are thought to vary widely as AD progresses (Mitew et al., 2013; Savioz et al., 2014; Kurbatskaya et al., 2016). A study from this group found that during mid-stage disease (Braak II-III), synaptic markers are significantly increased, possibly indicating compensation mechanisms in the face of initial synaptic dysfunction. By late stage AD, the same synaptic marker levels are significantly reduced demonstrating the loss of synapses and neurons at end stage AD (Kurbatskaya et al., 2016).

It is also important to note that there are some individuals with AD-like molecular pathology that do not show clinical AD symptoms during their lifetime. One study compared the molecular differences in post-mortem brain from these "mismatches" in comparison to control and AD cases. Activated glia and the mislocalisation of tau to synaptic compartments were found to be the best correlates of cognitive impairment and dementia during life (Perez-Nievas et al., 2013). It was important for the work presented in this thesis to investigate changes in glial markers and tau in post-mortem brains from all stages of AD since this should provide valuable insights in to the timing and contribution of astrocytes to the development of tau pathology in AD, and determine whether the results obtained from cell and animal models are directly relevant to human AD. Classification of AD stages by Braak and Braak was originally proposed based on correlation of the spread of tau pathology in post-mortem brain and the severity of clinical symptoms (Braak and Braak, 1995). It is now thought that this tau spread occurs via the trans-synaptic release and uptake of pathological tau between anatomically connected neurons, creating the pattern of tau spread that Braak originally described (Clavaguera et al., 2015). Experiments described in Chapter 3 (**section 3.3**) suggested that mechanisms and signalling pathways driving the development of tau pathology differed in different brain regions. Research using mouse models and post-mortem brain also suggests that the role of astrocytes and their immune response, in particular, are different in distinct brain regions (Rodriguez et al., 2014;

Rodriguez-Arellano et al., 2016). Investigating changes in glial markers and tau in all Braak stages may therefore provide further insights into how astrocytes, neuroinflammatory responses and disease-associated changes in tau are temporally and regionally associated.

The aims of this chapter are to use post-mortem samples from control and Braak stage I-VI AD temporal cortex and hippocampus to investigate changes in the following during disease development:

- Disease-associated changes in tau, including phosphorylation, cleavage and aggregation
- Activation of astrocytes and microglia
- Markers of synapse function.

These findings will then be compared to determine if there are specific regional associations between glia and tau at different stages of disease.

5.2 Methods

The methods and materials used in this chapter, including methodology for the homogenisation of human brain tissue, are described in Chapter 2 (**section 2.4.1**). Briefly, brain tissue was homogenised according to the protocol described in Chapter 2 (**section 2.4.1**). Homogenates were run on 10 % tris-glycine gels for western blotting and were immunoblotted with antibodies against NSE and ß-actin to allow normalisation of sample concentrations according to total neuronal proteins and all neural cells, respectively (**Chapter 2, section 2.6**).

Three separate groups of post-mortem brain samples were obtained from the London Neurodegenerative Diseases Brain Bank for these studies:

Group 1: Control (n=20) and Braak stages V/VI AD (n=20) temporal cortex, for which ApoE genotype had been determined (**Table 5.1**).

No.	Age	Sex	Post-mortem delay (PMD, h)	Notes	ApoE
1	80	M	41	AD, Braak VI, severe amyloid angiopathy	3/4
2	91	F	29	AD, definite Braak VI	3/4
3	88	M	46	AD, definite Braak VI	3/4
4	92	F	42	AD, Braak VI	3/4
5	80	F	13	AD, Braak V, mild amyloid angiopathy	3/4
6	69	F	16	AD, Braak VI	3/4
7	84	F	<24	AD, Braak V	4/4
8	81	F	<72	AD, Braak VI	4/4
9	81	M	74	AD, Braak VI	4/4
10	82	F	69	AD, Braak V, mild amyloid angiopathy	4/4
11	84	F	36	AD, Braak V/VI	4/4
12	90	F	23	AD	3/3
13	98	F	3.5	AD, BNE IV, CERAD probable	3/3
14	82	M	80	AD definite	3/3
16	89	F	15	AD, BNE stage IV, amyloid angiopathy	3/3
17	97	F	12	AD, Braak V	2/3
18	89	M	19	AD definite	2/3
19	86	M	26	AD, Braak V, moderate amyloid angiopathy	2/4
20	87	F	48	AD, Braak VI, moderate amyloid angiopathy	2/4
21	82	F	43	Normal brain	3/3
22	81	F	17	Mild ageing changes, Braak I	3/3
23	92	F	17	Control brain, some tau deposition	3/3
24	86	M	6	Normal adult brain	3/3
25	55	F	12	Minimal tau pathology consistent with HP-tau stage I	3/3
26	80	M	21	Widespread acute infarcts and acute ischaemic changes; old infarcts	3/3
27	90	F	50	Control brain, mild alzheimer-type changes (modified Braak stage II) mild amyloid angiopathy	3/3
28	87	F	22	Normal adult brain	3/3
29	81	M	18	Control, old cerebral infarct (Braak I)	3/3
30	78	M	10	Ageing changes, mild	2/3
31	79	M	47	Early tau pathology Braak II, no neuritic plaques	2/3
32	82	F	13	Argyrophilic grains low to moderate density	2/3
33	59	M	50	Normal adult brain	4/4
34	40	M	40	Normal adult brain	3/4

Table 5.1: Details of post-mortem control and Braak stage V-VI temporal cortex
Sample number, age, sex, PMD (in h), neuropathologist notes and ApoE genotype of each sample is shown.

No.	Sex	Age	PMD	Notes
1	F	87	22	Normal adult brain
2	M	86	6	Normal adult brain
3	M	59	50	Normal adult brain
4	M	40	40	Normal adult brain
5	M	78	10	Ageing changes, mild
6	F	82	13	Argyrophilic grains, low to moderate density
7	F	92	17	Control brain, some tau deposition
8	F	55	12	Minimal tau pathology consistent with HP-tau stage I
9	F	81	17	Mild ageing changes, Braak I
10	M	79	47	Early tau pathology, Braak II, no neuritic plaques
11	F	90	50	Control brain, mild alzheimer-type changes (modified Braak stage II), mild amyloid angiopathy
12	M	93	~33	Mild AD type changes, Braak II
13	F	84	35	AD changes, Braak II, consistent with normal aging
14	M	92	11	Mild AD type changes due to ageing Braak III
15	F	70	38	Possible AD (CERAD) Braak III (limbic), BNE stage III
16	M	86	52	Ageing changes, AD modified Braak stage 3, suitable as control
17	M	82	28	AD, modified Braak stage IV, limbic TDP-43 pathology
18	M	86	53	AD, modified Braak stage IV, extensive severe amyloid angiopathy
19	F	83	22	AD, limbic stage, modified Braak stage IV, moderate to severe amyloid angiopathy
20	F	89	56	AD, HP tau stage IV severely affecting limbic system, moderately extending to neocortex.
21	F	80	13	AD, Braak V, mild amyloid angiopathy
22	F	82	69	AD, Braak V, mild amyloid angiopathy
23	M	86	26	AD, Braak V, moderate amyloid angiopathy
24	M	81	74	AD, Braak VI
25	F	87	48	AD, Braak VI, moderate amyloid angiopathy
26	M	72	5	AD, Braak VI, marked amyloid angiopathy

Table 5.2: Details of temporal post-mortem brain samples
Sample number, sex, age, PMD (in h) and neuropathologist notes for each sample is shown.

No.	Sex	Age	PMD (h)	Pathological diagnosis
3	M	59	50	Normal adult brain
7	F	92	17	Control brain, some tau deposition
8	F	55	12	Minimal tau pathology consistent with HP-tau stage I
10	M	79	47	Early tau pathology, Braak II, no neuritic plaques
11	F	90	50	Control brain, mild AD-type changes, modified Braak stage II, mild amyloid angiopathy
12	M	93	~33	Mild AD type changes, Braak II
13	F	84	35	AD changes, Braak II, consistent with normal aging
14	M	92	11	Mild AD type changes due to ageing, Braak III
15	F	70	38	Possible AD (CERAD), Braak III (limbic), BNE stage III
16	M	86	52	Ageing changes, AD modified Braak stage III, suitable as control
17	M	82	28	AD, modified Braak stage IV, limbic TDP-43 pathology
18	M	86	53	AD, modified Braak stage IV, extensive severe amyloid angiopathy
19	F	83	22	AD, limbic stage, modified Braak stage IV, moderate to severe amyloid angiopathy
20	F	89	56	AD, HP tau stage IV, severely affecting limbic system, moderately extending to neocortex.
21	F	80	13	AD, Braak V, mild amyloid angiopathy
22	F	82	69	AD, Braak V, mild amyloid angiopathy
23	M	86	26	AD, Braak V, moderate amyloid angiopathy
25	F	87	48	AD, Braak VI, moderate amyloid angiopathy
26	M	72	5	AD, Braak VI, marked amyloid angiopathy
27	F	84	36	AD, Braak V/VI
28	M	88	46	AD, definite Braak VI
29	F	92	42	AD, Braak VI
30	F	69	16	AD, Braak VI

Table 5.3: Details of hippocampal post-mortem brain samples
Sample number, sex, age, PMD (in h) and neuropathologist notes for each sample is shown.

The second (temporal cortex, **Table 5.2**) and third (hippocampal, **Table 5.3**) groups contained control and AD brain of all stages (Braak stage I through to VI). Where possible, these samples were matched, with temporal and hippocampal samples coming from the same individual. It was not always possible to obtain hippocampal tissue from all samples due to the relative scarcity of these tissues. In addition, slides with brain sections from Brodmann Area 10 in the prefrontal cortex were obtained from the MRC London Neurodegenerative Diseases Brain Bank. 7 µm tissue sections were stained with hematoxylin and eosin (H&E) and immunolabelled with antibodies against phosphorylated tau and Aß (Kurbatskaya et al., 2016). Slides were imaged

and photographed to obtain data for this thesis using an EVOS XL Core Cell Imaging System in this laboratory.

5.3 Results

5.3.1 Preliminary work

Confirmation of Braak staging in brain sections

To confirm the progressive development of Aß and tau pathology with increasing Braak stage, slides of stained brain sections, taken from Brodmann Area 10 in the frontal cortex, were obtained from the London Neurodegenerative Diseases Brain Bank. Sections were stained with H&E which stains nuclei and cytoplasm, and allows visualisation of tissue damage and cell loss. Sections were also immunolabelled with AT8, which detects tau phosphorylated at Ser202/Thr205, or 6E10, which is raised against the N-terminus of Aß.

Visualisation of these slides using an EVOS XL Core Cell Imaging System showed a progressive increase in tissue damage with H&E staining as Braak stage increases. In Braak stages IV-VI, H&E staining revealed increasing vacuolisation and decreased numbers of cells (**Figure 5.1, left column**). AT8 staining shows increasing amounts of tau phosphorylation with increasing Braak stage; pre-tangles and many neuropil threads being apparent in early-mid Braak stages and culminating with the appearance of mature NFTs at Braak stages IV and VI. (**Figure 5.1, middle column**). Immunolabelling with 6E10 clearly demonstrated the build-up of Aß as AD progresses. The occurrence and density of Aß plaques increases from Braak stages II through to VI in association with the development of tau pathology and loss of neural cells (**Figure 5.1, right column**). This allowed confirmation of the Braak stages to which tissues used in subsequent biochemical characterisation had been assigned.

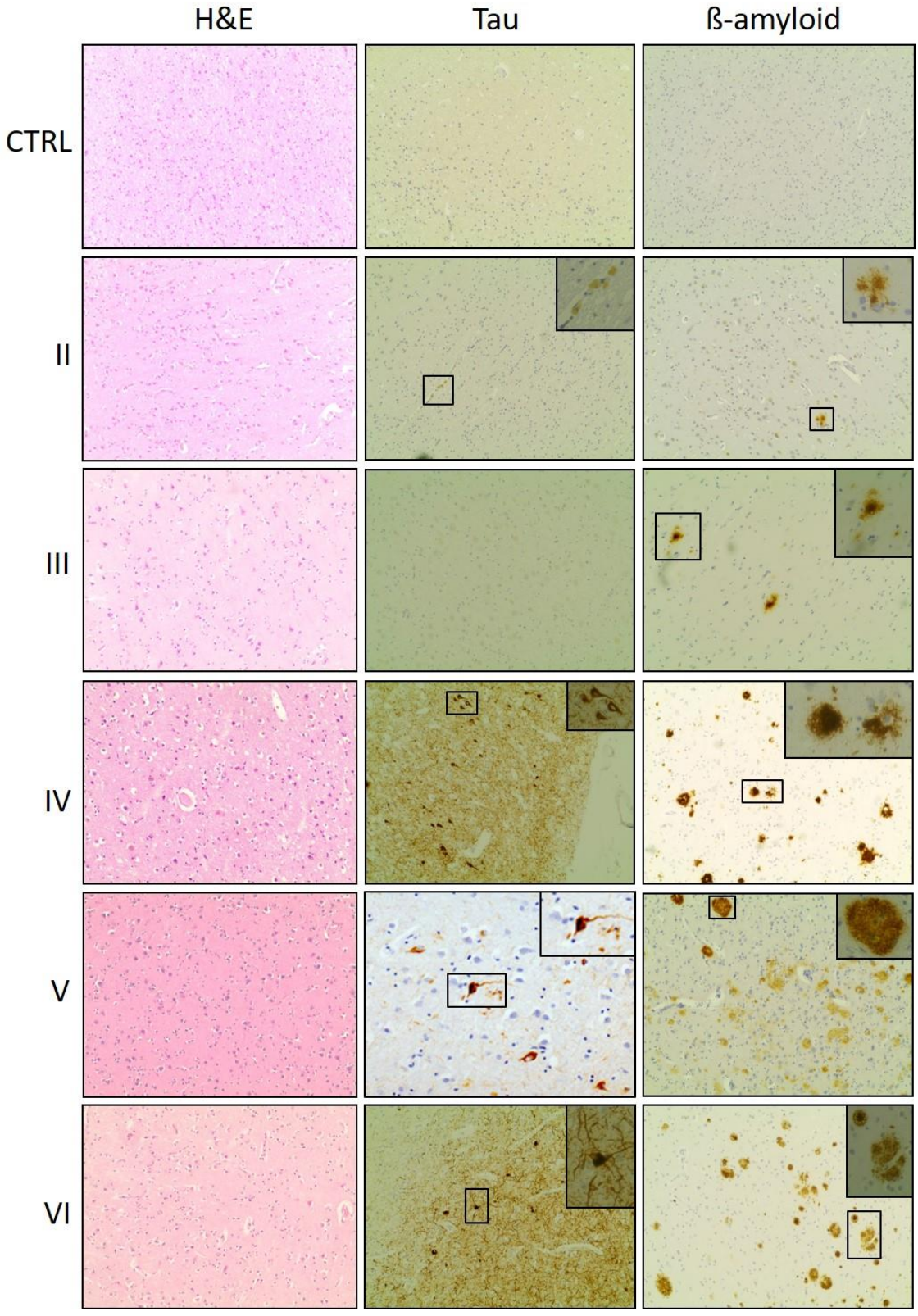

Figure 5.1: Characterisation of Aß and tau pathology and tissue integrity in control and Braak stage I-VI tissues.

Representative immunohistochemistry images showing sections from Brodmann area 10 in brains at different Braak stages (I to VI) and controls. Haematoxylin and eosin (H&E) staining and immunohistochemistry with AT8 (tau phosphorylated at Ser202/Thr205) and 6E10 (N-terminal Aß) are shown.

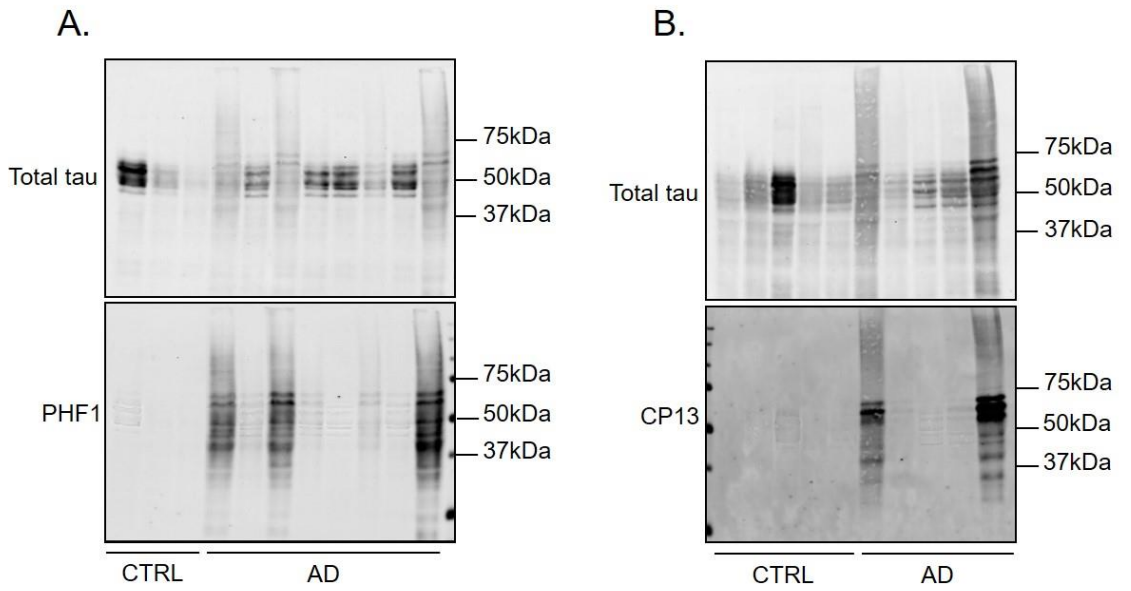

Figure 5.2: Increased tau phosphorylation in late stage AD
Representative western blots of temporal cortex homogenates from control (CTRL) and late stage (Braak V/VI) AD (AD) brain probed with antibodies against total tau (DAKO) and **A.** PHF1 (tau phosphorylated at Ser396/404) and **B.** CP13 (tau phosphorylated at Ser202). Molecular weight markers are shown on the right (kDa). Control n=14; AD n=19.

Investigating differences in glial markers and tau in control and late stage AD brain

In order to confirm published data showing changes in glial cell markers and tau in end-stage AD, western blotting was first used to examine biochemical differences in control and late stage (Braak V/VI) AD temporal cortex only.

Samples were immunoblotted with antibodies against total and phosphorylated tau. Antibodies against the PHF1 (tau phosphorylated at Ser396/404) and CP13 (tau phosphorylated at Ser202) epitopes were used, since these sites are abnormally phosphorylated in PHF tau extracted from AD brain (Hanger et al., 2009) and phosphorylation at these sites is important for microtubule destabilisation and initiation of tau aggregation (Evans et al., 2000; Augustinack et al., 2002). Visualisation of these signals showed that total tau levels varied considerably within groups of post-mortem brain samples (**Figure 5.2 A, B**). Furthermore, while phosphorylated tau was only detected in AD samples, there was a high variability in the amounts of tau phosphorylated at PHF1 and CP13 epitopes in AD cases. This is somewhat expected in human post-mortem brain samples that can be affected by many parameters including cause of death, post-mortem delay,

tissue pH, co-occurring morbidities, and exposure to different prescribed medications (Hanger et al., 2009). Nevertheless, substantial amounts of phosphorylated tau were only detected in AD cases, supporting previous findings that tau is abnormally phosphorylated in AD (Hanger et al., 2009; Kurbatskaya et al., 2016; Lau et al., 2016).

Differences in astrocyte markers between control and late stage AD post-mortem brain samples were next investigated. Homogenised temporal cortex samples were run on western blots and probed with an antibody against GFAP, widely considered to be a reliable indicator of activated astrocytes (Eng et al., 2000). This revealed a main band of approximately 50 kDa corresponding to full-length GFAP and several smaller bands, which likely represent cleaved fragments of GFAP (Zoltewicz et al., 2012) (**Figure 5.3 A**). Quantification of detected proteins on western blots showed that GFAP levels are significantly elevated in Braak stage V-VI temporal cortex homogenates compared to controls, suggesting that there is a marked increase in the number of activated astrocytes in late stage AD (**Figure 5.3 A, B**). This is consistent with a wide body of literature showing that astrocytes are activated in AD and that these cells play an important role in disease progression (Simpson et al., 2010; Sofroniew and Vinters, 2010; Phillips et al., 2014; Zhang and Jiang, 2015; Hu et al., 2016).

Results were next stratified according to ApoE genotype to determine if ApoE, a genetic risk factor for AD that is produced predominantly by astrocytes, is associated with astrocyte activation. The ApoE ε4 variant is the largest known genetic risk factor for AD, with over 60 % of individuals diagnosed with AD harbouring at least one ε4 allele (Riedel et al., 2016). In contrast the ε2 variant is protective against AD, significantly reducing the risk of AD in carriers (Suri et al., 2013). Results were stratified into three groups: those carrying one copy of the ε2 variant (ε2/ε3 or ε2/ε4), those homozygous for ε3 (ε3/ε3) or carrying one copy of the ε4 allele (ε3/ε4), and those homozygous for ApoE ε4 (ε4/ε4). Statistical analysis showed that there were no significant differences in GFAP levels between the three groups (**Figure 5.3 C**). However, samples with at least one ApoE ε4 allele appeared to contain the lowest GFAP amounts, whereas those with one ApoE ε2 allele showed the highest levels of astrocyte activation.

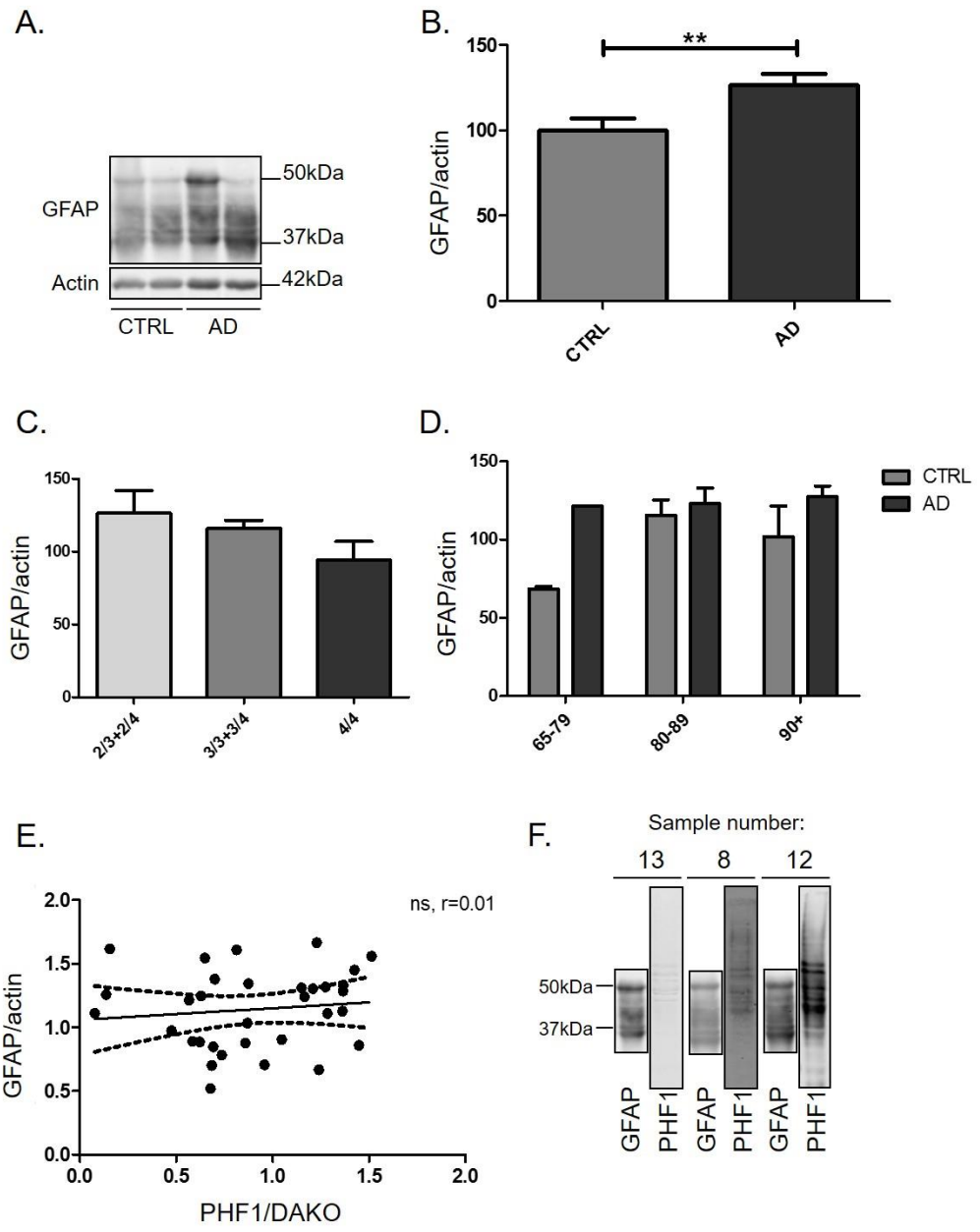

Figure 5.3: Astrocyte activation is increased in late stage AD temporal cortex relative to controls

A. Representative western blots showing homogenates of control (CTRL) and late stage (Braak V/VI) AD temporal cortex probed with an antibody against GFAP (50 kDa). Blots were also probed with an antibody against ß-actin (42 kDa) as a loading control. Molecular weight markers are shown on the right. **B.** Bar chart shows GFAP amounts following normalisation to ß-actin in the same sample. Data are shown as % control (CTRL). Control n=14; AD n=19. **C-D.** Bar chart show amounts of GFAP, following standardisation to ß-actin as a function of **C.** ApoE genotype (2/3 + 2/4 n = 7, 3/3 n = 13, 3/4 + 4/4 n = 13) and **D.** age in control and AD samples (65-79 n = 3, 80-89 n = 20, 90+ n = 7). **E.** Scatter plot showing correlation between levels of GFAP/actin and PHF1/total tau (DAKO). ns = not significant, r = correlation coefficient. Control n=14; AD n=19. **F.** Direct comparison of representative western blots probed with antibodies against GFAP and PHF1 showing no correlation between antibody levels. Molecular weight markers are shown on the left. Sample numbers are indicated. Data in graphs are mean ± SEM. Data were analysed using: **B.** two-tailed t-test, **C.** one-way ANOVA, **D.** two-way ANOVA. **E.** Spearman's correlation. ** = $p<0.01$.

Age is also suggested to be involved in the inflammatory response in AD (Craft, 2005; Simpson et al., 2010; Calvo et al., 2015; Riedel et al., 2016; Rodriguez et al., 2016). Low level systemic inflammation accompanies normal aging and is thought to prime glia resulting in an increased susceptibility to AD and other age-related diseases (Franceschi and Campisi, 2014). Specifically, age is thought to exacerbate Aß-related inflammation in AD (Craft, 2005). To examine possible associations between astrocyte activation and age in these samples, results were analysed following stratification into three age groups: 65-79, 80-89 and 90+ years old. The small number of samples from individuals younger than 65 were excluded from this analysis. Since there appears to be dissociation between age-related effects in normal aging and disease (Liddell et al., 2007), samples were further stratified into control and AD groups. The results of this analysis showed that GFAP amounts appeared to be lower in the age 65-79 control group compared to all others, and all ages of control groups showed less GFAP amounts compared to their AD counterparts. However, statistical analysis revealed that these differences were not significant (**Figure 5.3 D**). This might be because of the limited sample size used here, particularly for the age 65-79 groups (control = 2, AD = 1).

Finally, to explore possible associations between astrocyte activation and tau phosphorylation, a Spearman's rank test was used to examine the correlation between GFAP and either PHF1 (tau phosphorylated at Ser396/404) or CP13 (tau phosphorylated at Ser202) amounts. No significant correlation was found between GFAP and tau phosphorylated at either epitope (CP13: data not shown, PHF1: **Figure 5.3 E, F**). This was somewhat unexpected as evidence from models of AD suggests that astrocyte activation induces disease-associated changes in tau such as its phosphorylation and cleavage (Garwood et al., 2011). However, as discussed in Chapter 4 (**section 4.4**), levels of GFAP are not necessarily completely indicative of astrocyte activation. Therefore, it is possible that other markers of astrocytic inflammatory response or levels of cytokine production (such as IL-1ß, for example) may correlate with tau phosphorylation.

Moreover, this data might suggest that results obtained in dissociated co-culture models is not representative of that which occurs in AD brain. These findings are likely further confounded by

recent results showing marked differences in the rodent and human astrocyte transcriptomes, variation that is further altered with aging (Zhang et al., 2016b).

In summary, these results suggest that there is a significant increase in astrocyte activation in end-stage AD. Astrocyte activation is probably not affected by age or ApoE genotype, and is not closely correlated with the abundance of phosphorylated tau.

To further explore the inflammatory response in late stage AD, microglial markers were also investigated. Microglia and the microglial inflammatory response have long been implicated in the development and progression of AD (Heneka et al., 2015; Jebelli et al., 2015; Heneka et al., 2016). Microglial phenotype is altered in AD (Perry, 2016), losing protective functions that allow microglia to phagocytose Aß and cell debris in an attempt to reduce the toxicity of the local environment (Boche et al., 2013). In parallel, microglia can mount a pro-inflammatory response, including cytokine and chemokine release, that can activate toxic signalling pathways in other glial cells and neurons (Cai et al., 2013).

To investigate microglial responses in the brain samples used in this thesis, homogenised post-mortem temporal cortex from control and late-stage AD brain (**Table 5.1**) were immunoblotted as described above, but using 12 % acrylamide gels, with an antibody against Iba1 (**Figure 5.4 A**). Iba1 is a microglia/macrophage-specific calcium-binding protein that is often used as a marker for microglial activation (Imai and Kohsaka, 2002). Western blots showed a single band of approximately 17 kDa corresponding to the expected size of Iba1. Quantification of Iba1 signal density, following normalisation to ß-actin amounts in the same sample, showed that there was no significant difference in Iba1 levels between control and late stage AD samples (**Figure 5.4 B**) suggesting that microglia are not significantly activated in these samples. Alternatively, these findings might suggest that Iba1 is not a good indicator of microglial activation (Boche et al., 2013).

Similar to described above for GFAP, further characterisation of Iba1 levels was carried out with respect to ApoE genotype and age. Statistical analysis showed that there is no significant interaction of ApoE genotype and Iba1 amounts (**Figure 5.4 C**). Similarly, there were no

significant differences in Iba1 amounts between different ages of control and AD groups (**Figure 5.4 D**). Again, as described above, it is possible that effects may be masked by the relatively small number of samples used in this study and the significant variation observed within groups.

Signalling between neurons and microglia is important for disease-associated changes in tau. In particular, knockout of microglial fractalkine receptors prevents neuron-derived fractalkine from maintaining microglia in a resting state, and causes neuroinflammatory responses that exacerbate the development of tau pathology in transgenic mouse models of AD (Bhaskar et al., 2010). Therefore, it was important to determine if there are any associations between Iba1 amounts and phosphorylated tau in these samples. Spearman's rank correlations were carried out to examine the association between Iba1 and PHF1 (tau phosphorylated at Ser396/404) or CP13 (tau phosphorylated at Ser202). There was no statistically significant correlation between Iba1 and CP13 amounts (data not shown). However, Iba1 and PHF1 were significantly positively correlated ($r = 0.57$, $p < 0.001$, **Figure 5.4 E**), and this was apparent when Iba1 and PHF1 amounts were examined on western blots of the same samples (**Figure 5.4 F**). This data suggests that increased microglial activation may contribute to increased tau phosphorylation in AD, at least at the PHF1 epitope.

To summarise, no significant changes were apparent in Iba1 amounts between AD and control brain. Iba1 amounts did not appear to dissociate with either ApoE genotype or age. Interestingly, however, Iba1 amounts significantly correlate with levels of tau phosphorylated at the PHF1 epitope. This suggests that microglia activation may be involved in the signalling pathways that result in phosphorylation of tau at this epitope. These results might further suggest that the large extent of variation in post-mortem brain makes it difficult to determine changes between control and disease states, whereas correlation analysis might provide more informative data regarding possible disease pathways.

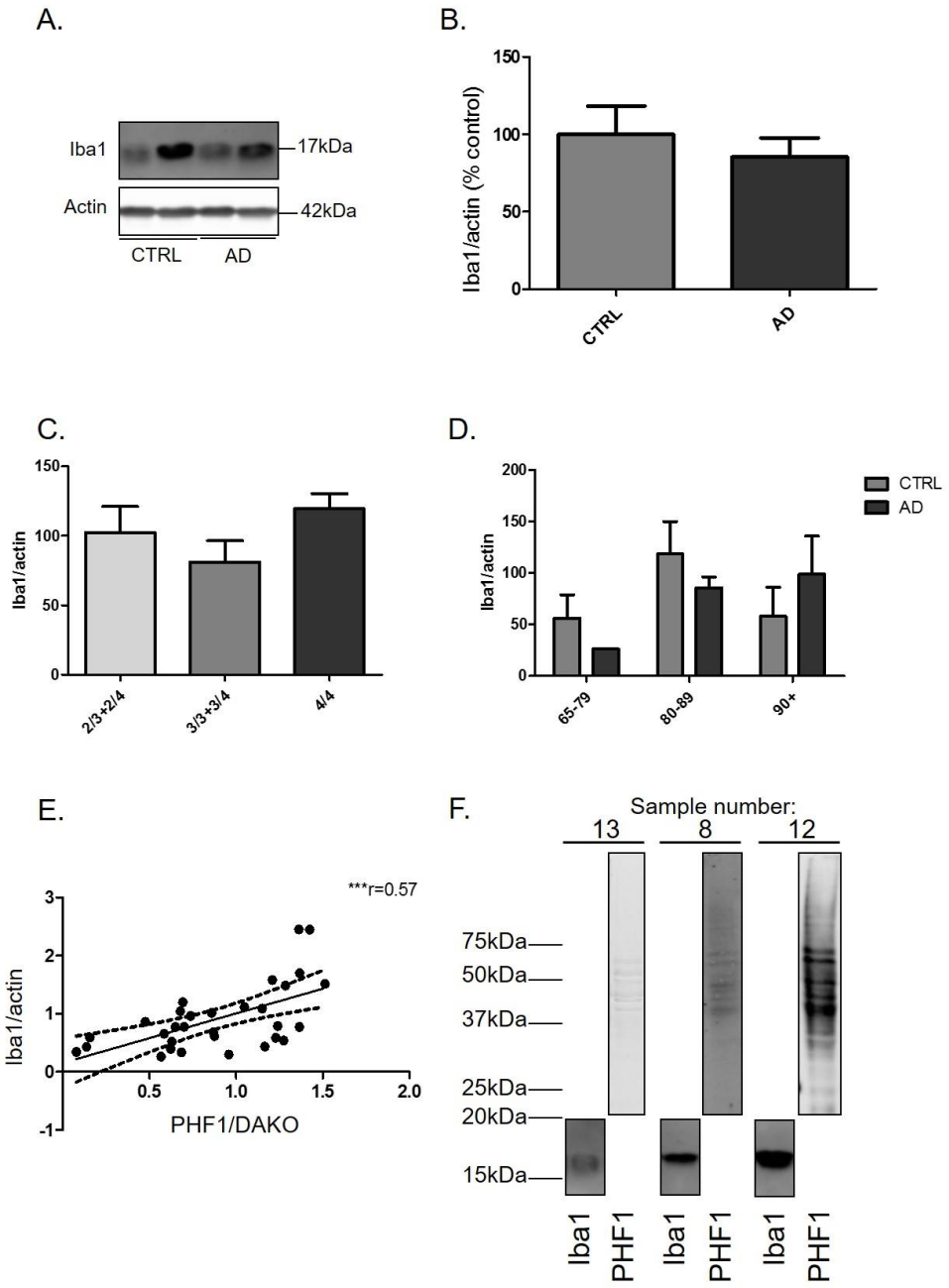

Figure 5.4: Amounts of the microglial marker Iba1 positively correlate with tau phosphorylation at the PHF1 epitope.

A. Representative western blots showing homogenates of control (CTRL) and late stage (Braak V/VI) AD temporal cortex probed with an antibody against Iba1 (17 kDa). Blots were also probed with an antibody against ß-actin (42 kDa) as a loading control. Molecular weight markers are shown on the right. **B.** Bar chart shows Iba1 amounts following normalisation to ß-actin in the same sample. Data are shown as % control (CTRL). Control n=14; AD n=19. **C-D.** Bar chart show amounts of Iba1, following standardisation to ß-actin as a function of **C.** ApoE genotype (2/3 + 2/4 n = 7, 3/3 n = 13, 3/4 + 4/4 n = 13), and **D.** age in control and AD samples (65-79 n = 3, 80-89 n = 20, 90+ n = 7). **E.** Scatter plot showing correlation between levels of Iba1/actin and PHF1/total tau (DAKO). ns = not significant, r = correlation coefficient. Control n=14; AD n=19. **F.** Direct comparison of representative western blots probed with antibodies against Iba1 and PHF1. Molecular weight markers are shown on the left. Sample numbers are indicated. Data in graphs are mean ± SEM. Data were analysed using: **B.** two-tailed t-test, **C.** one-way ANOVA, **D.** two-way ANOVA. **E.** Spearman's correlation. **** = p<0.001.

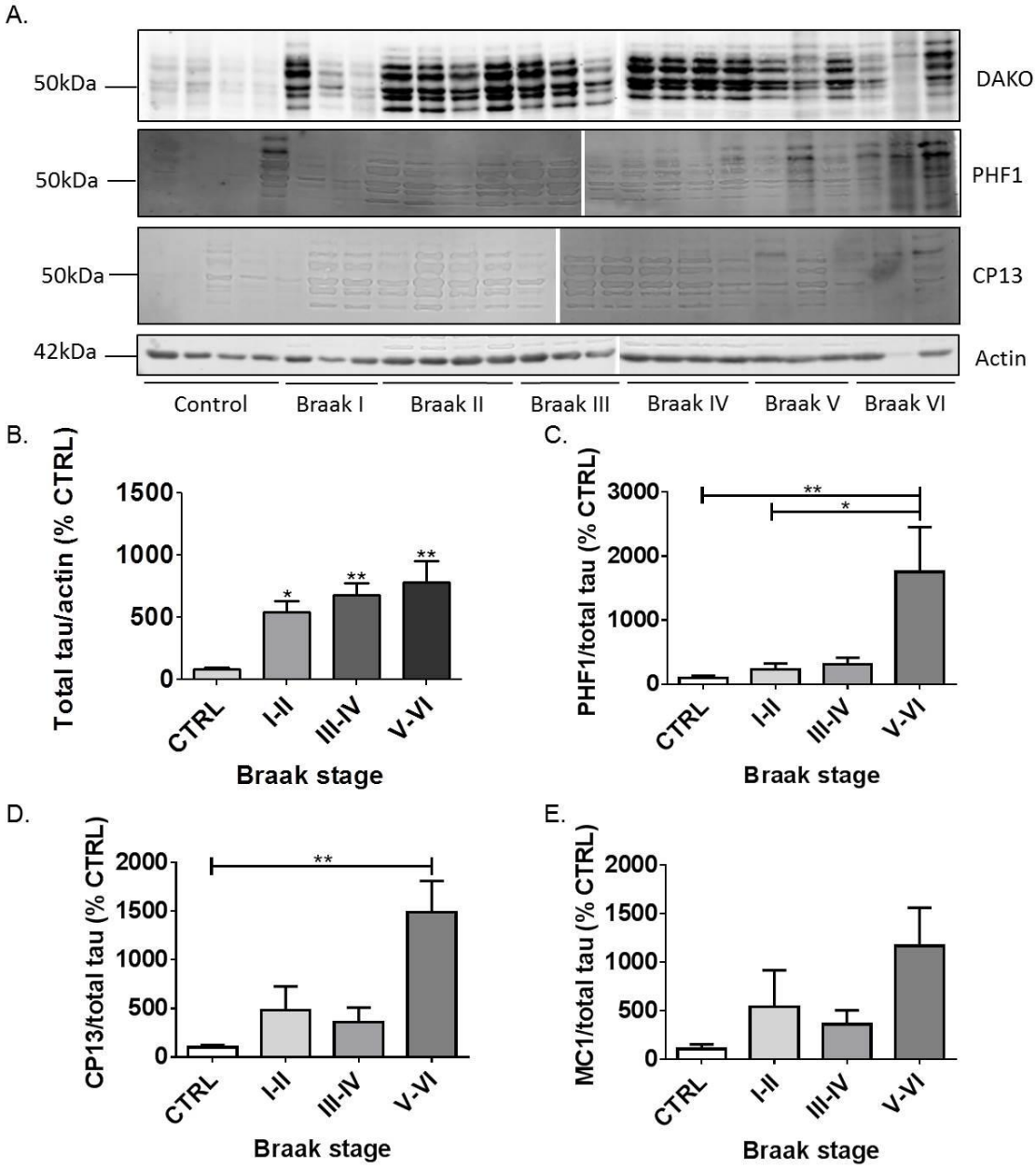

Figure 5.5: Total and phosphorylated tau increase as AD progresses

A. Representative immunoblots of temporal cortical homogenates from post-mortem control and Braak stage I-VI brain. Blots were probed with antibodies to detect total (phosphorylated and non-phosphorylated) tau (DAKO), tau phosphorylated at Ser396/404 (PHF-1) and Ser202 (CP13), all at 50 to 70 kDa. Blots were also probed with an antibody against ß-actin as a loading control. Molecular weight markers are shown on the left. **B.** Bar chart shows quantification of total tau amount detected by western blotting as a proportion of ß-actin in the same sample. **C-E.** Bar charts showing quantification of standard tau ELISAs using antibodies **E.** PHF1, **F.** CP13 and **G.** MC1, all graphed and analysed as a proportion of total tau. Values shown are mean ± SEM as percentage control (CTRL). N= 3-4 per Braak stage. Data was analysed using one-way ANOVA. * = $p<0.05$, ** = $p<0.01$.

Having determined that there are some differences in temporal cortex between control and end-stage AD brain, and established methods with which to examine glial markers and tau in these tissues, the next step of this study was to determine if there are key points in AD development at which these changes occur and/or if there are regional differences. To this end, glial markers and tau processing was examined in temporal cortex and hippocampus from cases at all Braak stages.

5.3.2 Characterisation of changes in tau and glia in temporal cortex during AD progression

Total and phosphorylated tau amounts increase in temporal cortex during AD development

Temporal cortex homogenates from control and Braak stage I-VI brain (**Table 5.2**) were immunoblotted with antibodies against total and phosphorylated (PHF1, CP13) tau, as described above. Blots appeared to show an increase in total and phosphorylated tau amounts with increasing Braak stage (**Figure 5.5 A**)**.** Quantification of total tau amounts following normalisation to ß-actin, showed a significant accumulation of total tau with increasing Braak stage (**Figure 5.5 B**)**.** For this and all other quantification of this sample set, sample 25, the second Braak VI sample shown on western blots, was excluded from analysis due to abnormal ß-actin levels, see **Figure 5.5 A**).

Western blots probed with PHF1 and CP13 antibodies showed increased levels of tau phosphorylation as AD progresses **(Figure 5.5 A**). However, these differences were not statistically significant (data not shown) due to high variation between samples and the relative insensitivity of western blotting in detecting subtle protein changes. Therefore, tau phosphorylation was also assessed using semi-quantitative tau ELISAs using the CP13 and PHF1 antibodies, in addition to an MC1 antibody which detects an abnormal conformation of tau (Jicha et al., 1999). Analysis of ELISA results showed that PHF1 levels were significantly increased in Braak stages V-VI compared to control samples and Braak stage I-II samples (**Figure 5.5 C**). CP13 amounts were also significantly increased at Braak stage V-VI compared to controls (**Figure**

5.5 D). Changes in MC1 were not statistically significant between groups suggesting that tau conformation does not change significantly as AD progresses (**Figure 5.5 E**). This is likely to be due to high variation between samples and low sample numbers in each group since there is robust evidence demonstrating that changes in tau conformation occur early in disease as tau aggregate formation begins (Weaver et al., 2000; Garcia-Sierra et al., 2003; Mondragon-Rodriguez et al., 2008b).

To determine if the increases in total tau observed in late stage AD brain reflect the accumulation of tau aggregates that are less prone to protein clearance and degradation machinery (Meraz-Rios et al., 2010), aggregated tau was isolated on the basis of its insolubility in sarkosyl, as we have previously described (Noble et al., 2003). This protocol results in three tau fractions, a low speed supernatant (LSS), sarkosyl-soluble (HSS) and sarkosyl-insoluble tau, all of which were immunoblotted with antibodies against total tau. These findings confirmed an increase in insoluble tau as a proportion of total tau in Braak stage V and VI tissues relative to earlier Braak stages and controls (**Figure 5.6**). Thus, the increase in total tau protein observed in **Figure 5.5 A** likely reflects the accumulation of this insoluble tau in temporal cortex homogenates.

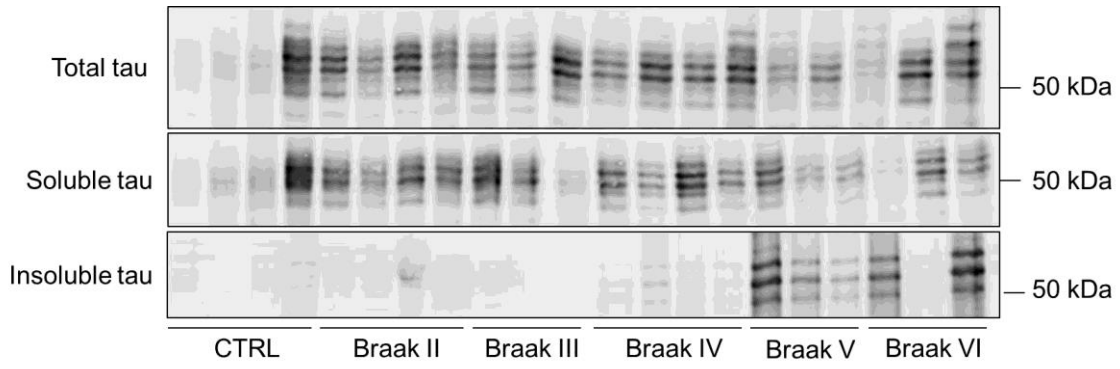

Figure 5.6: Sarkosyl insoluble tau increases as AD progresses
Representative immunoblots of sarkosyl extraction protocols showing total, soluble and insoluble fractions from temporal cortical homogenates from post-mortem control and Braak stage I-VI brain. Blots were probed with antibodies to detect total tau (DAKO), at 50 to 70 kDa. Molecular weight markers are shown on the right. N= 3-4 per Braak stage.

Increased tau phosphorylation may be caused by increases in GSK-3 activity in early Braak stages

Increases in tau phosphorylation as AD progresses are known to be caused, largely, by increases in tau kinase activity. Research shows GSK-3 is a key tau kinase in AD, and is significantly increased in AD brain (Hanger et al., 2009). GSK-3 has two isoforms: GSK-3α and GSK-3ß, both of which are inhibited by phosphorylation – at Ser21 and Ser9, respectively (Fang et al., 2000). Reduced levels of phosphorylation increase levels of GSK-3 activity, increasing tau phosphorylation. To investigate changes in GSK-3 activity as AD progresses, control and Braak stage I-VI AD post-mortem homogenates were analysed on western blots probed for antibodies against total and phosphorylated (Ser21/9) GSK-3α/ß. Quantification of western blots, following standardisation of phosphorylated GSK-3 to total GSK-3, showed a trend towards a reduction in phosphorylated GSK-3 amounts at Braak stage II, compared to controls (p=0.07; **Figure 5.7**). Only one prominent band was detected in the phospho GSK-3 antibody. This is likely to represent Ser9 on GSK-3ß as the antibody used shows a preference for this epitope. For this reason, GSK-3α and ß were quantified together. This indicates that GSK-3 activity may be increased in early Braak stages, and may possibly be responsible for the increased tau phosphorylation that follows later in disease. However, this reduction in GSK-3 phosphorylation, and therefore increase in activity, is not maintained throughout disease (**Figure 5.7**). This suggests that GSK-3 may be involved in increased tau phosphorylation during early stage AD but may not be as active during the later, more severe stages of the disease.

No significant changes in glial markers were detected in temporal cortex of different Braak stages

Temporal cortex homogenates from control and Braak stage I-VI brains (**Table 5.2**) were western blotted with antibodies that detect specific astrocyte and microglial markers to determine if there are changes in glial activation during AD development. Unfortunately, despite extensive attempts at optimisation, protein bands at the correct molecular weight could not be reliably

detected in these samples using the anti-Iba1 antibody (data not shown), so no results for Iba1 are described here.

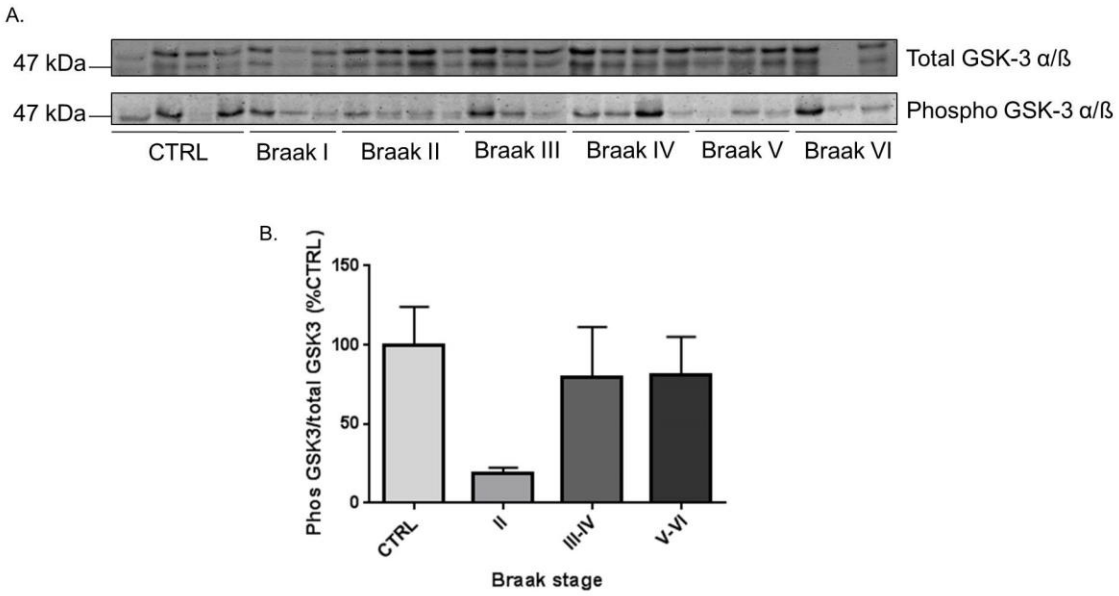

Figure 5.7: Phosphorylated GSK-3 levels are significantly reduced in early Braak stages
A. Representative blots of temporal cortex homogenates from post-mortem control and Braak stage I-VI brain. Blots were probed with antibodies against total and phosphorylated (Ser21/9) GSK-3α/ß. Molecular weight markers are shown on the left. **B.** Bar charts show quantification of phosphorylated GSK-3α/ß as a proportion of total GSK-3α/ß in each sample. Values shown are mean ± SEM as percentage control (CTRL). N= 3-4 per Braak stage. Data was analysed using one-way ANOVA. * = $p<0.05$.

Western blots were probed with an antibody against the active astrocytic marker GFAP as described above, and additionally with an antibody against vimentin. Vimentin is another intermediate filament protein that is also reported to be upregulated in reactive astrocytes (Pekny and Nilsson, 2005). Both antibodies detected bands at the expected sizes of 50 and 57 kDa, respectively, as well as a number of smaller protein fragments (**Figure 5.8 A**). Vimentin antibodies have detected small fragments of protein in previously published paper, however it is unclear what vimentin fragments are present therefore only full length vimentin was quantified (Yang et al., 2002). Quantification of GFAP and vimentin signal intensities on western blots showed that there are no statistically significant changes in GFAP or vimentin in different Braak stages (**Figure 5.8 B, C**). This suggests that general astrocyte activation does not

significantly change in the temporal cortex as AD develops and progresses. This is inconsistent with both the results described in **section 5.3.1** and previous publications describing that progressive increases in astrocyte inflammatory responses are characteristic of AD (Sofroniew and Vinters, 2010). It is likely that the negative finding reported here reflects the variation in astrocytic responses in cases of similar Braak stages, as can also be observed when examining other proteins. It is possible that, with larger numbers of samples in each group, significant differences may have become apparent.

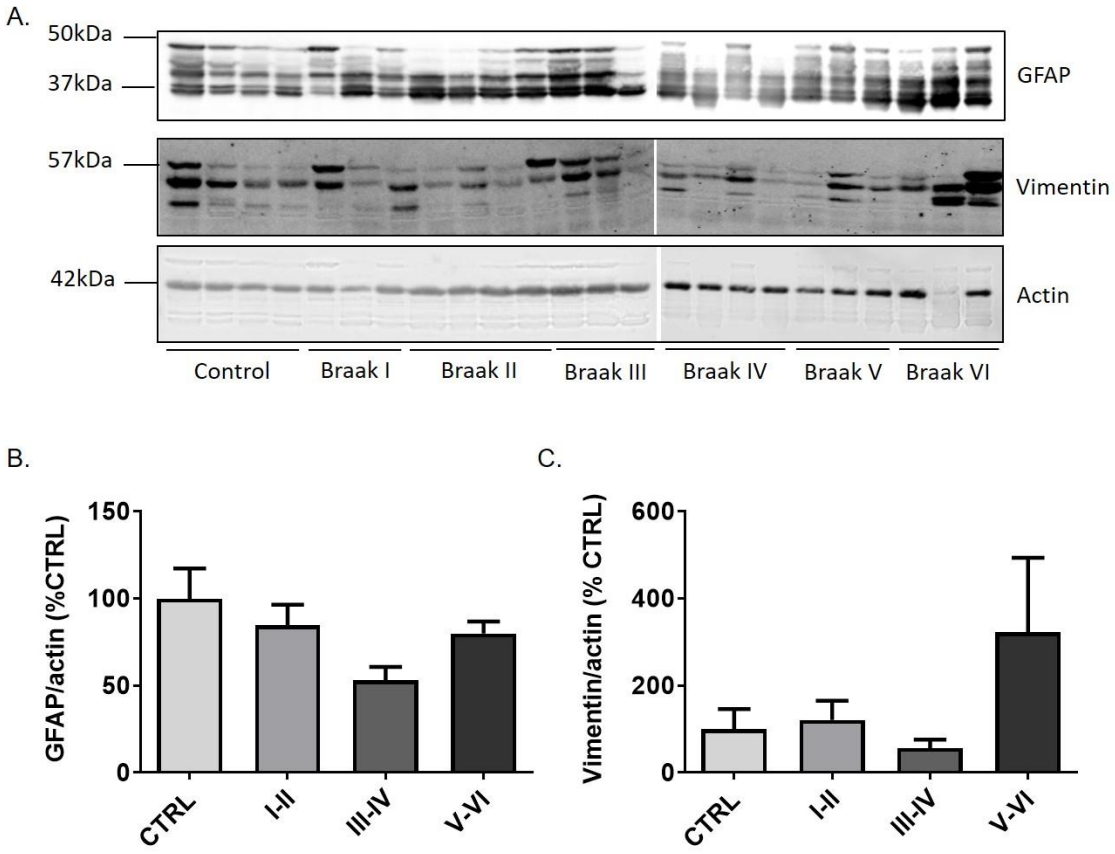

Figure 5.8: Astrocytic marker levels do not change with increasing Braak stage
A. Representative blots of temporal cortex homogenates from post-mortem control and Braak stage I-VI brain. Blots were probed with antibodies against GFAP and vimentin. ß-actin was used as a loading control. Molecular weight markers are shown on the left. Bar charts show quantification, following normalisation to ß-actin of **B.** GFAP, and **C.** vimentin. Values shown are mean ± SEM as percentage control (CTRL). N= 3-4 per Braak stage. Data was analysed using one-way ANOVA.

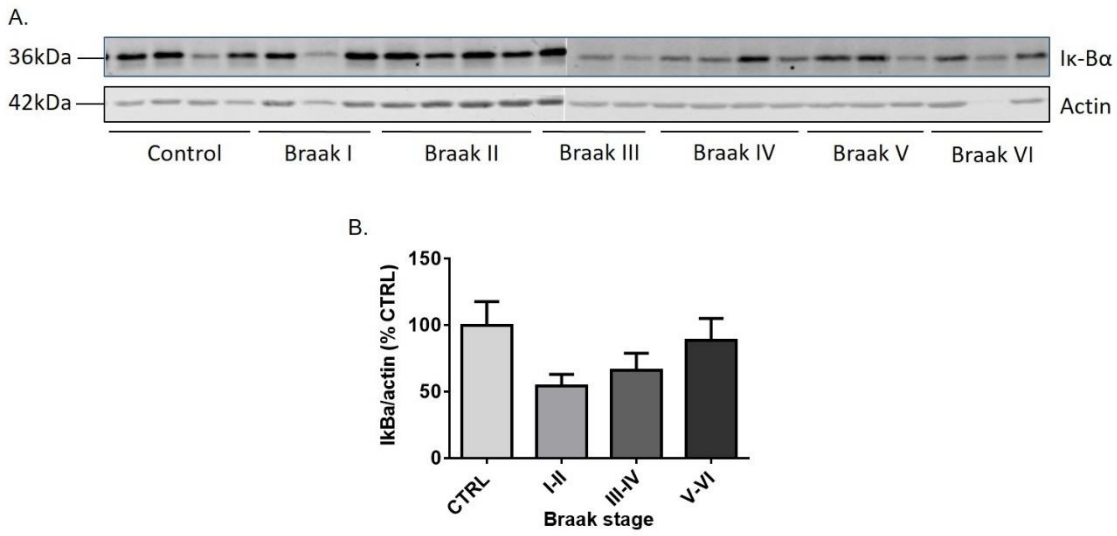

Figure 5.9: There are no changes in IκBα levels with increasing Braak stage in temporal cortex A. Representative blots of temporal cortex homogenates from post-mortem control and Braak stage I-VI brain. Blots were probed with antibodies against IκBα and ß-actin as a loading control. Molecular weight markers are shown on the left. **B.** Bar charts show quantification of IκBα as a proportion of ß-actin. Values shown are mean ± SEM as percentage control (CTRL). N= 3-4 per Braak stage. Data was analysed using one-way ANOVA.

IκBα levels suggest NF-κB activation does not change as AD progresses

Evidence from the literature suggests the activity of NF-κB, a transcription factor known to control the production and release of multiple immune-related proteins (Granic et al., 2009), increases as part of the astrocytic activation response in AD (Shi et al., 2016). Experiments described in Chapter 3 (**section 4.3.4**), also provide evidence that NF-κB levels are increased in response to Aß in primary cortical cultures. To determine if there are changes in NF-κB activity in post-mortem AD brain, temporal cortex homogenates were western blotted and probed for IκBα. IκBα is an endogenous inhibitor of NF-κB, being bound to inactive NF-κB in the cytoplasm. When phosphorylated via signalling pathways that can be activated by Aß and other cell stressors (Kaltschmidt et al., 1997; Lin et al., 2013), IκBα releases NF-κB and it translocates to the nucleus where it can increase transcription of multiple inflammatory mediators, including pro-inflammatory cytokines and chemokines (Bauernfeind et al., 2009). Increased inflammatory mediator production can subsequently activate pathological signalling pathways in other glial and neuronal cells (Shi et al., 2016). Probing western blots with an IκBα antibody detected

proteins of 36 kDa corresponding to the expected molecular weight of IκBα. Quantification of IκBα amounts relative to ß-actin showed that there were no statistically significant differences between control tissue and any Braak stages (**Figure 5.9**). This data may suggest that there are no changes in NF-κB activation in the temporal cortex with increasing Braak stage. However, it is possible that changes in IκBα phosphorylation are occurring in the absence of changes in total IκBα, which would affect activation of NF-κB. Unfortunately, antibodies to examine phospho-IκBα were not available for investigation in this project.

Changes in synaptic markers indicate synaptic compensation in early-mid stages of AD

Synaptic loss occurs early in AD and is thought to underlie neuron death and cognitive impairment (Busche and Konnerth, 2016). Both Aß and tau have been suggested to cause synaptic dysfunction and loss (Thies and Mandelkow, 2007; Ondrejcak et al., 2010; Crimins et al., 2013). Additionally, synaptic dysfunction is thought to drive abnormal tau processing, possibly creating a pathological feed-forward loop (Amadoro et al., 2006; Li et al., 2014b). Changes in synaptic markers were therefore examined in control and Braak stage I-VI post-mortem temporal cortex (**Table 5.2**). Blots were probed with an antibody against post-synaptic density-95 (PSD-95, 95 kDa), an integral scaffolding component of the post-synapse that is also commonly used a marker for loss of synapses in AD models (Savioz et al., 2014). Quantification of PSD-95 amounts relative to ß-actin showed that PSD-95 levels appear to decrease with increasing Braak stage (**Figure 5.10 A**). However, these differences were not statistically significant (**Figure 5.10 B**) despite PSD-95 levels at all Braak stages being substantially lower than those detected in control samples. There is high variability in the control group and the lack of significance might have been the result of an anomalous sample (first control sample), that did not meet criteria for being removed as an outlier (**Figure 5.10 A**).

Western blots were also probed with antibodies against the pre-synaptic markers, synapsin-1 and synaptophysin. Synapsin-1 is a neuron specific phosphoprotein localized to the cytoplasmic side of small synaptic vesicles that plays an important role in synaptic vesicle release by

exocytosis (Bahler et al., 1990), and was apparent as two bands at approximately 70 and 74 kDa on blots (**Figure 5.10 A**). Synaptophysin is a 38 kDa synaptic vesicle glycoprotein that interacts with synaptobrevin to regulate synaptic vesicle positioning and release (Yao et al., 2003) (**Figure 5.10 A**). Quantification of synapsin-1 immunoreactivity showed that synapsin-1 levels are significantly increased at Braak stage III-IV compared to control samples (**Figure 5.10 A, C**). This may suggest an innate attempt to compensate for the synaptic dysfunction caused by Aß and other AD insults. However, this increase in synapsin is not maintained in Braak stages V-VI suggesting that any compensation is only temporary and is overcome by significant synaptotoxic challenges in later disease stages.

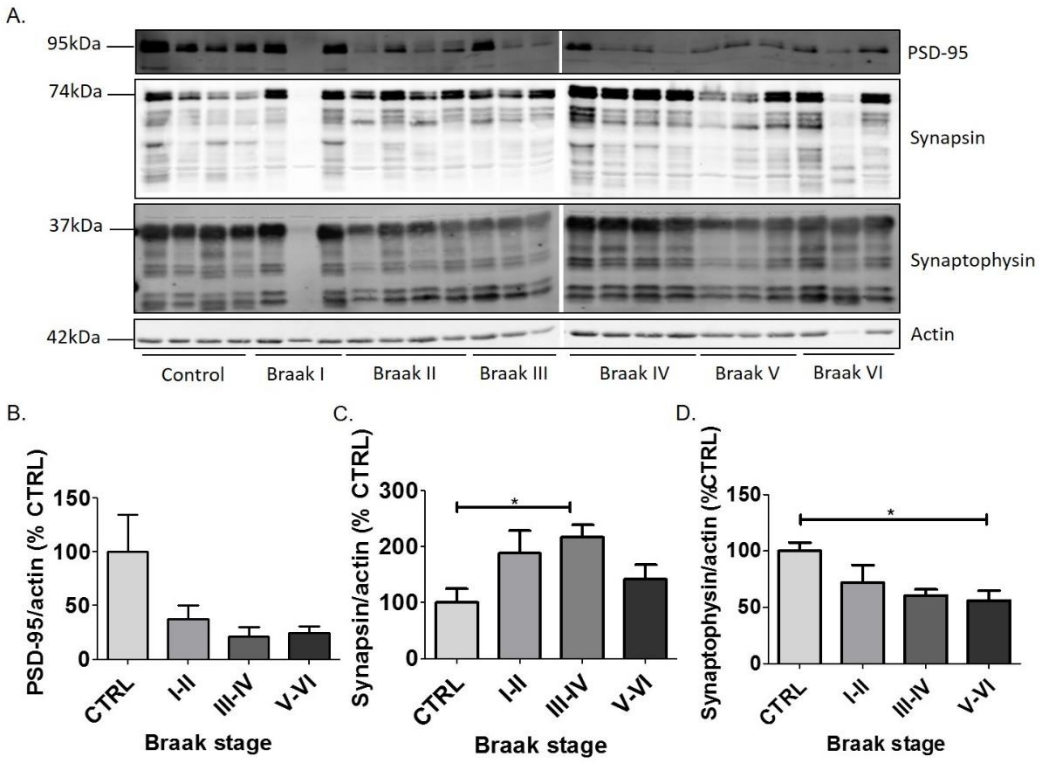

Figure 5.10: Changes in synaptic markers indicate possible compensatory mechanisms prior to loss of synapses at late-stage AD

A. Representative blots of temporal cortex homogenates from post-mortem control and Braak stage I-VI brain. Blots were probed with antibodies against PSD-95, synapsin, synaptophysin and ß-actin as a loading control. Molecular weight markers are shown on the left. Bar charts show **B.** PSD-95, **C.** synapsin, and **D.** synaptophysin quantified as a proportion of ß-actin. Values shown are mean ± SEM as percentage control (CTRL). N= 3-4 per Braak stage. Data were analysed using one-way ANOVA. * = $p<0.05$.

Quantification of western blots probed with the pre-synaptic marker, synaptophsyin, showed significantly decreased synaptophysin amounts in Braak stage V-VI samples compared to controls (**Figure 5.10 A, D**), suggesting that synapses are lost in Braak stages V-VI. These results further suggest that different synaptic markers have different utilities for examining synaptic degeneration in post-mortem tissues, an issue discussed in detail by Honer (2003).

Taken together, the results of these experiments suggest that there may be compensatory responses in prodromal AD (Braak stages III-IV) that are overcome by end-stage AD. Enhanced function and plasticity of healthy synapses in an area of degenerating neurons has been previously demonstrated (Neuman et al., 2015). If the mechanisms underlying the improved function of these synapses could be elucidated, it is possible they could be used to reverse synaptic dysfunction in AD-affected neurons.

In summary, analysis of post-mortem temporal cortex has shown increases in total, phosphorylated and aggregated tau with increasing Braak stage. Changes in tau phosphorylation and aggregation were preceded by elevations in GSK-3 activity. There were no consistent changes in markers of astrocyte activation, or NF-κB activity in different Braak stages, so the association between astrocytes and these changes in tau remains elusive. The results suggest that there may be a synaptic compensatory response in Braak stages III-IV as an attempt to protect from synaptic dysfunction and as AD progresses, that is overcome in late-stage AD at which point synaptic proteins are lost.

5.3.3 Characterisation of changes in tau and glia in hippocampus during AD progression

Total and phosphorylated tau amounts increase in hippocampus during AD development

Control and Braak stage II-VI hippocampal post-mortem homogenates (see **Table 5.3**) were western blotted and probed for antibodies against total and phosphorylated tau as described above for temporal cortex. Similar to changes observed in temporal cortex, quantification of total tau relative to NSE showed accumulation of total tau amounts with increasing Braak stage

(**Figure 5.11 A**), with a significant difference found between control and Braak stage V-VI hippocampus (**Figure 5.11 B**). This is consistent with findings from experiments using temporal cortex post-mortem samples (**section 5.3.2**) and is most likely due to the formation of tau aggregates and NFTs as AD progresses.

Assessment of tau phosphorylation using the antibodies PHF1 and CP13 also showed increases in phosphorylated tau with advancing Braak stage (**Figure 5.11 A**). However, the high levels of variability within groups was the probable reason that these differences did not reach statistical significance (**Figure 5.11 C, D**). This is consistent with findings from temporal cortex samples which suggest that western blotting is not a sufficiently sensitive method to detect subtle change in phosphorylated tau in post-mortem brain (**section 5.3.2**). However, phosphorylated tau was more consistently detected in earlier Braak stages in the hippocampus when compared to the cortex, consistent with staging criteria showing that tau pathology occurring in the hippocampus before spreading to the temporal cortex (Braak and Braak, 1995).

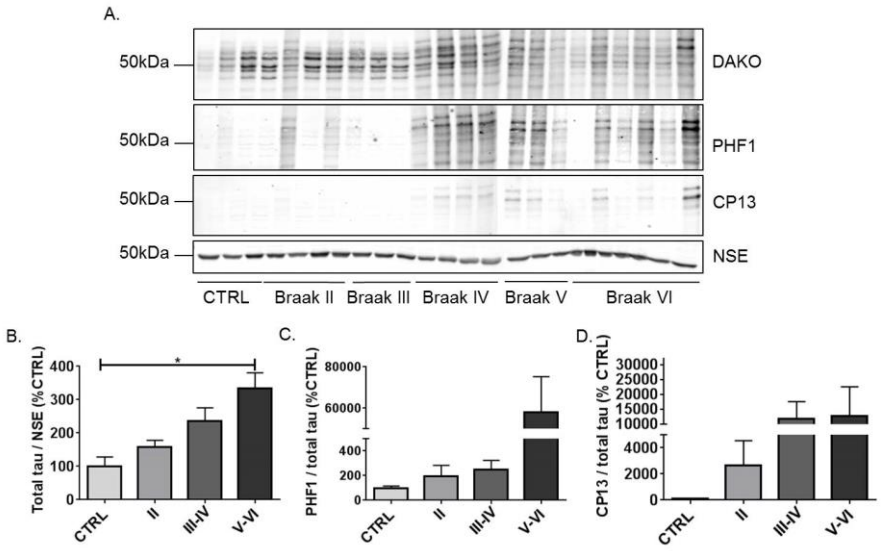

Figure 5.11: Levels of total and phosphorylated hippocampal tau are elevated with increasing Braak stage

A. Representative blots of hippocampal homogenates from post-mortem control and Braak stage I-VI brain. Blots were probed with antibodies against total tau (DAKO), tau phosphorylated at Ser396/404 (PHF1) and Ser202 (CP13). NSE was used as a loading control. Molecular weight markers are shown on the left. Bar charts show **B.** total tau measured as a proportion of NSE, **C.** PHF1 and **D.** CP13 measured as a proportion of total tau. Values shown are mean ± SEM as percentage control (CTRL). N= 3-6 per Braak stage. Data was analysed using one-way ANOVA. * = $p<0.05$.

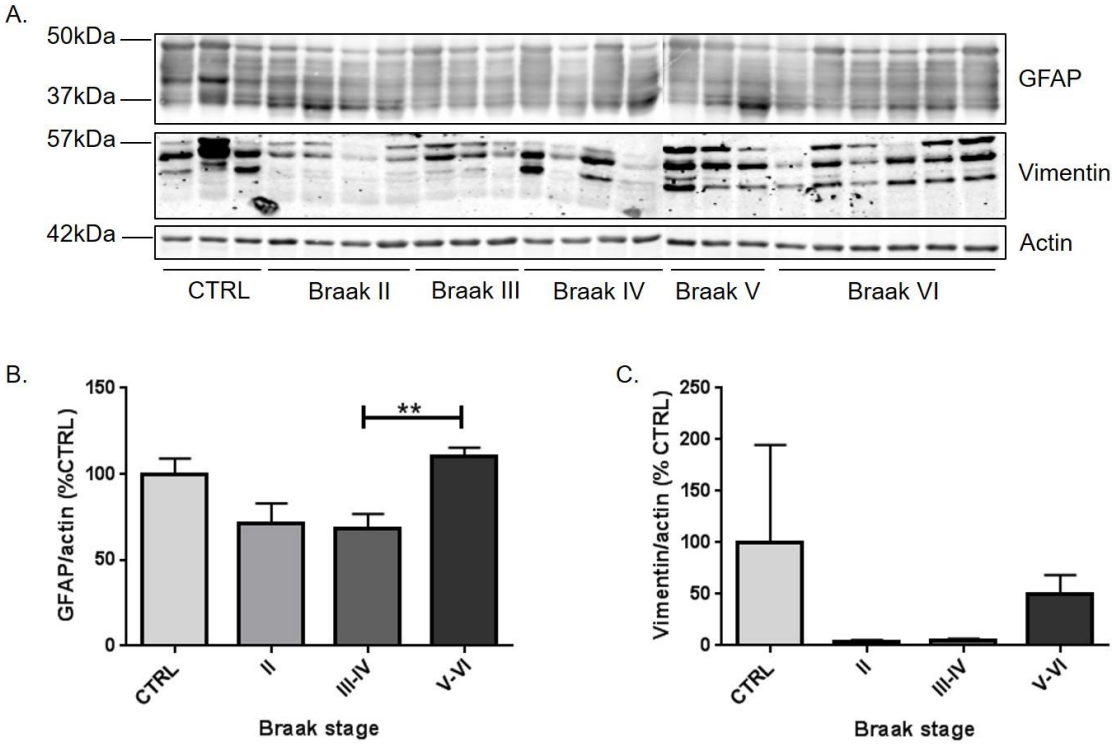

Figure 5.12: Hippocampal GFAP levels increase between Braak stages II-IV and V-VI
A. Representative blots of hippocampal homogenates from post-mortem control and Braak stage I-VI brain. Blots were probed with antibodies against GFAP and vimentin. ß-actin was used as a loading control. Molecular weight markers are shown on the left. Bar charts show quantification of **B.** GFAP, and **C.** vimentin as a proportion of ß-actin. Values shown are mean ± SEM as percentage control (CTRL). N= 3-6 per Braak stage. Data was analysed using one-way ANOVA. ** = $p<0.01$.

GFAP levels increase in late Braak stage hippocampus

To investigate changes in astrocyte activation in the hippocampus as AD progresses, homogenates were run on western blots and probed with the GFAP antibody. The results showed a non-significant descrease in GFAP amounts in Braak stages II-IV followed by a significant increase in GFAP amounts in Braak stage V-VI samples, when compared to Braak stage III-IV samples, but not to earlier Braak stages or controls (**Figure 5.12 A, B**). This might suggest that there is a period of intensive astrocyte activation towards end stage AD in the hippocampus. When western blots were probed with the vimentin antibody, no significant changes were found between any groups (**Figure 5.12 A, C**). Indeed, the vimentin immunolabelling was extremely

variable between groups and inconsistencies in the findings prevent any firm conclusions being drawn from this result.

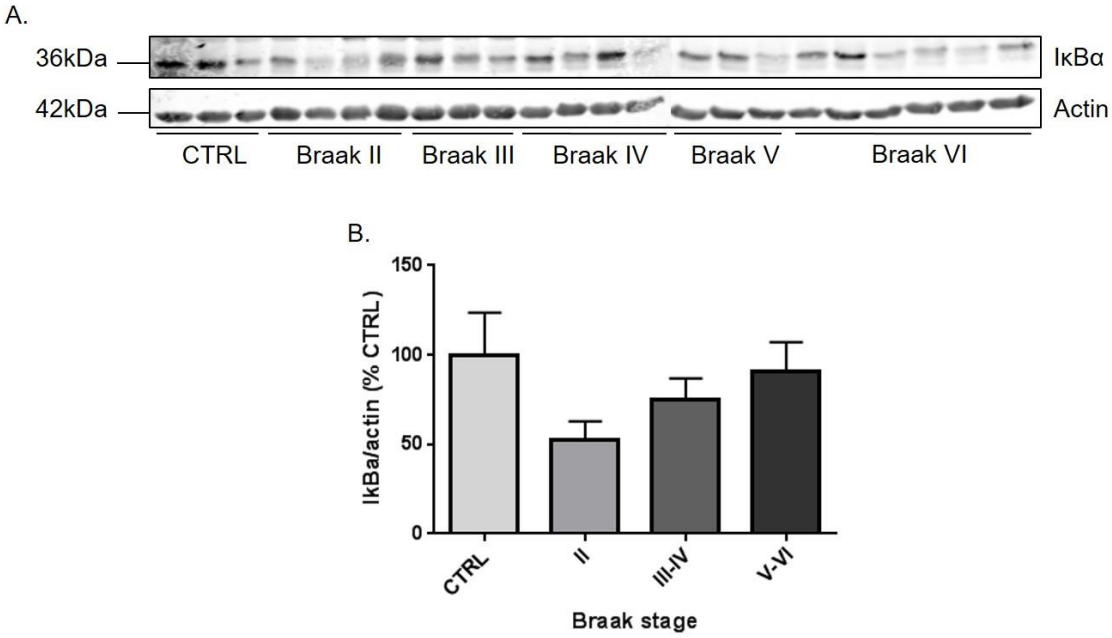

Figure 5.13: Hippocampal IκBα levels do not change with increasing Braak stage
A. Representative blots of hippocampal homogenates from post-mortem control and Braak stage I-VI brain. Blots were probed with antibodies against IκBα and ß-actin as a loading control. Molecular weight markers are shown on the left. **B.** Bar chart shows quantification of IκBα as a proportion of ß-actin. Values shown are mean ± SEM as percentage control (CTRL). N= 3-6 per Braak stage. Data was analysed using one-way ANOVA.

IκBα levels suggest hippocampal NF-κB activation does not change as AD progresses

To investigate possible changes in NF-κB activation, as an indicator of neuroinflammatory responses, in the hippocampus as AD progresses, western blots of control and Braak stage II-VI AD hippocampal homogenates were probed with the antibody against IκBα. Quantification of western blots showed that there were no statistically significant changes in IκBα levels between groups, suggesting that there may be no global changes in NF-κB activity in hippocampus during AD development (**Figure 5.13**). This is consistent with the results from IκBα temporal cortex post-mortem western blots described earlier in this chapter (**section 5.3.2**). However, interpretation of these results is subject to the same caveats. IκBα amounts did appear to be

markedly reduced in Braak stage II-IV tissues, and while these reductions were not significant relative to controls, this might suggest upregulation of NF-κB occurs at the beginning of AD pathogenesis.

Synaptic markers are relatively stable in the hippocampus with increasing Braak stage

To determine if the possible synaptic compensatory mechanisms identified in temporal cortex (**section 5.3.2**) are also evident in hippocampus, hippocampal homogenates were immunoblotted using antibodies against the post-synaptic marker, PSD-95, and the pre-synaptic markers, synapsin and synaptophysin (**Figure 5.14 A**). Unlike results with temporal cortex homogenates, quantification of protein amounts following western blotting of hippocampal homogenates showed that there are no significant changes in either pre- or post- synaptic markers with increasing Braak stage (**Figure 5.14 B-D**). These results were unexpected since synaptic loss is one of the earliest changes to occur in AD (Crimins et al., 2013). However, there is a large and variable literature in this area, reviewed in detail by Honer (2003) and Sze et al., 2000. A number of factors may influence the results of this type of study including sample size, the white/grey matter composition of tissues, pH, post-mortem delay and methods used for tissue processing.

To summarise, total and phosphorylated tau were found to accumulate in hippocampus with advancing Braak stage. There were significant increases in astrocyte activation between Braak stages III-IV and V-VI, and marked, but non-significant, reductions in IκBα in the earliest Braak stages. Surprisingly, there were no alterations in synaptic markers as AD progressed.

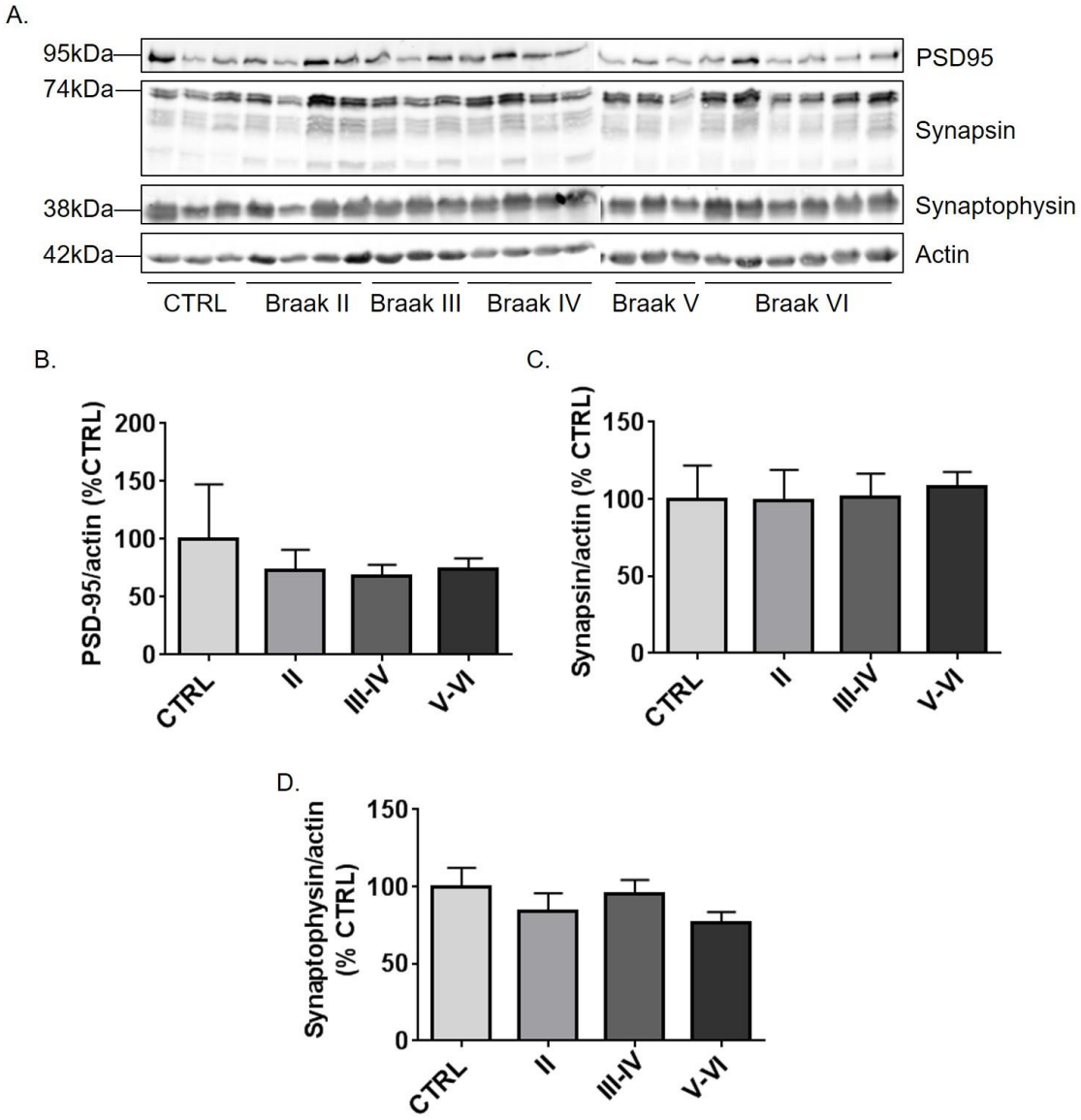

Figure 5.14: Hippocampal synaptic markers do not change with increasing Braak stage
A. Representative blots of hippocampal homogenates from post-mortem control and Braak stage I-VI brain. Blots were probed with antibodies against PSD-95, synapsin, synaptophysin and ß-actin as a loading control. Molecular weight markers are shown on the left. Bar charts show quantification of **B.** PSD-95, **C.** synapsin, and **D.** synaptophysin as a proportion of ß-actin. Values shown are mean ± SEM as percentage control (CTRL). N= 3-6 per Braak stage. Data was analysed using one-way ANOVA.

5.3.4 Summary

The results in this chapter describe changes in glial proteins and tau in post-mortem control and AD brain. The results reveal some differences in the stage at which changes were observed in different brain regions. To allow better visualisation of these alterations in glial proteins and tau in temporal cortex relative to hippocampus, the following table uses shade to represent different fold changes from control samples for different Braak stages.

	Braak I-II		Braak III-IV		Braak V-VI	
	Cortical	Hippo	Cortical	Hippo	Cortical	Hippo
Total tau	*		**		**	*
PHF1					**	
CP13					**	
GFAP						*
Vimentin						
IκBα						
PSD-95						
Synapsin			*			
Synaptophysin					*	

Table 5.4: Summary of protein changes in temporal cortex and hippocampal homogenates with increasing Braak stage
Compared to control sample levels: white = 0-50 %, light grey = 50-100 %, mid-grey = 100-300 %, mid-dark grey = 300-600 %, dark grey = 600+ %. * = $p<0.05$, ** = $p<0.01$, all compared to control, except hippocampal GFAP Braak stages V/VI which is compared to Braak stages III/IV. Hippo = hippocampal.

This set of experiments demonstrates there are some temporal and regional differences in protein changes with increasing Braak stage. In particular, phosphorylated tau was increased in earlier Braak stages in the hippocampus relative to the temporal cortex. There was a period between Braak stages III-IV and V-VI in which hippocampal astrocyte activation occurred which was not apparent in temporal cortex, and IκBα levels showed non-significant reductions in early Braak stages in the hippocampus but not temporal cortex. Finally, unlike results obtained using temporal cortex, hippocampal homogenates did not show results indicative of synaptic compensation in mid-Braak stages or loss of synaptic proteins in late stage AD. In conclusion,

while there are clearly broad similarities between protein changes as Braak stages advance in the hippocampus and temporal cortex, it is also clear that there are likely region-specific influences that underlie AD development in different brain regions.

5.4 Discussion

The main aim of this chapter was to investigate the changes in tau phosphorylation, glial, inflammatory and synaptic markers in post-mortem human AD brain relative to controls. In addition, regional differences in these proteins were investigated since results from cell culture experiments suggested different influences of astrocytes following stimulation with Aß in cultures prepared from different brain regions.

Results from this chapter showing increases in total and phosphorylated tau with advancing Braak stage are consistent with the methods used to stage neuropathological tissues according to the amounts and spread of phosphorylated and aggregated tau throughout the brain (Braak and Braak, 1995). The results presented here show significant decreases in inhibitory phosphorylation of GSK-3 during early stages of disease in temporal cortex, suggesting that increases in GSK-3 activity precede increases in tau phosphorylation in later Braak stages. This is consistent with many publications showing that GSK-3 is a prominent tau kinase in AD (reviewed by Hanger et al., 2009).

The results obtained from assessment of glial markers and inflammatory proteins were less consistent. Although analysis of a large set of control and Braak stage V-VI AD temporal cortex showed increased GFAP activation in AD, this was not verified when a smaller group of samples, including those from earlier Braak stages were assessed. There appeared to be reductions in IκBα in early Braak stage hippocampus but not temporal cortex, which might be indicative of the induction of neuroinflammatory pathways in the hippocampus during AD pathogenesis. Finally, some significant increases in synaptic protein amounts, followed by loss of synaptic markers were found in temporal cortex, but not hippocampus. The statistical analysis of these later

results was likely underpowered, with considerable (normal) variation within groups, reducing the likelihood of obtaining significant results. Unfortunately, tissues from early Braak stage cases were difficult to obtain, otherwise this sample set would have been extended. In addition, the "control" cases used in these experiments may have influenced the results. The controls were selected on the basis that they showed no disease-related alterations in tau or Aß. They were age-matched as closely as possible with AD cases in the same samples sets, and showed no significant difference in average post-mortem delay. However, these cases are somehow protected from AD, and it may be that the endogenous mechanisms that confer this protection affect the proteins that were studied here, thereby skewing the results obtained.

5.4.1 Total and phosphorylated tau increase in the temporal cortex and hippocampus as AD progresses

AD is molecularly characterised by the presence of extracellular Aß plaques and intracellular NFTs. A definite diagnosis of AD can only be confirmed post-mortem by the presence of these lesions. In particular, NFT density and spread throughout the brain post-mortem correlates well with symptom severity before death (Braak and Braak, 1991; Braak et al., 2011). As a result, post-mortem diagnostic and disease staging criteria is commonly based on the development, spread and density of tau aggregates (Braak and Braak, 1995). Abnormal processing of tau, including increased phosphorylation, is believed to precede the formation of tau aggregates (Bancher et al., 1989; Ding et al., 2006), therefore it would be expected that phosphorylated tau also increases as AD progresses. The results presented here are consistent with this literature, showing increases in total, phosphorylated and aggregated tau with advancing Braak stage. Similar findings have been reported in these tissues by multiple groups (Santpere et al., 2006; Hanger et al., 2007; Mondragon-Rodriguez et al., 2008b; Hanger and Wray, 2010; Braak et al., 2011; Lau et al., 2016). It is worth noting, however, that a recent study showed that tau in tauopathy brain is largely dephosphorylated (Kimura et al., 2016) and this may explain the relative scarcity of phosphorylated tau in early Braak stage tissues.

Furthermore, results from this chapter suggest that increased activity of GSK-3, a prominent tau kinase (Fang et al., 2000), could mediate increases in tau phosphorylation, at least through its influence in early Braak stages. GSK-3 has long been implicated in abnormal tau phosphorylation in AD and is known to phosphorylate tau at multiple epitopes (Hanger et al., 2009). Several of these sites, including Thr231, Ser235 and Ser262, control microtubule binding of tau. Pre-phosphorylation of these sites by one of several kinases, followed by phosphorylation by GSK-3 has been demonstrated to result in the inhibition of tau binding to microtubules, an event also believed to occur early in disease development (Sengupta et al., 1998). Therefore, phosphorylation of tau at early Braak stages by GSK-3 may result in an increased pool of soluble cytosolic tau that aggregates in a concentration-dependent manner into oligomers and is subsequently deposited in NFTs as AD progresses.

No alterations in tau conformation were observed in temporal cortex as AD develops, in contrast with previous findings (Weaver et al., 2000; Garcia-Sierra et al., 2003). The reason for this discrepancy is not clear, but might reflect differences in the preparation of homogenates used in different studies. Tau in abnormal conformations is particularly prone to aggregation (Noble et al., 2005), and it might be that assessing MC1 amounts in sarkosyl-insoluble fractions would have shown different findings. Unfortunately, there were insufficient amounts of the sarkosyl insoluble fraction obtained from the tissues used for these analyses to allow this work to be carried out.

5.4.2 Glial markers are not consistently upregulated with advancing Braak stage in different brain regions

A widespread activation of glial cells and associated neuroinflammatory response is increasingly regarded as another key hallmark of AD brain. It is thought that Aß can activate glial cells initiating the release of cytokines and chemokines and triggering multiple pro-inflammatory signalling pathways (Rubio-Perez and Morillas-Ruiz, 2012; Shi et al., 2016; Zheng et al., 2016). These complex inflammatory events can influence neuronal signalling pathways to increase tau

phosphorylation and aggregation in nearby neurons, thereby driving the progression of AD (Sofroniew and Vinters, 2010; Phillips et al., 2014; Selkoe and Hardy, 2016). The results presented here showed that increased GFAP activation in late stage AD relative to controls, that was not verified when a smaller group of samples, including those from earlier Braak stages, were later assessed. However, there were significant increases in astrocyte activation in the hippocampus, but not temporal cortex, between Braak stages III-IV and V-VI. The difference in results from these brain regions may reflect differences in the contributions of astrocytes to the progression of AD in different environments at different stages of disease. Previous studies from the literature suggest that astrocytes behave differently in different brain regions, possibly distinguishing different astrocyte subtypes. Astrocytes from different brain regions show different glycoprotein markers in culture, suggesting that, like neurons, regional astrocytes may represent distinct cell types (Barbin et al., 1988). Further evidence suggesting a regional influence of astrocyte contributions to disease have come from analysis of transgenic mouse models of AD. GFAP levels were shown to increase in the hypertrophied hippocampus of aging mice, but this same increase in astrocyte reactivity was not found in the entorhinal cortex of 3xTg-AD mice (Rodriguez et al., 2014). This suggests different regional astrocytes may respond to aging differently, possibly contributing to the increased susceptibility of some brain regions to Aß and neurotoxicity. Additional support for this theory comes from a study that showed atrophy and no astrogliosis of entorhinal cortex astrocytes suggesting neurons may be particularly vulnerable in the absence of astrocyte activation (Yeh et al., 2011). This is consistent with the findings of this thesis, that suggest astrocytes are activated in the hippocampus, but not the temporal cortex, of AD brain. Furthermore, astrocytes in different brain regions respond differently to Aß, with the calcium response in different brain regions being more susceptible to Aß toxicity (Grolla et al., 2013). These results may further explain the susceptibility of specific brain regions to Aß, with astrocytes from the entorhinal cortex showing an increased sensitivity and calcium response to Aß, compared to the hippocampus (Grolla et al., 2013). Additionally, they may also explain differences seen in synaptic marker levels between the hippocampus and

temporal cortex in this thesis, as different calcium responses from regional astrocytes may affect regional neurotoxicity, synaptic health and compensation. Astrocyte activation has been implicated in AD progression via multiple pathways, controlled by the release of different cytokines and chemokines (Zheng et al., 2016). Different responses of astrocytes in different areas of the brain may result in the activation of different signalling pathways via the release of different cytokines and chemokines. These studies support the results described here which suggest differences in the timing of astrocyte activation in hippocampal, but not temporal, AD brain samples.

ApoE is generally thought to be associated with an anti-inflammatory phenotype of astrocytes since ApoE treatment of cell cultures reduces macrophage activation and ApoE knockout mice have increased neuroinflammatory responses (Grainger et al., 2004; Baitsch et al., 2011). However, the ε4 variant may trigger pro-inflammatory responses, possibly exacerbating AD progression (Jofre-Monseny et al., 2007; Belinson and Michaelson, 2009). The number of samples used to investigate ApoE correlation with astrocyte activation in this study is too small to draw any definitive conclusions. However, they may suggest that the pro-inflammatory effects of ApoE ε4 are not particularly associated with astrocyte activation and induction of astrocytic inflammatory responses. There is evidence to suggest ApoE may help mediate neuroinflammation via microglia, the primary immune cells of the brain. ApoE has been found to be involved in the mediation of the innate immune system, via TLR4 receptor signalling pathways (Tai et al., 2015). Furthermore, Aß can increase production of ApoE, which in turn has been found in exacerbate the inflammatory response (Guo et al., 2004). Also, TREM2 production is lower in microglia with the ε4 allele suggesting that this allele may have similar effects to TREM2 variations that increase AD risk (Li et al., 2015).

Iba1 was visualised in temporal cortex homogenates from control and Braak stage V-VI. No significant differences were observed in Iba1 amounts in these tissues, and for reasons that were never determined, this antibody failed to detect any proteins in the Braak-staged samples sets. It is therefore not possible to comment on changes in microglial proteins in these samples. In

any case, it is likely that assessment of microglial morphology might have provided more informative results concerning microglial activation state, since microglial phenotypes are complex to distinguish, as described by Perry and Teeling (2013), Perry and Holmes (2014) and Perry (2016).

Finally, there appeared to be reductions in IκBα in early Braak stage hippocampus but not temporal cortex, which might be indicative of the induction of neuroinflammatory pathways in the hippocampus during AD pathogenesis. Cytokine array analysis of other post-mortem brain tissues by colleagues in the lab supports this idea. Indeed, there is a vast literature showing increased amounts of different pro-inflammatory cytokines in AD brain (Di Bona et al., 2008; Ojala et al., 2009; Zheng et al., 2016). Time constraints prevented similar analyses from being conducted for this thesis.

5.4.3 Synaptic compensation may occur in the temporal cortex in mid-Braak stages

Results from these experiments suggest that, in temporal cortex, there is an increase in synapsin, a pre-synaptic marker, during mid-stages of AD. According to general theories of the progression of AD, this is unexpected as synapses are meant to become dysfunctional and then be lost as AD progresses (Selkoe and Hardy, 2016). However, these data support those from other studies which suggest that there is an upregulation of some synaptic proteins in the mid-stage of disease which may be an innate neuroprotective mechanism in attempt to improve synaptic function and rescue the dysfunction that progressively develops in AD (Neuman et al., 2015). However, there is some evidence to suggest that synaptic compensation may actually be detrimental rather than protective. One study found that, in aging rats, synaptic compensation occurred only at large synapses, leaving smaller synapses to degenerate (Bloss et al., 2013). Furthermore, the head volume of thin dendritic spines, from smaller synapses, has been found to correlate best with cognitive status in rhesus monkeys, suggesting it is smaller synapses that may be most important for memory loss (Dumitriu et al., 2010).

These studies might therefore suggest that the increases in synapsin-1 that are found in mid Braak stages could represent an additional neurodegenerative step rather than synaptic rescue.

On the other hand, local synthesis of synaptic proteins is linked with learning and memory, and protection from synaptic loss (Tiwari et al., 2015), so further investigations are necessary to untangle the significance of this finding.

Reductions in synaptic markers, particularly synaptophysin, in Braak stage V-VI temporal cortex samples indicate there is a level of synaptic loss at these stages of disease. This is consistent with the literature, demonstrating synaptic dysfunction and subsequently synaptic loss throughout the brain in AD (LaFerla and Oddo, 2005), although the results of different studies vary widely (Sze et al., 2000; Honer, 2003). Synaptic dysfunction is particularly associated with abnormal tau processing. For example, activation of NMDA receptors, via increased glutamate or cytokine activation, may lead to excitotoxicity and activation of signalling pathways that result in increased kinase activity and tau phosphorylation (Curran and O'Connor, 2001; Amadoro et al., 2006). Conversely, there is also evidence tau and Aß may converge to exacerbate synaptic dysfunction (Crimins et al., 2013), resulting in a feed-forward loop that continually affects synapse health. The reductions in synaptophysin concurrent with increased phosphorylated tau observed in Braak stage V-VI temporal cortex homogenates is consistent with these reports. Finally, the regional differences in synaptic protein alterations might suggest that temporal cortex synapses show greater sensitivity to toxic Aß and tau species resulting in a greater extent of synaptic loss than is observed in the hippocampus. Alternatively, increased activation of astrocytes in hippocampal brain regions may be providing protection at the synapse, maintaining synaptic function for longer during disease progression.

5.4.4 Conclusions

In summary, the data shown here might support the idea that there are spatiotemporal differences in the pathways underlying AD progression. Being able to tease out these differences may result in new drug targets and signalling pathways being identified. Furthermore, these temporal and regional differences need to be taken into account when both developing drugs and running clinical trials. As AD pathology spreads through different brain regions in a well-

characterised way, it is possible that effective disease-modifying drugs could show no benefit if administered to an individual at the wrong stage of disease. Further characterisation of these regional differences will allow better stratification of patients in clinical trials. New PET ligands against specific astrocyte and microglial markers have been developed which should also aid in these investigations (Politis and Piccini, 2012; Politis et al., 2012).

Chapter 6: Discussion

The main aims of this thesis were to investigate the relationship between astrocytes and tau in models of AD. In addition, this thesis aimed to explore differences in the effects of astrocytes in different brain regions and explore how these differences may affect drug discovery and repurposing for AD treatment.

The studies described in this thesis used primary cortical cultures to investigate the contributions of astrocytes to Aß-induced cell death and abnormal tau processing by creating two distinct populations of cell cultures: mixed neuron and astrocyte cultures and predominantly neuronal cultures. To achieve this, the two cell culture types were treated with synthetic Aß. In addition, cultures were treated with the anti-inflammatory agent minocycline to allow investigation of the role of astrocytic inflammatory signalling pathways for Aß-induced changes. These experiments were repeated in primary hippocampal cultures in order to investigate possible differences in astrocytic contributions in different brain regions.

Primary cell culture experiments showed that there were differences in the effects of Aß in cortical and hippocampal cultures. Hippocampal astrocytes appeared to accelerate Aß-induced hippocampal neuron death, since Aß induced significant levels of toxicity in mixed, but not predominantly neuronal cultures. In contrast, non-significant increases in cell death of similar magnitude were observed following Aß treatment in both cortical mixed and neuronal cultures. This data might suggest different mechanisms of Aß-induced toxicity in different brain regions. In turn this might imply that different drugs may be more or less effective at different stages of disease, depending on the brain regions most affected at that time.

Minocycline has previously been shown by this laboratory to reduce the release of pro-inflammatory cytokines released from astrocytes upon stimulation with Aß (Garwood et al., 2011), in keeping with its anti-inflammatory effects in various models of neurodegeneration (Hunter et al., 2004; Ryu et al., 2004; Festoff et al., 2006; Peng et al., 2006; Garwood et al., 2010). However, in the experiments described here, no neuroprotective effects of minocycline were identified in either mixed or predominantly neuronal hippocampal or cortical cultures. While

the reasons for this lack of effect in these experiments were not clear, it is clear from the literature that the beneficial anti-inflammatory effects of minocycline are not always clearly defined and appear to be highly context dependent (Diguet et al., 2004).

There were also no clearly defined effects of Aß or astrocytes on tau phosphorylation or cleavage in treated cultures in these experiments. Again, this is somewhat surprising considering previous publications from this laboratory (Williamson et al., 2002; Garwood et al., 2011) and others (Town et al., 2002; Jin and Selkoe, 2015). As discussed in Chapter 3, it is possible that the lack of Aß-induced tau effects may have arisen from batch-to-batch Aß variations, insufficient levels of toxic Aß-species and/or issues with culture health.

Nevertheless, the potential benefits of anti-inflammatory agents in other models was worthy of further exploration, especially considering the close association of glial activation and inflammatory mediators with tau pathology development *in vivo* (Bellucci et al., 2004; Schindowski et al., 2006; Garwood et al., 2010; Schwab et al., 2010). Therefore, the effects of DMF, an already licenced drug with anti-inflammatory action, were tested first in primary cortical cultures and then in a mouse model of tauopathy with the aim of determining if this drug has potential for repurposing for AD. In primary cortical cultures, DMF was found to dose-dependently reduce tau phosphorylation at several epitopes known to be abnormally phosphorylated in AD, supporting its further investigation in tau transgenic mice. Preliminary trials examining DMF effects on mice at early- and mid- stages of tauopathy were less promising, as effects of DMF on possible cognitive impairment was unable to be determined and DMF treatment lead to increases in the accumulation of sarkosyl-insoluble tau aggregates. These differences between primary culture and transgenic mouse model may have been due to the accumulation of tau aggregates in htau mice, which are not present in primary cultures, since DMF is known to affect the activity of Nrf2, which in turn is implicated in tau-specific autophagy via the autophagy adapter protein NDP52 (Jo et al., 2014). Regardless of mechanism, these results suggest DMF does not show significant changes in htau mice.

Finally, since it is critical that any results from mammalian cell and animal models of AD have relevance to human disease, human post-mortem brain samples from control and Braak stages I-VI temporal cortex and hippocampus were homogenised to allow investigations of regional differences in glial markers and pathological changes in tau during AD progression. These data suggested there were increased activation states of glia in late-stage AD, coinciding with large increases in tau phosphorylation. However, the mechanistic links between these two observations remains elusive.

To summarise, the primary findings of this thesis were:

- **Astrocytes contribute to Aß-induced cell death to different extents in primary cell cultures from different brain regions.** Experiments presented in this thesis show astrocytes affect Aß-induced neurotoxicity in hippocampal, but not cortical, cell cultures. This suggests the underlying mechanisms driving Aß-induced cell changes are different in primary cell cultures from different brain regions. Furthermore, in primary cortical cultures, astrocytes appear to be involved in mediating extracellular tau levels in basal conditions.
- **DMF does not improve tauopathy-like symptoms in htau mice.** Results from primary cell culture experiments with DMF showed dose-dependent reductions in tau phosphorylation in primary cortical cultures. However, small preliminary preclinical trials of DMF treatment of a mouse model of tauopathy failed to show any benefits suggesting repurposing DMF as a tauopathy durg treatment is unlikely to slow disease progression or symptoms.
- **Differences in astrocyte activation and abnormal tau processing are observed in different regions of post-mortem AD brain.** Experiments investigating changes in tau, glial and synaptic markers as AD progressed from early Braak stages to severe AD (Braak stages V-VI) showed that abnormal tau phosphorylation occurred at an earlier Braak stage in hippocampal samples than was found in cortical samples. Additionally,

astrocyte activation was increased in hippocampal but not cortical samples suggesting astrocytes from different brain regions may contribute differently to AD progression. Further support for the idea that different mechanisms underlie pathological changes in different brain regions was shown in regional differences in synaptic marker changes: in cortical samples, synaptic marker levels suggest possible synaptic compensation during Braak stages III-IV while hippocampal samples show no indication of neuroprotective events as disease progresses. These findings are in partial agreement with primary cell culture findings.

Taken together, these results suggest there are likely to be regional differences in astrocyte activation and pathological tau processing in AD. In particular, the contribution of astrocytes appears to differ significantly between the cortex and hippocampus. These differences should not be overlooked as they may have significant implications for highlighting and developing potential drug treatments for the treatment of AD.

6.1 Regional differences in the development and progression of AD

One of the main ideas underlying this project was that there are likely specific neurodegenerative mechanisms in different brain regions that will come into play at different stages of disease progression. There is considerable published data to support this hypothesis. Even in healthy brain, astrocytes from different brain regions show significant differences in their expression of surface glycoproteins (Barbin et al., 1988). Differences in astrocyte structure and function, not only between brain regions of interest (e.g. hippocampus and nearby cortex), but also within the same brain region, demonstrate a heterogeneity similar to that found in neurons. Recently Liu et al. (2015a) have shown two different subpopulations of cortical astrocytes, which can be distinguished by their growth patterns, exert markedly different effects upon neurite outgrowth. One of these subpopulations, characterised by an atypical growth pattern, including random orientation and homogenous cell clusters, inhibited neurite growth

and provoked a dystrophic appearance of neurites, but did not affect neuron survival (Liu et al., 2015a). This has resulted in suggestions that astrocytes from the same and different brain regions may be distinct subspecies of cell type, in the same way as motor neurons and sensory neurons differ (Verkhratsky et al., 2012; Stobart and Anderson, 2013; Hu et al., 2016). This is not surprising as converging lines of evidence show astrocytes have a wide range of functions, supporting neuron health and maintaining synapse function in environments with different positive and negative synaptic inputs (Sofroniew and Vinters, 2010; Garwood et al., 2016; Hu et al., 2016; Rodriguez-Arellano et al., 2016). Furthermore, regional differences in the function and structure of neurons suggests different astrocytic support would be required in order to maintain neuronal function and health.

In disease models, aged hippocampal neurons have higher resting calcium levels and are more susceptible to excitotoxicity than younger hippocampal neuron cultures (Calvo et al., 2015). Hippocampal sensitivity in AD is demonstrated by the early death of hippocampal neurons and subsequent short-term memory impairment (Braak and Braak, 1995). Hippocampal atrophy is evident early following AD diagnosis and now, with improved imaging resolution (e.g. for MRI imaging), it is possible to track disease progression based on the speed of hippocampal atrophy (de Flores et al., 2015). Furthermore, hippocampal sensitivity to insult has been found to not just be limited to Aß and AD-related pathology. For example, evidence shows the hippocampus is more sensitive to structural and functional damage from traumatic brain injury than other brain areas (Lifshitz et al., 2003; Deng and Xu, 2011).

However, the precise mechanisms by which hippocampal neurons show increased susceptibility to disease-related insults are not clear. Evidence from traumatic brain injury research, where the injury sustained can be better controlled and monitored, suggests hippocampal neuron susceptibility may be due to increased mitochondrial damage and impaired response to injury, compared to cortical neurons (Lifshitz et al., 2003). Furthermore, hippocampal neurons have been found to be more sensitive to post-injury excitotoxicity (Deng and Xu, 2011). Pro-inflammatory cytokines have been shown to increase in response to hippocampal injury, and

inhibition of these cytokines has been demonstrated to attenuate damage as a result of global cerebral ischaemia suggesting glial activation may influence hippocampal neuron susceptibility to injury (Xing and Lu, 2016).

Evidence from studies described in this thesis also suggests glial activation, and possibly inflammation, may contribute to differences found between hippocampal and cortical neuron responses to Aß. Experiments from Chapter 3 show the increased sensitivity of primary hippocampal cultures finding increased levels of cell death in response to Aß compared to cortical cultures. However, higher levels of cell death are only significant in mixed neuron and astrocyte cultures, suggesting astrocytes may be exacerbating Aß-induced neurotoxicity in hippocampal cultures. In comparison, the presence of astrocytes in primary cortical cultures has no effect on levels of cell death or tau phosphorylation with Aß or minocycline treatment in these studies.

Differences in the roles of astrocytes during AD progression have been described previously in the literature. Differences in hippocampal and cortical astrocyte markers including GFAP, glutamine synthase and s100ß in WT mice of different ages suggest astrocytes from different regions of the brain undergo specific remodelling as mice age (Rodriguez et al., 2014). Furthermore, astrocytes from the entorhinal cortex and hippocampus of control and transgenic mice have previously been found to respond differently to Aß, with increased activation and calcium sensitivity in hippocampal astrocytes while entorhinal astrocytes showed no Aß-induced changes (Grolla et al., 2013). This may be consistent with the results of cell culture experiments described here, with astrocytes appearing to contribute more to the primary hippocampal culture response than the cortical culture response. Thus, regional differences in the environment required for both physiological astrocyte and neuron function may result in these cells having different responses in neurodegenerative diseases such as AD, with different pathological mechanisms being implicated as the disease spreads across affected brain. This has implications for understanding disease progression as well as developing new, disease-modifying drug targets.

6.1.1 Implications of regional differences in neurodegenerative mechanisms for preclinical and clinical trials

Regional differences in the way astrocytic and other mechanisms drive abnormal tau processing and neurodegenerative pathways are of the utmost importance for understanding disease progression and when developing efficient drug treatment protocols with the capacity of slowing or halting disease development. As AD progresses, tau pathology spreads from the entorhinal cortex and hippocampus in the earliest, prodromal stages (Braak stages I-II) throughout the cortex in the latest stages (Braak stages V-VI). This pattern of spread is well-characterised and is used to diagnose and stage AD post-mortem (Braak and Braak, 1995). This means that at different stages of disease, when tau and Aß pathology is developing in specific brain areas, region-specific neurodegenerative mechanisms could be involved. This clearly has important implications for the design of preclinical and clinical trials. For example, screening of possible disease-modifying drugs in mouse models of AD that only recapitulate one stage of disease may result in a drug that may provide benefits at a different stage of disease being overlooked, or even worse the drug deemed ineffective when it may have been beneficial if tested at a different stage of disease progression. As a result, it seems important to examine the effects of treatment at different stages or severities of disease.

6.1.2 Importance of biomarkers for drug development

As described above, a good knowledge of disease stage may be critical for preclinical and clinical testing. Early diagnosis of AD is a challenge as clinical symptoms only manifest themselves after widespread neuron loss across the brain (Braak and Braak, 1995). However, treatments may be most effective at earlier stages of disease, before substantial neuron death has occurred (Mattsson et al., 2015). Therefore, determination of early and mid-AD stages using a blood test or other non-invasive biomarker is critical to the development of potential disease-modifying drug treatments of AD.

Detection of abnormally high levels of Aß, in the CSF or the blood, has been investigated as a potential biomarker for AD. The presence of Aß monomers and oligomers particularly in the CSF

can predict the severity and progression of prodromal AD, however CSF testing is invasive and expensive making it difficult to use on a large scale (Zhou et al., 2016). Levels of Aß in the blood, however, are much lower and difficult to detect, with many other proteins of higher concentration interfering with detection. Additionally, levels of Aß in the blood do not appear to be specific to AD patients or to reflect the severity of disease, suggesting blood tests for Aß may not be an ideal biomarker for AD (Pesaresi et al., 2006; Zhou et al., 2016).

Detection of tau in the CSF and blood has also been considered in the search of an AD biomarker. However, measurements of tau in CSF have the same disadvantages as amyloid tests, while tau blood levels are increased in patients with other tauopathies as well as those suffering from AD (Mattsson et al., 2015; Shanthi et al., 2015). So, while tau levels in blood may reveal the presence of a tauopathy, they cannot be used to diagnose or stage AD.

More recent attempts at developing a biomarker for AD have involved advanced imaging with positron emission tomography (PET), whereby Aß or tau are labelled with a specific tracer and measured using a PET scanner (Villemagne, 2016). These techniques, while expensive, are non-invasive and have increasingly good resolution, allowing diagnosis of AD in individuals prior to the start of clinical symptoms (Schierle et al., 2016). It is hoped that these advanced diagnostic tools may allow more careful staging of patients (and indeed animals) for preclinical and clinical trials. Of considerable interest to this thesis, a number of inflammation-related PET ligands have recently been described. These include markers of activated astrocytes and microglia. For example, carbon-11-labelled (R)-PK11195 is a PET ligand for peripheral benzodiazepine sites, a group of receptors with increased expression on activated microglia, compared to resting microglia (Cagnin et al., 2001). Astrocyte levels and activation have also been measured using PET ligand (11)C-deuterium-L-deprenyl to measure monoamine oxidase B in astrocytes, and found the marker suggested increases in astrocyte activation in patients with MCI (Carter et al., 2012). These new PET markers will obviously be of particular use for trials in which inflammatory pathways are being targeted. In addition, serial imaging with the astrocyte PET ligand and a tau

ligand will allow much more precise information about the spatiotemporal association of activated astrocytes and pathological tau changes to be identified.

6.2 DMF and the repurposing of drugs for AD treatment

To explore the relationship between inflammation and the development of tau pathology in vivo, the effectiveness of DMF to reduce abnormal tau species was investigated in the htau mouse model of tauopathy. Repurposing of already licenced drugs such as DMF is considered a valuable approach to identifying disease-modifying treatments for AD since their progression to the clinic can be made more rapidly (Corbett et al., 2012).

Results from experiments investigating the effects of DMF treatment on a mouse model of tauopathy found no significant biochemical differences between groups of treated and untreated mice. Furthermore, behavioural impairment of htau mice, compared to WT mice, was not found to be significant preventing conclusions about DMF-related memory improvements and making it difficult to demonstrate that this drug is suitable for repurposing as a treatment for AD. No effects on astrocyte activation were apparent and biochemical analysis of the brains of younger mice showed a trend toward increases in sarkosyl-insoluble tau levels with DMF treatment, indicating the drug may be influencing the propensity of tau to aggregate. This was unexpected as DMF has known anti-inflammatory action and was expected to reduce astrocytic activity in the htau mice, a model of tauopathy. However, it is likely DMF could affect other inflammatory pathways that do not involve astrocytes, or that are very specific. Astrocytes and microglia can activate many different signalling cascades with capacity to affect neighbouring cells, including through the release of cytokines and chemokines into the extracellular space (Zheng et al., 2016). DMF treatment could affect the release and activity of multiple cytokines and their downstream signalling cascades. Many cytokines, for example IL-6 and TNF-α, have been associated with AD-like changes in tau phosphorylation (Quintanilla et al., 2004; Gabbita

et al., 2015) and there is evidence suggesting DMF may reduce the synthesis of some of these specific cytokines (Wilms et al., 2010).

Evidence extensively supports the role of IL-1ß, in particular, in abnormal tau phosphorylation. Overexpression of IL-1ß in the 3xTg mouse model of AD resulted in rapid exacerbation of pathological tau species, while IL-1ß receptor antagonists have been found to reduce tau pathology and improve cognitive impairment *in vivo* (Ghosh et al., 2013; Ben-Menachem-Zidon et al., 2014). Additionally, IL-1ß inhibition reduces the activity of multiple tau kinases including cdk5 (Kitazawa et al., 2012), a kinase experiments presented in **Chapter 4:** highlight as possibly being involved in DMF-affected pathways. DMF was shown to reduce tau phosphorylation in primary cultures in this thesis (**Chapter 4:**), and one possible explanation of the effects seen in primary cortical cultures is that DMF treatment acts on activated astrocytes, reducing inflammatory activity such as IL-1ß production and release (Wilms et al., 2010). This would reduce the activation of pathological neuronal signalling cascades, including p25 levels and, therefore, cdk5 activity. This could account for the reduced phosphorylation observed at Ser199/202/Thr205 after DMF treatment, since these sites can be phosphorylated by cdk5 (Hanger et al., 2009).

In contrast, no effects on tau phosphorylation were observed following DMF treatment of htau mice, although a trend towards increased tau aggregation, indicated by accumulation of sarkosyl-insoluble tau species, was observed when mice at an early disease stage were treated. The presence of tau aggregates correlate well with symptom progression in AD and are used for Braak staging (Braak and Braak, 1991). However, there is now a significant body of evidence to suggest tau aggregates are not the cause of toxicity, as once assumed, but a neuronal attempt at preventing toxicity (Meraz-Rios et al., 2010; Cowan and Mudher, 2013).

Soluble tau oligomers are increasingly thought to be the toxic tau species. Tau oligomers impair memory and induce tauopathy-like synaptic and mitochondrial dysfunction in wild-type mice (Lasagna-Reeves et al., 2011). Treatment of mouse models of tauopathy with an antibody raised specifically against tau oligomers improved memory impairments and reduced oligomer, but not

NFT, load, strongly suggesting tau oligomers underlie the characteristic memory deficits displayed by these mice (Ward et al., 2012; Castillo-Carranza et al., 2014). Furthermore, large tau aggregates, such as those species insoluble in sarkosyl, have been suggested as neuroprotective, acting to sequester tau oligomers and prevent them from causing further damage (Meraz-Rios et al., 2010). Therefore, the increased sarkosyl-insoluble tau amounts detected here following DMF treatment of younger htau mice could potentially be neuroprotective, by reducing the amount of highly toxic soluble tau oligomers in htau brain.

Despite these preliminary studies with DMF not being conclusive, they demonstrate some methods by which already licenced drugs could be preclinically tested for tauopathies. In particular, testing a drug at multiple ages/disease stages is an important consideration. If carried out in conjunction with biomarkers that can more accurately determine disease stage, it is possible to envisage previously disregarded drugs, or drugs originally approved for other diseases, could be found to slow or prevent AD progression.

Moreover, a better understanding of the contributions of glia and glial signalling pathways could identify new targets for drug development. Previous research into broad-range anti-inflammatories, such as NSAIDs, have concluded there is no significant improvement in clinical symptoms following drug treatment (Miguel-Alvarez et al., 2015). However, significant evidence suggests targeting specific cytokines, such as IL-1ß, may be beneficial (Li et al., 2003; Quintanilla et al., 2004; Ghosh et al., 2013; Salani et al., 2013). These promising preclinical trials which describe improvements in biochemical and behavioural AD-like symptoms suggest controlling cytokine levels may provide a way of modulating disease progression (Rothwell and Luheshi, 2000; McAlpine et al., 2009). Of particular interest is the IL-1 receptor antagonist (IL-1RA), an endogenous inhibitor of the IL-1 receptor, that has been found to have anti-inflammatory effects (Rubio-Perez and Morillas-Ruiz, 2012). A recombinant version of human IL-1RA, anakinra, has been licenced for treatment of rheumatoid arthritis (Hallegua and Weisman, 2002). However, a preclinical trial was unable to detect the drug in the CNS after perispinal injection (Roerink et al.,

2015), and it is still unclear whether inhibition of IL-1 in the brain could cause widespread side-effects.

In addition to highlighting possible drug targets, further knowledge of underlying mechanisms of AD would allow design of trials involving therapies that may target specific mechanisms implicated at only some stages of disease progression. The data described above begins to demonstrate the continued challenges of drug discovery and trials in AD research, highlighting the need for further basic research into underlying mechanisms of AD progression and the need for understanding possible differences in signalling pathways in different brain regions and at different stages of the disease.

6.3 Comparisons between cell culture models and post-mortem AD brain

Models of AD, both on a cellular and whole organism level, do not accurately recapitulate human AD. However, they recapitulate at least some important disease aspects and can be used to determine useful information about underlying mechanisms and for drug discovery. Many mouse models, for example the htau mouse used in this thesis, model only some pathological aspects of AD: the htau mouse, like other tau transgenic lines, models the development of tau, but not Aß, pathology (Lewis et al., 2000; Andorfer et al., 2003; DaRocha-Souto et al., 2012; Bondulich et al., 2016). While htau mice may provide useful information about the development of tau pathology, it is not possible to examine pathological APP processing or Aß accumulation and therefore the synaptotoxic interaction of Aß and tau in these mice. As such they can be considered an incomplete model of AD. In general, only multigenic lines, such as the 3xTg-AD mouse, develop AD-like Aß and tau pathology (Lewis et al., 2001; Oddo et al., 2003; Platt et al., 2011). The 3xTg-AD mouse line shows age-dependent Aß and tau pathology and glial inflammation, along with progressive cognitive deficits, suggesting this model represents AD progression to a good extent (Oddo et al., 2003). However, this model is widely criticised due to

its lack of relevance to human AD since it relies on overexpression of three mutant human transgenes that have never been found to co-occur in patients.

Therefore, it is always important to validate findings from animal models using human tissues. However, most studies using post mortem brain samples focus on end stages of disease in comparison with control brain (Chen et al., 2016; Lau et al., 2016; Nasaruddin et al., 2016). This is partly due to difficulties in acquiring post-mortem brain from early and mid-disease stages.

The studies using human post-mortem brain presented in this thesis aimed to investigate possible changes in tau, glial and synaptic markers as AD progresses using tissue from control and Braak-staged brain. In addition to the expected increase in total and phosphorylated tau, two other patterns of changes were found. The first was an apparent synaptic compensation in cortical samples at Braak stages III-IV, demonstrated by a significant increase in amounts of synapsin, a pre-synaptic marker (Kurbatskaya et al., 2016). This may suggest an attempt by these neurons to counteract disease-related synapse dysfunction occurring at this stage of disease. Interestingly, these changes were not seen in hippocampal post-mortem samples. Taken together with the data described in primary cultures in **Chapter 3:**, this might suggest neurodegenerative cascades are different in different regions of the brain, with hippocampal neurons being particularly susceptible to neurodegeneration.

Secondly, in the set of samples including cases from all Braak stages, increases in markers of activated astrocytes were only seen in the hippocampus in late stage (Braak stages V-VI) AD. Unexpectedly, in the temporal cortex there was no evidence of any glial changes at earlier disease stages. As discussed throughout this thesis, astrocyte activation and neuroinflammation are key components of AD pathology (Phillips et al., 2014; Hu et al., 2016; Rodriguez-Arellano et al., 2016). However, there is also evidence from other groups suggesting glial activation is not present in the entorhinal cortex of aging mice, despite evidence of activation in the hippocampus (Rodriguez et al., 2014). Activation of astrocyte roles in the hippocampus but not the cortex in AD was also supported by primary cell culture experiments from **Chapter 3:** of this thesis.

Similarities between results from disease models and those from experiments using human post-mortem brain samples are important as they suggest experimental models used are replicating some aspects of human disease with some accuracy. These comparisons are reassuring as experiments using primary culture and human post-mortem brain samples show broadly similar results, suggesting different signalling mechanisms may be involved in the hippocampus and cortex, and astrocytes appear to play a more central role in degenerative processes in the hippocampus, compared to the cortex.

6.4 Limitations of this work

For all studies presented in this thesis, everything possible was done to ensure all experiments were carefully planned and controlled. However, there are limitations of this work that need to be discussed.

6.4.1 Limitations of rodent primary cell culture models

Using primary cell cultures has many advantages, including that they allow the manipulation of active and maturing neurons in connected networks over short periods of time. While not as complex or physiologically relevant as mouse models, the relative ease of maintenance, the low cost, and speed at which experiments can be completed make primary cell cultures a popular choice for biochemical experiments (Barbin et al., 1988; Chen and Herrup, 2008; Ferreira et al., 2012; Zhou and Klein, 2012; Calvo et al., 2015). However, there are also some important limitations to consider when interpreting results obtained using rodent primary cultures. First and foremost, cells in culture are not in the same physiological conditions as if they were developing in a living brain. Cells no longer have the same physical contact with each other or the same chemicals in the extracellular environment (Chen and Herrup, 2008). In addition, the percentage of each neural cell type varies dramatically in different cultures. For example, at 14 DIV there was approximately 19 % astrocytes in the mixed cortical cultures used in this thesis,

in comparison there are approximately five times as many astrocytes as neurons in some regions of the adult human brain (Sofroniew and Vinters, 2010).

Additionally, it was assumed that the primary cultures used in experiments in this thesis do not contain microglia as they are made from embryonic rat brains at a developmental stage shown to precede microglial infiltration of the brain (Streit and Xue, 2009; Jebelli et al., 2015). Microglia play a key role in supporting and maintaining neuron health in a living brain and neuron cultures in the absence of these cells will inevitably be less resistant to stress and disease (Nimmerjahn et al., 2005; Jebelli et al., 2015). Additionally, the possible lack of microglia may have revealed additional effects of DMF treatment in line with evidence of its anti-inflammatory action in other studies (Heiligenhaus et al., 2004; Wierinckx et al., 2005; Schilling et al., 2006; Wilms et al., 2010; Brennan et al., 2016). The aim of this thesis was specifically to investigate the role of astrocytes and, to allow this, conditions were used in which microglia were unlikely to be present. However, as the absence of microglia has not been confirmed in the primary cultures used in these experiments, it is possible that some of the results described may be due to low levels of microglia in the cell cultures.

Furthermore, while basic characterisation of the primary cell cultures was carried out, this thesis would have benefited from more in depth investigation into the make up and development of the primary cell cultures used. Phase images of cells would provide further insight into the development and health of cell cultures, and demonstrate clear morphological differences between neurons and astrocytes. Moreover, probing western blots of primary cell lysates with other antibodies, including both neuron- and microglia-specific markers, alongside western blots probed with tau, could further confirm neuron enrichment and the absence of microglia in predominantly neuronal cultures. Increased levels of neuron markers in predominantly neuronal cultures, compared to total protein markers, would indicate a higher percentage of total cultured cells were neurons.

In addition, microglial cells were assumed to be absent based on previous work carried out with similar primary cell cultures in this laboratory (Garwood et al., 2011) and elsewhere (Streit and

Xue, 2009). However, using immunocytochemistry to stain primary cultures for microglial-specific markers (such as OX42) would demonstrate primary cell cultures grown for this project do not contain microglia.

An important point when considering the implication of the data presented here is that the primary cell culture experiments presented in this thesis were carried out during a period of time when our laboratories were moving to a new building. There were many issues with the cell culture facilities we were using such as with fans needed to provide a sterile environment in tissue culture hoods, with the ultrapure water supply and maintenance of CO_2 supply to incubators. Unfortunately, no easily accessible or convenient alternative facilities were available. Despite as much as possible being done to minimise artefacts from these poor tissue culture conditions, there were issues with higher than expected levels of cell death and inevitably poorer cell health. The effects of poor cell health on the development and presence of synapses is of particular concern. While the presence of synapses in 14 DIV neuron cultures is widely reported in the literature (Cullen et al., 2010; Chai et al., 2016; He et al., 2016), it may be that poorer cell health may be impairing synapse growth or increasing synapse degeneration. To demonstrate synapses are present in the primary cell cultures used in this thesis it would be highly beneficial to probe for synaptic markers on western blots run using primary cell lysates. Increased levels of cell death and poor cell health are likely to explain some of the unexpected findings reported in **Chapter 3:**. That said, the results from these primary cell culture experiments appear to correspond, at least in part, to findings from human post-mortem brain. It is also important to consider species differences. For example, human astrocytes are much larger and complex, with human protoplasmic astrocytes estimated to have tenfold more processes than their rodent counterparts (Oberheim et al., 2009). Whilst mouse astrocytes have been shown to promote neuronal survival and synapse formation to a similar extent as human astrocytes, marked changes in glutamate response and transcription profile have been described between murine and human astrocytes (Zhang et al., 2016b). Recent advances in induced pluripotent stem (iPS) cells mean that iPS cells from control and AD individuals could

now be used as an alternative model to primary rat cultures. For example, investigations into the positive effects of hypothermia using iPS cells have found tau phosphorylation is protective during cooling conditions, reducing oxidative stress and neurotoxicity and suggesting tau phosphorylation may be a physiological response under cooling conditions (Rzechorzek et al., 2016). This study, and others like it, may provide molecular explanations for the hyperphosphorylation of tau and other pathological responses underlying AD progression (Rzechorzek et al., 2015). Alongside experiments in primary rat cultures, iPS cells could help eliminate problems surrounding species differences. Another alternative method to using primary rodent cultures is using primary human astrocytes retrieved from post-mortem human brain (De Groot et al., 1997). Astrocytic and microglial Aß uptake has been demonstrated to be dependent on Aß aggregation state and ApoE in primary human astrocytes, showing these primary human cells can be used as an alternative method to investigate pathological mechanisms in AD (Nielsen et al., 2010; Mulder et al., 2014).

Limitations of using soluble Aß as a cell culture treatment

As mentioned briefly in **Chapter 3:**, the use of soluble, synthetic Aß as a cell culture treatment has come under criticism due to limitations surrounding the production and use of the peptide. Poor consistency between and within batches causes variability between experiments despite batch testing (Soto et al., 1995; Stohr et al., 2012). This is likely to be due to impurities in the peptide and the structure of individual peptide molecules affecting the fibrillisation and aggregation propensity and speed (Soto et al., 1995; Finder et al., 2010). In addition, there is no standard protocol for resuspending or aggregating Aß peptide prior to cell treatment making it difficult to compare results from different research groups. Finally, synthetic Aß has been criticised as not being physiological, with much higher concentrations of synthetically produced peptide required to produce the same results as those caused by physiological Aß in a human brain (Walsh et al., 2005). Furthermore, physiologically released Aß, such as that from 7PA2 CHO cells or cultured Tg2576 neurons, have also been found to have more toxic effects at synapses than synthetically produced Aß (Walsh et al., 2002; Reed et al., 2011). Experiments presented in

this thesis show that while 7PA2-derived Aß caused activation of caspase-3, it did not cause overt cell death and appeared not to activate astrocytes in the same manner as synthetic Aß. For these reasons, although clearly not ideal, synthetic Aß was used for a large part of the work presented here.

6.4.2 Limitations of DMF treatment of htau mice

The results from preclinical trials investigating possible effects of DMF on age-related pathological changes in the htau mouse model of tauopathy (**Chapter 4:**) showed very little difference between DMF treated and control groups, with the exception of increases in insoluble tau amounts in young htau mice. The most likely explanation for this is that DMF is not having an effect on the specific parameters investigated here. However, there are some limitations to the protocols used in these experiments. Potential statistical noise resulting from variation in the precise dose of drug orally administered may have obscured subtle drug effects. However, the decision to use this method of administration was based on the welfare of the mice, which is of the utmost importance (Eichenbaum et al., 2011).

In particular, behavioural testing of older (mid-disease stage) htau mice showed high levels of variability within groups, and no statistically significant differences between either htau and wild-type mice or between htau mice dosed with DMF or vehicle in the Morris water maze.

The Morris water maze is one of the most commonly used behavioural tests for experimental rodents and has been widely characterised (Wahlsten et al., 2005; Bromley-Brits et al., 2011; Vorhees and Williams, 2014a). It is cheap, easy to use and requires rodents to undergo only basic training. Furthermore, having undergone extensive testing, the water maze has been demonstrated as a robust test of allocentric spatial learning (spatial learning and memory) based on external, environmental cues (Vorhees and Williams, 2014a)). All these advantages make the Morris water maze the most popular, and usually first, choice for assessing spatial memory deficits in rodents. However, this maze was originally designed for use with rats and there have been some suggestions that the task is less appropriate for mice (Vorhees and Williams, 2014b). In particular, the water maze has been found to be significantly affected by mouse strain

differences, however a previous study with C57BL/6 mice (the background strain used in these studies) suggest that the performance of this strain in the maze is good (Wahlsten et al., 2005). Additionally, performance in the water maze can be affected by high levels of anxiety. Studies suggest some mice find the Morris water maze stressful, demonstrating increased corticosteroid levels that negatively correlate with maze performance (Harrison et al., 2009). Animals with high stress levels often display 'wall hugging' or floating behaviours (Wahlsten et al., 2005). Although not quantitatively measured, wall hugging and a tendency to continual circle the maze was observed in htau mice in this study, possibly suggesting anxiety and potentially obscuring differences in spatial memory abilities between groups.

Finally, the water maze is not a suitable test for animal with motor impairments. Research shows htau locomotor activity is equal to that of control mice (Polydoro et al., 2009). Generally, this was also found in this study of the mice, however, one mouse displayed swimming problems due to problems with back limb control. This mouse showed no signs of pain or distress outside of the maze, however the mouse was removed from water maze experiments and excluded from analysis. It is most likely that motor problems were unrelated to the htau phenotype, possibly caused by spontaneous illness (e.g. ischaemia), as no other mice in the experiment were affected by similar impairments.

Additionally, it is possible that DMF treatment could be affecting htau mouse behaviour in ways undetectable by the Morris water maze. Ideally multiple behavioural tests would have been carried out in this study. In particular, novel object recognition paradigms could have yielded interesting results as this is another area in which htau mice have been found to show impairment (Polydoro et al., 2009). However, in general, rodent behavioural tests are time consuming and often have higher statistical noise due to high variability in general behaviour between animals, making significant results difficult to obtain, particularly in relatively small groups (Hanell and Marklund, 2014).

6.4.3 Limitations of using post-mortem brain samples

Studies using human post-mortem brain samples to investigate changes in AD, like the experiments described in **Chapter 5:**, have the advantage of being one of the only ways to view disease-related changes in a human brain. While mouse, cell culture and computational models of disease are useful to provide insights into signalling pathways and mechanisms underlying disease development and progression, it is important to validate findings in diseased brain. However, there are some general limitations to using post-mortem brain that need to be considered when interpreting the experimental results described in **Chapter 5:**.

First and foremost, it is vital to remember that the human tissues are obtained post-mortem. Therefore, even using Braak-staged tissues does not allow comment on the development of disease events, but rather represents a snap-shot of changes taking place at distinct times in different brains. Similarly, legal and ethical considerations make it difficult to collect a donated brain for some time after death. The time between death and the collection of a brain is referred to as the post-mortem delay and the length of delay has significant effects on the quality of the brain samples. The post-mortem delay for each human brain sample used is recorded in the sample tables of methods section of Chapter 5 (**section 5.2**). These tables demonstrate the variation of this delay, from several hours to several days. While some research from the field suggests brain samples maintain their integrity for several days (Gonzalez-Maeso et al., 2002), there is evidence of biochemical changes and particularly sample degradation occurring from as early as 6 hours in rat brain (De Groot et al., 1995). In addition, there are many other variables that can affect the quality and degradation of post-mortem brain samples (Stan et al., 2006). For example, brain pH has been found to have significant effects on hippocampal gene expression profiles, and has been shown to have greater predictive value than disease in a group of control and schizophrenic post-mortem brain samples (Mexal et al., 2006). Information detailing the collection of post-mortem brain used in these studies did not include variables such as pH or time taken to cool brains, therefore effects caused by such variables may explain some of the variation between samples but no final conclusions can be drawn.

Additionally, there is often considerable variation between post-mortem brain that is not seen in relatively homogenous colonies of transgenic mice. This is due to genetic variation and environmental factors including illnesses suffered, medications being taken and factors such as whether or not an individual smoked (Harrison, 2011). It is also difficult to obtain tissues from very early disease stages, particularly from the hippocampus for which there is great demand. Therefore, low sample sizes can make it difficult to generate statistically meaningful data. Nevertheless, further understanding the differences in signalling mechanisms underlying neurodegeneration in different brain regions (and no doubt in different individuals) will hopefully aid the development of stage-specific disease-modifying drugs, allowing for a more 'personalised' approach to the treatment of AD and other brain diseases.

6.5 Future directions

Data presented in this thesis demonstrates differences in astrocyte contribution in hippocampus and cortex at different stages of AD using both primary cell culture and human post-mortem brain samples. In addition, it shows repurposing of drugs could help accelerate drug trial procedures, despite pre-clinical trials with the anti-inflammatory DMF being inconclusive. With more time, future experiments could investigate the precise mechanisms underlying the regional differences in AD and the molecular targets of DMF. The following are some suggestions of possible future research avenues.

6.5.1 The role of astrocytes and inflammation in disease-associated tau processing in primary cell culture models

Previous data from this laboratory determined a range of inflammatory mediators upregulated by Aß that are associated with changes in tau phosphorylation (Garwood et al., 2011). Experiments could be designed to determine the effects of specific targeting of these molecules. For example, immunodepleting astrocyte-conditioned culture medium of a specific cytokine prior to application of this medium to neurons, downregulating cytokines or cytokine receptors

using siRNAs, or blocking cytokine receptors with specific antagonists allow inhibition of specific signalling pathways that could start to elucidate the role of astrocyte-derived inflammatory mediators in Aß-induced hippocampal cell death. Some attempts were made to conduct these experiments (data not shown), but cytokine antibodies are generally quite poor, making it difficult to ascertain the quality of immunodepletion experiments. Alternatively, while inflammatory mediators have been implicated in disease-associated tau processing, other astrocytic secretions (for example, gliotransmitters) may also be important. Proteomic analysis assessing astrocytic secretions in the conditioned medium of control and Aß-treated astrocyte cultures could highlight astrocytic released proteins, whether those proteins are inflammatory mediators or other astrocytic secretions, that contribute to abnormal tau processing in primary cell culture models (Dowell et al., 2009; Han et al., 2014).

To determine if it is hippocampal astrocytes rather than increased susceptibility of hippocampal neurons to AD-like insults that is important, hippocampal astrocytes could be co-cultured with cortical neurons, and *vice versa*.

In addition, if specific astrocytic signalling pathways are found to contribute to hippocampal Aß-induced changes, drugs targeting key steps in these pathways could be tested to investigate potential beneficial effects of inhibiting or activating these events. Drug discovery via evidence of the involvement of specific pathways is likely to give better results than trials of general anti-inflammatories, such as NSAIDs (Miguel-Alvarez et al., 2015).

Furthermore, experiments described in **Chapter 3:** show astrocytes play a role in the maintenance of extracellular tau levels in primary cortical cultures. These experiments were only preliminary and there are many further experiments that could be carried out to further investigate this avenue of research, including:

1. **Investigations into regional differences in tau release**. All experiments investigating the role of astrocytes in tau release were carried out in primary cortical cultures. Other experiments described in this thesis have suggested that astrocytes may play an

increasingly important role in the hippocampus, therefore a natural extension of this work would be to examine the effect of astrocytes on tau release in hippocampal cultures.

2. **Investigations into Aß-induced tau release using the tau sandwich ELISA**. Experiments investigating the role of astrocytes in Aß-induced tau release were carried out at Eli Lilly using Alphascreens. It was expected that Alphascreens would be sensitive enough to detect differences extracellular tau in concentrated medium, but results showed no change in the level of extracellular tau in neuronal cultures treated with AraC to prevent astrocyte proliferation. However, in a tau sandwich ELISA developed in-house, the presence of astrocytes in cortical mixed cultures was robustly associated with increased accumulation of extracellular tau, suggesting that the Alphascreen may not be sensitive enough to detect small changes in tau levels. Therefore, it is worth using the tau ELISA to look at conditioned medium from cultures treated with Aß and/or minocycline.
3. **Investigations into astrocytic uptake of extracellular tau**. Experiments described in this thesis have demonstrated astrocytes play a role in maintaining extracellular tau levels, however, there are several mechanisms that could underlie maintenance of tau levels. Previous research in the field has shown it is possible for astrocytes to take up tau following its trans-synaptic propagation (de Calignon et al., 2012), therefore providing one possible mechanism for astrocytic control of extracellular tau. Simple ICC experiments investigating tau uptake in cultured astrocytes, with and without neuronal stimulation, could elucidate whether this is an important mechanism used to maintain extracellular tau levels. A likely limitation of this experiment will be the low levels of tau released and potentially taken up which may be below the sensitivity of conventional immunofluorescence imaging techniques.
4. **Investigations into the role of astrocytic glutamate uptake in tau release.** Alternatively, astrocytes may influence tau release via the contributions they make to maintaining synaptic glutamate levels (Anderson and Swanson, 2000). Increased glutamate in the

synapse can lead to increased post-synaptic activity, known to increase levels of tau released (Pooler et al., 2013; Talantova et al., 2013). By modifying glutamate transporters in primary astrocytic cultures or culturing cells from glutamate transporter knock-out mice and measuring levels of extracellular tau compared to wildtype cultures, it would be possible to determine if astrocytic glutamate uptake was involved in mediating neuronal tau release.

Finally, in terms of the culture model itself, in the brain, astrocytes interact with neurons in a three-dimensional fashion, and consequently the two-dimensional culturing methods used here have a limited ability to emulate this physiological environment (Maclean et al., 2015). In addition to reduced GFAP expression, astrocytes grown on nanofiber scaffolds also exhibit increased expression of BDNF and EAAT2, consistent with a 'healthy brain' phenotype (Lau et al., 2014). Astrocytes grown on such three-dimensional structures actively proliferate, migrate into these scaffolds and adopt a stellate morphology, thus mimicking *in vivo* phenotypes (Lau et al., 2014). Future studies using neural cells grown on such three-dimensional scaffolds may allow us to explore further the influence of astrocytes under more physiological conditions, and investigate whether they retain the highly heterogenic morphology and cell size observed in our culture conditions.

As mentioned in the limitations section of this chapter (**section 6.4.1**), species differences between rat and human astrocytes limit the use of the primary culture model used in these experiments (Oberheim et al., 2009). To overcome this problem, motor neurons differentiated from iPS cells from control individuals and those with amyotrophic lateral sclerosis (ALS)/FTD have been used to investigate differences in signalling pathways in human motor neuron cultures in this disease (Serio et al., 2013). In the same way, neurons and astrocytes differentiated from iPS cells from AD patients could be compared with those from control individuals to investigate differences in astrocytic signalling pathways. Similarly, neuronal cells differentiated from embryonic stem cells could be cultured with primary human astrocytes from

control and AD brain to investigate the effects of aged and AD astrocytes on young control neurons (Re et al., 2014).

6.5.2 Identification of DMF targets

If time had allowed, further experiments could have been conducted to further elucidate the molecular targets of DMF in cell cultures and htau mice. Experiments investigating the effects of DMF in primary cortical cultures found treatment significantly reduced tau phosphorylation at Ser199/202/Thr205. However, there was no change in GFAP levels in primary cultures despite DMF having known anti-inflammatory effects. However, GFAP is not the only indicator of astrocytes, and also does not label all activated astrocytes (Garwood et al., 2016). Therefore, it is possible that astrocyte activation, or at least changes in some astrocytic signalling pathways, may be occurring in the absence of reductions in GFAP levels.

With more time, experiments investigating whether astrocytes are necessary for DMF-dependent reductions in tau phosphorylation could easily be carried out. Treating cell cultures with AraC at 3 DIV, in the same way as experiments described in **Chapter 3:**, would result in neuronal primary cultures. Predominantly neuronal and mixed primary cultures could be treated with DMF, and if a reduction in tau phosphorylation was not seen following DMF treatment of predominantly neuron cultures this would indicate astrocytes are necessary for DMF to be effective in reducing tau phosphorylation.

Additionally, experiments investigating the mechanisms by which DMF reduces tau phosphorylation implicated signalling pathways involving cdk5, a tau kinase. In particular, since IL-1ß is known to affect cdk5 activity (Kitazawa et al., 2011), the results might suggest DMF could reduce the activity of an IL-1ß - cdk5 signalling pathway. In order to test this hypothesis, IL-1ß could be targeted using the methods described above and the downstream effects on cdk5 and tau determined.

It would also be interesting to further investigate the impact of DMF on Nrf2 signalling since this is important for the selective autophagy of tau aggregates (Jo et al., 2014a). However, these

experiments may also prove challenging as antibodies raised against proteins in this signalling pathway have so far been found to be of poor quality.

6.5.3 Further analysis of post-mortem AD brain

Further information about the role of glia and neuroinflammation in the progression of AD could be elucidated using the same human post-mortem brain samples as used in the experiments in **Chapter 5:** by investigating the role of a wide range of cytokines using antibody arrays. This would allow the assembly of a regional and Braak-stage specific heat map which may highlight specific cytokine families as being important in different tissues or stages of disease. An alternative approach would be to use gene expression arrays and network analysis with the help of a biostatistician.

Additionally, with more time, investigations into changes in microglial markers would be a priority. Attempts to optimise an anti-Iba1 antibody were carried out but protein bands at the correct size were not found in the full set of post-mortem temporal cortex samples. However, there are multiple other microglial markers that could be assessed including CD45, CD68 and more recently developed Tmem119 (Cuadros et al., 2006; Bennett et al., 2016). It would be expected that there would be significant changes in microglia levels and activation, as microglial release of cytokines and their anti-inflammatory roles, as mentioned in Chapter 1 (**section 1.7**), have been previously found to be important in the development and progression of AD (Pocock and Kettenmann, 2007; Crehan et al., 2012; Gomez-Nicola and Perry, 2016; Perry, 2016; Wes et al., 2016).

Finally, recent papers have shown activated glial cells cluster around amyloid plaques and pathological tau aggregates in transgenic mouse and human AD brain (Olabarria et al., 2010; de Calignon et al., 2012; Bouvier et al., 2016). Additional IHC experiments using paraffin-fixed sections from the same brains as those samples used in the post-mortem studies described in **Chapter 5:** could be carried out to investigate changes in morphology and localisation of astrocytes and microglia as disease progresses. Staining of samples from Braak stage I-VI with antibodies for glial markers and (phosphorylated) tau or Aß could provide insights into glial

behaviour throughout disease, extending studies examining these associations in control and late stage AD (Olabarria et al., 2010; Bouvier et al., 2016). Furthermore, it may be possible to compare differences in glial morphology and localisation in different brain regions as AD progresses, hopefully gaining more information about differences in regional astrocytic behaviour.

6.6 Final conclusions

Overall, the studies presented in this thesis suggest there are likely regional differences in the contributions of astrocytes to pathological changes in tau and neurodegeneration during the progression of AD. In particular, the contribution of astrocytes appeared to differ between cortical and hippocampal regions. These differences can be seen in both primary cell culture models and human post-mortem brain samples; this suggests that the primary cell culture models used in this thesis are recapitulating at least some important aspects of disease successfully.

Efforts to further understand the implications of these regional differences will be critical for increasing our understanding of important disease mechanisms. Furthermore, this knowledge will allow better stratification criteria for clinical trials which might result in a higher likelihood of promising drugs reaching patients. Together, this would allow the development of more personalised disease-modifying treatments for AD and related neurodegenerative diseases.

References

Abbott NJ, Ronnback L, Hansson E (2006) Astrocyte-endothelial interactions at the blood-brain barrier. Nature reviews Neuroscience 7:41-53.

Agulhon C, Sun MY, Murphy T, Myers T, Lauderdale K, Fiacco TA (2012) Calcium Signaling and Gliotransmission in Normal vs. Reactive Astrocytes. Frontiers in pharmacology 3:139.

Ahmed Z, Cooper J, Murray TK, Garn K, McNaughton E, Clarke H, Parhizkar S, Ward MA, Cavallini A, Jackson S, Bose S, Clavaguera F, Tolnay M, Lavenir I, Goedert M, Hutton ML, O'Neill MJ (2014) A novel in vivo model of tau propagation with rapid and progressive neurofibrillary tangle pathology: the pattern of spread is determined by connectivity, not proximity. Acta neuropathologica 127:667-683.

Akira S, Hemmi H (2003) Recognition of pathogen-associated molecular patterns by TLR family. Immunol Lett 85:85-95.

Alavi Naini SM, Soussi-Yanicostas N (2015) Tau Hyperphosphorylation and Oxidative Stress, a Critical Vicious Circle in Neurodegenerative Tauopathies? Oxidative medicine and cellular longevity 2015:151979.

Alberdi E, Wyssenbach A, Alberdi M, Sanchez-Gomez MV, Cavaliere F, Rodriguez JJ, Verkhratsky A, Matute C (2013) Ca(2+) -dependent endoplasmic reticulum stress correlates with astrogliosis in oligomeric amyloid beta-treated astrocytes and in a model of Alzheimer's disease. Aging Cell 12:292-302.

Albrecht P, Bouchachia I, Goebels N, Henke N, Hofstetter HH, Issberner A, Kovacs Z, Lewerenz J, Lisak D, Maher P, Mausberg AK, Quasthoff K, Zimmermann C, Hartung HP, Methner A (2012) Effects of dimethyl fumarate on neuroprotection and immunomodulation. Journal of neuroinflammation 9:163.

Allaman I, Belanger M, Magistretti PJ (2011) Astrocyte-neuron metabolic relationships: for better and for worse. Trends Neurosci 34:76-87.

Allen NJ, Barres BA (2009) Neuroscience: Glia - more than just brain glue. Nature 457:675-677.

Alloisio S, Di Garbo A, Barbieri R, Bozzo L, Ferroni S, Nobile M (2010) Evidence for two conductive pathways in P2X receptor: differences in modulation and selectivity. Journal of neurochemistry 113:796-806.

Alzheimer A, Stelzmann RA, Schnitzlein HN, Murtagh FR (1995) An English translation of Alzheimer's 1907 paper, "Uber eine eigenartige Erkankung der Hirnrinde". Clinical anatomy (New York, NY) 8:429-431.

Amadoro G, Ciotti MT, Costanzi M, Cestari V, Calissano P, Canu N (2006) NMDA receptor mediates tau-induced neurotoxicity by calpain and ERK/MAPK activation. Proceedings of the National Academy of Sciences of the United States of America 103:2892-2897.

Amadoro G, Corsetti V, Ciotti MT, Florenzano F, Capsoni S, Amato G, Calissano P (2011) Endogenous Abeta causes cell death via early tau hyperphosphorylation. Neurobiology of aging 32:969-990.

Anderson CM, Swanson RA (2000) Astrocyte Glutamate Transport: Review of Properties, Regulation, and Physiological Functions. Glia 32:1-14.

Andorfer C, Acker CM, Kress Y, Hof PR, Duff K, Davies P (2005) Cell-cycle reentry and cell death in transgenic mice expressing nonmutant human tau isoforms. The Journal of neuroscience : the official journal of the Society for Neuroscience 25:5446-5454.

Andorfer C, Kress Y, Espinoza M, De Silva R, Tucker KL, Barde Y-A, Duff K, Davies P (2003) Hyperphosphorylation and aggregation of tau in mice expressing normal human tau isoforms. J Neurochem 86:582-590.

Andreadis A, Brown WM, Kosik KS (1992) Structure and novel exons of the human tau gene. Biochemistry 31:10626-10633.

Anisman H (2009) Cascading effects of stressors and inflammatory immune system activation: implications for major depressive disorder. Journal of psychiatry & neuroscience : JPN 34:4-20.

Appleby BS, Nacopoulos D, Milano N, Zhong K, Cummings JL (2013) A review: treatment of Alzheimer's disease discovered in repurposed agents. Dementia and geriatric cognitive disorders 35:1-22.

Arai H, Lee VM, Messinger ML, Greenberg BD, Lowery DE, Trojanowski JQ (1991) Expression patterns of beta-amyloid precursor protein (beta-APP) in neural and nonneural human tissues from Alzheimer's disease and control subjects. Ann Neurol 30:686-693.

Arnold CS, Johnson GV, Cole RN, Dong DL, Lee M, Hart GW (1996) The microtubule-associated protein tau is extensively modified with O-linked N-acetylglucosamine. J Biol Chem 271:28741-28744.

Ashutosh, Kou W, Cotter R, Borgmann K, Wu L, Persidsky R, Sakhuja N, Ghorpade A (2011) CXCL8 protects human neurons from amyloid-beta-induced neurotoxicity: relevance to Alzheimer's disease. Biochem Biophys Res Commun 412:565-571.

Augustinack JC, Schneider A, Mandelkow EM, Hyman BT (2002) Specific tau phosphorylation sites correlate with severity of neuronal cytopathology in Alzheimer's disease. Acta neuropathologica 103:26-35.

Avila-Munoz E, Arias C (2014) When astrocytes become harmful: functional and inflammatory responses that contribute to Alzheimer's disease. Ageing research reviews 18:29-40.

Azizi G, Khannazer N, Mirshafiey A (2014) The Potential Role of Chemokines in Alzheimer's Disease Pathogenesis. Am J Alzheimers Dis Other Demen 29:415-425.

Bahler M, Benfenati F, Valtorta F, Greengard P (1990) The synapsins and the regulation of synaptic function. Bioessays 12:259-263.

Bahmanyar S, Higgins GA, Goldgaber D, Lewis DA, Morrison JH, Wilson MC, Shankar SK, Gajdusek DC (1987) Localization of amyloid beta protein messenger RNA in brains from patients with Alzheimer's disease. Science 237:77-80.

Baitsch D, Bock HH, Engel T, Telgmann R, Muller-Tidow C, Varga G, Bot M, Herz J, Robenek H, von Eckardstein A, Nofer JR (2011) Apolipoprotein E induces antiinflammatory phenotype in macrophages. Arterioscler Thromb Vasc Biol 31:1160-1168.

Ballatore C, Lee VM, Trojanowski JQ (2007) Tau-mediated neurodegeneration in Alzheimer's disease and related disorders. Nature reviews Neuroscience 8:663-672.

Bancher C, Brunner C, Lassmann H, Budka H, Jellinger K, Wiche G, Seitelberger F, Grundke-Iqbal I, Iqbal K, Wisniewski HM (1989) Accumulation of abnormally phosphorylated tau precedes the formation of neurofibrillary tangles in Alzheimer's disease. Brain Res 477:90-99.

Barbin G, Katz DM, Chamak B, Glowinski J, Prochiantz A (1988) Brain astrocytes express region-specific surface glycoproteins in culture. Glia 1:96-103.

Baroja-Mazo A, Martin-Sanchez F, Gomez AI, Martinez CM, Amores-Iniesta J, Compan V, Barbera-Cremades M, Yague J, Ruiz-Ortiz E, Anton J, Bujan S, Couillin I, Brough D, Arostegui JI, Pelegrin P (2014) The NLRP3 inflammasome is released as a particulate danger signal that amplifies the inflammatory response. Nat Immunol 15:738-748.

Barres BA (2008) The mystery and magic of glia: a perspective on their roles in health and disease. Neuron 60:430-440.

Basurto-Islas G, Luna-Munoz J, Guillozet-Bongaarts AL, Binder LI, Mena R, Garcia-Sierra F (2008) Accumulation of aspartic acid421- and glutamic acid391-cleaved tau in neurofibrillary tangles correlates with progression in Alzheimer disease. Journal of neuropathology and experimental neurology 67:470-483.

Bauernfeind FG, Horvath G, Stutz A, Alnemri ES, MacDonald K, Speert D, Fernandes-Alnemri T, Wu J, Monks BG, Fitzgerald KA, Hornung V, Latz E (2009) Cutting edge: NF-kappaB activating pattern recognition and cytokine receptors license NLRP3 inflammasome activation by regulating NLRP3 expression. J Immunol 183:787-791.

Baumann K, Mandelkow EM, Biernat J, Piwnica-Worms H, Mandelkow E (1993) Abnormal Alzheimer-like phosphorylation of tau-protein by cyclin-dependent kinases cdk2 and cdk5. FEBS Lett 336:417-424.

Beart PM, O'Shea RD (2007) Transporters for L-glutamate: an update on their molecular pharmacology and pathological involvement. Br J Pharmacol 150:5-17.

Beharry C, Cohen LS, Di J, Ibrahim K, Briffa-Mirabella S, Alonso Adel C (2014) Tau-induced neurodegeneration: mechanisms and targets. Neuroscience bulletin 30:346-358.

Belinson H, Michaelson DM (2009) ApoE4-dependent Abeta-mediated neurodegeneration is associated with inflammatory activation in the hippocampus but not the septum. J Neural Transm (Vienna) 116:1427-1434.

Bellucci A, Westwood AJ, Ingram E, Casamenti F, Goedert M, Spillantini MG (2004) Induction of inflammatory mediators and microglial activation in mice transgenic for mutant human P301S tau protein. The American journal of pathology 165:1643-1652.

Ben-Menachem-Zidon O, Ben-Menahem Y, Ben-Hur T, Yirmiya R (2014) Intra-hippocampal transplantation of neural precursor cells with transgenic over-expression of IL-1 receptor antagonist rescues memory and neurogenesis impairments in an Alzheimer's disease model. Neuropsychopharmacology : official publication of the American College of Neuropsychopharmacology 39:401-414.

Benilova I, Karran E, De Strooper B (2012) The toxic Abeta oligomer and Alzheimer's disease: an emperor in need of clothes. Nature neuroscience 15:349-357.

Benito C, Tolon RM, Castillo AI, Ruiz-Valdepenas L, Martinez-Orgado JA, Fernandez-Sanchez FJ, Vazquez C, Cravatt BF, Romero J (2012) beta-Amyloid exacerbates inflammation in astrocytes lacking fatty acid amide hydrolase through a mechanism involving PPAR-alpha, PPAR-gamma and TRPV1, but not CB(1) or CB(2) receptors. Br J Pharmacol 166:1474-1489.

Bennett ML, Bennett FC, Liddelow SA, Ajami B, Zamanian JL, Fernhoff NB, Mulinyawe SB, Bohlen CJ, Adil A, Tucker A, Weissman IL, Chang EF, Li G, Grant GA, Hayden Gephart MG, Barres BA (2016) New tools for studying microglia in the mouse and human CNS. Proceedings of the National Academy of Sciences of the United States of America 113:E1738-1746.

Bentahir M, Nyabi O, Verhamme J, Tolia A, Horre K, Wiltfang J, Esselmann H, De Strooper B (2006) Presenilin clinical mutations can affect gamma-secretase activity by different mechanisms. Journal of neurochemistry 96:732-742.

Berger Z, Roder H, Hanna A, Carlson A, Rangachari V, Yue M, Wszolek Z, Ashe K, Knight J, Dickson D, Andorfer C, Rosenberry TL, Lewis J, Hutton M, Janus C (2007) Accumulation of pathological tau species and memory loss in a conditional model of tauopathy. The Journal of neuroscience : the official journal of the Society for Neuroscience 27:3650-3662.

Bernardinelli Y, Muller D, Nikonenko I (2014) Astrocyte-synapse structural plasticity. Neural plasticity 2014:232105.

Berne BJ, Pecora R (1976) Dynamic light scattering: with applications to chemistry, biology, and physics. In: Courier Corporation.

Bertram L, Lill CM, Tanzi RE (2010) The genetics of Alzheimer disease: back to the future. Neuron 68:270-281.

Bhaskar K, Konerth M, Kokiko-Cochran ON, Cardona A, Ransohoff RM, Lamb BT (2010) Regulation of tau pathology by the microglial fractalkine receptor. Neuron 68:19-31.

Biber K, Owens T, Boddeke E (2014) What is microglia neurotoxicity (Not)? Glia 62:841-854.

Birch AM, Katsouri L, Sastre M (2014) Modulation of inflammation in transgenic models of Alzheimer's disease. Journal of neuroinflammation 11:25.

Block ML, Zecca L, Hong JS (2007) Microglia-mediated neurotoxicity: uncovering the molecular mechanisms. Nature reviews Neuroscience 8:57-69.

Bloss EB, Puri R, Yuk F, Punsoni M, Hara Y, Janssen WG, McEwen BS, Morrison JH (2013) Morphological and molecular changes in aging rat prelimbic prefrontal cortical synapses. Neurobiology of aging 34:200-210.

Boche D, Perry VH, Nicoll JA (2013) Review: activation patterns of microglia and their identification in the human brain. Neuropathol Appl Neurobiol 39:3-18.

Boluda S, Toledo JB, Irwin DJ, Raible KM, Byrne MD, Lee EB, Lee VM, Trojanowski JQ (2014) A comparison of Abeta amyloid pathology staging systems and correlation with clinical diagnosis. Acta neuropathologica 128:543-550.

Bondulich MK, Guo T, Meehan C, Manion J, Rodriguez Martin T, Mitchell JC, Hortobagyi T, Yankova N, Stygelbout V, Brion JP, Noble W, Hanger DP (2016) Tauopathy induced by low level expression of a human brain-derived tau fragment in mice is rescued by phenylbutyrate. Brain : a journal of neurology 139:2290-2306.

Bossu P, Ciaramella A, Salani F, Bizzoni F, Varsi E, Di Iulio F, Giubilei F, Gianni W, Trequattrini A, Moro ML, Bernardini S, Caltagirone C, Spalletta G (2008) Interleukin-18 produced by peripheral blood cells is increased in Alzheimer's disease and correlates with cognitive impairment. Brain Behav Immun 22:487-492.

Bouvier DS, Jones EV, Quesseveur G, Davoli MA, T AF, Quirion R, Mechawar N, Murai KK (2016) High Resolution Dissection of Reactive Glial Nets in Alzheimer's Disease. Scientific reports 6:24544.

Braak H, Braak E (1991) Neuropathological stageing of Alzheimer-related changes. Acta neuropathologica 82:239-259.

Braak H, Braak E (1995) Staging of Alzheimer's Disease-Related Neurofibrillary Changes. Neurobiology of aging 16:271-278.

Braak H, Thal DR, Ghebremedhin E, Del Tredici K (2011) Stages of the pathologic process in Alzheimer disease: age categories from 1 to 100 years. Journal of neuropathology and experimental neurology 70:960-969.

Brace N, Snelgar, R., Kemp R. (2012) SPSS for Psychologists: Palgrave Macmillan.

Braddock M, Quinn A (2004) Targeting IL-1 in inflammatory disease: new opportunities for therapeutic intervention. Nature reviews Drug discovery 3:330-339.

Bradford MM (1976) A rapid and sensitive method for the quantitation of microgram quantities of protein utilizing the principle of protein-dye binding. Anal Biochem 72:248-254.

Brennan MS, Patel H, Allaire N, Thai A, Cullen P, Ryan S, Lukashev M, Bista P, Huang R, Rhodes KJ, Scannevin RH (2016) Pharmacodynamics of Dimethyl Fumarate Are Tissue Specific and Involve NRF2-Dependent and -Independent Mechanisms. Antioxidants & redox signaling 24:1058-1071.

Bromley-Brits K, Deng Y, Song W (2011) Morris water maze test for learning and memory deficits in Alzheimer's disease model mice. J Vis Exp:2920.

Bu G (2009) Apolipoprotein E and its receptors in Alzheimer's disease: pathways, pathogenesis and therapy. Nature reviews Neuroscience 10:333-344.

Buee L, Delacourte A (1999) Comparative biochemistry of tau in progressive supranuclear palsy, corticobasal degeneration, FTDP-17 and Pick's disease. Brain pathology (Zurich, Switzerland) 9:681-693.

Burda JE, Sofroniew MV (2014) Reactive gliosis and the multicellular response to CNS damage and disease. Neuron 81:229-248.

Busche MA, Konnerth A (2016) Impairments of neural circuit function in Alzheimer's disease. Philosophical transactions of the Royal Society of London Series B, Biological sciences 371.

Butterfield DA (2002) Amyloid beta-peptide (1-42)-induced oxidative stress and neurotoxicity: implications for neurodegeneration in Alzheimer's disease brain. A review. Free radical research 36:1307-1313.

Caceres A, Kosik KS (1990) Inhibition of neurite polarity by tau antisense oligonucleotides in primary cerebellar neurons. Nature 343:461-463.

Cagnin A, Brooks DJ, Kennedy AM, Gunn RN, Myers R, Turkheimer FE, Jones T, Banati RB (2001) In-vivo measurement of activated microglia in dementia. Lancet 358:461-467.

Cahoy JD, Emery B, Kaushal A, Foo LC, Zamanian JL, Christopherson KS, Xing Y, Lubischer JL, Krieg PA, Krupenko SA, Thompson WJ, Barres BA (2008) A transcriptome database for

astrocytes, neurons, and oligodendrocytes: a new resource for understanding brain development and function. The Journal of neuroscience : the official journal of the Society for Neuroscience 28:264-278.

Cai Z, Delwar Hussain M, Yan LJ (2013) Microglia, neuroinflammation, and Abeta in Alzheimer's disease. The International journal of neuroscience 124:307-321.

Calvo M, Sanz-Blasco S, Caballero E, Villalobos C, Nunez L (2015) Susceptibility to excitotoxicity in aged hippocampal cultures and neuroprotection by non-steroidal anti-inflammatory drugs: role of mitochondrial calcium. Journal of neurochemistry 132:403-417.

Carrero I, Gonzalo MR, Martin B, Sanz-Anquela JM, Arevalo-Serrano J, Gonzalo-Ruiz A (2012) Oligomers of beta-amyloid protein (Abeta1-42) induce the activation of cyclooxygenase-2 in astrocytes via an interaction with interleukin-1beta, tumour necrosis factor-alpha, and a nuclear factor kappa-B mechanism in the rat brain. Exp Neurol 236:215-227.

Carter SF, Scholl M, Almkvist O, Wall A, Engler H, Langstrom B, Nordberg A (2012) Evidence for astrocytosis in prodromal Alzheimer disease provided by 11C-deuterium-L-deprenyl: a multitracer PET paradigm combining 11C-Pittsburgh compound B and 18F-FDG. Journal of nuclear medicine : official publication, Society of Nuclear Medicine 53:37-46.

Caselli RJ, Reiman EM (2013) Characterizing the preclinical stages of Alzheimer's disease and the prospect of presymptomatic intervention. Journal of Alzheimer's disease : JAD 33 Suppl 1:S405-416.

Castellano JM, Kim J, Stewart FR, Jiang H, DeMattos RB, Patterson BW, Fagan AM, Morris JC, Mawuenyega KG, Cruchaga C, Goate AM, Bales KR, Paul SM, Bateman RJ, Holtzman DM (2011) Human apoE isoforms differentially regulate brain amyloid-beta peptide clearance. Science translational medicine 3:89ra57.

Castillo-Carranza DL, Sengupta U, Guerrero-Munoz MJ, Lasagna-Reeves CA, Gerson JE, Singh G, Estes DM, Barrett AD, Dineley KT, Jackson GR, Kayed R (2014) Passive Immunization with Tau Oligomer Monoclonal Antibody Reverses Tauopathy Phenotypes without Affecting Hyperphosphorylated Neurofibrillary Tangles. The Journal of neuroscience : the official journal of the Society for Neuroscience 34:4260-4272.

Cavallucci V, D'Amelio M, Cecconi F (2012) Abeta toxicity in Alzheimer's disease. Mol Neurobiol 45:366-378.

Chai J, Wang Y, Li H, He W, Zou W, Zhou Y, Hu X, Chai Q (2016) [Distribution of postsynaptic density protein 95 (PSD95) and synaptophysin during neuronal maturation]. Xi bao yu fen zi mian yi xue za zhi = Chinese journal of cellular and molecular immunology 32:1619-1622.

Chai X, Dage JL, Citron M (2012) Constitutive secretion of tau protein by an unconventional mechanism. Neurobiology of disease 48:356-366.

Chakrabarty P, Li A, Ceballos-Diaz C, Eddy JA, Funk CC, Moore B, DiNunno N, Rosario AM, Cruz PE, Verbeeck C, Sacino A, Nix S, Janus C, Price ND, Das P, Golde TE (2015) IL-10 alters immunoproteostasis in APP mice, increasing plaque burden and worsening cognitive behavior. Neuron 85:519-533.

Chami L, Buggia-Prevot V, Duplan E, Del Prete D, Chami M, Peyron JF, Checler F (2012) Nuclear factor-kappaB regulates betaAPP and beta- and gamma-secretases differently at physiological and supraphysiological Abeta concentrations. J Biol Chem 287:24573-24584.

Chan G, White CC, Winn PA, Cimpean M, Replogle JM, Glick LR, Cuerdon NE, Ryan KJ, Johnson KA, Schneider JA, Bennett DA, Chibnik LB, Sperling RA, Bradshaw EM, De Jager PL (2015) CD33 modulates TREM2: convergence of Alzheimer loci. Nature neuroscience 18:1556-1558.

Chartier-Harilni MC, Partita M, Legrain S, Perez-Tur J, Brousseau T, Evans A, Berr C, Vldal O, Roques P, Gouriet V, Fruchart JC, Delacourte A, Rossor M, Philippe Amouyel P (1994) Apolipoprotein E, e4 allele as a major risk factor for sporadic early and late-onset forms of Alzheimer's disease: analysis of the 19q13.2 chromosomal region. Human molecular genetics 3:569-574.

Chen J, Herrup K (2008) Selective vulnerability of neurons in primary cultures and in neurodegenerative diseases. Reviews in the neurosciences 19:317-326.
Chen M, Ona VO, Li M, Ferrante RJ, Fink KB, Zhu S, Bian J, Guo L, Farrell LA, Hersch SM, Hobbs W, Vonsattel JP, Cha JH, Friedlander RM (2000) Minocycline inhibits caspase-1 and caspase-3 expression and delays mortality in a transgenic mouse model of Huntington disease. Nat Med 6:797-801.
Chen Y, Liu C, Parker WD, Chen H, Beach TG, Liu X, Serrano GE, Lu Y, Huang J, Yang K, Wang C (2016) Mitochondrial DNA Rearrangement Spectrum in Brain Tissue of Alzheimer's Disease: Analysis of 13 Cases. PloS one 11:e0154582.
Choi AJ, Ryter SW (2014) Inflammasomes: molecular regulation and implications for metabolic and cognitive diseases. Molecules and cells 37:441-448.
Choi SS, Lee HJ, Lim I, Satoh J, Kim SU (2014) Human astrocytes: secretome profiles of cytokines and chemokines. PloS one 9:e92325.
Chow VW, Mattson MP, Wong PC, Gleichmann M (2010) An overview of APP processing enzymes and products. Neuromolecular medicine 12:1-12.
Chung CW, Song YH, Kim IK, Yoon WJ, Ryu BR, Jo DG, Woo HN, Kwon YK, Kim HH, Gwag BJ, Mook-Jung IH, Jung YK (2001) Proapoptotic effects of tau cleavage product generated by caspase-3. Neurobiology of disease 8:162-172.
Cisneros-Mejorado A, Perez-Samartin A, Gottlieb M, Matute C (2015) ATP signaling in brain: release, excitotoxicity and potential therapeutic targets. Cell Mol Neurobiol 35:1-6.
Clavaguera F, Hench J, Goedert M, Tolnay M (2015) Invited review: Prion-like transmission and spreading of tau pathology. Neuropathol Appl Neurobiol 41:47-58.
Clavaguera F, Akatsu H, Fraser G, Crowther RA, Frank S, Hench J, Probst A, Winkler DT, Reichwald J, Staufenbiel M, Ghetti B, Goedert M, Tolnay M (2013) Brain homogenates from human tauopathies induce tau inclusions in mouse brain. Proceedings of the National Academy of Sciences of the United States of America 110:9535-9540.
Cohen TJ, Guo JL, Hurtado DE, Kwong LK, Mills IP, Trojanowski JQ, Lee VM (2011) The acetylation of tau inhibits its function and promotes pathological tau aggregation. Nature communications 2:252.
Colangelo AM, Alberghina L, Papa M (2014) Astrogliosis as a therapeutic target for neurodegenerative diseases. Neurosci Lett 565:59-64.
Coleman P, Federoff H, Kurlan R (2004) A focus on the synapse for neuroprotection in Alzheimer disease and other dementias. Neurology 63:1155-1162.
Congdon EE, Kim S, Bonchak J, Songrug T, Matzavinos A, Kuret J (2008) Nucleation-dependent tau filament formation: the importance of dimerization and an estimation of elementary rate constants. J Biol Chem 283:13806-13816.
Corbett A, Pickett J, Burns A, Corcoran J, Dunnett SB, Edison P, Hagan JJ, Holmes C, Jones E, Katona C, Kearns I, Kehoe P, Mudher A, Passmore A, Shepherd N, Walsh F, Ballard C (2012) Drug repositioning for Alzheimer's disease. Nature reviews Drug discovery 11:833-846.
Cowan CM, Mudher A (2013) Are tau aggregates toxic or protective in tauopathies? Frontiers in neurology 4:114.
Craft S (2005) Insulin resistance syndrome and Alzheimer's disease: age- and obesity-related effects on memory, amyloid, and inflammation. Neurobiology of aging 26 Suppl 1:65-69.
Crain JM, Nikodemova M, Watters JJ (2013) Microglia express distinct M1 and M2 phenotypic markers in the postnatal and adult central nervous system in male and female mice. J Neurosci Res 91:1143-1151.
Crehan H, Hardy J, Pocock J (2012) Microglia, Alzheimer's disease, and complement. International journal of Alzheimer's disease 2012:983640.
Crehan H, Hardy J, Pocock J (2013) Blockage of CR1 prevents activation of rodent microglia. Neurobiology of disease 54:139-149.

Crimins JL, Pooler A, Polydoro M, Luebke JI, Spires-Jones TL (2013) The intersection of amyloid beta and tau in glutamatergic synaptic dysfunction and collapse in Alzheimer's disease. Ageing research reviews 12:757-763.

Cruz JC, Tseng HC, Goldman JA, Shih H, Tsai LH (2003) Aberrant Cdk5 activation by p25 triggers pathological events leading to neurodegeneration and neurofibrillary tangles. Neuron 40:471-483.

Cuadros MA, Santos AM, Martin-Oliva D, Calvente R, Tassi M, Marin-Teva JL, Navascues J (2006) Specific immunolabeling of brain macrophages and microglial cells in the developing and mature chick central nervous system. The journal of histochemistry and cytochemistry : official journal of the Histochemistry Society 54:727-738.

Cullen DK, Gilroy ME, Irons HR, Laplaca MC (2010) Synapse-to-neuron ratio is inversely related to neuronal density in mature neuronal cultures. Brain Res 1359:44-55.

Cunningham C, Campion S, Lunnon K, Murray CL, Woods JF, Deacon RM, Rawlins JN, Perry VH (2009) Systemic inflammation induces acute behavioral and cognitive changes and accelerates neurodegenerative disease. Biological psychiatry 65:304-312.

Curran B, O'Connor JJ (2001) The pro-inflammatory cytokine interleukin-18 impairs long-term potentiation and NMDA receptor-mediated transmission in the rat hippocampus in vitro. Neuroscience 108:83-90.

Cutler NR, Sramek JJ (2001) Review of the next generation of Alzheimer's disease therapeutics: challenges for drug development. Progress in neuro-psychopharmacology & biological psychiatry 25:27-57.

DaRocha-Souto B, Coma M, Perez-Nievas BG, Scotton TC, Siao M, Sanchez-Ferrer P, Hashimoto T, Fan Z, Hudry E, Barroeta I, Sereno L, Rodriguez M, Sanchez MB, Hyman BT, Gomez-Isla T (2012) Activation of glycogen synthase kinase-3 beta mediates beta-amyloid induced neuritic damage in Alzheimer's disease. Neurobiology of disease 45:425-437.

Davis RC, Marsden IT, Maloney MT, Minamide LS, Podlisny M, Selkoe DJ, Bamburg JR (2011) Amyloid beta dimers/trimers potently induce cofilin-actin rods that are inhibited by maintaining cofilin-phosphorylation. Molecular neurodegeneration 6:10.

de Calignon A, Polydoro M, Suarez-Calvet M, William C, Adamowicz DH, Kopeikina KJ, Pitstick R, Sahara N, Ashe KH, Carlson GA, Spires-Jones TL, Hyman BT (2012) Propagation of tau pathology in a model of early Alzheimer's disease. Neuron 73:685-697.

de Flores R, La Joie R, Chetelat G (2015) Structural imaging of hippocampal subfields in healthy aging and Alzheimer's disease. Neuroscience 309:29-50.

De Groot CJ, Theeuwes JW, Dijkstra CD, van der Valk P (1995) Postmortem delay effects on neuroglial cells and brain macrophages from Lewis rats with acute experimental allergic encephalomyelitis: an immunohistochemical and cytochemical study. J Neuroimmunol 59:123-134.

De Groot CJ, Langeveld CH, Jongenelen CA, Montagne L, Van Der Valk P, Dijkstra CD (1997) Establishment of human adult astrocyte cultures derived from postmortem multiple sclerosis and control brain and spinal cord regions: immunophenotypical and functional characterization. J Neurosci Res 49:342-354.

de Pablo Y, Nilsson M, Pekna M, Pekny M (2013) Intermediate filaments are important for astrocyte response to oxidative stress induced by oxygen-glucose deprivation and reperfusion. Histochemistry and cell biology 140:81-91.

De Strooper B, Annaert W (2010) Novel research horizons for presenilins and gamma-secretases in cell biology and disease. Annu Rev Cell Dev Biol 26:235-260.

De Strooper B, Karran E (2016) The Cellular Phase of Alzheimer's Disease. Cell 164:603-615.

De Strooper B, Iwatsubo T, Wolfe MS (2012) Presenilins and gamma-secretase: structure, function, and role in Alzheimer Disease. Cold Spring Harbor perspectives in medicine 2:a006304.

De Zeeuw CI, Hoogland TM (2015) Reappraisal of Bergmann glial cells as modulators of cerebellar circuit function. Frontiers in cellular neuroscience 9:246.

Decker H, Lo KY, Unger SM, Ferreira ST, Silverman MA (2010) Amyloid-beta peptide oligomers disrupt axonal transport through an NMDA receptor-dependent mechanism that is mediated by glycogen synthase kinase 3beta in primary cultured hippocampal neurons. The Journal of neuroscience : the official journal of the Society for Neuroscience 30:9166-9171.

Deng P, Xu ZC (2011) Contribution of Ih to neuronal damage in the hippocampus after traumatic brain injury in rats. Journal of neurotrauma 28:1173-1183.

Deng Y, Lu X, Wang L, Li T, Ding Y, Cao H, Zhang Y, Guo X, Yu G (2014) Curcumin inhibits the AKT/NF-kappaB signaling via CpG demethylation of the promoter and restoration of NEP in the N2a cell line. The AAPS journal 16:649-657.

Derkinderen P, Scales TM, Hanger DP, Leung KY, Byers HL, Ward MA, Lenz C, Price C, Bird IN, Perera T, Kellie S, Williamson R, Noble W, Van Etten RA, Leroy K, Brion JP, Reynolds CH, Anderton BH (2005) Tyrosine 394 is phosphorylated in Alzheimer's paired helical filament tau and in fetal tau with c-Abl as the candidate tyrosine kinase. The Journal of neuroscience : the official journal of the Society for Neuroscience 25:6584-6593.

Dhikav V, Anand K (2011) Potential predictors of hippocampal atrophy in Alzheimer's disease. Drugs & aging 28:1-11.

Di Bona D, Plaia A, Vasto S, Cavallone L, Lescai F, Franceschi C, Licastro F, Colonna-Romano G, Lio D, Candore G, Caruso C (2008) Association between the interleukin-1beta polymorphisms and Alzheimer's disease: a systematic review and meta-analysis. Brain Res Rev 59:155-163.

di Nuzzo L, Orlando R, Nasca C, Nicoletti F (2014) Molecular pharmacodynamics of new oral drugs used in the treatment of multiple sclerosis. Drug design, development and therapy 8:555-568.

Diaz-Hernandez M, Gomez-Ramos A, Rubio A, Gomez-Villafuertes R, Naranjo JR, Miras-Portugal MT, Avila J (2010) Tissue-nonspecific alkaline phosphatase promotes the neurotoxicity effect of extracellular tau. J Biol Chem 285:32539-32548.

Diguet E, Gross CE, Tison F, Bezard E (2004) Rise and fall of minocycline in neuroprotection: need to promote publication of negative results. Exp Neurol 189:1-4.

Dinarello CA, Mier JW (1986) Interleukins. Annu Rev Med 37:173-178.

Ding H, Matthews TA, Johnson GV (2006) Site-specific phosphorylation and caspase cleavage differentially impact tau-microtubule interactions and tau aggregation. J Biol Chem 281:19107-19114.

Dixit R, Ross JL, Goldman YE, Holzbaur EL (2008) Differential regulation of dynein and kinesin motor proteins by tau. Science 319:1086-1089.

Dong Y, Benveniste EN (2001) Immune function of astrocytes. Glia 36:180-190.

Dowell JA, Johnson JA, Li L (2009) Identification of astrocyte secreted proteins with a combination of shotgun proteomics and bioinformatics. Journal of proteome research 8:4135-4143.

Duff K, Knight H, Refolo LM, Sanders S, Yu X, Picciano M, Malester B, Hutton M, Adamson J, Goedert M, Burki K, Davies P (2000) Characterization of pathology in transgenic mice over-expressing human genomic and cDNA tau transgenes. Neurobiology of disease 7:87-98.

Duff K, Eckman C, Zehr C, Yu X, Prada CM, Perez-tur J, Hutton M, Buee L, Harigaya Y, Yager D, Morgan D, Gordon MN, Holcomb L, Refolo L, Zenk B, Hardy J, Younkin S (1996) Increased amyloid-beta42(43) in brains of mice expressing mutant presenilin 1. Nature 383:710-713.

Dujardin S, Begard S, Caillierez R, Lachaud C, Delattre L, Carrier S, Loyens A, Galas MC, Bousset L, Melki R, Auregan G, Hantraye P, Brouillet E, Buee L, Colin M (2014) Ectosomes: a new mechanism for non-exosomal secretion of tau protein. PloS one 9:e100760.

Dumitriu D, Hao J, Hara Y, Kaufmann J, Janssen WG, Lou W, Rapp PR, Morrison JH (2010) Selective changes in thin spine density and morphology in monkey prefrontal cortex

correlate with aging-related cognitive impairment. The Journal of neuroscience : the official journal of the Society for Neuroscience 30:7507-7515.

Dyrks T, Weidemann A, Multhaup G, Salbaum JM, Lemaire HG, Kang J, Muller-Hill B, Masters CL, Beyreuther K (1988) Identification, transmembrane orientation and biogenesis of the amyloid A4 precursor of Alzheimer's disease. The EMBO journal 7:949-957.

Eichenbaum G, Damsch S, Looszova A, Vandenberghe J, Van den Bulck K, Roels K, Megens A, Knight E, Hillsamer V, Feyen B, Kelley MF, Tonelli A, Lammens L (2011) Impact of gavage dosing procedure and gastric content on adverse respiratory effects and mortality in rat toxicity studies. Journal of applied toxicology : JAT 31:342-354.

Eisen A, Turner MR (2013) Does variation in neurodegenerative disease susceptibility and phenotype reflect cerebral differences at the network level? Amyotrophic lateral sclerosis & frontotemporal degeneration 14:487-493.

Eliasson C, Sahlgren C, Berthold CH, Stakeberg J, Celis JE, Betsholtz C, Eriksson JE, Pekny M (1999) Intermediate filament protein partnership in astrocytes. J Biol Chem 274:23996-24006.

Ellrichmann G, Petrasch-Parwez E, Lee DH, Reick C, Arning L, Saft C, Gold R, Linker RA (2011) Efficacy of fumaric acid esters in the R6/2 and YAC128 models of Huntington's disease. PloS one 6:e16172.

Elobeid A, Rantakomi S, Soininen H, Alafuzoff I (2014) Alzheimer's disease-related plaques in nondemented subjects. Alzheimer's & dementia : the journal of the Alzheimer's Association 10:522-529.

Eng LF, Ghirnikar RS, Lee YL (2000) Glial fibrillary acidic protein: GFAP-thirty-one years (1969-2000). Neurochem Res 25:1439-1451.

Engel T, Lucas JJ, Hernandez F, Avila J (2007) A mouse model to study tau pathology related with tau phosphorylation and assembly. J Neurol Sci 257:250-254.

Engmann O, Giese KP (2009) Crosstalk between Cdk5 and GSK3beta: Implications for Alzheimer's Disease. Frontiers in molecular neuroscience 2:2.

Eugenin J, Vecchiola A, Murgas P, Arroyo P, Cornejo F, von Bernhardi R (2016) Expression Pattern of Scavenger Receptors and Amyloid-beta Phagocytosis of Astrocytes and Microglia in Culture are Modified by Acidosis: Implications for Alzheimer's Disease. Journal of Alzheimer's disease : JAD 53:857-873.

Evans DB, Rank KB, Bhattacharya K, Thomsen DR, Gurney ME, Sharma SK (2000) Tau phosphorylation at serine 396 and serine 404 by human recombinant tau protein kinase II inhibits tau's ability to promote microtubule assembly. J Biol Chem 275:24977-24983.

Fa M, Orozco IJ, Francis YI, Saeed F, Gong Y, Arancio O (2010) Preparation of oligomeric beta-amyloid 1-42 and induction of synaptic plasticity impairment on hippocampal slices. J Vis Exp.

Familian A, Boshuizen RS, Eikelenboom P, Veerhuis R (2006) Inhibitory effect of minocycline on amyloid beta fibril formation and human microglial activation. Glia 53:233-240.

Fang X, Yu SX, Lu Y, Bast RC, Jr., Woodgett JR, Mills GB (2000) Phosphorylation and inactivation of glycogen synthase kinase 3 by protein kinase A. Proceedings of the National Academy of Sciences of the United States of America 97:11960-11965.

Feinstein SC, Wilson L (2005) Inability of tau to properly regulate neuronal microtubule dynamics: a loss-of-function mechanism by which tau might mediate neuronal cell death. Biochimica et biophysica acta 1739:268-279.

Fernandez MA, Klutkowski JA, Freret T, Wolfe MS (2014) Alzheimer presenilin-1 mutations dramatically reduce trimming of long amyloid beta-peptides (Abeta) by gamma-secretase to increase 42-to-40-residue Abeta. J Biol Chem 289:31043-31052.

Ferreira IL, Bajouco LM, Mota SI, Auberson YP, Oliveira CR, Rego AC (2012) Amyloid beta peptide 1-42 disturbs intracellular calcium homeostasis through activation of GluN2B-containing N-methyl-d-aspartate receptors in cortical cultures. Cell calcium 51:95-106.

Festoff BW, Ameenuddin S, Arnold PM, Wong A, Santacruz KS, Citron BA (2006) Minocycline neuroprotects, reduces microgliosis, and inhibits caspase protease expression early after spinal cord injury. Journal of neurochemistry 97:1314-1326.

Fiacco TA, McCarthy KD (2006) Astrocyte calcium elevations: properties, propagation, and effects on brain signaling. Glia 54:676-690.

Finder VH, Vodopivec I, Nitsch RM, Glockshuber R (2010) The recombinant amyloid-beta peptide Abeta1-42 aggregates faster and is more neurotoxic than synthetic Abeta1-42. J Mol Biol 396:9-18.

Fontaine SN, Zheng D, Sabbagh JJ, Martin MD, Chaput D, Darling A, Trotter JH, Stothert AR, Nordhues BA, Lussier A, Baker J, Shelton L, Kahn M, Blair LJ, Stevens SM, Jr., Dickey CA (2016) DnaJ/Hsc70 chaperone complexes control the extracellular release of neurodegenerative-associated proteins. The EMBO journal 35:1537-1549.

Forabosco P, Ramasamy A, Trabzuni D, Walker R, Smith C, Bras J, Levine AP, Hardy J, Pocock JM, Guerreiro R, Weale ME, Ryten M (2013) Insights into TREM2 biology by network analysis of human brain gene expression data. Neurobiology of aging 34:2699-2714.

Fox RJ, Miller DH, Phillips JT, Hutchinson M, Havrdova E, Kita M, Yang M, Raghupathi K, Novas M, Sweetser MT, Viglietta V, Dawson KT (2012) Placebo-controlled phase 3 study of oral BG-12 or glatiramer in multiple sclerosis. The New England journal of medicine 367:1087-1097.

Frakes AE, Ferraiuolo L, Haidet-Phillips AM, Schmelzer L, Braun L, Miranda CJ, Ladner KJ, Bevan AK, Foust KD, Godbout JP, Popovich PG, Guttridge DC, Kaspar BK (2014) Microglia induce motor neuron death via the classical NF-kappaB pathway in amyotrophic lateral sclerosis. Neuron 81:1009-1023.

Franceschi C, Campisi J (2014) Chronic inflammation (inflammaging) and its potential contribution to age-associated diseases. The journals of gerontology Series A, Biological sciences and medical sciences 69 Suppl 1:S4-9.

Frank S, Burbach GJ, Bonin M, Walter M, Streit W, Bechmann I, Deller T (2008) TREM2 is upregulated in amyloid plaque-associated microglia in aged APP23 transgenic mice. Glia 56:1438-1447.

Freeman LC, Ting JP (2016) The pathogenic role of the inflammasome in neurodegenerative diseases. Journal of neurochemistry 136 Suppl 1:29-38.

Friedman LG, Qureshi YH, Yu WH (2015) Promoting autophagic clearance: viable therapeutic targets in Alzheimer's disease. Neurotherapeutics : the journal of the American Society for Experimental NeuroTherapeutics 12:94-108.

Gabbita SP, Johnson MF, Kobritz N, Eslami P, Poteshkina A, Varadarajan S, Turman J, Zemlan F, Harris-White ME (2015) Oral TNFalpha Modulation Alters Neutrophil Infiltration, Improves Cognition and Diminishes Tau and Amyloid Pathology in the 3xTgAD Mouse Model. PloS one 10:e0137305.

Gamblin TC, Chen F, Zambrano A, Abraha A, Lagalwar S, Guillozet AL, Lu M, Fu Y, Garcia-Sierra F, LaPointe N, Miller R, Berry RW, Binder LI, Cryns VL (2003) Caspase cleavage of tau: linking amyloid and neurofibrillary tangles in Alzheimer's disease. Proceedings of the National Academy of Sciences of the United States of America 100:10032-10037.

Garcia-Marin V, Garcia-Lopez P, Freire M (2007a) Cajal's contributions to glia research. Trends Neurosci 30:479-487.

Garcia-Marin V, Garcia-Lopez P, Freire M (2007b) Cajal's contributions to the study of Alzheimer's disease. Journal of Alzheimer's disease : JAD 12:161-174.

Garcia-Segura LM, McCarthy MM (2004) Minireview: Role of glia in neuroendocrine function. Endocrinology 145:1082-1086.

Garcia-Sierra F, Ghoshal N, Quinn B, Berry RW, Binder LI (2003) Conformational changes and truncation of tau protein during tangle evolution in Alzheimer's disease. Journal of Alzheimer's disease : JAD 5:65-77.

Garg SK, Kipnis J, Banerjee R (2009) IFN-gamma and IL-4 differentially shape metabolic responses and neuroprotective phenotype of astrocytes. Journal of neurochemistry 108:1155-1166.

Garwood CJ, Cooper JD, Hanger DP, Noble W (2010) Anti-inflammatory impact of minocycline in a mouse model of tauopathy. Frontiers in psychiatry 1:136-144.

Garwood CJ, Pooler AM, Atherton J, Hanger DP, Noble W (2011) Astrocytes are important mediators of Abeta-induced neurotoxicity and tau phosphorylation in primary culture. Cell death & disease 2:e167-e176.

Garwood CJ, Ratcliffe LE, Simpson JE, Heath PR, Ince PG, Wharton SB (2016) Review: Astrocytes in Alzheimer's disease and other age-associated dementias; a supporting player with a central role. Neuropathol Appl Neurobiol.

Gerson J, Kayed R (2016) Therapeutic approaches targeting pathological tau aggregates. Curr Pharm Des.

Ghosh S, Wu MD, Shaftel SS, Kyrkanides S, LaFerla FM, Olschowka JA, O'Banion MK (2013) Sustained interleukin-1beta overexpression exacerbates tau pathology despite reduced amyloid burden in an Alzheimer's mouse model. The Journal of neuroscience : the official journal of the Society for Neuroscience 33:5053-5064.

Giese KP (2014) Generation of the Cdk5 activator p25 is a memory mechanism that is affected in early Alzheimer's disease. Frontiers in molecular neuroscience 7:36.

Glatz DC, Rujescu D, Tang Y, Berendt FJ, Hartmann AM, Faltraco F, Rosenberg C, Hulette C, Jellinger K, Hampel H, Riederer P, Moller HJ, Andreadis A, Henkel K, Stamm S (2006) The alternative splicing of tau exon 10 and its regulatory proteins CLK2 and TRA2-BETA1 changes in sporadic Alzheimer's disease. Journal of neurochemistry 96:635-644.

Glenner GG, Wong CW (1984) Alzheimer's disease: initial report of the purification and characterization of a novel cerebrovascular amyloid protein. Biochem Biophys Res Commun 120:885-890.

Goate A, Chartier-Harlin MC, Mullan M, Brown J, Crawford F, Fidani L, Giuffra L, Haynes A, Irving N, James L, et al. (1991) Segregation of a missense mutation in the amyloid precursor protein gene with familial Alzheimer's disease. Nature 349:704-706.

Goedert M, Jakes R (1990) Expression of separate isoforms of human tau protein: correlation with the tau pattern in brain and effects on tubulin polymerization. The EMBO journal 9:4225-4230.

Gold M, El Khoury J (2015) beta-amyloid, microglia, and the inflammasome in Alzheimer's disease. Seminars in immunopathology 37:607-611.

Gold R, Kappos L, Arnold DL, Bar-Or A, Giovannoni G, Selmaj K, Tornatore C, Sweetser MT, Yang M, Sheikh SI, Dawson KT (2012) Placebo-controlled phase 3 study of oral BG-12 for relapsing multiple sclerosis. The New England journal of medicine 367:1098-1107.

Golomb J, Kluger A, Ferris SH (2004) Mild cognitive impairment: historical development and summary of research. Dialogues in clinical neuroscience 6:351-367.

Gomez-Nicola D, Perry VH (2016) Analysis of Microglial Proliferation in Alzheimer's Disease. Methods Mol Biol 1303:185-193.

Gomez-Ramos A, Diaz-Hernandez M, Rubio A, Diaz-Hernandez JI, Miras-Portugal MT, Avila J (2009) Characteristics and consequences of muscarinic receptor activation by tau protein. European neuropsychopharmacology : the journal of the European College of Neuropsychopharmacology 19:708-717.

Gong CX, Liu F, Grundke-Iqbal I, Iqbal K (2006) Impaired brain glucose metabolism leads to Alzheimer neurofibrillary degeneration through a decrease in tau O-GlcNAcylation. Journal of Alzheimer's disease : JAD 9:1-12.

Gonzalez-Maeso J, Torre I, Rodriguez-Puertas R, Garcia-Sevilla JA, Guimon J, Meana JJ (2002) Effects of age, postmortem delay and storage time on receptor-mediated activation of G-proteins in human brain. Neuropsychopharmacology : official publication of the American College of Neuropsychopharmacology 26:468-478.

Gordon S, Martinez FO (2010) Alternative activation of macrophages: mechanism and functions. Immunity 32:593-604.

Gotz J, Chen F, van Dorpe J, Nitsch RM (2001) Formation of neurofibrillary tangles in P301l tau transgenic mice induced by Abeta 42 fibrils. Science 293:1491-1495.

Grabrucker A, Vaida B, Bockmann J, Boeckers TM (2009) Synaptogenesis of hippocampal neurons in primary cell culture. Cell Tissue Res 338:333-341.

Graeber MB, Li W, Rodriguez ML (2011) Role of microglia in CNS inflammation. FEBS Lett 585:3798-3805.

Grainger DJ, Reckless J, McKilligin E (2004) Apolipoprotein E modulates clearance of apoptotic bodies in vitro and in vivo, resulting in a systemic proinflammatory state in apolipoprotein E-deficient mice. J Immunol 173:6366-6375.

Granic I, Dolga AM, Nijholt IM, van Dijk G, Eisel UL (2009) Inflammation and NF-kappaB in Alzheimer's disease and diabetes. Journal of Alzheimer's disease : JAD 16:809-821.

Greenberg SG, Davies P (1990) A preparation of Alzheimer paired helical filaments that displays distinct tau proteins by polyacrylamide gel electrophoresis. Proceedings of the National Academy of Sciences of the United States of America 87:5827-5831.

Griffith JW, Sokol CL, Luster AD (2014) Chemokines and chemokine receptors: positioning cells for host defense and immunity. Annu Rev Immunol 32:659-702.

Grolla AA, Sim JA, Lim D, Rodriguez JJ, Genazzani AA, Verkhratsky A (2013) Amyloid-beta and Alzheimer's disease type pathology differentially affects the calcium signalling toolkit in astrocytes from different brain regions. Cell death & disease 4:e623-670.

Grundke-Iqbal I, Iqbal K, Quinlan M, Tung YC, Zaidi MS, Wisniewski HM (1986) Microtubule-associated protein tau. A component of Alzheimer paired helical filaments. J Biol Chem 261:6084-6089.

Guerreiro R et al. (2013) TREM2 variants in Alzheimer's disease. The New England journal of medicine 368:117-127.

Guo JL, Lee VM (2011) Seeding of normal Tau by pathological Tau conformers drives pathogenesis of Alzheimer-like tangles. J Biol Chem 286:15317-15331.

Guo L, LaDu MJ, Van Eldik LJ (2004) A dual role for apolipoprotein e in neuroinflammation: anti- and pro-inflammatory activity. Journal of molecular neuroscience : MN 23:205-212.

Guthrie PB, Knappenberger J, Segal M, Bennett MV, Charles AC, Kater SB (1999) ATP released from astrocytes mediates glial calcium waves. The Journal of neuroscience : the official journal of the Society for Neuroscience 19:520-528.

Haass C, Kaether C, Thinakaran G, Sisodia S (2012) Trafficking and proteolytic processing of APP. Cold Spring Harbor perspectives in medicine 2:a006270.

Hallegua DS, Weisman MH (2002) Potential therapeutic uses of interleukin 1 receptor antagonists in human diseases. Ann Rheum Dis 61:960-967.

Hamby ME, Coppola G, Ao Y, Geschwind DH, Khakh BS, Sofroniew MV (2012) Inflammatory mediators alter the astrocyte transcriptome and calcium signaling elicited by multiple G-protein-coupled receptors. The Journal of neuroscience : the official journal of the Society for Neuroscience 32:14489-14510.

Han D, Jin J, Woo J, Min H, Kim Y (2014) Proteomic analysis of mouse astrocytes and their secretome by a combination of FASP and StageTip-based, high pH, reversed-phase fractionation. Proteomics 14:1604-1609.

Hanell A, Marklund N (2014) Structured evaluation of rodent behavioral tests used in drug discovery research. Frontiers in behavioral neuroscience 8:252.

Hanger DP, Wray S (2010) Tau cleavage and tau aggregation in neurodegenerative disease. Biochemical Society transactions 38:1016-1020.

Hanger DP, Anderton BH, Noble W (2009) Tau phosphorylation: the therapeutic challenge for neurodegenerative disease. Trends Mol Med 15:112-119.

Hanger DP, Hughes K, Woodgett JR, Brion JP, Anderton BH (1992) Glycogen synthase kinase-3 induces Alzheimer's disease-like phosphorylation of tau: generation of paired helical filament epitopes and neuronal localisation of the kinase. Neurosci Lett 147:58-62.

Hanger DP, Lau DH, Phillips EC, Bondulich MK, Guo T, Woodward BW, Pooler AM, Noble W (2014) Intracellular and Extracellular Roles for Tau in Neurodegenerative Disease. Journal of Alzheimer's disease : JAD.

Hanger DP, Byers HL, Wray S, Leung KY, Saxton MJ, Seereeram A, Reynolds CH, Ward MA, Anderton BH (2007) Novel phosphorylation sites in tau from Alzheimer brain support a role for casein kinase 1 in disease pathogenesis. J Biol Chem 282:23645-23654.

Hanslick JL, Lau K, Noguchi KK, Olney JW, Zorumski CF, Mennerick S, Farber NB (2009) Dimethyl sulfoxide (DMSO) produces widespread apoptosis in the developing central nervous system. Neurobiology of disease 34:1-10.

Hardy J, Allsop D (1991) Amyloid deposition as the central event in the aetiology of Alzheimer's disease. Trends Pharmacol Sci 12:383-388.

Hardy J, Selkoe DJ (2002) The amyloid hypothesis of Alzheimer's disease: progress and problems on the road to therapeutics. Science 297:353-356.

Hardy J, Duff K, Hardy KG, Perez-Tur J, Hutton M (1998) Genetic dissection of Alzheimer's disease and related dementias: amyloid and its relationship to tau. Nature neuroscience 1:355-358.

Harold D et al. (2009) Genome-wide association study identifies variants at CLU and PICALM associated with Alzheimer's disease. Nat Genet 41:1088-1093.

Harrison FE, Hosseini AH, McDonald MP (2009) Endogenous anxiety and stress responses in water maze and Barnes maze spatial memory tasks. Behav Brain Res 198:247-251.

Harrison PJ (2011) Using our brains: the findings, flaws, and future of postmortem studies of psychiatric disorders. Biological psychiatry 69:102-103.

Hasegawa M (2006) Biochemistry and molecular biology of tauopathies. Neuropathology 26:484-490.

Hasegawa M, Watanabe S, Kondo H, Akiyama H, Mann DM, Saito Y, Murayama S (2014) 3R and 4R tau isoforms in paired helical filaments in Alzheimer's disease. Acta neuropathologica 127:303-305.

Hashiguchi M, Saito T, Hisanaga S, Hashiguchi T (2002) Truncation of CDK5 activator p35 induces intensive phosphorylation of Ser202/Thr205 of human tau. J Biol Chem 277:44525-44530.

Hashimoto T, Serrano-Pozo A, Hori Y, Adams KW, Takeda S, Banerji AO, Mitani A, Joyner D, Thyssen DH, Bacskai BJ, Frosch MP, Spires-Jones TL, Finn MB, Holtzman DM, Hyman BT (2012) Apolipoprotein E, especially apolipoprotein E4, increases the oligomerization of amyloid beta peptide. The Journal of neuroscience : the official journal of the Society for Neuroscience 32:15181-15192.

He Z, Zhang S, Song Q, Li W, Liu D, Li H, Tang M, Chai R (2016) The structural development of primary cultured hippocampal neurons on a graphene substrate. Colloids and surfaces B, Biointerfaces 146:442-451.

Hebron ML, Algarzae NK, Lonskaya I, Moussa C (2013) Fractalkine signaling and Tau hyper-phosphorylation are associated with autophagic alterations in lentiviral Tau and Abeta(1-42) gene transfer models. Exp Neurol 251:127-138.

Heiligenhaus A, Li H, Wasmuth S, Bauer D (2004) Influence of dimethylfumarate on experimental HSV-1 necrotizing keratitis. Graefe's archive for clinical and experimental ophthalmology = Albrecht von Graefes Archiv fur klinische und experimentelle Ophthalmologie 242:870-877.

Hellstrand E, Boland B, Walsh DM, Linse S (2010) Amyloid beta-protein aggregation produces highly reproducible kinetic data and occurs by a two-phase process. ACS chemical neuroscience 1:13-18.

Heneka M et al. (2016) Targeting innate immunity for neurodegenerative disorders of the central nervous system. Journal of neurochemistry.

Heneka MT, Rodriguez JJ, Verkhratsky A (2010) Neuroglia in neurodegeneration. Brain Res Rev 63:189-211.

Heneka MT, Kummer MP, Stutz A, Delekate A, Schwartz S, Vieira-Saecker A, Griep A, Axt D, Remus A, Tzeng TC, Gelpi E, Halle A, Korte M, Latz E, Golenbock DT (2012) NLRP3 is activated in Alzheimer's disease and contributes to pathology in APP/PS1 mice. Nature 493:674-678.

Heneka MT et al. (2015) Neuroinflammation in Alzheimer's disease. The Lancet Neurology 14:388-405.

Heppner FL, Ransohoff RM, Becher B (2015) Immune attack: the role of inflammation in Alzheimer disease. Nature reviews Neuroscience 16:358-372.
Hippius H, Neundorfer G (2003) The discovery of Alzheimer's disease. Dialogues in clinical neuroscience 5:101-108.
Hol EM, Pekny M (2015) Glial fibrillary acidic protein (GFAP) and the astrocyte intermediate filament system in diseases of the central nervous system. Curr Opin Cell Biol 32:121-130.
Hollingworth P et al. (2011) Common variants at ABCA7, MS4A6A/MS4A4E, EPHA1, CD33 and CD2AP are associated with Alzheimer's disease. Nat Genet 43:429-435.
Holmin S, Hojeberg B (2004) In situ detection of intracerebral cytokine expression after human brain contusion. Neurosci Lett 369:108-114.
Honer WG (2003) Pathology of presynaptic proteins in Alzheimer's disease: more than simple loss of terminals. Neurobiology of aging 24:1047-1062.
Horowitz PM, Patterson KR, Guillozet-Bongaarts AL, Reynolds MR, Carroll CA, Weintraub ST, Bennett DA, Cryns VL, Berry RW, Binder LI (2004) Early N-terminal changes and caspase-6 cleavage of tau in Alzheimer's disease. The Journal of neuroscience : the official journal of the Society for Neuroscience 24:7895-7902.
Hoshino M, Katou H, Hagihara Y, Hasegawa K, Naiki H, Goto Y (2002) Mapping the core of the beta(2)-microglobulin amyloid fibril by H/D exchange. Nat Struct Biol 9:332-336.
Hsiao K, Chapman P, Nilsen S, Eckman C, Harigaya Y, Younkin S, Yang F, Cole G (1996) Correlative memory deficits, Abeta elevation, and amyloid plaques in transgenic mice. Science 274:99-102.
Hu X, Yuan Y, Wang D, Su Z (2016) Heterogeneous astrocytes: Active players in CNS. Brain Res Bull 125:1-18.
Huang HC, Nguyen T, Pickett CB (2002) Phosphorylation of Nrf2 at Ser-40 by protein kinase C regulates antioxidant response element-mediated transcription. J Biol Chem 277:42769-42774.
Hughes EG, Maguire JL, McMinn MT, Scholz RE, Sutherland ML (2004) Loss of glial fibrillary acidic protein results in decreased glutamate transport and inhibition of PKA-induced EAAT2 cell surface trafficking. Brain research Molecular brain research 124:114-123.
Hunter CL, Bachman D, Granholm AC (2004) Minocycline prevents cholinergic loss in a mouse model of Down's syndrome. Ann Neurol 56:675-688.
Hyman BT, West HL, Rebeck GW, Lai F, Mann DM (1995) Neuropathological changes in Down's syndrome hippocampal formation. Effect of age and apolipoprotein E genotype. Arch Neurol 52:373-378.
Iba M, McBride JD, Guo JL, Zhang B, Trojanowski JQ, Lee VM (2015) Tau pathology spread in PS19 tau transgenic mice following locus coeruleus (LC) injections of synthetic tau fibrils is determined by the LC's afferent and efferent connections. Acta neuropathologica 130:349-362.
Illes P, Verkhratsky A, Burnstock G, Franke H (2012) P2X receptors and their roles in astroglia in the central and peripheral nervous system. Neuroscientist 18:422-438.
Imai Y, Kohsaka S (2002) Intracellular signaling in M-CSF-induced microglia activation: role of Iba1. Glia 40:164-174.
Institute of Medicine (US) Forum on Drug Discovery D, and Translation (2010) Transforming Clinical Research in the United States: Challenges and Opportunities: Workshop Summary. Washington DC: National Academy of Sciences.
Iqbal K, Liu F, Gong CX (2016) Tau and neurodegenerative disease: the story so far. Nature reviews Neurology 12:15-27.
Ittner LM, Ke YD, Delerue F, Bi M, Gladbach A, van Eersel J, Wolfing H, Chieng BC, Christie MJ, Napier IA, Eckert A, Staufenbiel M, Hardeman E, Gotz J (2010) Dendritic function of tau mediates amyloid-beta toxicity in Alzheimer's disease mouse models. Cell 142:387-397.

Jack CS, Arbour N, Manusow J, Montgrain V, Blain M, McCrea E, Shapiro A, Antel JP (2005) TLR signaling tailors innate immune responses in human microglia and astrocytes. J Immunol 175:4320-4330.

Jacob A, Alexander JJ (2014) Complement and blood-brain barrier integrity. Mol Immunol 61:149-152.

Jahn H (2013) Memory loss in Alzheimer's disease. Dialogues in clinical neuroscience 15:445-454.

James G, Butt AM (2001) P2X and P2Y purinoreceptors mediate ATP-evoked calcium signalling in optic nerve glia in situ. Cell calcium 30:251-259.

Jana A, Pahan K (2010) Fibrillar amyloid-beta-activated human astroglia kill primary human neurons via neutral sphingomyelinase: implications for Alzheimer's disease. The Journal of neuroscience : the official journal of the Society for Neuroscience 30:12676-12689.

Jay TR, Miller CM, Cheng PJ, Graham LC, Bemiller S, Broihier ML, Xu G, Margevicius D, Karlo JC, Sousa GL, Cotleur AC, Butovsky O, Bekris L, Staugaitis SM, Leverenz JB, Pimplikar SW, Landreth GE, Howell GR, Ransohoff RM, Lamb BT (2015) TREM2 deficiency eliminates TREM2+ inflammatory macrophages and ameliorates pathology in Alzheimer's disease mouse models. The Journal of experimental medicine 212:287-295.

Jebelli J, Su W, Hopkins S, Pocock J, Garden GA (2015) Glia: guardians, gluttons, or guides for the maintenance of neuronal connectivity? Ann N Y Acad Sci 1351:1-10.

Ji K, Akgul G, Wollmuth LP, Tsirka SE (2013) Microglia actively regulate the number of functional synapses. PloS one 8:e56293.

Jia Z, Misra HP (2007) Reactive oxygen species in in vitro pesticide-induced neuronal cell (SH-SY5Y) cytotoxicity: role of NFkappaB and caspase-3. Free radical biology & medicine 42:288-298.

Jicha GA, Berenfeld B, Davies P (1999) Sequence requirements for formation of conformational variants of tau similar to those found in Alzheimer's disease. J Neurosci Res 55:713-723.

Jimenez-Blasco D, Santofimia-Castano P, Gonzalez A, Almeida A, Bolanos JP (2015) Astrocyte NMDA receptors' activity sustains neuronal survival through a Cdk5-Nrf2 pathway. Cell Death Differ 22:1877-1889.

Jin M, Selkoe DJ (2015) Systematic analysis of time-dependent neural effects of soluble amyloid beta oligomers in culture and in vivo: Prevention by scyllo-inositol. Neurobiology of disease 82:152-163.

Jin M, Shepardson N, Yang T, Chen G, Walsh D, Selkoe DJ (2011) Soluble amyloid beta-protein dimers isolated from Alzheimer cortex directly induce Tau hyperphosphorylation and neuritic degeneration. Proceedings of the National Academy of Sciences of the United States of America 108:5819-5824.

Jing R, Wilhelmsson U, Goodwill W, Li L, Pan Y, Pekny M, Skalli O (2007) Synemin is expressed in reactive astrocytes in neurotrauma and interacts differentially with vimentin and GFAP intermediate filament networks. J Cell Sci 120:1267-1277.

Jiwrajka M, Phillips A, Butler M, Rossi M, Pocock JM (2016) The Plant-Derived Chalcone 2,2',5'-Trihydroxychalcone Provides Neuroprotection against Toll-Like Receptor 4 Triggered Inflammation in Microglia. Oxidative medicine and cellular longevity 2016:6301712.

Jo C, Gundemir S, Pritchard S, Jin YN, Rahman I, Johnson GV (2014a) Nrf2 reduces levels of phosphorylated tau protein by inducing autophagy adaptor protein NDP52. Nature communications 5:3496.

Jo WK, Law AC, Chung SK (2014b) The neglected co-star in the dementia drama: the putative roles of astrocytes in the pathogeneses of major neurocognitive disorders. Mol Psychiatry 19:159-167.

Jofre-Monseny L, Loboda A, Wagner AE, Huebbe P, Boesch-Saadatmandi C, Jozkowicz A, Minihane AM, Dulak J, Rimbach G (2007) Effects of apoE genotype on macrophage inflammation and heme oxygenase-1 expression. Biochem Biophys Res Commun 357:319-324.

Johnson GV, Seubert P, Cox TM, Motter R, Brown JP, Galasko D (1997) The tau protein in human cerebrospinal fluid in Alzheimer's disease consists of proteolytically derived fragments. Journal of neurochemistry 68:430-433.

Jonsson T et al. (2012) A mutation in APP protects against Alzheimer's disease and age-related cognitive decline. Nature 488:96-99.

Jucker M, Walker LC (2011) Pathogenic protein seeding in Alzheimer disease and other neurodegenerative disorders. Ann Neurol 70:532-540.

Jucker M, Walker LC (2013) Self-propagation of pathogenic protein aggregates in neurodegenerative diseases. Nature 501:45-51.

Julien C, Bretteville A, Planel E (2012) Biochemical isolation of insoluble tau in transgenic mouse models of tauopathies. Methods Mol Biol 849:473-491.

Kaltschmidt B, Uherek M, Volk B, Baeuerle PA, Kaltschmidt C (1997) Transcription factor NF-kappaB is activated in primary neurons by amyloid beta peptides and in neurons surrounding early plaques from patients with Alzheimer disease. Proceedings of the National Academy of Sciences of the United States of America 94:2642-2647.

Kaltschmidt C, Kaltschmidt B, Neumann H, Wekerle H, Baeuerle PA (1994) Constitutive NF-kappa B activity in neurons. Mol Cell Biol 14:3981-3992.

Kanaan NM, Morfini G, Pigino G, LaPointe NE, Andreadis A, Song Y, Leitman E, Binder LI, Brady ST (2012) Phosphorylation in the amino terminus of tau prevents inhibition of anterograde axonal transport. Neurobiology of aging 33:826.e815-830.

Kanaan NM, Morfini GA, LaPointe NE, Pigino GF, Patterson KR, Song Y, Andreadis A, Fu Y, Brady ST, Binder LI (2011) Pathogenic forms of tau inhibit kinesin-dependent axonal transport through a mechanism involving activation of axonal phosphotransferases. The Journal of neuroscience : the official journal of the Society for Neuroscience 31:9858-9868.

Kang J, Lemaire HG, Unterbeck A, Salbaum JM, Masters CL, Grzeschik KH, Multhaup G, Beyreuther K, Muller-Hill B (1987) The precursor of Alzheimer's disease amyloid A4 protein resembles a cell-surface receptor. Nature 325:733-736.

Kanmert D, Cantlon A, Muratore CR, Jin M, O'Malley TT, Lee G, Young-Pearse TL, Selkoe DJ, Walsh DM (2015) C-Terminally Truncated Forms of Tau, But Not Full-Length Tau or Its C-Terminal Fragments, Are Released from Neurons Independently of Cell Death. The Journal of neuroscience : the official journal of the Society for Neuroscience 35:10851-10865.

Karch CM, Goate AM (2015) Alzheimer's disease risk genes and mechanisms of disease pathogenesis. Biological psychiatry 77:43-51.

Karch CM, Cruchaga C, Goate AM (2014) Alzheimer's disease genetics: from the bench to the clinic. Neuron 83:11-26.

Kelleher I, Garwood C, Hanger DP, Anderton BH, Noble W (2007) Kinase activities increase during the development of tauopathy in htau mice. Journal of neurochemistry 103:2256-2267.

Kesavapany S, Li BS, Amin N, Zheng YL, Grant P, Pant HC (2004) Neuronal cyclin-dependent kinase 5: role in nervous system function and its specific inhibition by the Cdk5 inhibitory peptide. Biochimica et biophysica acta 1697:143-153.

Khanahmadi M, Farhud DD, Malmir M (2015) Genetic of Alzheimer's Disease: A Narrative Review Article. Iranian journal of public health 44:892-901.

Kim S, Lee D, Song JC, Cho SJ, Yun SM, Koh YH, Song J, Johnson GV, Jo C (2014) NDP52 associates with phosphorylated tau in brains of an Alzheimer disease mouse model. Biochem Biophys Res Commun 454:196-201.

Kim SH, Leem JY, Lah JJ, Slunt HH, Levey AI, Thinakaran G, Sisodia SS (2001) Multiple effects of aspartate mutant presenilin 1 on the processing and trafficking of amyloid precursor protein. J Biol Chem 276:43343-43350.

Kim TS, Lim HK, Lee JY, Kim DJ, Park S, Lee C, Lee CU (2008) Changes in the levels of plasma soluble fractalkine in patients with mild cognitive impairment and Alzheimer's disease. Neurosci Lett 436:196-200.

Kimura T, Hatsuta H, Masuda-Suzukake M, Hosokawa M, Ishiguro K, Akiyama H, Murayama S, Hasegawa M, Hisanaga S (2016) The Abundance of Nonphosphorylated Tau in Mouse and Human Tauopathy Brains Revealed by the Use of Phos-Tag Method. The American journal of pathology 186:398-409.

Kirkwood B, Sterne, J. (2003) Essential Medical Statistics. Wiley-Blackwell 2:512.

Kitaguchi N, Takahashi Y, Tokushima Y, Shiojiri S, Ito H (1988) Novel precursor of Alzheimer's disease amyloid protein shows protease inhibitory activity. Nature 331:530-532.

Kitazawa M, Medeiros R, Laferla FM (2012) Transgenic mouse models of Alzheimer disease: developing a better model as a tool for therapeutic interventions. Curr Pharm Des 18:1131-1147.

Kitazawa M, Cheng D, Tsukamoto MR, Koike MA, Wes PD, Vasilevko V, Cribbs DH, LaFerla FM (2011) Blocking IL-1 signaling rescues cognition, attenuates tau pathology, and restores neuronal beta-catenin pathway function in an Alzheimer's disease model. J Immunol 187:6539-6549.

Klyubin I, Walsh DM, Lemere CA, Cullen WK, Shankar GM, Betts V, Spooner ET, Jiang L, Anwyl R, Selkoe DJ, Rowan MJ (2005) Amyloid beta protein immunotherapy neutralizes Abeta oligomers that disrupt synaptic plasticity in vivo. Nat Med 11:556-561.

Koffie RM, Meyer-Luehmann M, Hashimoto T, Adams KW, Mielke ML, Garcia-Alloza M, Micheva KD, Smith SJ, Kim ML, Lee VM, Hyman BT, Spires-Jones TL (2009) Oligomeric amyloid beta associates with postsynaptic densities and correlates with excitatory synapse loss near senile plaques. Proceedings of the National Academy of Sciences of the United States of America 106:4012-4017.

Komuro Y, Xu G, Bhaskar K, Lamb BT (2015) Human tau expression reduces adult neurogenesis in a mouse model of tauopathy. Neurobiology of aging 36:2034-2042.

Kondo K, Hashimoto H, Kitanaka J, Sawada M, Suzumura A, Marunouchi T, Baba A (1995) Expression of glutamate transporters in cultured glial cells. Neurosci Lett 188:140-142.

Kopitar-Jerala N (2015) Innate Immune Response in Brain, NF-Kappa B Signaling and Cystatins. Frontiers in molecular neuroscience 8:73.

Kouri N, Whitwell JL, Josephs KA, Rademakers R, Dickson DW (2011) Corticobasal degeneration: a pathologically distinct 4R tauopathy. Nature reviews Neurology 7:263-272.

Kovacs GG (2015) Invited review: Neuropathology of tauopathies: principles and practice. Neuropathol Appl Neurobiol 41:3-23.

Kraft AW, Hu X, Yoon H, Yan P, Xiao Q, Wang Y, Gil SC, Brown J, Wilhelmsson U, Restivo JL, Cirrito JR, Holtzman DM, Kim J, Pekny M, Lee JM (2013) Attenuating astrocyte activation accelerates plaque pathogenesis in APP/PS1 mice. FASEB journal : official publication of the Federation of American Societies for Experimental Biology 27:187-198.

Kramer VC, Calabrese DM, Nickerson KW (1980) Growth of Enterobacter cloacae in the presence of 25% sodium dodecyl sulfate. Appl Environ Microbiol 40:973-976.

Kretner B, Fukumori A, Gutsmiedl A, Page RM, Luebbers T, Galley G, Baumann K, Haass C, Steiner H (2011) Attenuated Abeta42 responses to low potency gamma-secretase modulators can be overcome for many pathogenic presenilin mutants by second-generation compounds. J Biol Chem 286:15240-15251.

Ksiezak-Reding H, Liu WK, Yen SH (1992) Phosphate analysis and dephosphorylation of modified tau associated with paired helical filaments. Brain Res 597:209-219.

Kuhn PH, Wang H, Dislich B, Colombo A, Zeitschel U, Ellwart JW, Kremmer E, Rossner S, Lichtenthaler SF (2010) ADAM10 is the physiologically relevant, constitutive alpha-secretase of the amyloid precursor protein in primary neurons. The EMBO journal 29:3020-3032.

Kurbatskaya K, Phillips EC, Croft CL, Dentoni G, Hughes MM, Wade MA, Al-Sarraj S, Troakes C, O'Neill MJ, Perez-Nievas BG, Hanger DP, Noble W (2016) Upregulation of calpain activity precedes tau phosphorylation and loss of synaptic proteins in Alzheimer's disease brain. Acta neuropathologica communications 4:34.

Laemmli UK (1970) Cleavage of structural proteins during the assembly of the head of bacteriophage T4. Nature 227:680-685.
LaFerla FM, Oddo S (2005) Alzheimer's disease: Abeta, tau and synaptic dysfunction. Trends Mol Med 11:170-176.
Lai W, Wu J, Zou X, Xie J, Zhang L, Zhao X, Zhao M, Wang Q, Ji J (2013) Secretome analyses of Abeta(1-42) stimulated hippocampal astrocytes reveal that CXCL10 is involved in astrocyte migration. Journal of proteome research 12:832-843.
Lammich S, Kojro E, Postina R, Gilbert S, Pfeiffer R, Jasionowski M, Haass C, Fahrenholz F (1999) Constitutive and regulated alpha-secretase cleavage of Alzheimer's amyloid precursor protein by a disintegrin metalloprotease. Proceedings of the National Academy of Sciences of the United States of America 96:3922-3927.
Larcher JC, Boucher D, Ginzburg I, Gros F, Denoulet P (1992) Heterogeneity of Tau proteins during mouse brain development and differentiation of cultured neurons. Dev Biol 154:195-204.
Lasagna-Reeves CA, Castillo-Carranza DL, Sengupta U, Clos AL, Jackson GR, Kayed R (2011) Tau oligomers impair memory and induce synaptic and mitochondrial dysfunction in wild-type mice. Molecular neurodegeneration 6:39.
Laske C, Stellos K, Eschweiler GW, Leyhe T, Gawaz M (2008) Decreased CXCL12 (SDF-1) plasma levels in early Alzheimer's disease: a contribution to a deficient hematopoietic brain support? Journal of Alzheimer's disease : JAD 15:83-95.
Lastres-Becker I, Garcia-Yague AJ, Scannevin RH, Casarejos MJ, Kugler S, Rabano A, Cuadrado A (2016) Repurposing the NRF2 Activator Dimethyl Fumarate as Therapy Against Synucleinopathy in Parkinson's Disease. Antioxidants & redox signaling 25:61-77.
Lau DH, Hogseth M, Phillips EC, O'Neill MJ, Pooler AM, Noble W, Hanger DP (2016) Critical residues involved in tau binding to fyn: implications for tau phosphorylation in Alzheimer's disease. Acta neuropathologica communications 4:49.
Lawrence T (2009) The nuclear factor NF-kappaB pathway in inflammation. Cold Spring Harbor perspectives in biology 1:a001651.
Lawson LJ, Perry VH, Gordon S (1992) Turnover of resident microglia in the normal adult mouse brain. Neuroscience 48:405-415.
Lebouvier T, Scales TM, Hanger DP, Geahlen RL, Lardeux B, Reynolds CH, Anderton BH, Derkinderen P (2008) The microtubule-associated protein tau is phosphorylated by Syk. Biochimica et biophysica acta 1783:188-192.
Lee DH, Gold R, Linker RA (2012) Mechanisms of oxidative damage in multiple sclerosis and neurodegenerative diseases: therapeutic modulation via fumaric acid esters. International journal of molecular sciences 13:11783-11803.
Lee G, Thangavel R, Sharma VM, Litersky JM, Bhaskar K, Fang SM, Do LH, Andreadis A, Van Hoesen G, Ksiezak-Reding H (2004) Phosphorylation of tau by fyn: implications for Alzheimer's disease. The Journal of neuroscience : the official journal of the Society for Neuroscience 24:2304-2312.
Lee S, Xu G, Jay TR, Bhatta S, Kim KW, Jung S, Landreth GE, Ransohoff RM, Lamb BT (2014) Opposing effects of membrane-anchored CX3CL1 on amyloid and tau pathologies via the p38 MAPK pathway. The Journal of neuroscience : the official journal of the Society for Neuroscience 34:12538-12546.
Lee VM, Goedert M, Trojanowski JQ (2001) Neurodegenerative tauopathies. Annu Rev Neurosci 24:1121-1159.
Lehre KP, Levy LM, Ottersen OP, Storm-Mathisen J, Danbolt NC (1995) Differential expression of two glial glutamate transporters in the rat brain: quantitative and immunocytochemical observations. The Journal of neuroscience : the official journal of the Society for Neuroscience 15:1835-1853.
Lemere CA, Blusztajn JK, Yamaguchi H, Wisniewski T, Saido TC, Selkoe DJ (1996) Sequence of deposition of heterogeneous amyloid beta-peptides and APO E in Down syndrome:

implications for initial events in amyloid plaque formation. Neurobiology of disease 3:16-32.
Lesuisse C, Martin LJ (2002) Long-term culture of mouse cortical neurons as a model for neuronal development, aging, and death. J Neurobiol 51:9-23.
Levkovitz Y, Fenchel D, Kaplan Z, Zohar J, Cohen H (2015) Early post-stressor intervention with minocycline, a second-generation tetracycline, attenuates post-traumatic stress response in an animal model of PTSD. European neuropsychopharmacology : the journal of the European College of Neuropsychopharmacology 25:124-132.
Levy-Lahad E, Wijsman EM, Nemens E, Anderson L, Goddard KA, Weber JL, Bird TD, Schellenberg GD (1995) A familial Alzheimer's disease locus on chromosome 1. Science 269:970-973.
Lewis J, Dickson DW, Lin WL, Chisholm L, Corral A, Jones G, Yen SH, Sahara N, Skipper L, Yager D, Eckman C, Hardy J, Hutton M, McGowan E (2001) Enhanced neurofibrillary degeneration in transgenic mice expressing mutant tau and APP. Science 293:1487-1491.
Lewis J, McGowan E, Rockwood J, Melrose H, Nacharaju P, Van Slegtenhorst M, Gwinn-Hardy K, Paul Murphy M, Baker M, Yu X, Duff K, Hardy J, Corral A, Lin WL, Yen SH, Dickson DW, Davies P, Hutton M (2000) Neurofibrillary tangles, amyotrophy and progressive motor disturbance in mice expressing mutant (P301L) tau protein. Nat Genet 25:402-405.
Li JJ, Dolios G, Wang R, Liao FF (2014a) Soluble beta-amyloid peptides, but not insoluble fibrils, have specific effect on neuronal microRNA expression. PloS one 9:e90770.
Li K, Jia H, She X, Cui B, Zhang N, Chen X, Xu C, An G, Ma Q (2014b) Role of NMDA receptors in noise-induced tau hyperphosphorylation in rat hippocampus and prefrontal cortex. J Neurol Sci.
Li S, Jin M, Koeglsperger T, Shepardson NE, Shankar GM, Selkoe DJ (2011) Soluble Abeta oligomers inhibit long-term potentiation through a mechanism involving excessive activation of extrasynaptic NR2B-containing NMDA receptors. The Journal of neuroscience : the official journal of the Society for Neuroscience 31:6627-6638.
Li X, Montine KS, Keene CD, Montine TJ (2015) Different mechanisms of apolipoprotein E isoform-dependent modulation of prostaglandin E2 production and triggering receptor expressed on myeloid cells 2 (TREM2) expression after innate immune activation of microglia. FASEB journal : official publication of the Federation of American Societies for Experimental Biology 29:1754-1762.
Li Y, Liu L, Barger SW, Griffin WS (2003) Interleukin-1 Mediates Pathological Effects of Microglia on Tau Phosphorylation and on Synaptophysin Synthesis in Cortical Neurons through a p38-MAPK Pathway. The Journal of Neuroscience 23:1605-1611.
Liddell BJ, Paul RH, Arns M, Gordon N, Kukla M, Rowe D, Cooper N, Moyle J, Williams LM (2007) Rates of decline distinguish Alzheimer's disease and mild cognitive impairment relative to normal aging: integrating cognition and brain function. J Integr Neurosci 6:141-174.
Lifshitz J, Friberg H, Neumar RW, Raghupathi R, Welsh FA, Janmey P, Saatman KE, Wieloch T, Grady MS, McIntosh TK (2003) Structural and functional damage sustained by mitochondria after traumatic brain injury in the rat: evidence for differentially sensitive populations in the cortex and hippocampus. Journal of cerebral blood flow and metabolism : official journal of the International Society of Cerebral Blood Flow and Metabolism 23:219-231.
Lilienbaum A, Israel A (2003) From calcium to NF-kappa B signaling pathways in neurons. Mol Cell Biol 23:2680-2698.
Lim D, Iyer A, Ronco V, Grolla AA, Canonico PL, Aronica E, Genazzani AA (2013) Amyloid beta deregulates astroglial mGluR5-mediated calcium signaling via calcineurin and Nf-kB. Glia 61:1134-1145.
Lim F, Hernandez F, Lucas JJ, Gomez-Ramos P, Moran MA, Avila J (2001) FTDP-17 mutations in tau transgenic mice provoke lysosomal abnormalities and Tau filaments in forebrain. Molecular and cellular neurosciences 18:702-714.

Lin S, Wei X, Xu Y, Yan C, Dodel R, Zhang Y, Liu J, Klaunig JE, Farlow M, Du Y (2003) Minocycline blocks 6-hydroxydopamine-induced neurotoxicity and free radical production in rat cerebellar granule neurons. Life Sci 72:1635-1641.

Lin W, Ding M, Xue J, Leng W (2013) The role of TLR2/JNK/NF-kappaB pathway in amyloid beta peptide-induced inflammatory response in mouse NG108-15 neural cells. Int Immunopharmacol 17:880-884.

Liu C, Cui G, Zhu M, Kang X, Guo H (2014) Neuroinflammation in Alzheimer's disease: chemokines produced by astrocytes and chemokine receptors. International journal of clinical and experimental pathology 7:8342-8355.

Liu F, Grundke-Iqbal I, Iqbal K, Gong CX (2005) Contributions of protein phosphatases PP1, PP2A, PP2B and PP5 to the regulation of tau phosphorylation. The European journal of neuroscience 22:1942-1950.

Liu F, Zaidi T, Iqbal K, Grundke-Iqbal I, Merkle RK, Gong CX (2002) Role of glycosylation in hyperphosphorylation of tau in Alzheimer's disease. FEBS Lett 512:101-106.

Liu K, Liu Y, Li L, Qin P, Iqbal J, Deng Y, Qing H (2016) Glycation alter the process of Tau phosphorylation to change Tau isoforms aggregation property. Biochimica et biophysica acta 1862:192-201.

Liu L, Drouet V, Wu JW, Witter MP, Small SA, Clleland C, Duff K (2012) Trans-Synaptic Spread of Tau Pathology In Vivo. PloS one 7:e31302.

Liu MC, Kobeissy F, Zheng W, Zhang Z, Hayes RL, Wang KK (2011a) Dual vulnerability of tau to calpains and caspase-3 proteolysis under neurotoxic and neurodegenerative conditions. ASN neuro 3:e00051.

Liu R, Wang Z, Gou L, Xu H (2015a) A cortical astrocyte subpopulation inhibits axon growth in vitro and in vivo. Molecular medicine reports 12:2598-2606.

Liu W, Tang Y, Feng J (2011b) Cross talk between activation of microglia and astrocytes in pathological conditions in the central nervous system. Life Sci 89:141-146.

Liu Z, Li T, Li P, Wei N, Zhao Z, Liang H, Ji X, Chen W, Xue M, Wei J (2015b) The Ambiguous Relationship of Oxidative Stress, Tau Hyperphosphorylation, and Autophagy Dysfunction in Alzheimer's Disease. Oxidative medicine and cellular longevity 2015:352723.

Lu W, Maheshwari A, Misiuta I, Fox SE, Chen N, Zigova T, Christensen RD, Calhoun DA (2005) Neutrophil-specific chemokines are produced by astrocytic cells but not by neuronal cells. Brain research Developmental brain research 155:127-134.

Madrigal JL, Leza JC, Polak P, Kalinin S, Feinstein DL (2009) Astrocyte-derived MCP-1 mediates neuroprotective effects of noradrenaline. The Journal of neuroscience : the official journal of the Society for Neuroscience 29:263-267.

Maeda E, Robinson HP, Kawana A (1995) The mechanisms of generation and propagation of synchronized bursting in developing networks of cortical neurons. The Journal of neuroscience : the official journal of the Society for Neuroscience 15:6834-6845.

Magistri M, Velmeshev D, Makhmutova M, Patel P, Sartor GC, Volmar CH, Wahlestedt C, Faghihi MA (2016) The BET-bromodomain inhibitor JQ1 reduces inflammation and tau phosphorylation at Ser396 in the brain of the 3xTg model of Alzheimer's disease. Current Alzheimer research 13:985-995.

Magnusson JP, Frisen J (2016) Stars from the darkest night: unlocking the neurogenic potential of astrocytes in different brain regions. Development 143:1075-1086.

Maher F (1995) Immunolocalization of GLUT1 and GLUT3 glucose transporters in primary cultured neurons and glia. J Neurosci Res 42:459-469.

Maher F, Davies-Hill TM, Lysko PG, Henneberry RC, Simpson IA (1991) Expression of two glucose transporters, GLUT1 and GLUT3, in cultured cerebellar neurons: Evidence for neuron-specific expression of GLUT3. Molecular and cellular neurosciences 2:351-360.

Majkutewicz I, Kurowska E, Podlacha M, Myslinska D, Grembecka B, Rucinski J, Plucinska K, Jerzemowska G, Wrona D (2016) Dimethyl fumarate attenuates intracerebroventricular

streptozotocin-induced spatial memory impairment and hippocampal neurodegeneration in rats. Behav Brain Res 308:24-37.
Mandelkow EM, Stamer K, Vogel R, Thies E, Mandelkow E (2003) Clogging of axons by tau, inhibition of axonal traffic and starvation of synapses. Neurobiology of aging 24:1079-1085.
Maphis N, Xu G, Kokiko-Cochran ON, Jiang S, Cardona A, Ransohoff RM, Lamb BT, Bhaskar K (2015) Reactive microglia drive tau pathology and contribute to the spreading of pathological tau in the brain. Brain : a journal of neurology 138:1738-1755.
Marcus JN, Schachter J (2011) Targeting post-translational modifications on tau as a therapeutic strategy for Alzheimer's disease. J Neurogenet 25:127-133.
Martin L, Latypova X, Terro F (2011) Post-translational modifications of tau protein: implications for Alzheimer's disease. Neurochem Int 58:458-471.
Martin L, Latypova X, Wilson CM, Magnaudeix A, Perrin ML, Yardin C, Terro F (2013) Tau protein kinases: involvement in Alzheimer's disease. Ageing research reviews 12:289-309.
Martinez FO, Gordon S (2014) The M1 and M2 paradigm of macrophage activation: time for reassessment. F1000prime reports 6:13.
Matos M, Augusto E, Oliveira CR, Agostinho P (2008) Amyloid-beta peptide decreases glutamate uptake in cultured astrocytes: involvement of oxidative stress and mitogen-activated protein kinase cascades. Neuroscience 156:898-910.
Mattsson N, Carrillo MC, Dean RA, Devous MD, Sr., Nikolcheva T, Pesini P, Salter H, Potter WZ, Sperling RS, Bateman RJ, Bain LJ, Liu E (2015) Revolutionizing Alzheimer's disease and clinical trials through biomarkers. Alzheimer's & dementia (Amsterdam, Netherlands) 1:412-419.
Matute C, Melone M, Vallejo-Illarramendi A, Conti F (2005) Increased expression of the astrocytic glutamate transporter GLT-1 in the prefrontal cortex of schizophrenics. Glia 49:451-455.
McAlpine FE, Lee JK, Harms AS, Ruhn KA, Blurton-Jones M, Hong J, Das P, Golde TE, LaFerla FM, Oddo S, Blesch A, Tansey MG (2009) Inhibition of soluble TNF signaling in a mouse model of Alzheimer's disease prevents pre-plaque amyloid-associated neuropathology. Neurobiology of disease 34:163-177.
McGeer EG, McGeer PL (2003) Inflammatory processes in Alzheimer's disease. Prog Neuro-Psychopharmacol Biol Psychiatry 27:741-749.
McGeer PL, McGeer EG (1996) Anti-inflammatory drugs in the fight against Alzheimer's disease. Ann N Y Acad Sci 777:213-220.
McGeer PL, McGeer EG (2013) The amyloid cascade-inflammatory hypothesis of Alzheimer disease: implications for therapy. Acta neuropathologica 126:479-497.
McKenna MC (2012) Substrate competition studies demonstrate oxidative metabolism of glucose, glutamate, glutamine, lactate and 3-hydroxybutyrate in cortical astrocytes from rat brain. Neurochem Res 37:2613-2626.
McKhann G, Drachman D, Folstein M, Katzman R, Price D, Stadlan EM (1984) Clinical diagnosis of Alzheimer's disease: report of the NINCDS-ADRDA Work Group under the auspices of Department of Health and Human Services Task Force on Alzheimer's Disease. Neurology 34:939-944.
Meraz-Rios MA, Lira-De Leon KI, Campos-Pena V, De Anda-Hernandez MA, Mena-Lopez R (2010) Tau oligomers and aggregation in Alzheimer's disease. Journal of neurochemistry 112:1353-1367.
Mergenthaler P, Lindauer U, Dienel GA, Meisel A (2013) Sugar for the brain: the role of glucose in physiological and pathological brain function. Trends Neurosci 36:587-597.
Mexal S, Berger R, Adams CE, Ross RG, Freedman R, Leonard S (2006) Brain pH has a significant impact on human postmortem hippocampal gene expression profiles. Brain Res 1106:1-11.
Meyer-Luehmann M, Prinz M (2015) Myeloid cells in Alzheimer's disease: culprits, victims or innocent bystanders? Trends Neurosci 38:659-668.

Middeldorp J, Hol EM (2011) GFAP in health and disease. Prog Neurobiol 93:421-443.
Miguel-Alvarez M, Santos-Lozano A, Sanchis-Gomar F, Fiuza-Luces C, Pareja-Galeano H, Garatachea N, Lucia A (2015) Non-steroidal anti-inflammatory drugs as a treatment for Alzheimer's disease: a systematic review and meta-analysis of treatment effect. Drugs & aging 32:139-147.
Min SW et al. (2015) Critical role of acetylation in tau-mediated neurodegeneration and cognitive deficits. Nat Med 21:1154-1162.
Minano-Molina AJ, Espana J, Martin E, Barneda-Zahonero B, Fado R, Sole M, Trullas R, Saura CA, Rodriguez-Alvarez J (2011) Soluble oligomers of amyloid-beta peptide disrupt membrane trafficking of alpha-amino-3-hydroxy-5-methylisoxazole-4-propionic acid receptor contributing to early synapse dysfunction. J Biol Chem 286:27311-27321.
Minogue AM, Stubbs AK, Frigerio CS, Boland B, Fadeeva JV, Tang J, Selkoe DJ, Walsh DM (2009) gamma-secretase processing of APLP1 leads to the production of a p3-like peptide that does not aggregate and is not toxic to neurons. Brain Res 1262:89-99.
Mitew S, Kirkcaldie MT, Dickson TC, Vickers JC (2013) Altered synapses and gliotransmission in Alzheimer's disease and AD model mice. Neurobiology of aging 34:2341-2351.
Mochizuki Y, Iida A, Lyons E, Kageyama R, Nakauchi H, Murakami A, Watanabe S (2014) Use of cell type-specific transcriptome to identify genes specifically involved in Muller glia differentiation during retinal development. Developmental neurobiology 74:426-437.
Moharregh-Khiabani D, Blank A, Skripuletz T, Miller E, Kotsiari A, Gudi V, Stangel M (2010) Effects of fumaric acids on cuprizone induced central nervous system de- and remyelination in the mouse. PloS one 5:e11769.
Molofsky AV, Krencik R, Ullian EM, Tsai HH, Deneen B, Richardson WD, Barres BA, Rowitch DH (2012) Astrocytes and disease: a neurodevelopmental perspective. Genes Dev 26:891-907.
Mondragon-Rodriguez S, Perry G, Luna-Munoz J, Acevedo-Aquino MC, Williams S (2014) Phosphorylation of tau protein at sites Ser(396-404) is one of the earliest events in Alzheimer's disease and Down syndrome. Neuropathol Appl Neurobiol 40:121-135.
Mondragon-Rodriguez S, Mena R, Binder LI, Smith MA, Perry G, Garcia-Sierra F (2008a) Conformational changes and cleavage of tau in Pick bodies parallel the early processing of tau found in Alzheimer pathology. Neuropathol Appl Neurobiol 34:62-75.
Mondragon-Rodriguez S, Basurto-Islas G, Santa-Maria I, Mena R, Binder LI, Avila J, Smith MA, Perry G, Garcia-Sierra F (2008b) Cleavage and conformational changes of tau protein follow phosphorylation during Alzheimer's disease. International journal of experimental pathology 89:81-90.
Morales I, Guzman-Martinez L, Cerda-Troncoso C, Farias GA, Maccioni RB (2014) Neuroinflammation in the pathogenesis of Alzheimer's disease. A rational framework for the search of novel therapeutic approaches. Frontiers in cellular neuroscience 8:112.
Morgello S, Uson RR, Schwartz EJ, Haber RS (1995) The human blood-brain barrier glucose transporter (GLUT1) is a glucose transporter of gray matter astrocytes. Glia 14:43-54.
Morris R (1984) Developments of a water-maze procedure for studying spatial learning in the rat. J Neurosci Methods 11:47-60.
Mrak RE, Griffin WS (2005) Glia and their cytokines in progression of neurodegeneration. Neurobiology of aging 26:349-354.
Mufson EJ, Ikonomovic MD, Counts SE, Perez SE, Malek-Ahmadi M, Scheff SW, Ginsberg SD (2016) Molecular and Cellular Pathophysiology of Preclinical Alzheimer's Disease. Behav Brain Res 311:54-69.
Mulder SD, Nielsen HM, Blankenstein MA, Eikelenboom P, Veerhuis R (2014) Apolipoproteins E and J interfere with amyloid-beta uptake by primary human astrocytes and microglia in vitro. Glia 62:493-503.
Muller T, Meyer HE, Egensperger R, Marcus K (2008) The amyloid precursor protein intracellular domain (AICD) as modulator of gene expression, apoptosis, and cytoskeletal dynamics-relevance for Alzheimer's disease. Prog Neurobiol 85:393-406.

Murgas P, Godoy B, von Bernhardi R (2012) Abeta potentiates inflammatory activation of glial cells induced by scavenger receptor ligands and inflammatory mediators in culture. Neurotoxicity research 22:69-78.

Naj AC et al. (2014) Effects of multiple genetic loci on age at onset in late-onset Alzheimer disease: a genome-wide association study. JAMA neurology 71:1394-1404.

Nasaruddin ML, Holscher C, Kehoe P, Graham SF, Green BD (2016) Wide-ranging alterations in the brain fatty acid complement of subjects with late Alzheimer's disease as detected by GC-MS. American journal of translational research 8:154-165.

Nash KR, Lee DC, Hunt JB, Jr., Morganti JM, Selenica ML, Moran P, Reid P, Brownlow M, Guang-Yu Yang C, Savalia M, Gemma C, Bickford PC, Gordon MN, Morgan D (2013) Fractalkine overexpression suppresses tau pathology in a mouse model of tauopathy. Neurobiology of aging 34:1540-1548.

Navarrete M, Perea G, Maglio L, Pastor J, Garcia de Sola R, Araque A (2013) Astrocyte calcium signal and gliotransmission in human brain tissue. Cereb Cortex 23:1240-1246.

Neuman KM, Molina-Campos E, Musial TF, Price AL, Oh KJ, Wolke ML, Buss EW, Scheff SW, Mufson EJ, Nicholson DA (2015) Evidence for Alzheimer's disease-linked synapse loss and compensation in mouse and human hippocampal CA1 pyramidal neurons. Brain structure & function 220:3143-3165.

Nielsen HM, Mulder SD, Belien JA, Musters RJ, Eikelenboom P, Veerhuis R (2010) Astrocytic A beta 1-42 uptake is determined by A beta-aggregation state and the presence of amyloid-associated proteins. Glia 58:1235-1246.

Niger C, Buo AM, Hebert C, Duggan BT, Williams MS, Stains JP (2012) ERK acts in parallel to PKCdelta to mediate the connexin43-dependent potentiation of Runx2 activity by FGF2 in MC3T3 osteoblasts. American journal of physiology Cell physiology 302:C1035-1044.

Nimmerjahn A, Kirchhoff F, Helmchen F (2005) Resting microglial cells are highly dynamic surveillants of brain parenchyma in vivo. Science 308:1314-1318.

Niture SK, Khatri R, Jaiswal AK (2014) Regulation of Nrf2-an update. Free radical biology & medicine 66:36-44.

Noble W, Garwood C, Hanger DP (2009a) Minocycline as a potential therapeutic agent in neurodegenerative disorders charactersied by protein misfolding. Prion 3:78-83.

Noble W, Hanger DP, Gallo JM (2010) Transgenic mouse models of tauopathy in drug discovery. CNS & neurological disorders drug targets 9:403-428.

Noble W, Hanger DP, Miller CC, Lovestone S (2013) The importance of tau phosphorylation for neurodegenerative diseases. Frontiers in neurology 4:83-94.

Noble W, Garwood C, Stephenson J, Kinsey AM, Hanger DP, Anderton BH (2009b) Minocycline reduces the development of abnormal tau species in models of Alzheimer's disease. FASEB journal : official publication of the Federation of American Societies for Experimental Biology 23:739-750.

Noble W, Olm V, Takata K, Casey E, Mary O, Meyerson J, Gaynor K, LaFrancois J, Wang L, Kondo T, Davies P, Burns M, Veeranna, Nixon R, Dickson D, Matsuoka Y, Ahlijanian M, Lau LF, Duff K (2003) Cdk5 is a key factor in tau aggregation and tangle formation in vivo. Neuron 38:555-565.

O'Brien RJ, Wong PC (2011) Amyloid precursor protein processing and Alzheimer's disease. Annu Rev Neurosci 34:185-204.

Oberheim NA, Takano T, Han X, He W, Lin JH, Wang F, Xu Q, Wyatt JD, Pilcher W, Ojemann JG, Ransom BR, Goldman SA, Nedergaard M (2009) Uniquely hominid features of adult human astrocytes. The Journal of neuroscience : the official journal of the Society for Neuroscience 29:3276-3287.

Oddo S, Caccamo A, Shepherd JD, Murphy MP, Golde TE, Kayed R, Metherate R, Mattson MP, Akbari Y, LaFerla FM (2003) Triple-transgenic model of Alzheimer's disease with plaques and tangles: intracellular Abeta and synaptic dysfunction. Neuron 39:409-421.

Ojala J, Alafuzoff I, Herukka SK, van Groen T, Tanila H, Pirttila T (2009) Expression of interleukin-18 is increased in the brains of Alzheimer's disease patients. Neurobiology of aging 30:198-209.

Olabarria M, Noristani HN, Verkhratsky A, Rodriguez JJ (2010) Concomitant astroglial atrophy and astrogliosis in a triple transgenic animal model of Alzheimer's disease. Glia 58:831-838.

Oltersdorf T, Fritz LC, Schenk DB, Lieberburg I, Johnson-Wood KL, Beattie EC, Ward PJ, Blacher RW, Dovey HF, Sinha S (1989) The secreted form of the Alzheimer's amyloid precursor protein with the Kunitz domain is protease nexin-II. Nature 341:144-147.

Ondrejcak T, Klyubin I, Hu NW, Barry AE, Cullen WK, Rowan MJ (2010) Alzheimer's disease amyloid beta-protein and synaptic function. Neuromolecular medicine 12:13-26.

Oppenheim JJ, Zachariae CO, Mukaida N, Matsushima K (1991) Properties of the novel proinflammatory supergene "intercrine" cytokine family. Annu Rev Immunol 9:617-648.

Orellana JA, Froger N, Ezan P, Jiang JX, Bennett MV, Naus CC, Giaume C, Saez JC (2011) ATP and glutamate released via astroglial connexin 43 hemichannels mediate neuronal death through activation of pannexin 1 hemichannels. Journal of neurochemistry 118:826-840.

Orre M, Kamphuis W, Dooves S, Kooijman L, Chan ET, Kirk CJ, Dimayuga Smith V, Koot S, Mamber C, Jansen AH, Ovaa H, Hol EM (2013) Reactive glia show increased immunoproteasome activity in Alzheimer's disease. Brain : a journal of neurology 136:1415-1431.

Ovanesov MV, Ayhan Y, Wolbert C, Moldovan K, Sauder C, Pletnikov MV (2008) Astrocytes play a key role in activation of microglia by persistent Borna disease virus infection. Journal of neuroinflammation 5:50.

Pankiewicz JE, Guridi M, Kim J, Asuni AA, Sanchez S, Sullivan PM, Holtzman DM, Sadowski MJ (2014) Blocking the apoE/Abeta interaction ameliorates Abeta-related pathology in APOE epsilon2 and epsilon4 targeted replacement Alzheimer model mice. Acta neuropathologica communications 2:75.

Park SY, Ferreira A (2005) The generation of a 17 kDa neurotoxic fragment: an alternative mechanism by which tau mediates beta-amyloid-induced neurodegeneration. The Journal of neuroscience : the official journal of the Society for Neuroscience 25:5365-5375.

Patel NS, Paris D, Mathura V, Quadros AN, Crawford FC, Mullan MJ (2005) Inflammatory cytokine levels correlate with amyloid load in transgenic mouse models of Alzheimer's disease. Journal of neuroinflammation 2:9.

Patrick GN, Zukerberg L, Nikolic M, de la Monte S, Dikkes P, Tsai LH (1999) Conversion of p35 to p25 deregulates Cdk5 activity and promotes neurodegeneration. Nature 402:615-622.

Pekny M, Pekna M (2004) Astrocyte intermediate filaments in CNS pathologies and regeneration. The Journal of pathology 204:428-437.

Pekny M, Nilsson M (2005) Astrocyte activation and reactive gliosis. Glia 50:427-434.

Pekny M, Wilhelmsson U, Pekna M (2014) The dual role of astrocyte activation and reactive gliosis. Neurosci Lett 565:30-38.

Pekny M, Leveen P, Pekna M, Eliasson C, Berthold CH, Westermark B, Betsholtz C (1995) Mice lacking glial fibrillary acidic protein display astrocytes devoid of intermediate filaments but develop and reproduce normally. The EMBO journal 14:1590-1598.

Pellerin L, Magistretti PJ (2012) Sweet sixteen for ANLS. Journal of cerebral blood flow and metabolism : official journal of the International Society of Cerebral Blood Flow and Metabolism 32:1152-1166.

Pellerin L, Bouzier-Sore AK, Aubert A, Serres S, Merle M, Costalat R, Magistretti PJ (2007) Activity-dependent regulation of energy metabolism by astrocytes: an update. Glia 55:1251-1262.

Pellerin L, Pellegri G, Bittar PG, Charnay Y, Bouras C, Martin JL, Stella N, Magistretti PJ (1998) Evidence supporting the existence of an activity-dependent astrocyte-neuron lactate shuttle. Dev Neurosci 20:291-299.

Peng J, Xie L, Stevenson FF, Melov S, Di Monte DA, Andersen JK (2006) Nigrostriatal dopaminergic neurodegeneration in the weaver mouse is mediated via neuroinflammation and alleviated by minocycline administration. The Journal of neuroscience : the official journal of the Society for Neuroscience 26:11644-11651.

Peppard J, Glickman F, He Y, Hu SI, Doughty J, Goldberg R (2003) Development of a high-throughput screening assay for inhibitors of aggrecan cleavage using luminescent oxygen channeling (AlphaScreen). J Biomol Screen 8:149-156.

Perea G, Navarrete M, Araque A (2009) Tripartite synapses: astrocytes process and control synaptic information. Trends Neurosci 32:421-431.

Perez-Nievas BG, Stein TD, Tai HC, Dols-Icardo O, Scotton TC, Barroeta-Espar I, Fernandez-Carballo L, de Munain EL, Perez J, Marquie M, Serrano-Pozo A, Frosch MP, Lowe V, Parisi JE, Petersen RC, Ikonomovic MD, Lopez OL, Klunk W, Hyman BT, Gomez-Isla T (2013) Dissecting phenotypic traits linked to human resilience to Alzheimer's pathology. Brain : a journal of neurology 136:2510-2526.

Perry VH (2016) Microglia. Microbiology spectrum 4.

Perry VH, Teeling J (2013) Microglia and macrophages of the central nervous system: the contribution of microglia priming and systemic inflammation to chronic neurodegeneration. Seminars in immunopathology 35:601-612.

Perry VH, Holmes C (2014) Microglial priming in neurodegenerative disease. Nature reviews Neurology 10:217-224.

Pesaresi M, Lovati C, Bertora P, Mailland E, Galimberti D, Scarpini E, Quadri P, Forloni G, Mariani C (2006) Plasma levels of beta-amyloid (1-42) in Alzheimer's disease and mild cognitive impairment. Neurobiology of aging 27:904-905.

Petrelli F, Bezzi P (2016) Novel insights into gliotransmitters. Curr Opin Pharmacol 26:138-145.

Phillips EC, Croft CL, Kurbatskaya K, O'Neill MJ, Hutton ML, Hanger DP, Garwood CJ, Noble W (2014) Astrocytes and neuroinflammation in Alzheimer's disease. Biochemical Society transactions 42:1321-1325.

Pisetsky DS (2012) The origin and properties of extracellular DNA: from PAMP to DAMP. Clinical immunology (Orlando, Fla) 144:32-40.

Platt B, Drever B, Koss D, Stoppelkamp S, Jyoti A, Plano A, Utan A, Merrick G, Ryan D, Melis V, Wan H, Mingarelli M, Porcu E, Scrocchi L, Welch A, Riedel G (2011) Abnormal cognition, sleep, EEG and brain metabolism in a novel knock-in Alzheimer mouse, PLB1. PloS one 6:e27068.

Pocock JM, Liddle AC (2001) Microglial signalling cascades in neurodegenerative disease. Prog Brain Res 132:555-565.

Pocock JM, Kettenmann H (2007) Neurotransmitter receptors on microglia. Trends Neurosci 30:527-535.

Polanco JC, Scicluna BJ, Hill AF, Gotz J (2016) Extracellular Vesicles Isolated from the Brains of rTg4510 Mice Seed Tau Protein Aggregation in a Threshold-dependent Manner. J Biol Chem 291:12445-12466.

Politis M, Piccini P (2012) Positron emission tomography imaging in neurological disorders. Journal of neurology 259:1769-1780.

Politis M, Su P, Piccini P (2012) Imaging of microglia in patients with neurodegenerative disorders. Frontiers in pharmacology 3:96.

Polydoro M, Acker CM, Duff K, Castillo PE, Davies P (2009) Age-dependent impairment of cognitive and synaptic function in the htau mouse model of tau pathology. The Journal of neuroscience : the official journal of the Society for Neuroscience 29:10741-10749.

Ponte P, Gonzalez-DeWhitt P, Schilling J, Miller J, Hsu D, Greenberg B, Davis K, Wallace W, Lieberburg I, Fuller F (1988) A new A4 amyloid mRNA contains a domain homologous to serine proteinase inhibitors. Nature 331:525-527.

Pooler AM, Noble W, Hanger DP (2014) A role for tau at the synapse in Alzheimer's disease pathogenesis. Neuropharmacology 76 Pt A:1-8.

Pooler AM, Phillips EC, Lau DH, Noble W, Hanger DP (2013) Physiological release of endogenous tau is stimulated by neuronal activity. EMBO reports 14:389-394.

Pooler AM, Usardi A, Evans CJ, Philpott KL, Noble W, Hanger DP (2012) Dynamic association of tau with neuronal membranes is regulated by phosphorylation. Neurobiology of aging 33:431 e427-438.

Pooler AM, Polydoro M, Maury EA, Nicholls SB, Reddy SM, Wegmann S, William C, Saqran L, Cagsal-Getkin O, Pitstick R, Beier DR, Carlson GA, Spires-Jones TL, Hyman BT (2015) Amyloid accelerates tau propagation and toxicity in a model of early Alzheimer's disease. Acta neuropathologica communications 3:14.

Portelius E, Olsson M, Brinkmalm G, Ruetschi U, Mattsson N, Andreasson U, Gobom J, Brinkmalm A, Holtta M, Blennow K, Zetterberg H (2013) Mass spectrometric characterization of amyloid-beta species in the 7PA2 cell model of Alzheimer's disease. Journal of Alzheimer's disease : JAD 33:85-93.

Powers KM, Kay DM, Factor SA, Zabetian CP, Higgins DS, Samii A, Nutt JG, Griffith A, Leis B, Roberts JW, Martinez ED, Montimurro JS, Checkoway H, Payami H (2008) Combined effects of smoking, coffee, and NSAIDs on Parkinson's disease risk. Movement disorders : official journal of the Movement Disorder Society 23:88-95.

Priller C, Bauer T, Mitteregger G, Krebs B, Kretzschmar HA, Herms J (2006) Synapse formation and function is modulated by the amyloid precursor protein. The Journal of neuroscience : the official journal of the Society for Neuroscience 26:7212-7221.

Prince MW, A.; Guerchet, M.; Ali G. C.; Wu, Y.; Prina, M. (2015) World Alzheimer Report 2015: The Global Impact of Dementia. Alzheimer's Disease International.

Pugazhenthi S, Zhang Y, Bouchard R, Mahaffey G (2013) Induction of an inflammatory loop by interleukin-1beta and tumor necrosis factor-alpha involves NF-kB and STAT-1 in differentiated human neuroprogenitor cells. PloS one 8:e69585.

Qian W, Liu F (2014) Regulation of alternative splicing of tau exon 10. Neuroscience bulletin 30:367-377.

Qiu T, Liu Q, Chen YX, Zhao YF, Li YM (2015) Abeta42 and Abeta40: similarities and differences. Journal of peptide science : an official publication of the European Peptide Society 21:522-529.

Quintanilla RA, Orellana DI, Gonzalez-Billault C, Maccioni RB (2004) Interleukin-6 induces Alzheimer-type phosphorylation of tau protein by deregulating the cdk5/p35 pathway. Exp Cell Res 295:245-257.

Ransohoff RM, Cardona AE (2010) The myeloid cells of the central nervous system parenchyma. Nature 468:253-262.

Rapoport M, Dawson HN, Binder LI, Vitek MP, Ferreira A (2002) Tau is essential to beta -amyloid-induced neurotoxicity. Proceedings of the National Academy of Sciences of the United States of America 99:6364-6369.

Re DB, Le Verche V, Yu C, Amoroso MW, Politi KA, Phani S, Ikiz B, Hoffmann L, Koolen M, Nagata T, Papadimitriou D, Nagy P, Mitsumoto H, Kariya S, Wichterle H, Henderson CE, Przedborski S (2014) Necroptosis drives motor neuron death in models of both sporadic and familial ALS. Neuron 81:1001-1008.

Reed MN, Hofmeister JJ, Jungbauer L, Welzel AT, Yu C, Sherman MA, Lesne S, LaDu MJ, Walsh DM, Ashe KH, Cleary JP (2011) Cognitive effects of cell-derived and synthetically derived Abeta oligomers. Neurobiology of aging 32:1784-1794.

Reynolds MR, Reyes JF, Fu Y, Bigio EH, Guillozet-Bongaarts AL, Berry RW, Binder LI (2006) Tau nitration occurs at tyrosine 29 in the fibrillar lesions of Alzheimer's disease and other tauopathies. The Journal of neuroscience : the official journal of the Society for Neuroscience 26:10636-10645.

Ribe EM, Perez M, Puig B, Gich I, Lim F, Cuadrado M, Sesma T, Catena S, Sanchez B, Nieto M, Gomez-Ramos P, Moran MA, Cabodevilla F, Samaranch L, Ortiz L, Perez A, Ferrer I, Avila J, Gomez-Isla T (2005) Accelerated amyloid deposition, neurofibrillary degeneration and

neuronal loss in double mutant APP/tau transgenic mice. Neurobiology of disease 20:814-822.
Riedel BC, Thompson PM, Brinton RD (2016) Age, APOE and sex: Triad of risk of Alzheimer's disease. The Journal of steroid biochemistry and molecular biology 160:134-147.
Roberson ED, Scearce-Levie K, Palop JJ, Yan F, Cheng IH, Wu T, Gerstein H, Yu GQ, Mucke L (2007) Reducing endogenous tau ameliorates amyloid beta-induced deficits in an Alzheimer's disease mouse model. Science 316:750-754.
Roberson ED, Halabisky B, Yoo JW, Yao J, Chin J, Yan F, Wu T, Hamto P, Devidze N, Yu GQ, Palop JJ, Noebels JL, Mucke L (2011) Amyloid-beta/Fyn-induced synaptic, network, and cognitive impairments depend on tau levels in multiple mouse models of Alzheimer's disease. The Journal of neuroscience : the official journal of the Society for Neuroscience 31:700-711.
Rodriguez-Arellano JJ, Parpura V, Zorec R, Verkhratsky A (2016) Astrocytes in physiological aging and Alzheimer's disease. Neuroscience 323:170-182.
Rodriguez-Martin T, Cuchillo-Ibanez I, Noble W, Nyenya F, Anderton BH, Hanger DP (2013) Tau phosphorylation affects its axonal transport and degradation. Neurobiology of aging 34:2146-2157.
Rodriguez JJ, Witton J, Olabarria M, Noristani HN, Verkhratsky A (2010) Increase in the density of resting microglia precedes neuritic plaque formation and microglial activation in a transgenic model of Alzheimer's disease. Cell death & disease 1:e1-6.
Rodriguez JJ, Butt AM, Gardenal E, Parpura V, Verkhratsky A (2016) Complex and differential glial responses in Alzheimer's disease and ageing. Current Alzheimer research 13:343-358.
Rodriguez JJ, Yeh CY, Terzieva S, Olabarria M, Kulijewicz-Nawrot M, Verkhratsky A (2014) Complex and region-specific changes in astroglial markers in the aging brain. Neurobiology of aging 35:15-23.
Roerink ME, Groen RJ, Franssen G, Lemmers-van de Weem B, Boerman OC, van der Meer JW (2015) Central delivery of iodine-125-labeled cetuximab, etanercept and anakinra after perispinal injection in rats: possible implications for treating Alzheimer's disease. Alzheimer's research & therapy 7:70.
Rosenberg RN, Lambracht-Washington D, Yu G, Xia W (2016) Genomics of Alzheimer Disease: A Review. JAMA neurology 73:867-874.
Rossi G, Dalpra L, Crosti F, Lissoni S, Sciacca FL, Catania M, Di Fede G, Mangieri M, Giaccone G, Croci D, Tagliavini F (2008) A new function of microtubule-associated protein tau: involvement in chromosome stability. Cell cycle (Georgetown, Tex) 7:1788-1794.
Rothhammer V, Quintana FJ (2015) Control of autoimmune CNS inflammation by astrocytes. Seminars in immunopathology 37:625-638.
Rothwell NJ, Relton JK (1993) Involvement of cytokines in acute neurodegeneration in the CNS. Neuroscience and biobehavioral reviews 17:217-227.
Rothwell NJ, Luheshi GN (2000) Interleukin 1 in the brain: biology, pathology and therapeutic target. Trends Neurosci 23:618-625.
Rovelet-Lecrux A, Hannequin D, Raux G, Le Meur N, Laquerriere A, Vital A, Dumanchin C, Feuillette S, Brice A, Vercelletto M, Dubas F, Frebourg T, Campion D (2006) APP locus duplication causes autosomal dominant early-onset Alzheimer disease with cerebral amyloid angiopathy. Nat Genet 38:24-26.
Rubio-Perez JM, Morillas-Ruiz JM (2012) A review: inflammatory process in Alzheimer's disease, role of cytokines. TheScientificWorldJournal 2012:756357.
Ryu JK, Choi HB, McLarnon JG (2006) Combined minocycline plus pyruvate treatment enhances effects of each agent to inhibit inflammation, oxidative damage, and neuronal loss in an excitotoxic animal model of Huntington's disease. Neuroscience 141:1835-1848.
Ryu JK, Franciosi S, Sattayaprasert P, Kim SU, McLarnon JG (2004) Minocycline inhibits neuronal death and glial activation induced by beta-amyloid peptide in rat hippocampus. Glia 48:85-90.

Rzechorzek NM, Connick P, Patani R, Selvaraj BT, Chandran S (2015) Hypothermic Preconditioning of Human Cortical Neurons Requires Proteostatic Priming. EBioMedicine 2:528-535.

Rzechorzek NM, Connick P, Livesey MR, Borooah S, Patani R, Burr K, Story D, Wyllie DJ, Hardingham GE, Chandran S (2016) Hypothermic Preconditioning Reverses Tau Ontogenesis in Human Cortical Neurons and is Mimicked by Protein Phosphatase 2A Inhibition. EBioMedicine 3:141-154.

Salani F, Ciaramella A, Bizzoni F, Assogna F, Caltagirone C, Spalletta G, Bossu P (2013) Increased expression of interleukin-18 receptor in blood cells of subjects with mild cognitive impairment and Alzheimer's disease. Cytokine 61:360-363.

Saman S, Kim W, Raya M, Visnick Y, Miro S, Saman S, Jackson B, McKee AC, Alvarez VE, Lee NC, Hall GF (2012) Exosome-associated tau is secreted in tauopathy models and is selectively phosphorylated in cerebrospinal fluid in early Alzheimer disease. J Biol Chem 287:3842-3849.

Santpere G, Puig B, Ferrer I (2006) Low molecular weight species of tau in Alzheimer's disease are dependent on tau phosphorylation sites but not on delayed post-mortem delay in tissue processing. Neurosci Lett 399:106-110.

Saura CA (2010) Presenilin/gamma-Secretase and Inflammation. Frontiers in aging neuroscience 2:16.

Savage JC, Jay T, Goduni E, Quigley C, Mariani MM, Malm T, Ransohoff RM, Lamb BT, Landreth GE (2015) Nuclear receptors license phagocytosis by trem2+ myeloid cells in mouse models of Alzheimer's disease. The Journal of neuroscience : the official journal of the Society for Neuroscience 35:6532-6543.

Savioz A, Leuba G, Vallet PG (2014) A framework to understand the variations of PSD-95 expression in brain aging and in Alzheimer's disease. Ageing research reviews 18:86-94.

Scannevin RH, Chollate S, Jung MY, Shackett M, Patel H, Bista P, Zeng W, Ryan S, Yamamoto M, Lukashev M, Rhodes KJ (2012) Fumarates promote cytoprotection of central nervous system cells against oxidative stress via the nuclear factor (erythroid-derived 2)-like 2 pathway. The Journal of pharmacology and experimental therapeutics 341:274-284.

Scemes E, Giaume C (2006) Astrocyte calcium waves: what they are and what they do. Glia 54:716-725.

Schellenberg GD, Montine TJ (2012) The genetics and neuropathology of Alzheimer's disease. Acta neuropathologica 124:305-323.

Scheuner D et al. (1996) Secreted amyloid beta-protein similar to that in the senile plaques of Alzheimer's disease is increased in vivo by the presenilin 1 and 2 and APP mutations linked to familial Alzheimer's disease. Nat Med 2:864-870.

Schierle GS, Michel CH, Gasparini L (2016) Advanced imaging of tau pathology in Alzheimer Disease: New perspectives from super resolution microscopy and label-free nanoscopy. Microsc Res Tech 79:677-683.

Schildge S, Bohrer C, Beck K, Schachtrup C (2013) Isolation and culture of mouse cortical astrocytes. J Vis Exp.

Schilling S, Goelz S, Linker R, Luehder F, Gold R (2006) Fumaric acid esters are effective in chronic experimental autoimmune encephalomyelitis and suppress macrophage infiltration. Clin Exp Immunol 145:101-107.

Schindowski K, Bretteville A, Leroy K, Begard S, Brion JP, Hamdane M, Buee L (2006) Alzheimer's disease-like tau neuropathology leads to memory deficits and loss of functional synapses in a novel mutated tau transgenic mouse without any motor deficits. The American journal of pathology 169:599-616.

Schroder J, Pantel J (2016) Neuroimaging of hippocampal atrophy in early recognition of Alzheimer's disease--a critical appraisal after two decades of research. Psychiatry research 247:71-78.

Schwab C, Klegeris A, McGeer PL (2010) Inflammation in transgenic mouse models of neurodegenerative disorders. Biochimica et biophysica acta 1802:889-902.

Scott CW, Blowers DP, Barth PT, Lo MM, Salama AI, Caputo CB (1991) Differences in the abilities of human tau isoforms to promote microtubule assembly. J Neurosci Res 30:154-162.
Selden SC, Pollard TD (1983) Phosphorylation of microtubule-associated proteins regulates their interaction with actin filaments. J Biol Chem 258:7064-7071.
Selenica ML, Brownlow M, Jimenez JP, Lee DC, Pena G, Dickey CA, Gordon MN, Morgan D (2013) Amyloid oligomers exacerbate tau pathology in a mouse model of tauopathy. Neuro-degenerative diseases 11:165-181.
Selkoe DJ, Hardy J (2016) The amyloid hypothesis of Alzheimer's disease at 25 years. EMBO molecular medicine 8:595-608.
Sengupta A, Kabat J, Novak M, Wu Q, Grundke-Iqbal I, Iqbal K (1998) Phosphorylation of tau at both Thr 231 and Ser 262 is required for maximal inhibition of its binding to microtubules. Archives of biochemistry and biophysics 357:299-309.
Sengupta U, Nilson AN, Kayed R (2016) The Role of Amyloid-beta Oligomers in Toxicity, Propagation, and Immunotherapy. EBioMedicine 6:42-49.
Serio A, Bilican B, Barmada SJ, Ando DM, Zhao C, Siller R, Burr K, Haghi G, Story D, Nishimura AL, Carrasco MA, Phatnani HP, Shum C, Wilmut I, Maniatis T, Shaw CE, Finkbeiner S, Chandran S (2013) Astrocyte pathology and the absence of non-cell autonomy in an induced pluripotent stem cell model of TDP-43 proteinopathy. Proceedings of the National Academy of Sciences of the United States of America 110:4697-4702.
Seshadri S et al. (2010) Genome-wide analysis of genetic loci associated with Alzheimer disease. Jama 303:1832-1840.
Sestero CM, McGuire DJ, De Sarno P, Brantley EC, Soldevila G, Axtell RC, Raman C (2012) CD5-dependent CK2 activation pathway regulates threshold for T cell anergy. J Immunol 189:2918-2930.
Shanthi KB, Krishnan S, Rani P (2015) A systematic review and meta-analysis of plasma amyloid 1-42 and tau as biomarkers for Alzheimer's disease. SAGE open medicine 3:2050312115598250.
Sheldon AL, Robinson MB (2007) The role of glutamate transporters in neurodegenerative diseases and potential opportunities for intervention. Neurochem Int 51:333-355.
Shen J, Kelleher RJ, 3rd (2007) The presenilin hypothesis of Alzheimer's disease: evidence for a loss-of-function pathogenic mechanism. Proceedings of the National Academy of Sciences of the United States of America 104:403-409.
Shepherd CE, Gregory GC, Vickers JC, Halliday GM (2005) Novel 'inflammatory plaque' pathology in presenilin-1 Alzheimer's disease. Neuropathol Appl Neurobiol 31:503-511.
Sheridan GK, Murphy KJ (2013) Neuron-glia crosstalk in health and disease: fractalkine and CX3CR1 take centre stage. Open biology 3:130181.
Sherrington R et al. (1995) Cloning of a gene bearing missense mutations in early-onset familial Alzheimer's disease. Nature 375:754-760.
Shi ZM, Han YW, Han XH, Zhang K, Chang YN, Hu ZM, Qi HX, Ting C, Zhen Z, Hong W (2016) Upstream regulators and downstream effectors of NF-kappaB in Alzheimer's disease. J Neurol Sci 366:127-134.
Shoji M, Golde TE, Ghiso J, Cheung TT, Estus S, Shaffer LM, Cai XD, McKay DM, Tintner R, Frangione B, et al. (1992) Production of the Alzheimer amyloid beta protein by normal proteolytic processing. Science 258:126-129.
Sierra A, Tremblay ME, Wake H (2014) Never-resting microglia: physiological roles in the healthy brain and pathological implications. Frontiers in cellular neuroscience 8:240.
Simic G, Babic Leko M, Wray S, Harrington C, Delalle I, Jovanov-Milosevic N, Bazadona D, Buee L, de Silva R, Di Giovanni G, Wischik C, Hof PR (2016) Tau Protein Hyperphosphorylation and Aggregation in Alzheimer's Disease and Other Tauopathies, and Possible Neuroprotective Strategies. Biomolecules 6:6.
Simpson JE, Ince PG, Lace G, Forster G, Shaw PJ, Matthews F, Savva G, Brayne C, Wharton SB (2010) Astrocyte phenotype in relation to Alzheimer-type pathology in the ageing brain. Neurobiology of aging 31:578-590.

Sinha S et al. (1999) Purification and cloning of amyloid precursor protein beta-secretase from human brain. Nature 402:537-540.
Sjoberg MK, Shestakova E, Mansuroglu Z, Maccioni RB, Bonnefoy E (2006) Tau protein binds to pericentromeric DNA: a putative role for nuclear tau in nucleolar organization. J Cell Sci 119:2025-2034.
Skaper SD (2011) Ion Channels on Microglia: Therapeutic Targets for Neuroprotection. CNS and neurological disorders 10:44-56.
Sleegers K, Brouwers N, Gijselinck I, Theuns J, Goossens D, Wauters J, Del-Favero J, Cruts M, van Duijn CM, Van Broeckhoven C (2006) APP duplication is sufficient to cause early onset Alzheimer's dementia with cerebral amyloid angiopathy. Brain : a journal of neurology 129:2977-2983.
Smith PK, Krohn RI, Hermanson GT, Mallia AK, Gartner FH, Provenzano MD, Fujimoto EK, Goeke NM, Olson BJ, Klenk DC (1985) Measurement of protein using bicinchoninic acid. Anal Biochem 150:76-85.
Snigdha S, Smith ED, Prieto GA, Cotman CW (2012) Caspase-3 activation as a bifurcation point between plasticity and cell death. Neuroscience bulletin 28:14-24.
Sofroniew MV (2009) Molecular dissection of reactive astrogliosis and glial scar formation. Trends Neurosci 32:638-647.
Sofroniew MV, Vinters HV (2010) Astrocytes: biology and pathology. Acta neuropathologica 119:7-35.
Song L, Lu SX, Ouyang X, Melchor J, Lee J, Terracina G, Wang X, Hyde L, Hess JF, Parker EM, Zhang L (2015) Analysis of tau post-translational modifications in rTg4510 mice, a model of tau pathology. Molecular neurodegeneration 10:14.
Sorbi S, Forleo P, Tedde A, Cellini E, Ciantelli M, Bagnoli S, Nacmias B (2001) Genetic risk factors in familial Alzheimer's disease. Mechanisms of ageing and development 122:1951-1960.
Soto C, Castano EM, Kumar RA, Beavis RC, Frangione B (1995) Fibrillogenesis of synthetic amyloid-beta peptides is dependent on their initial secondary structure. Neurosci Lett 200:105-108.
Spillantini MG, Goedert M (2013) Tau pathology and neurodegeneration. The Lancet Neurology 12:609-622.
Spires-Jones TL, Stoothoff WH, de Calignon A, Jones PB, Hyman BT (2009) Tau pathophysiology in neurodegeneration: a tangled issue. Trends Neurosci 32:150-159.
Spittaels K, Van den Haute C, Van Dorpe J, Bruynseels K, Vandezande K, Laenen I, Geerts H, Mercken M, Sciot R, Van Lommel A, Loos R, Van Leuven F (1999) Prominent axonopathy in the brain and spinal cord of transgenic mice overexpressing four-repeat human tau protein. The American journal of pathology 155:2153-2165.
St George-Hyslop PH, Tanzi RE, Polinsky RJ, Haines JL, Nee L, Watkins PC, Myers RH, Feldman RG, Pollen D, Drachman D, et al. (1987) The genetic defect causing familial Alzheimer's disease maps on chromosome 21. Science 235:885-890.
Stamer K, Vogel R, Thies E, Mandelkow E, Mandelkow EM (2002) Tau blocks traffic of organelles, neurofilaments, and APP vesicles in neurons and enhances oxidative stress. The Journal of cell biology 156:1051-1063.
Stan AD, Ghose S, Gao XM, Roberts RC, Lewis-Amezcua K, Hatanpaa KJ, Tamminga CA (2006) Human postmortem tissue: what quality markers matter? Brain Res 1123:1-11.
Stephenson D, Yin T, Smalstig EB, Hsu MA, Panetta J, Little S, Clemens J (2000) Transcription factor nuclear factor-kappa B is activated in neurons after focal cerebral ischemia. Journal of cerebral blood flow and metabolism : official journal of the International Society of Cerebral Blood Flow and Metabolism 20:592-603.
Stewart CR, Stuart LM, Wilkinson K, van Gils JM, Deng J, Halle A, Rayner KJ, Boyer L, Zhong R, Frazier WA, Lacy-Hulbert A, El Khoury J, Golenbock DT, Moore KJ (2010) CD36 ligands promote sterile inflammation through assembly of a Toll-like receptor 4 and 6 heterodimer. Nat Immunol 11:155-161.

Stobart JL, Anderson CM (2013) Multifunctional role of astrocytes as gatekeepers of neuronal energy supply. Frontiers in cellular neuroscience 7:38.

Stohr J, Watts JC, Mensinger ZL, Oehler A, Grillo SK, DeArmond SJ, Prusiner SB, Giles K (2012) Purified and synthetic Alzheimer's amyloid beta (Abeta) prions. Proceedings of the National Academy of Sciences of the United States of America 109:11025-11030.

Streit WJ, Xue QS (2009) Life and death of microglia. Journal of neuroimmune pharmacology : the official journal of the Society on NeuroImmune Pharmacology 4:371-379.

Strittmatter WJ, Saunders AM, Schmechel D, Pericak-Vance M, Enghild J, Salvesen GS, Roses AD (1993) Apolipoprotein E: high-avidity binding to beta-amyloid and increased frequency of type 4 allele in late-onset familial Alzheimer disease. Proceedings of the National Academy of Sciences of the United States of America 90:1977-1981.

Sullivan SM, Lee A, Bjorkman ST, Miller SM, Sullivan RK, Poronnik P, Colditz PB, Pow DV (2007) Cytoskeletal anchoring of GLAST determines susceptibility to brain damage: an identified role for GFAP. J Biol Chem 282:29414-29423.

Suri S, Heise V, Trachtenberg AJ, Mackay CE (2013) The forgotten APOE allele: a review of the evidence and suggested mechanisms for the protective effect of APOE varepsilon2. Neuroscience and biobehavioral reviews 37:2878-2886.

Sutinen EM, Pirttila T, Anderson G, Salminen A, Ojala JO (2012) Pro-inflammatory interleukin-18 increases Alzheimer's disease-associated amyloid-beta production in human neuron-like cells. Journal of neuroinflammation 9:199.

Suzuki A, Stern SA, Bozdagi O, Huntley GW, Walker RH, Magistretti PJ, Alberini CM (2011) Astrocyte-neuron lactate transport is required for long-term memory formation. Cell 144:810-823.

Szczepankiewicz O, Linse B, Meisl G, Thulin E, Frohm B, Sala Frigerio C, Colvin MT, Jacavone AC, Griffin RG, Knowles T, Walsh DM, Linse S (2015) N-Terminal Extensions Retard Abeta42 Fibril Formation but Allow Cross-Seeding and Coaggregation with Abeta42. J Am Chem Soc 137:14673-14685.

Sze CI, Bi H, Kleinschmidt-DeMasters BK, Filley CM, Martin LJ (2000) Selective regional loss of exocytotic presynaptic vesicle proteins in Alzheimer's disease brains. J Neurol Sci 175:81-90.

Szendrei GI, Lee VM, Otvos L, Jr. (1993) Recognition of the minimal epitope of monoclonal antibody Tau-1 depends upon the presence of a phosphate group but not its location. J Neurosci Res 34:243-249.

Tai LM, Ghura S, Koster KP, Liakaite V, Maienschein-Cline M, Kanabar P, Collins N, Ben-Aissa M, Lei AZ, Bahroos N, Green SJ, Hendrickson B, Van Eldik LJ, LaDu MJ (2015) APOE-modulated Abeta-induced neuroinflammation in Alzheimer's disease: current landscape, novel data, and future perspective. Journal of neurochemistry 133:465-488.

Takahashi K, Rochford CD, Neumann H (2005) Clearance of apoptotic neurons without inflammation by microglial triggering receptor expressed on myeloid cells-2. The Journal of experimental medicine 201:647-657.

Takahashi M, Tsujioka Y, Yamada T, Tsuboi Y, Okada H, Yamamoto T, Liposits Z (1999) Glycosylation of microtubule-associated protein tau in Alzheimer's disease brain. Acta neuropathologica 97:635-641.

Talantova M et al. (2013) Abeta induces astrocytic glutamate release, extrasynaptic NMDA receptor activation, and synaptic loss. Proceedings of the National Academy of Sciences of the United States of America 110:e2518-2527.

Tam WY, Ma CH (2014) Bipolar/rod-shaped microglia are proliferating microglia with distinct M1/M2 phenotypes. Scientific reports 4:7279.

Tan MS, Yu JT, Jiang T, Zhu XC, Guan HS, Tan L (2014) IL12/23 p40 inhibition ameliorates Alzheimer's disease-associated neuropathology and spatial memory in SAMP8 mice. Journal of Alzheimer's disease : JAD 38:633-646.

Tanaka K (2000) Functions of glutamate transporters in the brain. Neuroscience research 37:15-19.

Tanuma N, Sakuma H, Sasaki A, Matsumoto Y (2006) Chemokine expression by astrocytes plays a role in microglia/macrophage activation and subsequent neurodegeneration in secondary progressive multiple sclerosis. Acta neuropathologica 112:195-204.

Tanzi RE (2012) The genetics of Alzheimer disease. Cold Spring Harbor perspectives in medicine 2.

Tanzi RE, McClatchey AI, Lamperti ED, Villa-Komaroff L, Gusella JF, Neve RL (1988) Protease inhibitor domain encoded by an amyloid protein precursor mRNA associated with Alzheimer's disease. Nature 331:528-530.

Taoufik E, Tseveleki V, Chu SY, Tselios T, Karin M, Lassmann H, Szymkowski DE, Probert L (2011) Transmembrane tumour necrosis factor is neuroprotective and regulates experimental autoimmune encephalomyelitis via neuronal nuclear factor-kappaB. Brain : a journal of neurology 134:2722-2735.

Tchelingerian JL, Vignais L, Jacque C (1994) TNF alpha gene expression is induced in neurones after a hippocampal lesion. Neuroreport 5:585-588.

Tebay LE, Robertson H, Durant ST, Vitale SR, Penning TM, Dinkova-Kostova AT, Hayes JD (2015) Mechanisms of activation of the transcription factor Nrf2 by redox stressors, nutrient cues, and energy status and the pathways through which it attenuates degenerative disease. Free radical biology & medicine 88:108-146.

Terwel D, Dewachter I, Van Leuven F (2002) Axonal transport, tau protein, and neurodegeneration in Alzheimer's disease. Neuromolecular medicine 2:151-165.

Thal DR, Rub U, Orantes M, Braak H (2002) Phases of A beta-deposition in the human brain and its relevance for the development of AD. Neurology 58:1791-1800.

Thies E, Mandelkow EM (2007) Missorting of tau in neurons causes degeneration of synapses that can be rescued by the kinase MARK2/Par-1. The Journal of neuroscience : the official journal of the Society for Neuroscience 27:2896-2907.

Thornton C, Bright NJ, Sastre M, Muckett PJ, Carling D (2011) AMP-activated protein kinase (AMPK) is a tau kinase, activated in response to amyloid beta-peptide exposure. The Biochemical journal 434:503-512.

Thornton P, Pinteaux E, Gibson RM, Allan SM, Rothwell NJ (2006) Interleukin-1-induced neurotoxicity is mediated by glia and requires caspase activation and free radical release. Journal of neurochemistry 98:258-266.

Thurston VC, Zinkowski RP, Binder LI (1996) Tau as a nucleolar protein in human nonneural cells in vitro and in vivo. Chromosoma 105:20-30.

Tikka TM, Koistinaho JE (2001) Minocycline provides neuroprotection against N-methyl-D-aspartate neurotoxicity by inhibiting microglia. J Immunol 166:7527-7533.

Tiwari SS, d'Orange M, Troakes C, Shurovi BN, Engmann O, Noble W, Hortobagyi T, Giese KP (2015) Evidence that the presynaptic vesicle protein CSPalpha is a key player in synaptic degeneration and protection in Alzheimer's disease. Molecular brain 8:6.

Toivari E, Manninen T, Nahata AK, Jalonen TO, Linne ML (2011) Effects of transmitters and amyloid-beta peptide on calcium signals in rat cortical astrocytes: Fura-2AM measurements and stochastic model simulations. PloS one 6:e17914.

Town T, Zolton J, Shaffner R, Schnell B, Crescentini R, Wu Y, Zeng J, DelleDonne A, Obregon D, Tan J, Mullan M (2002) p35/Cdk5 pathway mediates soluble amyloid-beta peptide-induced tau phosphorylation in vitro. J Neurosci Res 69:362-372.

Trinczek B, Ebneth A, Mandelkow EM, Mandelkow E (1999) Tau regulates the attachment/detachment but not the speed of motors in microtubule-dependent transport of single vesicles and organelles. J Cell Sci 112 (Pt 14):2355-2367.

Tripathy D, Thirumangalakudi L, Grammas P (2010) RANTES upregulation in the Alzheimer's disease brain: a possible neuroprotective role. Neurobiology of aging 31:8-16.

Tucker KL, Meyer M, Barde YA (2001) Neurotrophins are required for nerve growth during development. Nature neuroscience 4:29-37.

Turner PR, O'Connor K, Tate WP, Abraham WC (2003) Roles of amyloid precursor protein and its fragments in regulating neural activity, plasticity and memory. Prog Neurobiol 70:1-32.

Ulrich JD, Holtzman DM (2016) TREM2 Function in Alzheimer's Disease and Neurodegeneration. ACS chemical neuroscience 7:420-427.

van Huizen F, Romijn HJ, Habets AM (1985) Synaptogenesis in rat cerebral cortex cultures is affected during chronic blockade of spontaneous bioelectric activity by tetrodotoxin. Brain Res 351:67-80.

Varvel NH, Grathwohl SA, Degenhardt K, Resch C, Bosch A, Jucker M, Neher JJ (2015) Replacement of brain-resident myeloid cells does not alter cerebral amyloid-beta deposition in mouse models of Alzheimer's disease. The Journal of experimental medicine 212:1803-1809.

Vassar R et al. (1999) Beta-secretase cleavage of Alzheimer's amyloid precursor protein by the transmembrane aspartic protease BACE. Science 286:735-741.

Venereau E, Ceriotti C, Bianchi ME (2015) DAMPs from Cell Death to New Life. Frontiers in immunology 6:422.

Verderio C, Matteoli M (2001) ATP mediates calcium signaling between astrocytes and microglial cells: modulation by IFN-gamma. J Immunol 166:6383-6391.

Verkhratsky A, Anderova M, Chvatal A (2009) Differential calcium signalling in neuronal-glial networks. Frontiers in bioscience (Landmark edition) 14:2004-2016.

Verkhratsky A, Sofroniew MV, Messing A, deLanerolle NC, Rempe D, Rodriguez JJ, Nedergaard M (2012) Neurological diseases as primary gliopathies: a reassessment of neurocentrism. ASN neuro 4:e131-150.

Villegas-Llerena C, Phillips A, Garcia-Reitboeck P, Hardy J, Pocock JM (2016) Microglial genes regulating neuroinflammation in the progression of Alzheimer's disease. Curr Opin Neurobiol 36:74-81.

Villemagne VL (2016) Amyloid imaging: Past, present and future perspectives. Ageing research reviews S1568-1637:30005-30008.

Vincent AJ, Gasperini R, Foa L, Small DH (2010) Astrocytes in Alzheimer's disease: emerging roles in calcium dysregulation and synaptic plasticity. Journal of Alzheimer's disease : JAD 22:699-714.

Vingtdeux V, Marambaud P (2012) Identification and biology of alpha-secretase. Journal of neurochemistry 120 Suppl 1:34-45.

Violet M, Delattre L, Tardivel M, Sultan A, Chauderlier A, Caillierez R, Talahari S, Nesslany F, Lefebvre B, Bonnefoy E, Buee L, Galas MC (2014) A major role for Tau in neuronal DNA and RNA protection in vivo under physiological and hyperthermic conditions. Frontiers in cellular neuroscience 8:84.

Volterra A, Meldolesi J (2005) Astrocytes, from brain glue to communication elements: the revolution continues. Nature reviews Neuroscience 6:626-640.

Vorhees CV, Williams MT (2014a) Value of water mazes for assessing spatial and egocentric learning and memory in rodent basic research and regulatory studies. Neurotoxicol Teratol 45:75-90.

Vorhees CV, Williams MT (2014b) Assessing spatial learning and memory in rodents. ILAR journal / National Research Council, Institute of Laboratory Animal Resources 55:310-332.

Vossel KA, Xu JC, Fomenko V, Miyamoto T, Suberbielle E, Knox JA, Ho K, Kim DH, Yu GQ, Mucke L (2015) Tau reduction prevents Abeta-induced axonal transport deficits by blocking activation of GSK3beta. The Journal of cell biology 209:419-433.

Vukic V, Callaghan D, Walker D, Lue LF, Liu QY, Couraud PO, Romero IA, Weksler B, Stanimirovic DB, Zhang W (2009) Expression of inflammatory genes induced by beta-amyloid peptides in human brain endothelial cells and in Alzheimer's brain is mediated by the JNK-AP1 signaling pathway. Neurobiology of disease 34:95-106.

Wahlsten D, Cooper SF, Crabbe JC (2005) Different rankings of inbred mouse strains on the Morris maze and a refined 4-arm water escape task. Behav Brain Res 165:36-51.

Waite LM (2015) Treatment for Alzheimer's disease: has anything changed? Australian prescriber 38:60-63.

Walsh DM, Selkoe DJ (2007) A beta oligomers - a decade of discovery. Journal of neurochemistry 101:1172-1184.

Walsh DM, Klyubin I, Fadeeva JV, Cullen WK, Anwyl R, Wolfe MS, Rowan MJ, Selkoe DJ (2002) Naturally secreted oligomers of amyloid beta protein potently inhibit hippocampal long-term potentiation in vivo. Nature 416:535-539.

Walsh DM, Klyubin I, Shankar GM, Townsend M, Fadeeva JV, Betts V, Podlisny MB, Cleary JP, Ashe KH, Rowan MJ, Selkoe DJ (2005) The role of cell-derived oligomers of Abeta in Alzheimer's disease and avenues for therapeutic intervention. Biochemical Society transactions 33:1087-1090.

Wang DD, Bordey A (2008) The astrocyte odyssey. Prog Neurobiol 86:342-367.

Wang JZ, Grundke-Iqbal I, Iqbal K (1996) Glycosylation of microtubule-associated protein tau: an abnormal posttranslational modification in Alzheimer's disease. Nat Med 2:871-875.

Wang T, Zhang X, Li JJ (2002) The role of NF-kappaB in the regulation of cell stress responses. Int Immunopharmacol 2:1509-1520.

Wang Y, Mandelkow E (2016) Tau in physiology and pathology. Nature reviews Neuroscience 17:22-35.

Wang Y, Cella M, Mallinson K, Ulrich JD, Young KL, Robinette ML, Gilfillan S, Krishnan GM, Sudhakar S, Zinselmeyer BH, Holtzman DM, Cirrito JR, Colonna M (2015) TREM2 lipid sensing sustains the microglial response in an Alzheimer's disease model. Cell 160:1061-1071.

Wang YP, Biernat J, Pickhardt M, Mandelkow E, Mandelkow EM (2007) Stepwise proteolysis liberates tau fragments that nucleate the Alzheimer-like aggregation of full-length tau in a neuronal cell model. Proceedings of the National Academy of Sciences of the United States of America 104:10252-10257.

Ward SM, Himmelstein DS, Lancia JK, Binder LI (2012) Tau oligomers and tau toxicity in neurodegenerative disease. Biochemical Society transactions 40:667-671.

Watanabe A, Hasegawa M, Suzuki M, Takio K, Morishima-Kawashima M, Titani K, Arai T, Kosik KS, Ihara Y (1993) In vivo phosphorylation sites in fetal and adult rat tau. J Biol Chem 268:25712-25717.

Weaver CL, Espinoza M, Kress Y, Davies P (2000) Conformational change as one of the earliest alterations of tau in Alzheimer's disease. Neurobiology of aging 21:719-727.

Weingarten MD, Lockwood AH, Hwo SY, Kirschner MW (1975) A protein factor essential for microtubule assembly. Proceedings of the National Academy of Sciences of the United States of America 72:1858-1862.

Welzel AT, Maggio JE, Shankar GM, Walker DE, Ostaszewski BL, Li S, Klyubin I, Rowan MJ, Seubert P, Walsh DM, Selkoe DJ (2014) Secreted amyloid beta-proteins in a cell culture model include N-terminally extended peptides that impair synaptic plasticity. Biochemistry 53:3908-3921.

Wes PD, Sayed FA, Bard F, Gan L (2016) Targeting microglia for the treatment of Alzheimer's Disease. Glia.

Whitmer RA, Gustafson DR, Barrett-Connor E, Haan MN, Gunderson EP, Yaffe K (2008) Central obesity and increased risk of dementia more than three decades later. Neurology 71:1057-1064.

Wiche G, Winter L (2011) Plectin isoforms as organizers of intermediate filament cytoarchitecture. Bioarchitecture 1:14-20.

Wierinckx A, Breve J, Mercier D, Schultzberg M, Drukarch B, Van Dam AM (2005) Detoxication enzyme inducers modify cytokine production in rat mixed glial cells. J Neuroimmunol 166:132-143.

Wilcock DM, Griffin WS (2013) Down's syndrome, neuroinflammation, and Alzheimer neuropathogenesis. Journal of neuroinflammation 10:84.

Willem M et al. (2015) eta-Secretase processing of APP inhibits neuronal activity in the hippocampus. Nature 526:443-447.

Williamson R, Scales T, Clark BR, Gibb G, Reynolds CH, Kellie S, Bird IN, Varndell IM, Sheppard PW, Everall I, Anderton BH (2002) Rapid tyrosine phosphorylation of neuronal proteins including tau and focal adhesion kinase in response to amyloid-beta peptide exposure: involvement of Src family protein kinases. The Journal of neuroscience : the official journal of the Society for Neuroscience 22:10-20.

Wilms H, Sievers J, Rickert U, Rostami-Yazdi M, Mrowietz U, Lucius R (2010) Dimethylfumarate inhibits microglial and astrocytic inflammation by suppressing the synthesis of nitric oxide, IL-1beta, TNF-alpha and IL-6 in an in-vitro model of brain inflammation. Journal of neuroinflammation 7:30.

Wirenfeldt M, Babcock AA, Vinters HV (2011) Microglia - insights into immune system structure, function, and reactivity in the central nervous system. Histology and histopathology 26:519-530.

Wray S, Saxton M, Anderton BH, Hanger DP (2008) Direct analysis of tau from PSP brain identifies new phosphorylation sites and a major fragment of N-terminally cleaved tau containing four microtubule-binding repeats. Journal of neurochemistry 105:2343-2352.

Wu HY, Hudry E, Hashimoto T, Uemura K, Fan ZY, Berezovska O, Grosskreutz CL, Bacskai BJ, Hyman BT (2012) Distinct dendritic spine and nuclear phases of calcineurin activation after exposure to amyloid-beta revealed by a novel fluorescence resonance energy transfer assay. The Journal of neuroscience : the official journal of the Society for Neuroscience 32:5298-5309.

Wu JW, Hussaini SA, Bastille IM, Rodriguez GA, Mrejeru A, Rilett K, Sanders DW, Cook C, Fu H, Boonen RA, Herman M, Nahmani E, Emrani S, Figueroa YH, Diamond MI, Clelland CL, Wray S, Duff KE (2016) Neuronal activity enhances tau propagation and tau pathology in vivo. Nature neuroscience 19:1085-1092.

Xia MQ, Bacskai BJ, Knowles RB, Qin SX, Hyman BT (2000) Expression of the chemokine receptor CXCR3 on neurons and the elevated expression of its ligand IP-10 in reactive astrocytes: in vitro ERK1/2 activation and role in Alzheimer's disease. J Neuroimmunol 108:227-235.

Xing J, Lu J (2016) HIF-1alpha Activation Attenuates IL-6 and TNF-alpha Pathways in Hippocampus of Rats Following Transient Global Ischemia. Cellular physiology and biochemistry : international journal of experimental cellular physiology, biochemistry, and pharmacology 39:511-520.

Yamada K, Holth JK, Liao F, Stewart FR, Mahan TE, Jiang H, Cirrito JR, Patel TK, Hochgrafe K, Mandelkow EM, Holtzman DM (2014) Neuronal activity regulates extracellular tau in vivo. The Journal of experimental medicine 211:387-393.

Yan R, Bienkowski MJ, Shuck ME, Miao H, Tory MC, Pauley AM, Brashier JR, Stratman NC, Mathews WR, Buhl AE, Carter DB, Tomasselli AG, Parodi LA, Heinrikson RL, Gurney ME (1999) Membrane-anchored aspartyl protease with Alzheimer's disease beta-secretase activity. Nature 402:533-537.

Yang DS, Stavrides P, Mohan PS, Kaushik S, Kumar A, Ohno M, Schmidt SD, Wesson D, Bandyopadhyay U, Jiang Y, Pawlik M, Peterhoff CM, Yang AJ, Wilson DA, St George-Hyslop P, Westaway D, Mathews PM, Levy E, Cuervo AM, Nixon RA (2011) Reversal of autophagy dysfunction in the TgCRND8 mouse model of Alzheimer's disease ameliorates amyloid pathologies and memory deficits. Brain : a journal of neurology 134:258-277.

Yang Y, Fujita J, Bandoh S, Ohtsuki Y, Yamadori I, Yoshinouchi T, Ishida T (2002) Detection of antivimentin antibody in sera of patients with idiopathic pulmonary fibrosis and non-specific interstitial pneumonia. Clin Exp Immunol 128:169-174.

Yang Z, Wang KK (2015) Glial fibrillary acidic protein: from intermediate filament assembly and gliosis to neurobiomarker. Trends Neurosci 38:364-374.

Yao PJ, Zhu M, Pyun EI, Brooks AI, Therianos S, Meyers VE, Coleman PD (2003) Defects in expression of genes related to synaptic vesicle trafficking in frontal cortex of Alzheimer's disease. Neurobiology of disease 12:97-109.

Yasojima K, McGeer EG, McGeer PL (1999) Tangled areas of Alzheimer brain have upregulated levels of exon 10 containing tau mRNA. Brain Res 831:301-305.

Ye S, Huang Y, Mullendorff K, Dong L, Giedt G, Meng EC, Cohen FE, Kuntz ID, Weisgraber KH, Mahley RW (2005) Apolipoprotein (apo) E4 enhances amyloid beta peptide production in cultured neuronal cells: apoE structure as a potential therapeutic target. Proceedings of the National Academy of Sciences of the United States of America 102:18700-18705.

Yeh CY, Vadhwana B, Verkhratsky A, Rodriguez JJ (2011) Early astrocytic atrophy in the entorhinal cortex of a triple transgenic animal model of Alzheimer's disease. ASN neuro 3:271-279.

Yin H, Kuret J (2006) C-terminal truncation modulates both nucleation and extension phases of tau fibrillization. FEBS Lett 580:211-215.

Yu Y, Ye RD (2015) Microglial Abeta receptors in Alzheimer's disease. Cell Mol Neurobiol 35:71-83.

Zagorski MG, Yang J, Shao H, Ma K, Zeng H, Hong A (1999) Methodological and chemical factors affecting amyloid beta peptide amyloidogenicity. Methods Enzymol 309:189-204.

Zhang F, Jiang L (2015) Neuroinflammation in Alzheimer's disease. Neuropsychiatric disease and treatment 11:243-256.

Zhang W, Potrovita I, Tarabin V, Herrmann O, Beer V, Weih F, Schneider A, Schwaninger M (2005) Neuronal activation of NF-kappaB contributes to cell death in cerebral ischemia. Journal of cerebral blood flow and metabolism : official journal of the International Society of Cerebral Blood Flow and Metabolism 25:30-40.

Zhang Y, Li P, Feng J, Wu M (2016a) Dysfunction of NMDA receptors in Alzheimer's disease. Neurological sciences : official journal of the Italian Neurological Society and of the Italian Society of Clinical Neurophysiology 37:1039-1047.

Zhang Y, Sloan SA, Clarke LE, Caneda C, Plaza CA, Blumenthal PD, Vogel H, Steinberg GK, Edwards MS, Li G, Duncan JA, 3rd, Cheshier SH, Shuer LM, Chang EF, Grant GA, Gephart MG, Barres BA (2016b) Purification and Characterization of Progenitor and Mature Human Astrocytes Reveals Transcriptional and Functional Differences with Mouse. Neuron 89:37-53.

Zhang YW, Thompson R, Zhang H, Xu H (2011) APP processing in Alzheimer's disease. Molecular brain 4:3.

Zhang Z, Song M, Liu X, Kang SS, Kwon IS, Duong DM, Seyfried NT, Hu WT, Liu Z, Wang JZ, Cheng L, Sun YE, Yu SP, Levey AI, Ye K (2014a) Cleavage of tau by asparagine endopeptidase mediates the neurofibrillary pathology in Alzheimer's disease. Nat Med 20:1254-1262.

Zhang ZH, Yu LJ, Hui XC, Wu ZZ, Yin KL, Yang H, Xu Y (2014b) Hydroxy-safflor yellow A attenuates Abeta(1)(-)(4)(2)-induced inflammation by modulating the JAK2/STAT3/NF-kappaB pathway. Brain Res 1563:72-80.

Zhao X, Kotilinek LA, Smith B, Hlynialuk C, Zahs K, Ramsden M, Cleary J, Ashe KH (2016) Caspase-2 cleavage of tau reversibly impairs memory. Nat Med 22:1268-1276.

Zheng C, Zhou XW, Wang JZ (2016) The dual roles of cytokines in Alzheimer's disease: update on interleukins, TNF-alpha, TGF-beta and IFN-gamma. Translational neurodegeneration 5:7.

Zhou Y, Klein WL (2012) Abeta oligomers-induced toxicity is attenuated in cells cultured with NbActiv4 medium. Neurotoxicity research 22:335-344.

Zhou Y, Liu L, Hao Y, Xu M (2016) Detection of Abeta Monomers and Oligomers: Early Diagnosis of Alzheimer's Disease. Chemistry, an Asian journal 11:805-817.

Zilka N, Kazmerova Z, Jadhav S, Neradil P, Madari A, Obetkova D, Bugos O, Novak M (2012) Who fans the flames of Alzheimer's disease brains? Misfolded tau on the crossroad of neurodegenerative and inflammatory pathways. Journal of neuroinflammation 9:47-56.

Zoltewicz JS, Scharf D, Yang B, Chawla A, Newsom KJ, Fang L (2012) Characterization of Antibodies that Detect Human GFAP after Traumatic Brain Injury. Biomarker insights 7:71-79.

Zorec R, Araque A, Carmignoto G, Haydon PG, Verkhratsky A, Parpura V (2012) Astroglial excitability and gliotransmission: an appraisal of Ca2+ as a signalling route. ASN neuro 4.

Zuchero JB, Barres BA (2015) Glia in mammalian development and disease. Development 142:3805-3809.